
Unterschrift des Betreuers



TECHNISCHE
UNIVERSITÄT
WIEN

Vienna University of Technology

MASTERARBEIT

Monitoring viral RNA (common cold virus) transfer into liposomes via molecular beacons and chip electrophoresis

ausgeführt am

Institut für Chemische Technologien und Analytik

der Technischen Universität Wien

unter der Anleitung von

Univ.Prof. Mag.pharm. Dr.rer.nat. Günter Allmaier

und

Univ.Ass. Mag.rer.nat. Dr.rer.nat.Victor U. Weiss

durch

Christina Bliem

Siebenbrunnengasse 8/4, 1050 Wien

Abstract

It was the aim of my thesis to set up and improve a fast and easy-to-handle analytical approach for detection of viral RNA release from the human rhinovirus (common cold virus) into liposomes employing molecular beacons (MB) and chip capillary electrophoresis.

The human rhinovirus is a small, non-enveloped, single-stranded RNA virus that belongs to the family of *Picornaviridae* and is well known for causing infections of the respiratory system. The viral capsid contains four viral proteins VP1 - VP4, 60 copies each. More than 160 serotypes of the virus are known to date. They can be divided into major and minor type group viruses depending on their receptor binding specificity. Cell infection normally takes place by clathrin-mediated endocytosis initiated by a cell surface receptor.

The idea was to set up an *in vitro* system to simulate the *in vivo* cell infection of the human rhinovirus serotype HRV-A2 employing liposomes, lipid bilayer vesicles, as cell models. Liposomes in different lipid composition were applied. Additionally, the influence of a HRV-A2 specific recombinant MBP-V33333 receptor as additive was investigated regarding the RNA transfer into the liposome nanoparticle.

As presented by Okun and colleagues (Analytical Chemistry 1999, 71 (20), 4480 – 4485) viral uncoating can be introduced either by increased temperature or by acidification to a pH lower than 5.8 to simulate the endosomal environment.

For detection a fast, sensitive and straightforward method for monitoring of the viral RNA release into the liposomes was required. Therefore a strategy using MBs and chip capillary electrophoresis (CE) was introduced and optimized during this master thesis. MBs are small probes which fluoresce upon hybridization to a complementary sequence. Three of these probes are designed to bind to complementary sequence regions of the HRV-A2 genome.

Challenges like decreasing stability of the MBs in different buffers systems and the influence of divalent cations like Mg^{2+} on the MBs had to be handled during this thesis. Weiss *et.al.* presented that the additive Trolox (6-hydroxy-2,5,7,8-tetramethylchroman-2-carboxylic acid), which is known for reduction of bleaching and blinking of fluorophores, increases the sensitivity of the chip CE setup by up to a factor of three (Analytical and Bioanalytical Chemistry, 2016, 408 (16), 1-9). However, in my work it was also shown that the reactivity of the MBs towards complementary oligonucleotide sequences deteriorates with increasing storage time due to the Trolox in the buffer. Hence, the sample buffer was modified to improve the storage conditions in order to retain the MBs' reactivity.

In particular, four different HRV-A2 preparations were selected for this work. We were able to detect viral RNA release into solution after heating the sample to 56 °C for 15 min as well as after acidification to pH < 5.6.

In addition viral material was incubated with various liposomes containing different MBs in various concentrations. RNA release into the liposome was detected in presence of a specific receptor to form a direct link between the cell model and viral capsid for two virus preparations. In absence of the receptor only partial release out of the virion was detected on the chip CE device.

In summary, detection of viral RNA transfer into liposomes as cell models is possible with the applied chip CE method using selected MBs. Our results suggest that the RNA transfer into the liposomes requires a receptor that is specific for HRV-A2.

Kurzfassung

Das Ziel der hier vorliegenden Arbeit war es, eine schnelle und einfach zu handhabende analytische Strategie zu etablieren, um die Freisetzung von viraler RNA aus dem humanen Rhinovirus (umgangssprachlich Schnupfenvirus) in Liposome als Zellmodell zu verfolgen. Zur Detektion sollen Molecular Beacons (MBs) in Kombination mit Chip-Kapillar-Elektrophorese eingesetzt werden.

Der humane Rhinovirus ist ein relativ kleines Virus ohne Lipidhülle mit einzelsträngiger RNA, das zur Familie der *Picornaviridae* gehört. Das humane Rhinovirus ist vor allem dafür bekannt, dass es Infektionen der Atemwege hervorruft. Das virale Kapsid ist aus vier viralen Proteinen VP1 - VP4 aufgebaut, welche jeweils in Form von 60 Kopien vorhanden sind. Bisher sind mehr als 160 Serotypen dieses Virus bekannt. Diese können in *major type* und *minor type* Viren eingeteilt werden. Diese Einteilung beruht auf der Spezifität der Rezeptoren, die Viren für die Zellinfektion benötigen. Zellinfektion wird in der Regel durch Clathrin-vermittelte Endozytose durch einen Zelloberflächenrezeptor initiiert.

Ziel des Projekts war es, ein *in vitro* System zu etablieren, um die *in vivo* Zellinfektion des humanen Rhinoviruses (Serotyp HRV-A2) durch den Einsatz von Liposomen als Zellmodell zu simulieren. Liposome, Lipid-Doppelschicht-Vesikel, in verschiedenen Lipidzusammensetzungen wurden mit dem viralen Material in Kontakt gebracht. Zusätzlich wurde dieser Ansatz um einen HRV-A2 spezifischen, rekombinanten MBP-V33333-Rezeptor erweitert und sein Einfluss auf den RNA Transfer in das Liposomnanopartikel betrachtet.

Wie bereits von Okun und Koautoren (Analytical Chemistry 1999, 71 (20), 4480 – 4485) berichtet, kann die Freisetzung des viralen Genomes entweder durch erhöhte Temperatur oder durch Ansäuern auf einen pH Wert < 5.8, um die endosomale Umgebung zu simulieren, erzielt werden.

Zur Beobachtung des viralen RNA Transfers in die Liposome ist eine schnelle, sensitive und einfache Analysenstrategie erforderlich. Dafür galt es, ein Setup für die Technik Chip-Kapillarelektrophorese (Chip CE) unter Verwendung von MBs zu entwickeln und während dieser Masterarbeit zu optimieren. MBs sind kleine Fluoreszenzsonden, die bei der Hybridisierung an eine komplementäre Sequenz fluoreszieren. Drei dieser Sonden, die spezifisch an Abschnitten des HRV-A2 Genoms binden, wurden in dieser Arbeit eingesetzt.

Herausforderungen wie die abnehmende Stabilität der MBs in verschiedenen Puffer-Systemen und der Einfluss von divalenten Kationen wie Mg^{2+} auf die MBs mussten während dieser Arbeit gemeistert werden. Wie in der Publikation von Weiss *et al.* (Analytical and Bioanalytical Chemistry, 2016, 408 (16), 1-9) beschrieben wurde, verringert der Zusatz von Trolox (6-Hydroxy-2,5,7,8-tetramethylchroman-2-carbonsäure) das Ausbleichen und Blinken des Fluorophors. Dies erhöht die Empfindlichkeit des Chip- CE Setups um bis zu einen Faktor drei. In der hier vorliegenden Arbeit wurde jedoch gezeigt, dass die Reaktivität der MBs gegenüber den komplementären Oligonukleotiden über längere Lagerzeit aufgrund von Trolox im Puffer abnimmt. Daher wurde der Probenpuffer für verbesserte Lagerbedingungen entsprechend angepasst um die Reaktivität der MBs zu erhalten.

Während dieser Arbeit wurden vier verschiedene hochreine HRV-A2 Präparationen untersucht. Nach Erhitzen der Proben auf 56 ° C für 15 min bzw. nach Ansäuern auf pH <5.6 konnte die Freisetzung viraler RNA in Lösung mittels der entwickelten Strategie detektiert werden.

Weiters wurden verschiedene Liposome, die verschiedene MBs in unterschiedlichen Konzentrationen in ihrem Lumen beinhalten, verwendet um den RNA Transfer zu studieren. Die Freisetzung der RNA in Liposome wurde in Gegenwart des spezifischen Rezeptors für zwei Viruspräparate gezeigt. Durch

Einsatz des Rezeptors konnte eine direkte Verbindung zum Zellmodell gezeigt werden und eine Interaktion mit dem viralen Kapsid erzielt werden. In Abwesenheit des Rezeptors konnte nur eine teilweise Freisetzung der RNA aus dem Virion mittels des MB Chip CE Ansatzes gezeigt werden.

Zusammenfassend lässt sich sagen, dass der Nachweis von viralem RNA Transfer in Liposome mit dem hier präsentierten CE-System unter Einsatz von MBs möglich ist und damit eine Bestätigung des Zellmodells erzielt werden konnte. Die Ergebnisse zeigten, dass für den Transfer von RNA in die Liposome die Anwesenheit eines spezifischen Rezeptors von wesentlicher Bedeutung ist.

Danksagung

An dieser Stelle möchte ich mich bei den folgenden Personen für ihre Unterstützung bedanken:

Zunächst gilt mein großer Dank meinem Betreuer Univ.Prof. Günter Allmaier, der mir diese Diplomarbeit ermöglichte. Ich bin ihm sehr dankbar für die freundliche Aufnahme in seine Arbeitsgruppe und seine Unterstützung.

Besonders bedanken möchte ich mich bei Dr. Victor U. Weiss für die sehr intensive und geduldige Betreuung meiner Arbeit. Ich bin ihm sehr dankbar dafür, dass er sich so viel Zeit für Fragen und Diskussionspunkte genommen hat und stets ein offenes Ohr für meine Anliegen hatte. Zudem unterstützte er mich mit Mitteln seines FWF Projekts (Project No P25749-B20 to VUW), was mir die Forschung an diesem Thema ermöglichte.

Mein herzlicher Dank gilt allen Kollegen der beiden Arbeitsgruppen Bio- und Polymeranalytik von Univ.Prof. Günter Allmaier und Omics Technologies von Associate Prof. Martina Marchetti-Deschmann für die gute Zusammenarbeit, für die zahlreichen Tipps, die sie mir gegeben haben, und für die schönen Momente, die ich mit ihnen erleben durfte. Ganz besonders bedanken möchte ich mich bei Maria Schneider, Victoria Dorrer und Nicole Engel, die mir stets mit guten Ratschlägen zur Seite standen und immer ein offenes Ohr sowohl für fachliche als auch für private Anliegen hatten.

Außerdem möchte ich mich bei all meinen Freunden, die mich durch das Studium begleitet haben, für die vielen schönen Stunden und die Unterstützung herzlich bedanken.

Weiters gebührt meinen Eltern Helmut und Maria und meinem Bruder Hans-Helmut ein ganz besonderes Dankeschön für ihre unermüdliche Unterstützung während meiner gesamten Ausbildung. Danke, dass ihr mir diesen Weg ermöglicht habt und mir auch in manch schwierigen Zeiten den Rücken gestärkt und immer an mich geglaubt habt.

Meinen größten Dank möchte ich meinem Ehemann Roland, der stets hinter mir stand, mich immer wieder aufs Neue ermutigte und mir Geduld und Verständnis entgegengebracht hat, aussprechen.

Table of Contents

Abstract	I
Kurzfassung	II
Danksagung	IV
Table of Contents	V
Abbreviation	VII
1. Introduction.....	1
1.1. Motivation	1
1.2. Human Rhinovirus	2
1.3. Liposomes as cell model.....	3
1.4. Molecular Beacons	4
1.5. Electrophoresis.....	6
1.5.1. Principles of electrophoresis	7
1.5.2. Capillary Electrophoresis	8
1.5.3. Capillary Electrophoresis on the chip.....	10
1.5.4. Gas-phase electrophoretic mobility molecular analyzer (GEMMA).....	13
2. Experimental	15
2.1. Reagents and materials	15
2.1.1. Reagents	15
2.1.2. Working solutions.....	20
2.1.3. Materials and Instrumentation	25
2.2. Molecular beacons (MB) – Proof of principle measurments	26
2.2.1. Comparison of two MB preparation batches.....	26
2.2.2. MB experiments with positive and negative control – DNA target	27
2.2.3. MB reactivity towards negative control - RNA ladder.....	31
2.2.4. Storage in different buffers	32
2.2.5. Influence of MgCl ₂ on the MB	33
2.3. Liposome preparation and characterization	35
2.3.1. Liposome preparations.....	35
2.3.2. Quality control of liposomes at GEMMA.....	37
2.3.3. Liposomes at Bioanalyzer 2100	38
2.3.3.1. Reactivity of the MB outside of the liposome.....	38
2.4. Biological Material.....	40
2.4.1. HRV-A2 virus desalting	40
2.4.2. MBP-V33333 receptor desalting	40

2.5.	RNA release into solution.....	42
2.5.1.	RNA release into solution.....	42
2.5.1.1.	RNA release triggered through temperature increase.....	42
2.5.1.2.	RNA release triggered through acidification	42
2.6.	RNA release into the liposomes	44
2.6.1.	RNA release triggered through acidification	44
2.7.	Study of the interaction between liposome, receptor and viral capsid.....	46
3.	Results and Discussion	47
3.1.	RNA release into solution.....	47
3.1.1.	Comparison of two MB preparation batches.....	68
3.1.2.	Specificity of the MB towards positive and negative controls.....	69
3.1.3.	Stability of the MB in different buffers	75
3.1.4.	Influence of MgCl ₂ on the MB	80
3.1.5.	Influence of incubation temperature.....	83
3.1.6.	MBs reactivity towards released viral RNA	84
3.1.6.1.	RNA release triggered by temperature	84
3.1.6.2.	RNA release triggered by acidification	88
3.1.6.3.	HRV-B14 as negative control -RNA release triggered by temperature	90
3.2.	Liposome preparation	92
3.2.1.	Quality control of liposomes at the GEMMA instrument	92
3.2.2.	Liposomes at the Bioanalyzer 2100 system	96
3.3.	Viral RNA release into liposomes	99
3.3.1.	Results on the Bioanalyzer 2100 system.....	99
3.3.2.	GEMMA results.....	117
3.3.3.	TEM results.....	119
4.	Summary.....	120
5.	Outlook.....	121
	References.....	122
	Appendix A	127
	Appendix B	147

Abbreviation

A2	HRV serotype A2
BA	Bioanalyzer 2100
B14	HRV serotype B14
BGE	Background Electrolyte
CH ₃ COOH	Acetic acid
CIM	Convective Interaction Media
DNA	Desoxyribonucleic acid
EM	Electrophoretic Mobility
EOF	Electroosmotic Flow
EPH	Electrophoretic Flow
FU	Fluorescence Unit
GEMMA	Gas-phase Electrophoretic Mobility Molecular Analyzer
HEPES	4-(2-hydroxyethyl)-1-piperazineethanesulfonic acid
HRV	Human Rhinovirus
IEF	Isoelectric Focusing
IPG	Immobilized pH Gradient
IS2	Internal Standard
MB	Molecular Beacon
MBP	Maltose binding Protein
MgCl ₂	Magnesium chloride
min	minute
mM	millimolar (mmol/l)
μM	micromolar (μmol/l)
Na	Sodium
nM	nanomolar (nmol/l)
NaOH	Sodium hydroxide
NH ₄ OAc	Ammonia acetate
n.a.	not available
p.a.	pro analysis
RNA	Ribonucleic acid
s	second
T	Temperature
Tris	Tris(hydroxymethyl)aminomethane
Trolox	6-hydroxy-2,5,7,8-tetramethylchroman-2-carboxylic acid
UHQ	Ultra High Quality water
°C	degree Celsius

1. Introduction

1.1. Motivation

The idea of the current thesis was to simulate the *in vivo* infection of a cell with the human rhinovirus in an *in vitro* system implementing liposomes as cell model. Liposomes in various lipid compositions should be used. The transfer of the viral RNA out of HRV-A2 into vesicles should be monitored via molecular beacons (MB) - small oligonucleotide probes fluorescing upon hybridization to a specific DNA or RNA target. Chip capillary electrophoresis, a simple and fast analytical setup, should be implemented to monitor this process.

The human rhinovirus (HRV), also known as common cold virus, is mainly known for causing infections of the human respiratory system [1]. An infection with HRV is either passed from human to human indirectly via droplets in the air (e.g. spread through sneezing) – liquid aerosols - or via direct contact to contaminated surfaces. Infections of the human rhinovirus can only be treated symptomatically, while an immunization is until now not available.

Serotype HRV-A2 should be used in this project as virus model, because its biological background is already well studied. Besides, the virus is relatively easy to cultivate in cell culture. Furthermore, the common cold virus is an ideal model to work with because of a low health risk that allows working in a standard laboratory environment. No special safety measures are necessary.

Some aspects of the HRV-A2 RNA transfer are already well understood, while others are hardly found or described in literature. From the biological point of view, infection of a cell with the common cold virus is initiated Clathrin-dependent by endocytosis [2]. Endocytosis is mediated by a specific receptor on the cells surface. The viral capsid is encapsulated into endosomes, vesicles that change the pH to acidic values upon their maturation. At pH < 5.6 the virus changes its conformation leading to RNA release out of the capsid through pores in the virus shell. The exact mechanism of RNA transfer through membranes is still unknown.

The group of *Dieter Blaas* (MFPL, Medical University of Vienna) reported the transfer of the viral RNA into the liposomes employing cDNA synthesis with reverse transcriptase encapsulated in the cell models for detection. cDNA was subsequently amplified using PCR [3].

Due to this reason it is of great interest to follow the transfer of viral RNA employing a fast analytical method introducing various liposomes of different lipid composition. Liposomes that do not reflect the natural cell wall as well as such mimicing physiological conditions should be applied in the experiments. For additional support of the viral RNA transfer, a recombinant MBP-V33333 receptor and a cations gradient across the liposomal membrane should be employed. The formation of the liposomes should be controlled by gas-phase electrophoresis (GEMMA).

1.2.Human Rhinovirus

The human rhinovirus (HRV) is a small, non-enveloped, single-stranded RNA virus of the *Picornaviridae* family and belongs to the genus of Enteroviruses [4]. All species of this viral family are relative small (approximately 30 nm in diameter), non-enveloped and with an icosahedral symmetry. The capsid is formed out of four viral proteins VP1- VP4, 60 copies each [5]. VP1, VP2 and VP3 are located on the outside of the virus shell, while VP4 is located at the inner side and is not accessible from the viral surface [6]. The viral positive sense, single-stranded RNA genome is about 7.2 kbases in length.

Human rhinoviruses can be divided into the groups of the minor and major type. The classification is based on their receptor specificity they use for cell infection. Serotypes of the major type group bind specific to the human intercellular adhesion molecule 1 (ICAM-1) [7] while serotypes of the minor type group attach members of the low-density lipoprotein receptor (LDLR) family [8, 9]. A new investigated serotype, HRV-C, binds specific to the cadherin-related family member 3 (CDHR3) [10]. Furthermore, rhinoviruses can be classified into antiviral group A, B and C based on their sensitivity towards antiviral compounds [11].

The HRV-A2 prototype strain that is in focus in this work belongs to the minor type group, while the HRV-B14 serotype that is used as negative control belongs to the major type group and differs significantly from the minor type HRV-A2 serotype.

In vivo cell infection with the human rhinovirus:

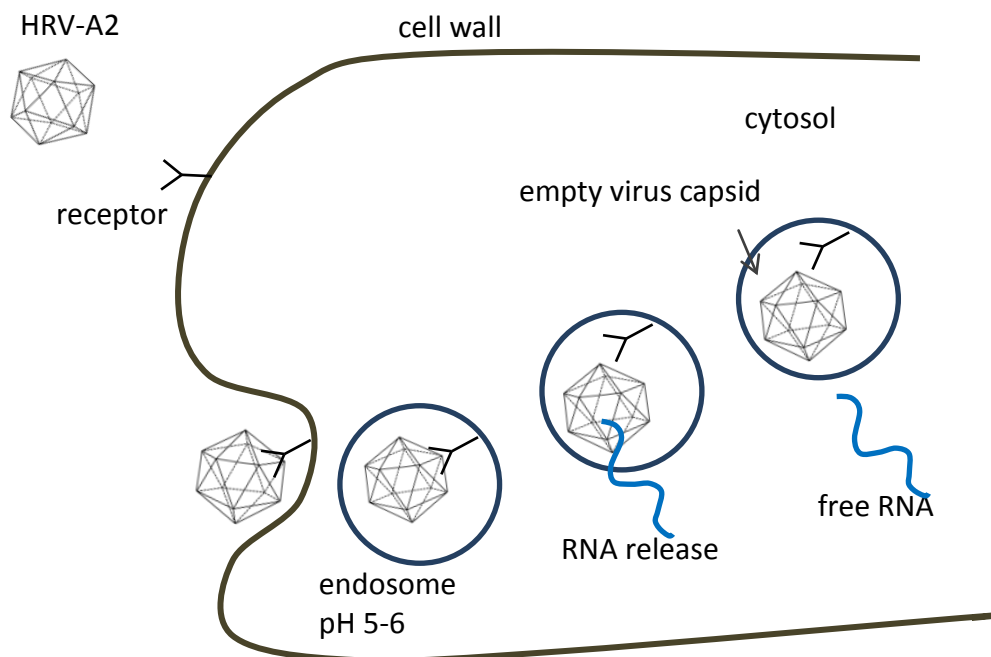


Figure 1: In vivo cell infection with HRV-A2 serotype of the common cold virus

Infection of a host cell with the common cold virus normally takes place by endocytosis [12], an encapsulation of the viral capsid by the cell wall and transfer into the cells cytosol as endosomal vesicle as shown in Figure 1. The binding of the viral capsid to the cell wall is initiated by a specific

cell-surface receptor [13]. *Snyers et.al* investigated that endocytosis of the human rhinovirus is supported by Clathrin, which is responsible for the formation of the endosomal vesicles [2]. In the cell the viral capsid undergoes a number of processes. Due to lowering of the pH to values of 5-6 in the endosomal environment, structural changes of the viral capsid occur and hence RNA release is induced. In following steps the released RNA passes through the endosomal membrane and enters the cytosol. There the RNA is translated in a replication procedure for amplification and further spreading of infectious viral particles [12].

Okun et al. showed that viral uncoating can be induced through heating the sample to 56 °C for > 10 min or by acidification to a pH lower 5.8 [14]. The process of viral uncoating and the RNA release out of the native virion and through the endosomal membrane proceeds under contribution of VP4 and VP1 building channel-like system through the lipid bilayer [2].

As already described above, HRVs of the minor type group attach specific to the cell via members of the low-density lipoprotein receptor (LDLR) family. These receptor molecules are formed out of different binding modules with various affinity to ligands [15]. In the current project a recombinant soluble receptor, MBP-V33333 was applied [16]. This receptor was modified to carry five repeats of the binding module 3 that allows binding to five VP1s on the HRV surface, a maltose-binding protein (MBP) for solubility and a His6-tag for purification and binding to Ni^{2+} carrying vesicles.

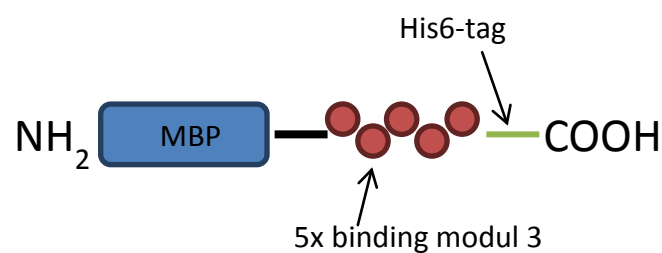


Figure 2: Schematically depiction of the recombinant MBP-V33333 receptor

1.3.Liposomes as cell model

Liposomes are self-assembled lipid bilayer particles to simulate the cell membrane. The lipid bilayer consists of hydrophilic heads on the outside and hydrophobic tails inside the bilayer formed out of lipids. An aqueous core can be found within the vesicle. Liposomes are mainly prepared out of phospholipids such as phosphatidylcholine (PC), phosphatidylethanolamine (PE), phosphatidylserine and phosphatidylglycerol [17]. Addition of cholesterol to the liposomes has a positive impact on the liposomal stability [18] and increases the vesicle size [19].

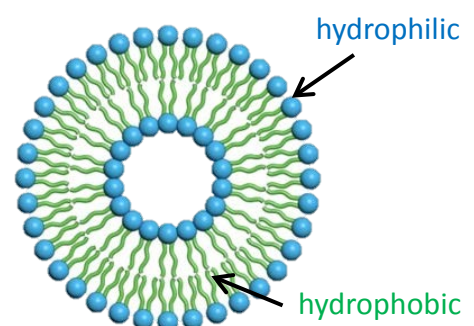


Figure 3: Schematically depiction of a liposome: hydrophilic outside and hydrophobic inside the lipid bilayer, adapted from [20]

Nowadays liposomes are commonly used for drug delivery, cancer treatment, cosmetics and as transport vesicles. Liposomes can carry drugs (or other small particles). Hydrophilic cargo can be found in the aqueous core, lipophilic cargo in the lipid bilayer or amphiphilic cargo attached to the liposomal surface [17].

In this project these lipid bilayer systems were chosen to simulate the membrane of the cell wall, which is also mainly formed out of phospholipids.

Liposome preparation techniques

Several techniques to produce multilamellar and unilamellar liposomes are known. The most conventional method is the formation of liposomes out of a thin lipid layer in a round bottom flask. Therefore the lipids are dissolved in an organic solvent. While evaporating the solvent a thin lipid layer in the round bottom flask is created. Rehydration of this lipid layer with an aqueous solution leads to the formation of multilamellar and unilamellar particles of different size. Particle size can be reduced by sonification or by multiple extrusion through polycarbonate filter membranes with certain pore size [21, 22].

Alternatively, liposomes can also be produced via injection of phospholipids dissolved in an organic phase in an aqueous phase [23], via reverse phase evaporation of organic – aqueous solvents containing the drug of interest and dissolved lipids or by using microfluidic systems [17].

1.4.Molecular Beacons

Molecular Beacons are small oligonucleotide probes tagged with a fluorophore and a quencher. 4-12 bp long complementary sequences of the oligonucleotide ends are forming a helix [24]. Consequently the fluorophore is unable to fluoresce as long as fluorophore and quencher are in close proximity (closed hairpin structure) [25].

The 15-30 bp long sequence between the stem regions is specific for a complementary RNA or DNA sequence. Once the molecular beacons interact with a specific target the MB undergoes a spontaneous conformational change [25]. The hairpin loop structure is opened and fluorophore and quencher are separated. This leads to an increased fluorescence signal.

Such probes are well known when performing qPCR to monitor the synthesis of a specific nucleic acid in a pool of other nucleic acids in real time [26, 27]. Further applications are the study of protein-DNA interactions [28] and the RNA expression in living cells [29].

In this project MBs should be used for detection of the RNA release out of viral capsid into solution or subsequently, after MB encapsulation inside liposomes, for detection of RNA transfer into lipid vesicles.



Figure 4: MB carrying a fluorophore (F) and a quencher (Q)

MB design

The most considerable parameters that show a significant impact on the hybridization specificity are the match of the loop sequence with the complementary target sequence, the length of the stem arms and their nucleotide content. The stability of the stem is mainly influenced by the GC-content, the number of complementary base pairs and the presence of divalent ions like magnesium chloride [25]. It was reported that too short stem regions as well as too long stem sequences mainly influence the behaviour of the probes. Stem regions that are too short are known to cause spontaneous opening of the stem-loop structures. Hence, fluorescence signals even without presence of any specific target are detectable, while too long stem sequences can lead to very stable constructs that do not open even in presence of a complementary target [30].

The length of the stem also influences the background fluorescence signal. Mostly short stem regions lead to higher background signals than longer, more stable stems. The closed structure of the stem is additionally influenced by the temperature of measurement. As presented by *Bonnet* and co-authors, heating the samples led also to structural changes of the MBs conformation. Further studies also showed a denaturation of a molecular beacon-target pair after heating the sample and a random reassembling of the MB structure after dissociation of the target [30].

For MB design mostly open source tools like *PrimeTime*, *qPCR*, *Primer Quest* and *RealTime PCR* are used [31]. Knowing the sequence of interest, the complementary base pairs are attached to stem regions carrying a fluorophore and quencher.

Independently from using such tools it is of great importance to check the self-binding possibilities of a MB construct to avoid the formation of internal secondary structures. Additionally a BLAST (basic local alignment search tool) to find regions of similarity between the viral and the MBs sequences and hence to check for specificity of the MBs sequences should be run [30]. Degradation of the biological material and nonspecific binding of DNA or RNA binding proteins should be avoided.

Introducing nucleic acids with a modified backbone, so called LNA (Locked Nucleic Acids), in the MBs sequence influence the target recognition of MB probes [31].

Four of such LNAs are implemented in the sequence of the MBs applied in this work for more stability of the MB/viral RNA complex.

1.5. Electrophoresis

Electrophoresis means the separation of analytes in an electric field and was first mentioned by the Swedish scientist *Arne Tiselius*. In 1948 *Tiselius* got the Nobel Prize for the separation of albumin, α -, β - and γ - globulin in horse blood serum in a U-shaped tube filled with buffer solutions of different pH and upon application of a constant voltage [32].

In principle the analytes migrate according to charge and size either to the cathode (negatively charged electrode) or to the anode (positively charged electrode). Forced by the applied voltage the charged particles migrate in a defined buffer system to the oppositely charged electrode as schematically depicted in Figure 5.

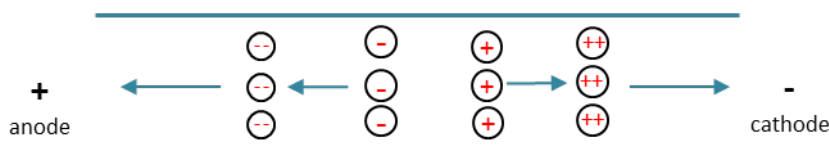


Figure 5: Principle of electrophoretic separation of charged ions in an electric field

Electrophoretic separation can be conducted in stabilizing matrices using thin gels layers or membranes or carrier free in the gas-phase or in the liquid phase. Free flow electrophoresis using a continuous buffer flow orthogonal to the electric field for example allows an efficient separation of the sample in different fractions.

Three principle variations have to be considered:

- **Zone electrophoresis:**

This separation technique is based on the difference in the electrophoretic mobility of the charged analytes in the applied electric field. The electrophoretic mobility μ is mainly influenced by the shape and size of the analytes and by the buffer system (pH, ionic strength I), which is crucial for the charge. Zone electrophoresis can be carried out in a carrier (anticonvective media) free system as well as using a carrier [33] but in constant, homogeneous buffer system.

- **Isotachophoresis**

Isotachophoresis means the migration of charged analytes that are moving within the same speed. Therefore the analytes migrate in a discontinuous buffer system between a leading buffer with higher mobility and a terminating buffer with lower mobility. The sample analytes are separated according to their mobility either near the leading or near the terminating electrolyte [34, 35].

- **Isoelectric focussing (IEF)**

The separation of the particles along a pH gradient is named isoelectric focusing (IEF). Analytes pass through the electrolyte electrophoretically until they reach the pH corresponding to their isoelectric point, whereby the netto charge of the analyte is zero and electrophoretically migration is no longer possible. The isoelectric point is specific for each analyte. IEF can be performed by using mobile carrier ampholytes, small low molecular, aliphatic oligo carbonic acids with different pI values, or using immobilized ampholytes on a so called IPG stripes (immobilized pH gradient). IEF is most likely used as first dimension in 2D electrophoresis previous to a SDS-PAGE, which additionally separates particles according to their size [36, 37].

1.5.1. Principles of electrophoresis

Separation of analytes in electrophoresis is driven by an electric field. Accelerating as well as decelerating forces influence the migration of the particles in the electric field. In the following these forces are described in more detail.

Because of the particles charge and the electric field an accelerating force, F_e , affects the particle in a positive manner, while the friction force, F_{fr} , acts against this motion in the electric field and harms the migration of the particle [33].

$$F_e = q * E$$

Equation 1

$$q = z * e$$

Equation 2

The decelerating force caused by the friction depends on the friction coefficient f_c , which is influenced by the viscosity of the medium and the pore size of the matrix, and the velocity v .

$$F_{fr} = f_c * v$$

Equation 3

F_e ... acceleration force
 q ... charge
 E ... electric field
 z ... charge number

e ... elementary charge
 F_{fr} ... friction force
 f_c ... friction coefficient
 v ... migration velocity

The equilibrium of these two forces leads to a constant migration of the particles in the electric field.

$$F_e = F_{fr}$$

Equation 4

$$q * E = f_c * v$$

Equation 5

The ratio of the migration velocity v and the electric field E is the electrophoretic mobility, μ , a parameter for the electrophoretic migration according to the charge.

$$\mu = \frac{v}{E} = \frac{q}{f_c} = \frac{z * e}{6 \pi * \eta * r}$$

Equation 6

The friction force of small round particles can be described by Stokes law as

$$F_R = 6 \pi * \eta * r * v .$$

Equation 7

η ... viscosity of the medium
 r ... stokes radius

v ... velocity

For non-spherical particles the friction force can be determined only by approximation [33].

Additionally, matrix effects caused by the carriers like glass or fused-silica capillaries are responsible for a second driving force besides the electrophoretic mobility - the electroosmotic flow. (For more details see also chapter 1.5.2.)

1.5.2. Capillary Electrophoresis

Nowadays, capillary electrophoresis (CE) is a state of the art technique in the protein and peptide analysis as well as in the analysis of carbohydrates, DNA and RNA.

Capillary electrophoresis was first mentioned by *Jorgenson* and *Lukacs* that were able to separate amino acids and peptides derivatives in a quartz capillary by applying a voltage of 30 kV to their separation system [38].

The big advantage of CE is the very high separation efficiency and resolution, while using only small sample and solvent volumes. In principle, the analytes are separated in a typically 20 - 100 cm long capillary that is about 50 μm in diameter filled with an electrolyte in capillary zone electrophoretic

manner or within a gel matrix in a gel electrophoresis manner. For sample injection the capillary tips into vials containing the sample on one side and into a waste vial on the other side. Injections can take place hydrodynamically by applying pressure in the sample vial or via vacuum at the detector side [33] as schematically depicted in Figure 6. Additionally, injections can be carried out electrokinetically applying a short high voltage pulse to the sample vials to force charged particle to enter the capillary system. Depending on the buffer, either positive or negative charged ions enter the capillary [40].

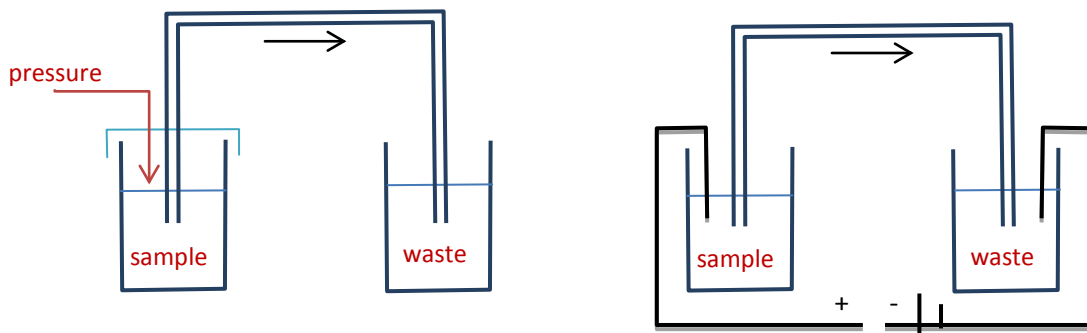


Figure 6: Scheme of hydrodynamically (left) and electrokinetically (right) injection in capillary electrophoresis, adapted from [39]

The driving force of a CE system is the already mentioned electroosmotic flow of the electrolyte, which is generated because of formation of a double layer on the inner capillary surface. This double layer forces a flow of the solution bulk towards the cathode.

Commonly used capillaries are made out of borosilicate or fused-silica glass. Hence, capillaries are carrying ionizable silanol (SiOH) groups on the surface. Depending on the ionic strength and the pH of the buffer either protonation or deprotonation of the silanol groups is induced [40]. Basic electrolytes force a deprotonation of the silanol groups (SiO^-) and induce the formation of a double layer along the capillaries surface. Positively charged ions of the electrolyte are attaching to the SiO^- groups. These ions migrate to the cathode when an electric field is applied leading to movements of the solution bulk - the electroosmotic flow E_{EOF} .

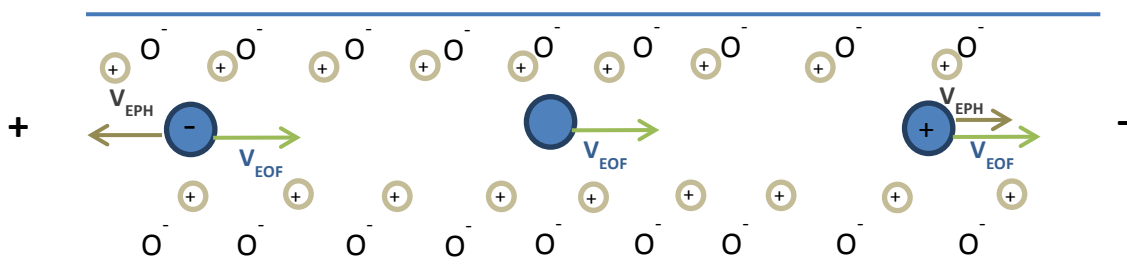


Figure 7: Scheme of the migration of charged ions in a capillary forced by the electroosmotic flow E_{EOF} and the electrophoretic mobility E_{EPH}


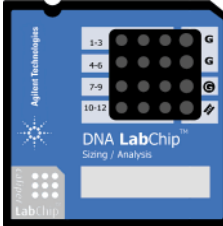

The electroosmotic flow (v_{EOF}) is enhanced or attenuated by the electrophoretic flow v_{EPH} of the particles itself based on their charge as shown in the scheme in Figure 7. Furthermore the EOF is strongly influenced by the pH and the ionic strength I of the buffer as well as the temperature. Due to this fact these parameters should be kept constant or under tight control during the experiments.

For detection, UV or fluorescence detectors are nowadays very common [39]. Therefore, special modified capillary segments, that allow the UV or fluorescence light to pass through, are necessary. A very interesting method is the coupling of CE with orthogonal techniques like mass spectrometry, which allows a separation and identification of analytes.

1.5.3. Capillary Electrophoresis on the chip

Capillary electrophoresis can be miniaturized to a chip format. *Agilent (Waldbronn, Germany)* provides a system for capillary gel electrophoresis on the chip, the Bioanalyzer 2100 system. This system allows the separation of RNA, DNA, intact cells and even proteins electrophoretically in a chip format, which is very timesaving considering sample preparation and analysis. Kits specialized either for RNA, DNA or protein samples make the sample preparation quite easy and fast to use. An overview of available kits provided from *Agilent (Waldbronn, Germany)* is given in Table 1.

Table 1: Overview of available kits for the *Agilent Bioanalyzer 2100 system* [41]

			
Kit	RNA LabChip	DNA LabChip	Protein LabChip
Sample volume	1 μ l	1 μ l	4 μ l (5 μ l)
Number of samples/chip	12 (Nano) or 11 (Pico and Small RNA)	12 (DNA kits) or 11 (High Sensitivity DNA)	10 (all kits)
Available kits specification	RNA 6000 Nano: 5- 500 ng/ μ l up to 6000 bases	DNA 1000: 0.1-50 ng/ μ l, 0.2-25-1000 bp	Protein 80: 6- 4000 ng/ μ l, 5- 80 kDa
	RNA 6000 Pico: 50- 5000 pg/ μ l up to 6000 bases	DNA 7500: 0.5-50 ng/ μ l 100 – 7500 bp	Protein 230: 6- 5000 ng/ μ l, 14- 230 kDa
	-	DNA 12500: 0.5-50 ng/ μ l 25-12000 bp	-
	Small RNA: 50- 2000 pg/ μ l, 6- 150 bases	High Sensitivity DNA: 5-500 pg/ μ l 50- 7000 bp	High sensitivity Protein 250: 1 pg/ μ l 10- 250 kDa

In addition *Kolivoška, Weiss* and colleagues presented in 2007 capillary electrophoresis on the chip in a zone electrophoresis manner using a background electrolyte for analysis of the human rhinovirus [42].

Agilent Bioanalyzer 2100

An *Agilent Bioanalyzer 2100* chip contains 16 wells, that are connected to a separation channel via a network of capillaries. Depending on the separation principle the capillary system is filled with a gel or a background electrolyte. Additionally 16 pin electrodes, one in each well, allow the application of voltage to each well, hence generating an electric field for electrophoresis.

In Figure 8 a step-by-step illustration of the procedure on the RNA chip is shown. First the samples will pass through the capillary system electrophoretically from the sample well to a waste well (1). Effectively only a small plug of the sample will enter the separation channel (2), where the analytes are separated according to charge and size (3). One analyte after the other will reach the detector (4).

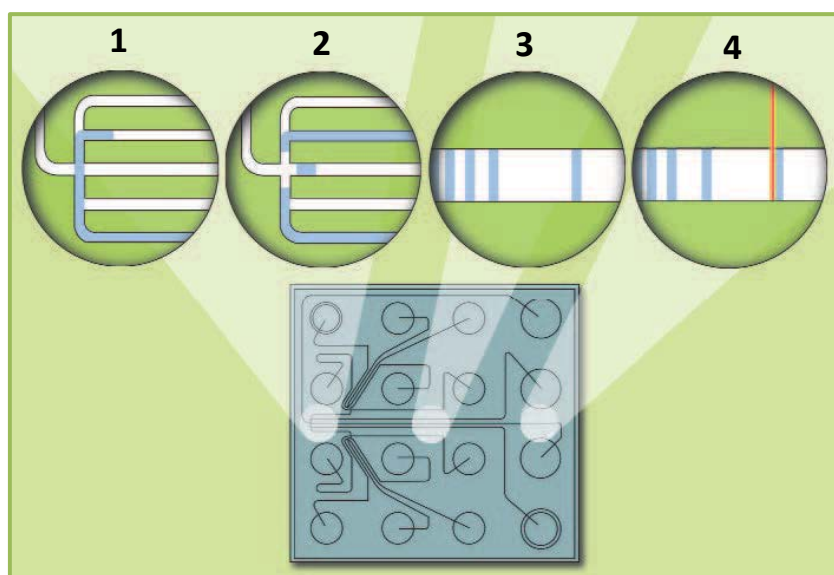


Figure 8: Step-by-step illustration of the analysis procedure on the *Agilent Bioanalyzer RNA* chip; adapted from [43]

The *Agilent Bioanalyzer 2100* system is equipped with two different excitation sources, a light-emitting diode (LED) ($\lambda_{\text{ex/em}} = 470/525 \text{ nm}$) and a red laser ($\lambda_{\text{ex/em}} = 635/685 \text{ nm}$). For detection, fluorescence emitting analytes are necessary. In case of samples without intrinsic fluorescence labelling with fluorescence dyes or introduction of MBs as fluorescence emitting probes that bind to the analyte of interest can be used.

Chip preparation

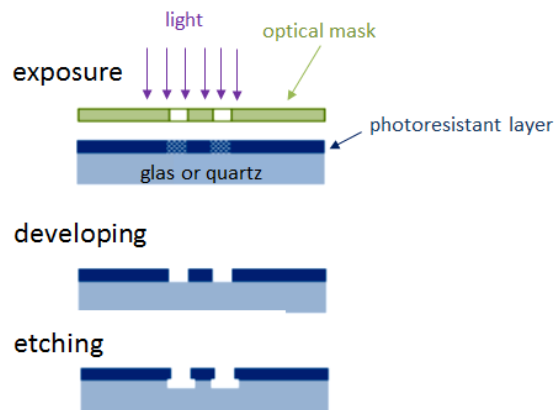


Figure 9: Scheme of the photolithographically chip preparations; adapted from [45]

areas can be removed by the treatment with a developing solution. In the last step precise trenches or holes are etched into the wafer to form the channel system. Finally the chip is covered with a thin layer to close the etched capillary system.

Chips are produced by *Caliper Technologies* (Hopkinton, Massachusetts, USA) using the principle of photolithography [44]. Figure 9 shows a schematical description of this process.

By the use of photolithography the pattern of interest is transferred to a substrate. First the pattern is placed on an optical photomask (e.g. glas). Using a laser or an electron beam the pattern can be drawn on the surface of the wafer. Now the wafer, that is covered with a photoresistant layer e.g. out of chromium, is exposed to UV to modify the photoresistant layer. Afterwards the treated photoresistant

Advantages of the Bioanalyzer 2100 system

The big advantages of the Bioanalyzer system are the time saving sample preparation by using kits and the short analysis time. Up to 12 samples can be analysed in 30 min automatically, while conventional planar/capillary electrophoresis is much more time consuming. Furthermore, only very low amounts of samples are necessary. For example, using RNA chips only ~ 50 pg of RNA (in 1 µl volume) are necessary for analysis, while for protein kits about 4 µl of sample (5 -5000 ng/µl protein) are needed.

Furthermore, the results are given immediately after analysis either as gel image, as electropherogram or in tabular form.

1.5.4. Gas-phase electrophoretic mobility molecular analyzer (GEMMA)

GEMMA is based on the electrophoretic separation of analytes in the gas-phase. This separation technique allows the determination of the particle size and the molecular weight of nanoparticles like viruses, liposomes, proteins, glycoproteins and polysaccharides [46, 47].

Therefore, the analytes have to be dissolved in an aqueous volatile electrolyte and are injected via a capillary by applying pressure from a sample vial to the instrument. Based on electrospray ionization in the Nano ES device (Nano electrospray) small, multiple-charged droplets carrying analytes are generated on the capillary tip upon application of a certain voltage as shown schematically in Figure 10. These droplets are subsequently dried in the gas phase. Using a ^{210}Po source as α - emitter the charge of the analytes is (mostly) reduced to zero. 1% of the analytes carry a single positive to or negative charge, which allows their separation only according to their dry particle size.

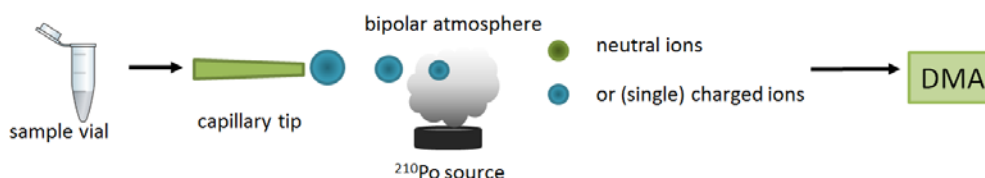


Figure 10: Schematic depiction of the sample injection and ionisation of the analytes in the nano electrospray GEMMA device

The analytes pass a differential mobility analyzer (DMA), where they are separated under ambient pressure according to their electrophoretic mobility diameter in a laminar sheath flow of dry air. Size separation of the particles is forced by a tuneable, orthogonal electric field that sorts analytes according to their different electrophoretic mobilities as shown in Figure 11. Particles of each electrophoretic mobility class leave the DMA subsequently and enter the so called condensation particle counter (CPC) for detection.

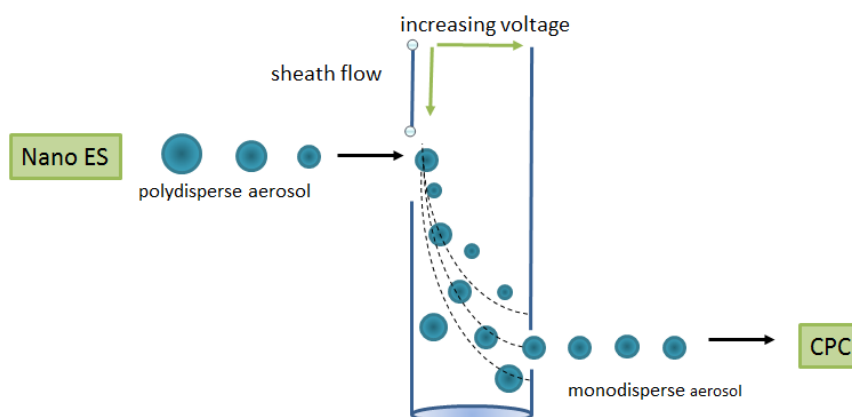


Figure 11: Schematically depiction of the differential mobility analyzer of the GEMMA instrument

In the condensation particle counter (CPC), monodisperse particles are covered by vapour condensation with n-butanol to form larger particles that can be detected by passing a laser beam (see Figure 12) [48].

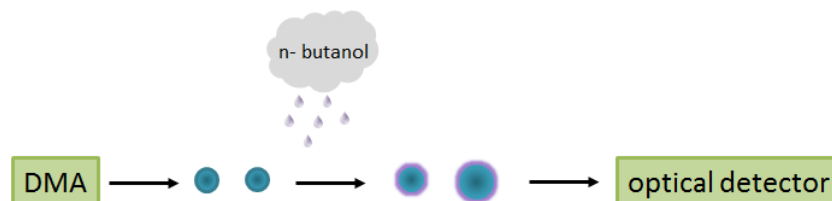


Figure 12: Schematically description of the condensation particle counter for analyte detection in the GEMMA instrument

Particles are counted related to the number of particle per volume and plotted versus particle size values (EM diameter). As an example Figure 13 shows a typically GEMMA spectra of a liposome as employed in this thesis.

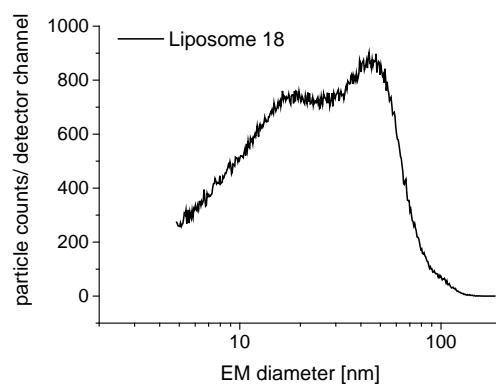


Figure 13: Typically GEMMA spectra of a liposome; EM diameter [nm] plotted against the particle counts detected per detector channel

2. Experimental

2.1. Reagents and materials

2.1.1. Reagents

In Table 2 a list of all used reagents and chemicals including their specifications is given. Lipids used for liposome preparation are listed in Table 3.

Table 2: List of reagents; MW are company given values

Reagent	Formula	Company	Purity	MW [g \cdot mol ⁻¹]*
Acetic acid	CH ₃ COOH	Sigma Aldrich, Steinheim, Germany	≥ 99.8 %	60.05
Ammonium acetate	NH ₄ OAc	Sigma Aldrich, Steinheim, Germany	≥ 99.99 %	77.08
Atto 488	-COOH	Atto Tec, Siegen, Germany	n.a.	804
Atto 495	-COOH	Atto Tec, Siegen, Germany	n.a.	452
Atto 633	-COOH	Atto Tec, Siegen, Germany	n.a.	652
Benzoic acid	C ₇ H ₆ O ₂	Fluka, Steinheim, Germany	p.a.	122.12
Benzonase endonuclease	-	Sigma Aldrich, Steinheim, Germany	> 99%	30 000
Boric acid	H ₃ BO ₃	Fluka, Steinheim, Germany	≥ 99.5 %	61.83
Chloroform for analysis	CHCl ₃	Merck, Darmstadt, Germany		119.37
Dimethyl sulfoxide (DMSO)	C ₂ H ₆ OS	Fluka, Steinheim, Germany	p.a.	78.13
Magnesium chloride-6-hydrate	MgCl ₂ * 6H ₂ O	Merck, Darmstadt, Germany	p.a.	203.30
Methanol (hypergrade)	CH ₃ OH	Merck, Darmstadt, Germany	≥ 99.9 %	32.05
Nitrogen gas	N ₂	Merck, Darmstadt, Germany	≥ 99.9 %	28.0
Sodium hydroxid	NaOH	Merck, Darmstadt, Germany	≥ 97 %	40.00
Trolox (6-hydroxy-2,5,7,8-tetramethylchroman-2-carboxylic acid)	C ₁₄ H ₁₈ O ₄	Sigma Aldrich, Steinheim, Germany	≥ 97 %	250.29
Tween 20	C ₅₈ H ₁₁₄ O ₂₆	Sigma Aldrich, Steinheim, Germany	n.a.	1227.54
UHQ (Ultra high quality) water (MilliQ water)	H ₂ O	Millipore, Billerica, MA, USA	18.2 MΩ cm/ 25 °C	18.02

Table 3: List of lipids for liposome preparation; MW vales given by Avanti lipids, Alabama, USA

Lipid	Formula	Company	Purity	MW* [gmol ⁻¹]
Chicken Egg SM (sphingomyelin)	C ₃₉ H ₇₉ N ₂ O ₆ P	Avanti lipids, Alabama, USA	>99 %	710.965 (average)
Cholesterol	C ₂₇ H ₄₆ O	Avanti lipids, Alabama, USA	>99 %	386.65
DGS-NTA (1,2-dioleoyl-sn-glycero-3-[(N-(5-amino-1-carboxypentyl)iminodiacetic acid)succinyl])	C ₅₃ H ₉₃ N ₂ O ₁₅ Ni	Avanti lipids, Alabama, USA	>99 %	1057.003 (average)
DSPE (1,2-distearoyl-sn-glycero-3-phosphoethanolamine)	C ₄₁ H ₈₂ NO ₈ P	Avanti lipids, Alabama, USA	>99 %	748.065 (average)
HSPC (L-α-phosphatidylcholine, hydrogenated (Soy))	C ₄₄ H ₈₈ NO ₈ P	Avanti lipids, Alabama, USA	>99 %	783.774 (average)
NBD-PC (1-Oleoyl-2-[12-[(7-nitro-2-1,3-benzoxadiazol-4-yl)amino]dodecanoyl]-sn-Glycero-3-Phosphocholine)	C ₄₄ H ₇₆ N ₅ O ₁₁ P	Avanti lipids, Alabama, USA	>99 %	882.075 (average)
SOPC (1-stearoyl-2-oleoyl-sn-glycero-3-phosphocholine)	C ₄₄ H ₈₆ NO ₈ P	Avanti lipids, Alabama, USA	>99 %	788.129 (average)
SoyPE (L-α-phosphatidylethanolamine)	C ₃₉ H ₇₄ NO ₈ P	Avanti lipids, Alabama, USA	>99 %	730.453 (average)

Table 4: List of the main fatty acids of the used lipids; values given by Avanti lipids, Alabama, USA

Fatty acid	Lipids						
	Chicken Egg SM	DGS-NTA	DSPE	HSPE	NBD-PC	SOPC	SoyPE
12:0	-	-	-	-	50	-	-
16:0	86	-	-	11.4	-	14.9	17.7
16:1	-	-	-	-	-	-	0.03
18:0	6	-	100	88.6	-	3.7	2.2
18:1	-	100	-	-	50	11.4	5
18:2	-	-	-	-	-	63	65.5
18:3	-	-	-	-	-	5.7	7.4
22:0	3	-	-	-	-	-	-
24:1	3	-	-	-	-	-	-
unknown	2	-	-	-	-	1.2	2.2

The complete sequence of the HRV-A2 genome is given below according to *Skern, T. et al. [49]*

(5') VPG -

ttaaaactggatccaggttggttcccacctggatttcccacagggagtggtactctgttattacggtaactttgta
cgccagttttatctcccttcccccatgtaacttagaagttttcacaaagaccaatagccggtaatcagccagat
tactgaaggtcaagcacttctgtttccccgggtcaatggtgatgctccaacagggcaaaaacaactgcatcgt
taaccgcaaagcgctacgcaaagcttagtagcatctttgaaatcggttggtcgatccgccatttcccctg
gtagacctggcagatgaggctagaaataccccactggcgacagtggttctagcctgctggtgctgcacacct
atgggtgtgaagccaaacaatggacaaggtgtgaagagccccgtgtgctcgtttgagtcctccggccccctgaat
gtggctaaccttaacctgacagctagagcacgtaacccaatgtgtatctagtcgtaatgagcaattgcgggatgg
gaccaactactttgggtgtccgtgtttcactttttccctttatatatttgcttat^{MBP12}ggtgacaatatatacaatat
atatattggcaccatgggtgcacaggtttcaagacaaaaat | gt | tggaaactcactccacgcaaaactctgtatca
aatgggtctagtttaaat¹¹attttaacatcaattatttcaaagatgctgcttcaaagtgtgcatcaaaactgga
attcacacaagatcctagtaaatctactgacccaggttaaggatgttttggaaaagggaataccaacactacagtc
ccccacagtggaggcttgtggatactctgataggattatacagattaccagaggagattcaaccataacctcaca
agatgtggctaattgctatcgttgcgatgggtgtttggccacattatctatcctccaaggatgcctctgcaattga
taaaccctctcaaccagatacatcttctaatagatttttatactctaaggagtgtagacctggagcagttcctcaaa
gggttgggtgggtggaaactacctgatgcactcaaggacatgggtatttttggtgaaaacatgttttatcattacct
gggtaggagtggtacacatacatgtgcagtgtaattgctagtaaatctcaccaggggtacactaattgttgctct
gatactgagcatcagattgcaagtgccttacatggcaatgtgaatgttgggttacaactacacacacccaggtga
aacaggcaggggaagttaaagctgagacgagattgaatcctgatctacaacctactgaagagatttggtcaaaactt
tgatgggacactccttggaaatattaccatattccctcatcaatttatcaacttgaggagtaataattctgccac
aataattgcccccttatgtcaatgcagttcctatggattcaatgaggagccacaataattggagtttggtaataat
accaatatgtcccccttgagacatcaagtgaattaacacaataacctattacaatatctataagccccatgtgtgc
agagttttccggcgcgctgccaaagcgtcaaggattaccagttttcatcacaccaggttcaggacagtttttgac
aacagatgattttccaatccccatgtgcacttccctgggtatcacccaactaaggaaatttctattccaggtgaggt
taaaaatttgggtgaaatttgtcaagtagacagcctagtaccaataaataaactgacacctacatcaatagtga
aaatatgtattctgttgtattgcaatcatcaattaatgcaccagataagatcttctctattcgaacagatgttgc
ttcccaaccttttagctactactttgattgggtgagatatctagctatttcacccactggacagggaggtctccgttt
cagcttcatgttttgggtactgccaacactactgttaagcttttgttggcatacacaccacctgggtatcgcaga
accaccacaaagaaaggatgcaatgctaggcactcatgttatatgggatgtgggggttgcagtcctacaatatcaat
ggtagtgccatggattagcgctagtcattatagaaacacatcacccaggtagatctacatctgggtacataacatg
ctgggtatcagactagattagtcattccacctcagacccacccaacagctagattgttatgttttgtatctgggtg
caaagacttttgccttgcgcatggcacgagataactaacctacacctgcaaagtgggtgcaatagcacagaacctgt
tgagaattatatagatgaagttcttaatgaagttttagttgtcccaaatattaatagtagtaacccacacaacatc
aaattctgccccagcattagatgctgcagaaacagggcacactagtaggttcaaccagaggatgtcattgaaac
taggtatgtgcagacatcacaaacaagagatgaaatgagtttagagagttttcttggcagatcaggatgcataca
tgaatctaaattagaggttacacttgcaattataacaaggagaattttacagtggtgggtctattaatctacaaga
aatgggtcaaattagaaggaaatttgaattgttcacctatactagggttgattctgaaataaccctagttccatg
catttccgccccttagtcaggacattggacacatcacaatgcaatacatgtatgttccaccaggtgcaccgggtgcc
caatagtagggacgattatgcatggcagtcctggcactaatgcctctgttttctggcaacatggacagggcttatcc
aagattttccttacctttcctaagtgtggcatctgcttattacatgttttatgatgggtatgatgaacaagatca
aaactatgggtacagcaaacacaaataacatgggggtcactatgctctaggatagtaacagagaaacacattcataa
agtacatatataatgacaagaatctatcacaaaggctaacaatgtcaaggcatgggtgtccacgcccacccagagcgct
tgagtatactcgtgctcatcgactaattttaaaattgaggataggagattcagacagcaattgtgaccagacc
aattatcactacagctggccccagtgacatgtatgttcatgtaggtaaccttatttatagaaatcttcatctttt
caactctgagatgcatgaatctattttgggtatcttattcatcagatttaatacatttaccgaacaaacactgtagg
tgatgattacattccctcttgtgattgtaccaagctacttattattgcaaacataaaaaatagatacttcccaat
tacagttacaagccatgactgggtatgaaatacaggaaagtgagtactatcccaaacacatacagtacaatttgtt
gattgggtgagggcccttgtgaaccaggtgactgtgggtggaaagttgctatgcaaacatgggtgtcataggatatgt
aacagctgggtgggtgataatcatgtggcttttattgaccttagacacttccattgtgctgaagaacaaggggttac
agattatatacatatgctaggagaagcatttggaaatggatttgtggatagtgtaaaagaacatatacatgccat
aaaccagtaggaaatatcagcaagaaaattttaaattggatgttgagaataatatcagcaatgggtcataataat

tagaaaactcttctgacccccaaactatattagcaacactcacactgattgggtgttctggatcacccctggagatt
tttaaaggaaaaattctgtaaatggacacagcttaattatatacacaagaatcagattcatgggttaaagaaatt
tactgaagcatgcaatgcagctagagggcttgaatggataggggaataagatatctaaatttattgaatggatgaa
gtcgatgctcccgcaagctcaattgaagggttaagtacttaaacgagcttaaaaaactcaacctatacgaaaagca
agttgagagcttgccgggtggctgacatgaaaacacaagaaaaaattaaaatggaaatagacactttacatgattt
gtcacgtaaatcttacccttctgtatgcaagtgaaggcaaaaaggataaaaaccctatacattaaatgtgataatat
catcaagcagaagaaaagatgtgaaccagtagctatagttattcatggaccacctgggtgctggcaaatctataac
aacaatttctctggccaaaatgataactaatgatagtgacatatactctctacctcctgatccaaaatattttga
tggttatgaccaacagagtgtagtaataatggatgacattatgcagaatccagccggggatgacatgacactgtt
ctgccaaatggtttctagtggttacattttataccaccaatgggtgatctaccagataaaaggcaaggcttttgattc
taggtttgtattatgcagcacaaatcattcccttctaacacccccgacaataacttcaactacctgcaatgaatag
aagatttttcttagatttagatataatagtagatgataacttcaaagatccacagggcaaaacttaatgtggcagc
agcgtttcgaccatgtgatgtagataatagaataggaaatgcacgttgttgtccatttgtgtgtggaaaagcagt
ttctttcaaagatcgtaactcttgcaacaaatacagccttgccgaggtgtacaacataatgattgaagaagacag
acggagaagacaagtgggtgatgtcatgacagctatattccaagggccaattgatatgaaaaaccaccaccacc
tgctattactgacttgctccagctctgttagaacccctgaagttattaagtattgtgagggtaatagatggataat
tccagcagaatgcaagatagaaaaggagttgaacttggttaacacaatcataacaatcattgcaaatgttattgg
tatggcgagaataatatatgttattttacaaacttttttgacattacagggaccatattcaggagaaccaaagcc
caagactaaaatcccagaaaggcgtgtagtaacacagggaccagaggaggaatttgggatgtctttaattaaaca
taactcatgtgttattacaacagaaaaatgggaaattcacaggtcttggagtatacgacagatttgtgggtcgtacc
aacacatgcagatcctggaaaggaaattcaggttgatgggtataactacaaaagtcattgactcatatgacctata
caacaagaatgggataaaagctagaaataacagtagcttaaatagatagaaatgaaaaatttagagatatcaggag
atatatacctaacaatgaagatgattacccaattgcaacttagcactgctagcaaaaccagcctgaaccaactat
aatcaatgttggagatgttgtatcctatggcaatatactgctcagtggaaccaaaccggctagaatgcttaaata
cagttacccaactaaatctgggttactgtggaggtgtcttatacaaaattgggcaagtgtcttgaatacatgttgg
gggcaatggtagggatgggtttctcagctatgttactcagatcctatttcaactgatgttcagggccaaataacggt
atcaaagaagaccagtgatgtaacctaccagtagatcacacccccatgcaaaaccaaattgcagcctagtggttt
ctatgatgtattccctgggttcaaaagaaccagctgtgttgtctgaaaaagatgcccggttacaagttgatttcaa
tgaagcactattttctaaatacaaaagggaatacagattgtccattaatgaccacataagaattgcatcatcaca
ttatgcagcacaaactcattaccttagatattgacccaaaacctattacacttgaggacagtgcttttggcactga
tggattagaggctcttgatttgaacactagcgcaggatttccatatattgcaatgggaggttaaaaagagagattt
aataaacaacaagaccaaggatataagcaaacttaagaagcaattgacaaatacggagttgacttacctatgggt
caccttcttgaaagatgaactcagaaagcatgaaaaggtaattaaagggtaaaactagagttattgaagctagtag
tgtgaatgataccctattattttagaacaacttttggcaacctcttttcaaagttccacttgaatcctggaattgt
tactggatcagcagttggatgtgatccagaggtgttttgggtcaaaaataaccagcaatgttggat⁵gataaatgta
ttatggcttttgattatacaaaattatgatggtagtatcacccc^{MBP13}tatttgggttgaagctcttaaacaggtac
tggtagatctatcatttaatccaacattaatagatagactatgcaagtctaaacacatcttcaaaaatacatact
atgaagtggagggaggtgtaccatctgggtgttcaggtagtagtatttttaacactatgatcaataatattatca
taaggaccttagtggttagatgcatacaagaatatagatctagataagcttaagataattgcctatgggtgatgatg
tcatattctcatacatacatgaactggacatggaggctatagcaatagaggggtgttaaataatgggttgactataa
ctcctgctgataaatctaacacatttgtaaaattagactatagcaatgttacttttttaaaaagaggggtttaagc
aagatgagaagtataactttctaatacatccaactttccctgaagatgaaatatttgaatccatcagatggacaa
agaaaccatcacaaatgcatgaacatgtgttgtctgtgtcacttaatgtggcacaatggacgtgacgcataca
aaaaatttgtggagaagatagcagtgtaagcgtgggtcgtgcaactgta^{P14}catccctccgtatgatttgcctttg^{MB}
^{P14}catgagtggtatgaaaaattttaagatat⁸agaaatagtaaactgatagttttattagttttataaaaaaaaaa
aa (3')

Table 5: List of molecular beacons used for detection of viral RNA release; MW value given by IDTDNA, Leuven, Belgium

Molecular Beacon	Abbreviation	Length	Company	Amount	MW* [g mol^{-1}]
MB P12S2_LNA_MB	MB P12	33 bases	IDTDNA, Leuven, Belgium	6.9 nmol	11.748
MB P13S2_LNA_MB	MB P13	33 bases	IDTDNA, Leuven, Belgium	4.8 nmol	11.631
MB P14S2_LNA_MB	MB P14	33 bases	IDTDNA, Leuven, Belgium	5.5 nmol	11.717

Table 6: List of oligonucleotide target sequences used for checking the reactivity of the MBs; MW value given by IDTDNA, Leuven, Belgium

Target	Length	Company
T12	40 bases	IDTDNA, Leuven, Belgium
T13	40 bases	IDTDNA, Leuven, Belgium
T14	40 bases	IDTDNA, Leuven, Belgium

The MBs sequences and the sequence of the corresponding oligonucleotide single-stranded DNA targets, designed by Victor U. Weiss, are given in follow for the three applied MBs. LNAs are marked in bold.

- **MB P12**

ccgtgttt**cactttttcctttatatttgcttat**ggtgacaa Target

5' tcgca ataag**g**caaat**tataaag**gaaaaag tcgca 3' Beacon

- **MB P13**

tgattata**caaattatgatggtagtatacaccc**tatttggt Target

5' tcgca ggg**g**tatact**taccat**cataatt tcgca 3' Beacon

- **MB P14**

Gcactgta**catccctccgtatgatttgcttttg**catgagtg Target

5' tcgca caaaa**g**caaat**cat**ac**g**aggga tcgca 3' Beacon

2.1.2. Working solutions

In following the used working solutions needed for the experiments and the way how they were prepared are given.

Solutions

- Solution A
 - dissolve 0.12 g NaOH in 1.0 ml UHQ
 - resulting in 3 M NaOH to adjust the pH
- Solution B (BGE for sample mixture)
 - dissolve 1.2366 g of boric acid in 80 ml of UHQ
 - adjust pH to 8.4 with solution A
 - fill up to 100 ml
 - filtrate buffer through sterile filter (0.2 µm pore size, CA, from Sartorius, Göttingen, Germany)
 - store at 4 °C
 - resulting in 200 mM Na-Borate, pH 8.4, as sample buffer
- Solution C (BGE for chip electrophoresis)
 - dissolve 50.06 mg of Trolox in 15.5 ml solution B
 - adjust pH to 8.4 with 66.67 µl of solution A
 - add 4.43 ml UHQ
 - mix gently
 - filtrate buffer through sterile filter (0.2 µm from Sartorius, Göttingen, Germany)
 - store at 4 °C
 - resulting in 155 mM Na-Borate, 10 mM Trolox, pH 8.4, as background electrolyte on the chip
- Solution D
 - dilute 0.5 µl of Atto 488 (2.5 mM in DMSO) and 0.5 µl of Atto 495 (3.3 mM in DMSO) in 24 µl solution B
 - mix well
 - store in the dark because of the fluorescence
 - resulting in a mixture of internal standards (Atto 488, Atto 495)(IS2) for the electropherogram alignment
- Solution E
 - dilute Atto 633 stock solution (2.5 mM in DMSO) 1:25000 (v/v) in solution B
 - store in the dark because of the fluorescence
 - resulting in the lens focusing solution for the Bioanalyzer 2100 instrument

- Solution F
 - mix 75 ml of Chloroform with 25 ml of Methanol in a bottle
 - resulting in Chloroform/Methanol (3/1, v/v) for liposome preparation
- Solution G
 - dissolve 277.488 mg NH_4OAc in 80 ml UHQ
 - adjust pH to 8.4 with 45.23 μl NH_4OH (28.2 %)
 - fill up to 90 ml with UHQ
 - filtrate buffer through sterile filter (0.2 μm from Sartorius, Göttingen, Germany)
 - resulting in 40 mM NH_4OAc , pH 8.4, as sample buffer for GEMMA measurements
- Solution H (cleaning solution for GEMMA)
 - mix solution G with 2 % Tween20
 - resulting in 40 mM NH_4OAc , pH 8.4, 0.02 % Tween20 for cleaning the GEMMA capillary
- Solution I
 - dissolve 20.33 mg Magnesium-6-hydrate in 10 ml UHQ
 - resulting in 10 mM MgCl_2 as stock solution for the liposome preparation
- Solution J
 - dissolve 21.787 mg CaCl_2 in solution B for 200 mM stock
 - dilute 200 mM stock 1:1000 (v/v) with solution B
 - filtrate solution through sterile filter (0.2 μm from Sartorius, Göttingen, Germany)
 - resulting in 200 mM Na-Borate, 0.2 mM CaCl_2 , pH 8.4, as buffer for receptor desalting
- Solution K
 - dilute 4.5 μl of concentrated CH_3COOH with 95.5 μl UHQ
 - resulting in 4.5 % CH_3COOH for acidification of the virus to induce the RNA release
- Solution X
 - take 35 μl of solution B
 - add 34.15 μl UHQ
 - add 1.2 μl solution A
 - add 8.75 μl solution D
 - mix gently
 - resulting in the reneutralizing solution after virus acidification to induce the RNA release
- Solution Z
 - take 100.5 μl of solution B
 - add 12.5 μl of solution D
 - mix gently

Molecular Beacons and controls

- Molecular Beacons
 - dissolve MB in 2 mM NH₄OAc, pH 7.4, to achieve a concentration of 0.5 mM according to Table 7

Table 7: MB dilution to 0.5 mM stock solutions

MB	Stock [nmol]	Concentration [mM]	Dissolve in x µl 2 mM NH ₄ OAc, pH 7.4
P12	6.9	0.5	13.8
P13	4.8	0.5	9.6
P14	5.5	0.5	11.0

- dilute 0.5 mM Stock 1:10 (v/v) in solution B for 50 µM Intermediate
 - dilute 50 µM MB intermediate 1:50 (v/v) in solution B for 1 µM Intermediate
 - dilute 1 µM MB intermediate 1:5 (v/v) in solution B for 200 nM Intermediate
- DNA target

Table 8: Overview of the available DNA target sequences that are specifically synthesized for the MBs

Target	Concentration [mM] in 2 mM NH ₄ OAc, pH 7.4
T12	0.5 (pre-exisiting)
T13	0.5 (pre-exisiting)
T14	0.5 (pre-exisiting)

- dilute 0.5 mM Stock 1:10 (v/v) in solution B for 50 µM Intermediate
 - dilute DNA target Stock (50 µM) 1:50 (v/v) in solution B for 1 µM Intermediate
- RNA ladder (provided from Agilent Technologies, Waldbronn, Germany)
 - incubated at 70 °C for 2 min for denaturation
 - cool down on ice
 - prepare 10 µl aliquots
 - stored on ice or in the freezer (-20 °C)

Biological material (obtained from MFPL, Medical University of Vienna, research group of Dieter Blaas)

- HRV—A2 preparation
 - either in 50 mM Tris or in 50 mM HEPES buffer

Table 9: List of HRV-A2 and HRV-B14 preparations

Preparation #	Preparation date	Concentration* [mg/ml]
A	04.10.2013, 1 st fraction	5.7
B	30.01.2015, 1 st fraction	4.7
C	05.11.2015	5.3
D	25.11.2015	1.7
E	22.01.2016, 1 st aliquot	2.4
F	22.01.2016, 2 nd aliquot	2.4
I	n.a.	2.0

* concentration determined at the GEMMA instrument by VUW

- receptor MBP-V33333
 - in TBSC buffer
 - unfreeze aliquot of receptor
 - (if required desalt receptor with solution B .as described in 2.4.2)

Lipids

- SOPC
 - dissolve certain amount of lipid in 1.5 ml solution F
 - calculate concentration
 - example: dissolve 7.8 mg in 1.5 ml solution F
→ concentration: 5.2 mg/ml
 - store in capped GC vial in freezer
- SoyPE
 - dissolve 25 mg aliquot in 1.5 ml solution F
→ concentration: 16.667 mg/ml
 - store in capped GC vial in freezer
- NGS- NTA (Ni^{2+} salt)
 - dissolve 8.5 mg aliquot in 1.5 ml solution F
→ concentration: 5.667 mg/ml
 - store in capped GC vial in freezer
- NBD- PC (labeled with fluorescence dye)
 - dissolve 1 mg aliquot in 1.5 ml solution F
→ concentration: 0.667 mg/ml
 - store in capped GC vial in freezer
 - avoid contact with light

2.1.3. Materials and Instrumentation

A capillary electrophoresis on the chip device from *Agilent Technologies (Waldbronn, Germany)* the Bioanalyzer 2100 system, was applied in the study to monitor viral RNA transfer. Besides the instrument itself (serial no. DE 34503981) a chip priming station as well as a special chip vortexer was provided. For data analysis the Agilent 2100 Expert software was used. Further data processing was carried out by Microsoft Office Excel and Origin 9.1 (*OriginLab Corporation, Northampton, MA, USA*).

For buffer filtration sterile 20 ml syringes with disposable sterile filters ((hydrophilic, 0.2 µm pore size from *Sartorius, Göttingen, Germany*) were used. CE sample preparation requires RNase free Eppendorf vials and tips (*Eppendorf, Hamburg, Germany*). An *Eppendorf Thermomixer comfort* device was used for incubation during experiments in which RNA release was induced either through increased temperature or acidification.

VWR (North America) centrifugal filters (10 kDa cut-off, modified PES, 500 µl) and the benchtop centrifuge of *Sigma, Osterode am Harz, Germany*, were used for desalting of the viral material and the liposomes.

For liposome preparation 50 ml round bottom flasks, an analytical and micro scale for lipid weighting and a desiccator for drying of the lipid layer were required.

An additional instrument to study the liposomes and their interaction with the viral material, the GEMMA instrument (*TSI Inc, Shoreview, MN, USA*), a gas-phase electrophoretic mobility molecular analyzer, was applied. The GEMMA system consists of a nano electrospray device (Nano ES; Electrospray Aerosol Generature, serial no. 3480), a nano differential mobility analyzer (DMA; Electrostatic Classifier, serial no. 3080) and an ultrafine condensation particle counter (CPC, serial no. 3015A). The determined spectra obtained from the MacroIMS software supplied by *TSI Inc (Shoreview, MN, USA)* were exported and plotted in Origin 9.1 (*OriginLab Corporation*).

2.2. Molecular beacons (MB) – Proof of principle measurements

2.2.1. Comparison of two MB preparation batches


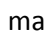
During my master thesis three different molecular beacons (MB), P12, P13 and P14, were used for detection of viral RNA release. These MBs bind specific to three different regions of the viral RNA genome of HRV-A2. For each MB two identical molecular beacon batches are available, an older one synthesized in 2014, which was already used in previous experiments at TU Wien, and a new synthesized batch from 2015, which was not used until the beginning of the present project. To evaluate these two preparations the MBs were separated electrophoretically using a capillary gel electrophoresis system, the RNA 6000 Nano Kit for *Agilent Bioanalyzer 2100*. The procedure used for comparison of the MB batches is given below.



Protocol (according to the quick guide for the RNA 6000 Nano kit from *Agilent Technologies* [50])

For sample preparation, the respective MB stock solutions (0.5 mM) were diluted in overall 1:50 (v/v) with UHQ. All further solutions were part of the RNA 6000 Nano kit and supplied by *Agilent Technologies (Waldbronn, Germany)*.

In order to prepare the chip, 10 µl of the ladder were incubate at 70 °C for 2 min for denaturation in an RNase free vial and afterwards cooled down on ice. In the next step 550 µl of RNA gel matrix was filtered through the provided spin filter in the centrifuge at 1.5×10^3 g for 10 min. Aliquots of 65 µl filtered gel were splitted to fresh 0.5 µl RNA free tubes and stored on ice.

For the Gel-Dye Mix, the RNA dye concentrate needed to equilibrate to room temperature. It was vortexed well followed by a short centrifugation step. One µl of dye was added to 65 µl of filtrated gel. The solution was mixed gently and centrifuged at 1.3×10^4 g for 10 min at room temperature.

Nine µl of Gel-Dye mix were loaded in the well marked by  (green marked well, Figure 14) and pressed into the capillary system using the *Agilent* priming station (syringe position C, base plate positioned at A). Therefore, the plunger was positioned at 1 ml. The chip priming station was closed and the plunger of the syringe was pressed down for 30 s. After 30 s the clip was released and the plunger pulls back automatically. Subsequently, in all wells marked by  (Figure 14, orange vials) 9 µl of Gel-Dye mix was loaded.

In each sample well and in the well marked by  5 µl of RNA marker was loaded. Either 1 µl of prepared ladder was added to the well marked by  (Figure 14, purple) or 1 µl of sample was added to the corresponding wells for the samples marked in blue in Figure 14. RNA marker and sample were mixed gently whereby bubbles should be avoided. The chip was placed horizontally in the chip vortexer, vortexed for 1 min at 2400 rpm and afterwards placed in the *Agilent Bioanalyzer 2100* instrument. For analysis the standard “*Eukaryote Total RNA Nano Series*” script supplied by *Agilent Technologies* was used.

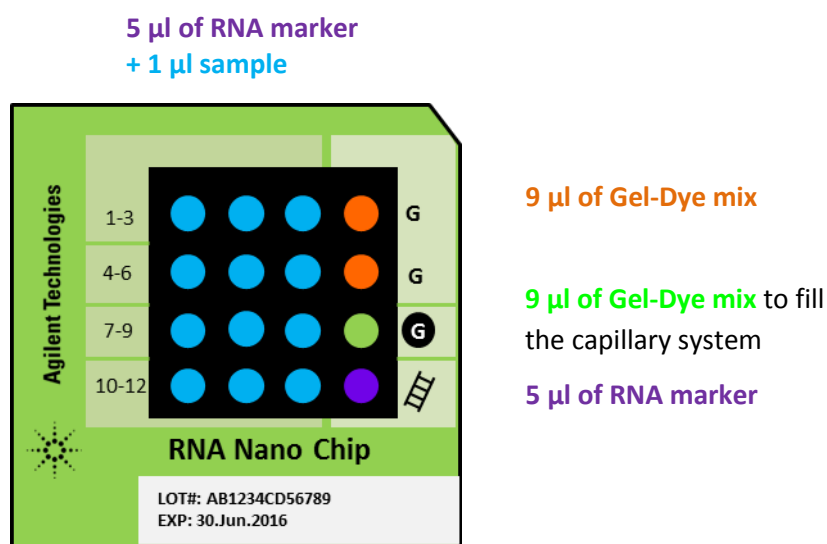


Figure 14: Loading scheme for the RNA 6000 Nano Kit Chip filled with a Gel-Dye mix as sieving solution

2.2.2. MB experiments with positive and negative control – DNA target

The reactivity of both MB batches against DNA target as positive control was tested. As negative control any unspecific DNA section can be used. The applied combinations of MBs and DNA targets are given in Table 10.

Protocol for preparation of one sample (25 µl):

First the 50 µM MB intermediate as well as the 50 µM Target intermediate were diluted 1:50 (v/v) with solution C to obtain 1 µM intermediates. The MBs 1 µM intermediate was further diluted 1:5 (v/v) with solution C, for a 200 nM intermediate that was used in the experiments. From this solution 1.0 µl was pipetted into a new RNase free Eppendorf vials and mixed with 5.0 µl corresponding DNA target (1 µM) as positive control or 5.0 µl unspecific DNA target (1 µM) as negative control. For alignment and calibration, 1.25 µl of solution D (IS2) were added, followed by 17.75 µl of solution C to obtain an end volume of 25 µl. The mixture was vortexed and incubated at ambient temperature for 5 minutes. Afterwards 6 µl of sample were loaded on a RNA Nano kit Bioanalyzer 2100 chip as described later in 2.2.2.1.

Table 10: MB incubated with positive control (specific DNA target) and negative control (unspecific DNA target) oligonucleotides

MB [nM]	DNA target as positive control [nM]	DNA target as negative control [nM]
40 nM P12	200 nM T12	200 nM T14
40 nM P13	200 nM T13	200 nM T12
40 nM P14	200 nM T14	200 nM T13

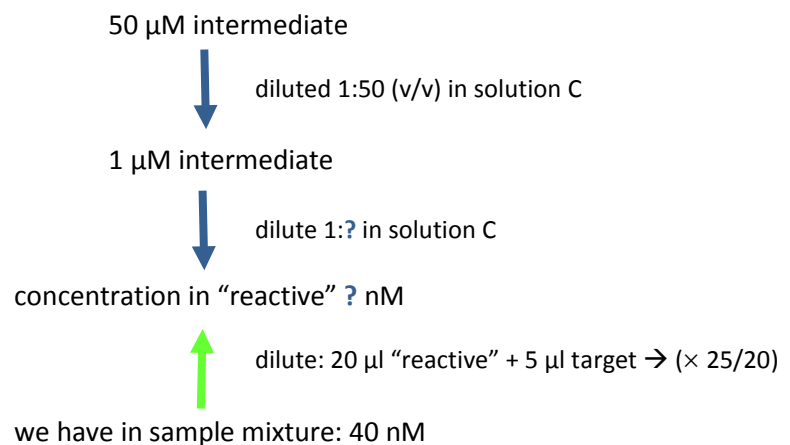
In control experiments without any target sequence, 5.0 μl of target were replaced with 5.0 μl solution B.

In order to avoid small pipetting volumes ($\leq 0.5 \mu\text{l}$) it is easier to prepare a pre- sample mixture that contains all components which are similar for more approaches. This pre-mixture is named “reactive” in following. Therefore a defined volume of MB, internal standards (IS2) and buffer were mixed in one step and distributed in samples vials afterwards. A calculation example is given below.

Calculation example- “reactive”:

The idea is to mix 20 μl “reactive” with 5 μl of target material (i.e. positive and negative control oligonucleotides, respectively, 1 μM intermediates) yielding in a solution containing 40 nM MB and 200 nM target material.

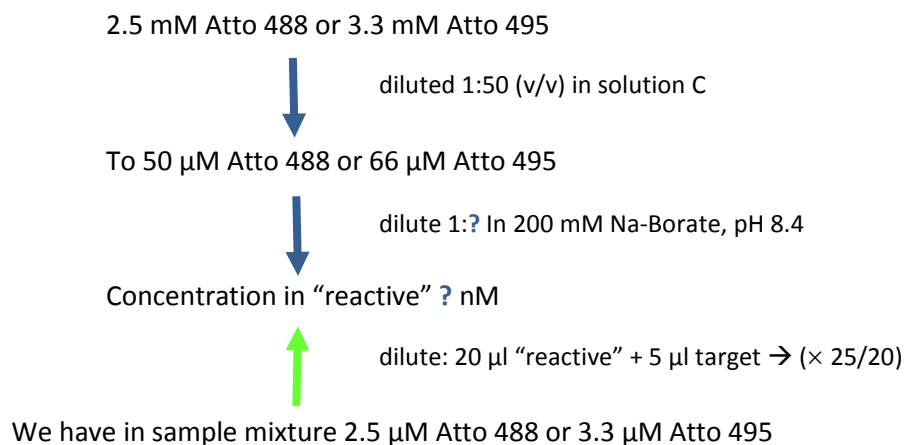
MB:



It follows that the 1 μM intermediate of the MB needed to be diluted 1:20 (v/v) in solution B ($40 \text{ nM} \times 25/20 = 50 \text{ nM}$ in “reactive”)

For comparison reasons the same calculations were also necessary for IS2 to guarantee exactly the same concentration of these internal standards in all experiments.

IS2:



It follows that the 50 µM intermediate of Atto 488 and the 66 µM intermediate of Atto 495 needs to be diluted 1:16 (v/v) in “reactive” ($25\text{ }\mu\text{M} \times 25/20 = 3.125\text{ }\mu\text{M}$ Atto 488 or $4.125\text{ }\mu\text{M}$ Atto 495 in “reactive”)

The volume of each component in “reactive” is calculated according to Equation 8

$$c_1V_1 = c_2V_2$$

Equation 8


Table 11 gives an example for the calculation of a “reactive” approach for three samples that can subsequently be incubated with different targets (e.g. positive and negative control as well as without target):

Table 11: calculation example for a „reactive“, calculated for 3 approaches

3 µl MB (1 µM) solution	
3.75 µl solution D (IS2)	
53.25 µl solution C	
<hr/>	
60.00 µl “reactive” solution	

2.2.2.1. Bioanalyzer 2100 loading procedure:

Before loading a chip to the instrument, the electrodes have to be cleaned by using a cleaning chip filled with 380 µl UHQ.

In case of using a background electrolyte instead of a sieving solution, as described below, the chip loading procedure differs from the original company-given protocol [50]. 12 µl of background electrolyte containing 10 mM Trolox (BGE) was pipetted into the well marked with **G** (green, Figure 15) of a fresh RNA 6000 Nano Chip. The BGE was pressed through the capillary system by pressing down the plunger of a 1 ml syringe in the priming station for 20 s. Therefore the plunger was positioned to the top position and the base plate to position C. After 20 s the plunger clip was released and the plunger was able to return back to the 1 ml start position. Remaining wells marked with **G** (orange, Figure 15) were filled with 12 µl of BGE while the well marked with a ladder  (purple, Figure 15) was filled with 12 µl of solution E for lens focusing. In each sample well (blue, Figure 15), 6 µl of samples were pipetted. The chip was mixed gently on the chip vortexer and placed in the Agilent Bioanalyzer 2100. After closing the lid the software *Expert2100* was employed using the modified *DNA 7500 series, Liposomes II, 1000 V, RT* script. Measurement were carried out at ambient temperature (approximately 22 °C during analysis) detecting the analytes at the cathodic end. The script is given in the Appendix A.

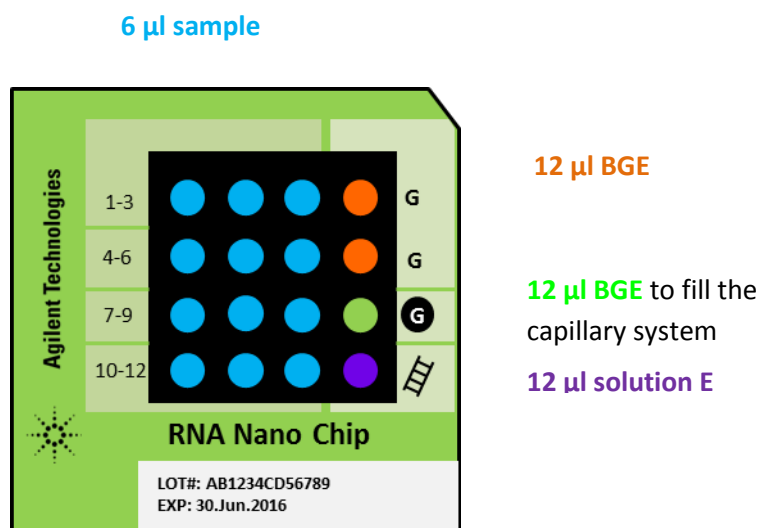


Figure 15: Loading scheme for the RNA 6000 Nano Chip filled with background electrolyte (BGE) as electrolyte

Data evaluation and peak alignment

The data was exported as .txt file and further processed in Microsoft Office Excel. Slight changes in the EOF result in a shift of electropherograms. This does not allow an exact overlay of electropherograms and hence making a peak comparison complicated. According to *Reijenga et.al* [51] an alignment of the electropherograms based on internal standards can be applied for the x axis. We employed two fluorophores, Atto 488 and Atto 495, detectable with the blue LED of the instrument and hence not interfering with analyte detection using the instruments red laser. Based on the peaks of the internal standards two correction factors for signal height were calculated and averaged for each run. This average allowed an alignment of electropherograms for the y axis. Variations in migration were corrected as described. Figure 16 gives an example for a not aligned (left) and aligned (right) overlay of four electropherograms of Atto 488 and Atto 495.

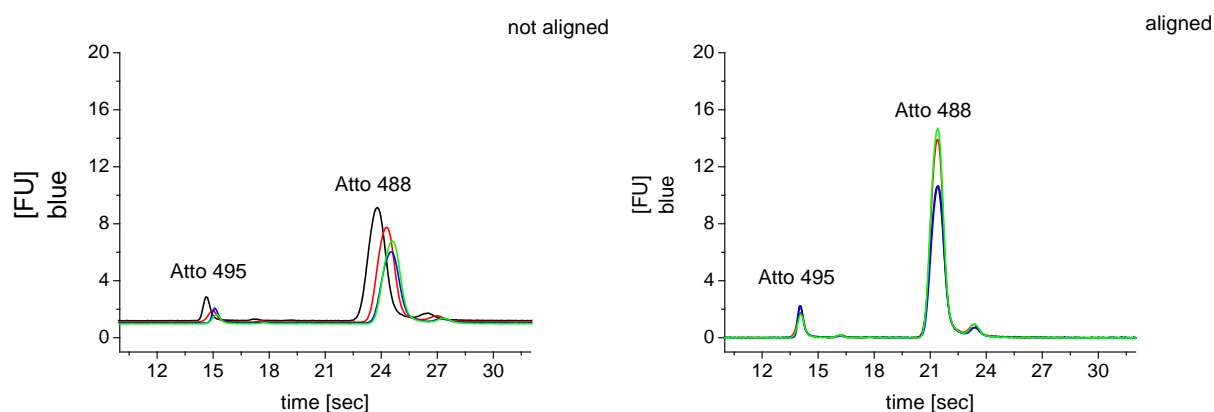


Figure 16: Comparison on a not aligned (left) and aligned (right) overlay of four electropherograms of internal standards

2.2.3. MB reactivity towards negative control - RNA ladder

Control experiments with unspecific target sequences were also done using the RNA ladder from the *Agilent RNA 6000 Nano Chip Kit*. The RNA ladder contains six RNA sequences of different length, which are randomly and hence not specific for the here used MBs. Due to the reason that the actual concentration of these RNA transcripts was not available, different volumes of the ladder were added to the MBs. Samples were incubated at ambient temperature for 5 minutes. For this the following protocol was used:

Protocol

In these experiments a pre-sample mixture named “reactive” was prepared as already described in 2.2.1. The calculated amount of each component is given in Table 12.

Table 12: sample composition for incubation of the MBs with different amounts of RNA ladder as negative control

Component	0 μ l ladder	1 μ l ladder	2 μ l ladder	3 μ l ladder
MB (1 μ M) [μ l]	0.48	0.576	0.6	0.8
IS2 [μ l]	0.6	0.72	0.75	1.0
BGE [μ l]	10.92	10.704	8.65	8.2
Σ “Reactive”	12.0	12.0	10.0	10.0
“Reactive” [μ l]	6.0	5.0	4.0	3.0
Ladder [μ l]	0.0	1.0	2.0	3.0
Σ Sample mixture [μ l]	6.0	6.0	6.0	6.0

MB, internal standards IS2 and BGE were mixed for the “reactive” that was subsequently mixed with RNA ladder material. After incubation at ambient temperature for 5 minutes 6 μ l of the sample mixture were loaded on the Bioanalyzer chip.

The ladder contains lots of constituents to stabilize the RNA. These constituents probably could also influence the behaviour of the MB and hence their reactivity towards the target sequence. The idea was to remove these additives prior to the application to the MBs. That is why the ladder was desalted with solution B using a 10 kDa spin filter membrane (*Sartorius, Göttingen, Germany*) prior introducing it to the samples. Removing these cofactors led to unstable RNA fragments and was not considered for further experiments anymore.

Chip electrophoresis, data evaluation and peak alignment were carried out as already described for the reactivity check towards a positive and negative target oligonucleotide sequence in 2.2.2.

2.2.4. Storage in different buffers

MBs were stored in 155 mM Na-Borate, 10 mM Trolox, pH 8.4, because it is already known that the vitamin D derivate Trolox increases the fluorescence signal and represses the bleaching of the fluorophore [52]. However, due to the loss of reactivity of the MB after an extended period of storage in this buffer, the buffer system had to be adapted. Therefore new 50 μ M intermediates out of the 0.5 mM stock solution of MB P14 are prepared in different buffers solutions (Table 13) and compared to the previous 50 μ M intermediate in UHQ.

Table 13: Overview of different applied buffer systems for MB and Target storage

Buffer system	50 μ M intermediate in	1 μ M intermediate in
Molecular beacon P14		
1	UHQ (already existing)	solution C
2	10 mM NH ₄ OAc	solution C
3	solution B	solution C
4	UHQ (new intermediate)	solution C
Target T14 as positive control		
a	UHQ (already existing)	solution C
b	solution B	solution C

The reactivity of 10 nM MB P14 against the corresponding positive control, 40 nM T14, was tested after different storage times. Therefore existing intermediates were compared to fresh prepared intermediates to monitor an eventual degradation/alteration of the MB. The reaction mixture is listed in following Table 14.

Table 14: Reaction mixture to monitor the stability of the MB and its reactivity towards the positive control

	Without target	With target
100 nM MB P14 [μ l]	1.25	1.25
200 nM target T14 [μ l]	0	2.5
Solution C (containing 10 mM Trolox)	10.625	8.125
Incubate @ 30 °C for 30 min		
IS2[μ l]	0.625	0.625
Sample mixture [μl]	12.5	12.5

The reactivity of the MB towards the positive control decreases significantly when storing the samples in 155 mM Na-Borate, pH 8.4 containing 10 mM Trolox. This let us assume that Trolox influences the MB decisively. Based on this knowledge Trolox was avoided in storage buffers for further experiments. To determine the optimal storage conditions for MBs at 4 °C new 50 μ M Intermediates out of the 0.5 mM stock solution (in 2 mM NH₄OAc) were again prepared in buffers without Trolox. A list of possible buffers is given in Table 15.

Table 15: Overview of possible buffers systems for long term storage of MBs without Trolox as buffer component

Buffer system	50 μ M intermediate in	1 μ M intermediate in
Molecular beacon P14		
I	UHQ (already existing)	UHQ
II	10 mM NH ₄ OAc, pH 7.15	10 mM NH ₄ OAc, pH 7.15
III	200 mM Na- Borate, pH 8.4	200 mM Na- Borate, pH 8.4
IV	UHQ (new intermediate)	UHQ
Target T14 as positive control		
A	UHQ (already existing)	UHQ
B	200 mM Na- Borate, pH 8.4	200 mM Na- Borate, pH 8.4

Again the reactivity of MB P14 was tested against the positive control in different time intervals as described in Table 16.

Table 16: Reaction mixture to monitor the stability of the MB and its reactivity towards the positive control in buffer systems without Trolox

	Without target	With target
100 nM MB P14 [μ l]	1.25	1.25
200 nM target T14 [μ l]	0	2.5
Solution B	10.625	8.125
Incubate @ 30 °C for 30 min		
IS2 [μ l]	0.625	0.625
Sample mixture [μl]	12.5	12.5

For further experiments and for the liposome preparation 200 mM Na- Borate, pH 8.4, was chosen as storage buffer for samples. The buffer containing Trolox was only used as background electrolyte directly on the chip.

2.2.5. Influence of MgCl₂ on the MB

In order to generate a cations gradient across the liposomal membrane MgCl₂ should be encapsulated in the liposomes. Mg²⁺ is suggested to have a pulling effect of the viral RNA through the membrane [53].

On the other hand, Mg²⁺ binds to the DNA and hence could influence the structure and reactivity of the MB. Due to this reason, the reactivity of the MB in presence of different amounts of this divalent cation has to be tested. In order to keep the ionic strength in the buffer system constant at 42 mM the composition of the BGE had to be adapted. The calculation of pH and ionic strength was carried out using the freeware program *Peakmaster* developed by the Department of Physical and Macromolecular Chemistry, Faculty of Science, Charles University, Prague, Czech Republic [54].

Following MgCl_2 concentrations in the buffer were considered:

Table 17: Buffer composition for different amounts of MgCl_2

Solution	[MgCl_2]	10 mM MgCl_2 [ml]	[Na- Borate] nominal	258.7 mM Na-Borate [ml]*	[NaOH] nominal	3 M NaOH [μl]	UHQ [ml]	pH
B	0 mM	0.0	200 mM	7.0	42.0 mM	0.0	3.0	8.4
L	0.1 mM	0.1	200 mM	7.0	41.75 mM	139.2	2.7608	8.4
M	0.25 mM	0.25	200 mM	7.0	41.3 mM	137.6	2.6124	8.4
N	0.5 mM	0.5	200 mM	7.0	40.5 mM	135	2.365	8.4
O	1.0 mM	1.0	200 mM	7.0	39.0 mM	130	1.870	8.4
P	2.0 mM	2.0	200 mM	7.0	36.0 mM	120	0.88	8.4

* The calculated amount of boric acid needed for 200 mM Na-Borate in 50 ml was dissolved only in 35 ml, which results in a higher concentration of 258.7 mM Na-Borate. During buffer preparation this stock solution was diluted to 200 mM Na-Borate, pH 8.4 according to Table 17.

All buffer solutions were filtrated through a sterile 0.2 μm syringe filter from *Sartorius (Göttingen, Germany)*.

MB P14 was incubated in solution L to P with the positive control DNA target to check the influence of these divalent ions on the reactivity of the MBs. It is known that divalent cations could stabilize the stem structure of the MBs and hence hamper the hybridization of the probe to the complementary sequence [53].

25 nM of MB were therefore incubated with 100 nM of the corresponding target as given in Table 18. For comparison reasons the samples were acidified to pH ~ 5.3 during incubation at 30 °C for 30 min to simulate the setup to initiate RNA release in later experiments, subsequently reneutralization with solution X (see also 2.1.2) to pH 8.4 for analysis on the CE chip was carried out.

Table 18: Pipetting scheme for the monitoring of the reactivity of MB P14 towards the positive control T14 in buffer containing MgCl_2

	Without target	With target
200 nM MB P14 in MgCl_2 buffer [μl]	3.125	3.125
1 μM target T14 in MgCl_2 buffer [μl]	0	2.5
buffer containing Na-Borate, MgCl_2 [μl]	9.875	7.375
CH_3COOH (4.5 %) or buffer [μl]	0.7	0.7
Incubate @ 30 °C for 30 min		
solution X or Z [μl]	11.3	11.3
sample mixture [μl]	25	25

These experiments were repeated for 0.0 mM, 1.0 mM and 2.0 mM MgCl_2 after one, two and four days in buffer to get an idea about the storability in MgCl_2 , and with incubation either at ambient temperature (approx. 22 °C), 30 °C or 37 °C.

2.3. Liposome preparation and characterization

2.3.1. Liposome preparations

Liposomes containing 10 mM lipid should be prepared. The chosen lipid composition of the different liposomes in physiological composition is listed in Table 18. Table 20 gives the composition of liposomes with a non-physiological constitution. A list of all liposome preparation is given in the Appendix B.

Table 19: Lipid composition for preparation of physiological liposomes, based on [3]

Lipid	Without NGS-NTA (Ni^{2+} salt)			With NGS-NTA (Ni^{2+} salt)		
	Lipid [mol%]	Lipid [mg]	Lipid _{dissolved} [μl]	Lipid [mol%]	Lipid [mg]	Lipid _{dissolved} [ml]
SOPC	22	0.867	166.7	21	0.828	159.23
SoyPE	22	0.803	48.18	21	0.767	48.18
Chicken egg SM	22	0.782	-	21	0.746	-
Cholesterol	33	0.638	-	31	0.599	-
NGS-NTA	-	-	-	5	0.264	46.588
NBD-PC	1	0.045	67.5	1	0.045	67.5

The lipid composition of the non-physiological liposomes was already known from previous experiments using liposomes and was provided by *Victor U. Weiss*.

Table 20: Lipid composition for preparation of non-physiological liposomes

Lipid	Lipid [mol%]	Lipid [mg]	Lipid _{dissolved} [μl]
HSPC	56	2.195	-
DSPE	5	0.187	-
Cholesterol	38	0.735	-
NBD-PC	1	0.045	67.5

Protocol

For liposome preparation a 50 ml round-bottom flask was pre-cleaned with solution F. Those lipids that can be handled easily on the scale (Cholesterol and chicken egg SM) were weighted in to the pre-cleaned, dried round-bottom flask, while all other lipids are added as liquid dissolved in solution F according to Table 19 or Table 20. Rotating the flask under a nitrogen flow led to evaporation of the solvents and to the production of a thin lipid film on the bottom of the flask. This lipid film had to be dried at least for 1 h in the dessicator. The flask was wrapped in aluminium foil to avoid bleaching of the fluorescence label lipid (NBD-PC) upon contact with light. The lipid film was rehydrated in 500 μl of solution B containing a defined amount of MB by vortexing the solution until a milky solution emerges. The dispersion is passed 21 times through a polycarbonate filter membrane of defined pore size to form unilamellar particles. Therefore an extruder as shown schematically in Figure 17 was

used. After extrusion a clear yellow solution of unilamellar liposomes remains that was stored in a capped vial at 4 °C in the dark.

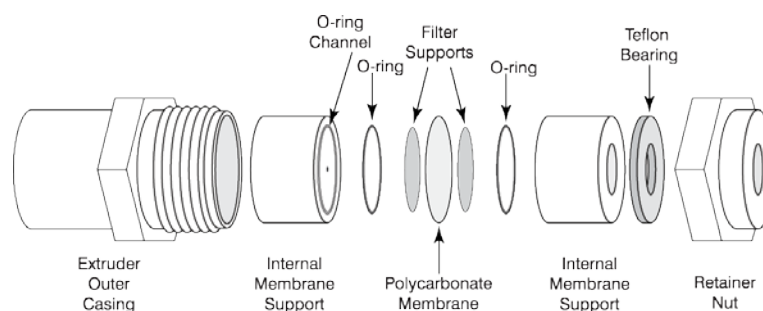


Figure 17: Scheme of the extrusion equipment, taken from [55]

Within these liposomes different MB of different concentrations - 50, 150 and 250 nM of MB P12, P13 or P14, respectively, were encapsulated. The first 10 liposomes preparations were dispersed in solution C containing 10 mM Trolox due to the reason that Trolox increases the fluorescence signal up to 3 times [52]. However because of the significant lower stability of the MB in the buffer containing Trolox, further liposomes were dispersed in solution B. As described above, the influence of $MgCl_2$ to the MBs and the viral RNA transfer was also tested. One mM $MgCl_2$ was co-encapsulated into the liposomes to generate a cations gradient across the membrane to force a transfer of viral RNA into the liposomes.

For comparison to the *in vivo* cell infection, which is strongly mediated by a receptor, an analogous system in the here present *in vitro* system was necessary. A specific recombinant receptor for HRV-A2 serotype for such a cell model system is already known [56]. The MBP-V33333 receptor carries a His6-tag on the N- terminus. This His6-tag allows a specific binding to liposomes carrying Ni^{2+} in the lipid bilayer. Therefore NGS-NTA, a Ni^{2+} complexing lipid, was introduced to the physiological lipid composition given in Table 18.

Liposomes carrying this Ni^{2+} salt in the lipid bilayer were produced either with 250 nM of MB or 250 nM of MB P14 inside.

These liposomes were passed through filter membranes with 400 nm, 200 nm and 100 nm pore size to form unilamellar particles of different sizes. Aliquots of liposome solutions for each vesicle size were drawn prior application of filters with smaller pore size. The dry particle size of the liposomes was determined via GEMMA measurements.

2.3.2. Quality control of liposomes at GEMMA

For measurement of the liposomes at the GEMMA system, the liposomes had to be previously desalted previously using a volatile electrolyte solution. Therefore 10 µl of the liposome preparation was weighed to 490 µl of solution G on a 10 kDa spin filter membrane. Desalting was done by spinning the buffer through the filter membrane at 9×10^3 g for 7 min. The permeate was removed and new buffer was added to the remaining solutions above the filter membrane. After a second spinning step the remaining supernatant was weighed out. Additionally, the filter membrane was washed with solution G and supernatant and washing solution were combined. Thereby a dilution of the liposomes of 1:25 (v/v) was reached.

Table 21: Parameter settings for GEMMA measurements of liposomes

Parameter	Setting
Detector	3025 high
Polarity	Negative
Tube length	9.6 inches
Macrolon	1.1
Sheath flow	2.5 lpm
Scan time/ retrace	150 s/ 30 s
Number of runs	1 x 4 runs
Pressure	4psid (approx.. 0.276 bar)
CO ₂	0.1 l
Air	1.0 l
Voltage	2.2 kV
Current	-300 up to -400 nA

For measurement, a 25 µm capillary was built in the GEMMA system for determination of the liposomal dry particle size. The parameter settings are given in Table 21.

Before injection of the sample, the capillary was flushed for at least 10 min with solution G and a blank was measured followed by the samples. After each sample the capillary had to be washed for 3 min with solution H containing Tween20, a detergent to remove residues of previous samples from the capillary surface. After application of the detergent the capillaries inlet and the electrode were cleaned by immersion for 1 min in buffer. The buffer aliquot was changed and the capillary flushed with solution G for at least 3 min. Before starting the measurement of a fresh sample the capillary was equilibrated for at least 3 min with sample until the measurement of four independent analyses per sample can be started.

After each measurement session, the capillary needs to be flushed for at least half an hour with solution G followed by drying of the capillary.

Data evaluation of GEMMA measurements

Raw data obtained from the GEMMA instruments *MacroIMS* software were exported as .txt files and further processed using Microsoft Office Excel. Four measurements were performed per sample. The median of these four repeated measurements was calculated. Using Origin 9.1 (*OriginLab Corporation, Northampton, MA, USA*) the electrophoretic mobility (EM) diameter was plotted against the particle counts per detector channel.

2.3.3. Liposomes at Bioanalyzer 2100

Additionally, the liposomes are analysed on the Bioanalyzer 2100 system. Therefore different concentrations of the liposomes were loaded on the chip to determine the lowest possible concentration of liposomes that can be detected. For detection of liposomes independently from the encapsulated MB, a fluorescence labeled lipid, NBD-PC, was integrated in the lipid bilayer. For each concentration again a “reactive” mixture was prepared to minimize sample preparation time and to avoid systematic errors. An example for such pipetting scheme is given in Table 21.

Table 22: Pipetting scheme for the determination of the lowest possible fluorescence signal of the liposomes that can be detected at the Bioanalyzer 2100 system

Component	Liposome dilution (v/v)					
	1:2	1:5	1:10	1:20	1:30	1:40
BGE [μl]	9.0	15.0	17.0	18.0	18.335	18.5
IS2 [μl]	1.0	1.0	1.0	1.0	1.0	1.0
Σ “Reactive” [μl]	10.0	16.0	18.0	19.0	19.335	19.5
Liposome [μl]	3.5	1.25	0.75	0.5	0.5	0.5
“Reactive” [μl]	3.5	6.0	6.75	9.5	14.5	19.5
Σ Sample mixture [μl]	7	7.25	7.5	10.0	15.0	20.0

The volume of MBs and IS2 for “reactive” was calculated as described above in 2.2.1 , but here the individual dilution factors of the liposomes were considered.

2.3.3.1. Reactivity of the MB outside of the liposome

In the next step the reactivity of the MB outside of the liposomes had to be checked after the liposome preparation procedure. Therefore, liposomes were diluted 1:10 (v/v) in solution B and incubated with 100 nM Target. This yielded samples containing 1 mM lipid, 250 nM MB inside and 25 nM MB outside liposomes. The latter probes should react to 100 nM target.

Protocol:

The prepared liposomes had to equilibrate to ambient temperature and vortexed properly. A volume of 2.5 µl of liposome were pipetted in an RNase free Eppendorf vial and mixed with 2.5 µl of the corresponding DNA target (1 µM) or with 2.5 µl of an unspecific target. To each sample 1.25 µl of solution D (IS2) and 18.75 µl of solution B were added to reach a final volume of 25 µl. The sample mixture was vortexed gently and incubated for 5 min at ambient temperature (approx. 22 °C). 6 µl of the sample were loaded on the Bioanalyzer chip as already described in 2.2.2.1.

For comparison reason the liposomes were incubated with the positive control also at acidified conditions. Therefore, the following procedure was used.

Procedure in case of acidification:

Again 2.5 µl liposome were pipetted in an RNase free Eppendorf vial and mixed with 2.5 µl corresponding DNA target (1 µM) for positive control or 2.5 µl unspecific DNA target (1 µM) for negative control. Afterwards, 8.0 µl solution B to achieve a volume of 13.0 µl, was added. The samples that should be compared to later experiments, whereby RNA release from virions is triggered by acidification, were mixed with 0.7 µl of solution K. 0.7 µl of solution B were added to the non-acidified control experiments. The samples were mixed gently and incubated at 30 °C for 30 min. Afterwards the samples were cooled down on ice and neutralized with 11.3 µl of solution X containing sodium hydroxide (defined in 2.1.2) for acidified samples or 11.3 µl of solution Z (defined in 2.1.2) for the non-acidified samples. The samples were vortexed and 6 µl were loaded on the Bioanalyzer chip.

The reactivity check of the MB outside of the liposomes allows a quick and simple testing of the quality of the MB probes after a certain storage time and after the whole procedure of liposome preparation including the extrusion step.

2.4. Biological Material

2.4.1. HRV-A2 virus desalting

The HRV-A2 preparations provided by the research group of *Dieter Blaas* at *MFPL (Max F. Perutz Laboratories, Medical University of Vienna; Vienna, Austria)* were stored either in 50 mM Tris Buffer, pH 7.4, or in 50 mM HEPES Buffer, pH 7.4. Both buffers contain a high amount of salts that could influence the viral release and the analysis at the Bioanalyzer 2100 system. Hence, the virus preparations needed to be desalted. Desalting was carried out for a virus aliquot prior a respective RNA release experiment.

Aliquots of the virus preparations were desalted with solution B using spin filter membranes (10 kDa cut off). During desalting, a dilution of the virus has to be calculated in order to obtain a stock solution for further experiments. The working procedure is given here:

First, the calculated volume of HRV-A2 for the planned experiment was weighed to a spin filter containing solution B (complete volume should be 500 µl). Centrifugation at 9×10^3 g for 7 min led to permeation of the buffer through the filter membrane while the biological material remained in the supernatant. Only a small amount of the supernatant should remain above the filter, otherwise the spinning step needs to be repeated. The permeate was removed and the filter was filled up with solution B to 500 µl. During the followed incubation step at 37 °C for 10 min in the Thermomixer a buffer exchange through pores in the viral capsid should take place. Afterwards the viral sample was cooled down on ice and centrifuged again at 9×10^3 g for 7 min. The desalted and diluted virus was weighed out into a new RNase free Eppendorf vial. The filter membrane was washed with solution B and the washing solution was also added to the desalted virus. Thereby, the maximal volume to achieve the calculated viral concentration for subsequent experiment should not be exceeded.

The release of RNA out of the viral capsid was detected using MBs and the Bioanalyzer 2100 system. The first two considered virus preparations from *MFPL* were not CIM purified, which means an until now undefined contaminant was not separated from the virus itself and might influence the behaviour of the viral RNA release. In contrast, more recent virus preparations are additionally CIM purified. As CIM purification works with buffers containing high amounts of salts, the incubation step at 37 °C for 10 min during desalting was necessary to remove the high amount of salts inside the virus capsid, which would probably inhibit the unfolding of the viral RNA structure. Consequently, the release of the genetic material and an interaction of the MB with the RNA would not be possible or strongly influenced.

2.4.2. MBP-V33333 receptor desalting

The provided MBP-V33333 receptor from *MFPL* was supplied in TBSC buffer (25 mM Tris-HCl pH 8.5, 150 mM NaCl, 2 mM CaCl_2) containing imidazole [56]. Potentially the presence of imidazole could influence the binding of the His₆-tag of the recombinant receptor to the Ni^{2+} in the liposomal membrane. Furthermore any cross reactions between the two buffer systems, TBSC buffer from the

receptor material and Na-Borate from the Bioanalyzer setup, could be avoided in case of an buffer exchange of the receptor material. Due to these reasons some experiments were also performed with desalted receptor aliquots. Desalting was carried out by the same procedure as described above for the virus in 2.4.1. An incubation step at 37 °C was not necessary due to the fact that the receptor is not coated by a capsid that needs to be penetrated by the buffer. The receptor material should not be diluted in the desalting step because of the low concentration in the stock solution and the high concentration needed in subsequent experiments.

2.5. RNA release into solution

2.5.1. RNA release into solution

In the next step the HRV-A2 virus RNA release into solution and in further consequence to liposomes was monitored by application of MBs. Additionally HRV-B14, a major type group virus, was introduced as negative control for the applied MBs.

RNA release of the viral capsid of HRV-A2 as well as HRV-B14 was either triggered by heating the sample to 56 °C for 15 min or by acidification of the sample to a pH lower than 5.6 to mimic the *in vivo* system in the early endosomes. Therefore the following procedures were carried out:

2.5.1.1. RNA release triggered through temperature increase

RNA release into solution triggered through temperature increase was monitored via MB P14 at least for each HRV preparation as pre-experiment to check for presence of detectable viral RNA.

Protocol

In case of RNA release triggered by heating the samples to 56 °C, 1.52 µl HRV-A2 or HRV-B14, respectively, needed to be desalted with solution B according to the procedure described above in 2.4.1. An amount of 22.75 µl of desalted and diluted HRV-A2 was pipetted into a new RNase free Eppendorf vial and mixed with of 1 µl MB (1 µM Intermediate). The samples were incubated at 56 °C for 15 min for RNA release followed by cooling on ice. Control experiments omitted the heating step; samples were incubated only on ice instead. Afterwards, the samples were centrifuged. 1.25 µl of solution D (IS2) were added to each sample for alignment of the electropherograms after analysis and the samples were mixed well. 6 µl of each sample mixture were loaded on the Bioanalyzer chip (see also 2.2.2.1)

2.5.1.2. RNA release triggered through acidification

RNA release into solution triggering by acidification was not carried out for each HRV-A2 preparation and each MB in order to save biological material for the RNA release into the liposomes. The used protocol for the RNA release into solution is given here.

Protocol

For the experiments in which RNA release was triggered by acidification to simulate the endosomal environment in the *in vivo* system, a defined and previous calculated amount of HRV-A2 needed to be desalted with solution B according to the protocol described in 2.4.1. A defined volume of desalted virus was pipetted in a new fresh RNase free Eppendorf vial and mixed with 3.125 µl of 200 nM MB intermediate. Solution B was added to reach a final volume of 13 µl that was acidified with 0.7 µl solution K to pH ~ 5.3 for RNA release triggering. The equal amount of solution B was added instead of acetic acid to the non-acidified control samples. The samples were vortexed and incubated at 30 °C for 30 min in the Thermomixer. After cooling down the samples on ice 11.3 µl of solution X containing sodium hydroxide (defined in 2.1.2) was added to the acidified samples and 11.3 µl of solution Z (defined in 2.1.2) to the non-acidified samples. After mixing all the samples, 6 µl were loaded on the Bioanalyzer chip as described in 2.2.2.1.

Data evaluation and peak alignment was carried out as described in 2.2.2.

2.6.RNA release into the liposomes

2.6.1. RNA release triggered through acidification

The key experiments of my thesis should be the monitoring of the viral RNA release out of the capsid and into the liposomes. Therefore liposomes carrying a Ni^{2+} salt, which allows a recombinant MBP-V33333 receptor to bind to the liposomes, liposomes without this possibility and even liposomes with 1 mM MgCl_2 (buffer solution O) inside to generate a cations gradient across the membrane were used.

According to the determined dry particle size of the liposomes, the employed lipid concentration and an approximately area cross-section of around 0.54 nm^2 per lipid, a ratio of liposome to virus of 1:2 was calculated based on amount of vesicles and hence their provided surface. The lowest concentration of liposome that can be detected on the Bioanalyzer system was predefined at a dilution of 1:10 (v/v) in the sample mixture. Based on this information the virus concentration was calculated. Desalted viral material was incubated with liposomes. The RNA release out of the viral capsid was triggered by acidification of the samples to a pH of approximately 5.3. The working protocols are given below.

Liposomes without receptor

A defined amount of HRV-A2 needed to be desalted with solution B according to the procedure described above in 2.4.1.

Using RNase free Eppendorf vials, 2.5 μl of the liposome preparation were mixed with the previous calculated amount of desalted and diluted HRV-A2. For control experiments without viral material, the same amount was replaced by an equal volume of solution B. The sample was adjusted to 13 μl with solution B. RNA release was triggered by mixing the sample with solution K, while those samples without RNA release triggering were mixed with 0.7 μl of solution B. The samples were vortexed gently and incubated at 30 °C for 30 min. After cooling down on ice and spinning down the samples in the vial 11.3 μl of solution X (for components see also 2.1.2) was added to acidified sample and 11.3 μl solution Z was added to the non-acidified sample. Again, the samples needed to be mixed and 6 μl of the sample were loaded on the Bioanalyzer chip. Loading procedure as well as data evaluation and peak alignment is described in 2.2.2.1.

Liposome with MBP-V33333 receptor

In case of introduction of a specific receptor to the liposome-virus sample, a previous incubation step of the liposome containing the Ni-complexing lipid and the receptor material was necessary.

Therefore 2.5 μl of liposome was pipetted in a fresh RNase free Eppendorf vial and mixed with 0.37 μl of receptor (35 μM). This mixture was incubated at 30 °C for 5 min and afterwards cooled down on ice to allow the binding of the receptor to the liposome to form a cell model. Further steps were as

described in the experiments without receptor, which means desalted virus was added, the sample volume was brought to 13.0 µl, followed by acidification of the sample with solution K and incubation at 30 °C for 30 min. Afterwards the acidified samples were reneutralized with solution X containing the internal standards for the alignment of the electropherograms and sodium hydroxide.

At least two analyses per sample were performed at the Bioanalyzer system for each sample prepared. Between the analyses samples were stored on ice in the dark.

To obtain an even higher repetition rate, the samples were recovered from the chip after the analysis and loaded on a new RNA chip for further measurements after storage at – 20 °C. However, as shown in later measurements degradation of the viral material took place. Hence, these latter data could not be considered.

2.6.2. Benzonase digest of the free RNA

For control experiments the free released RNA as well as the MB outside the liposomes were digested with endonuclease Benzonase. Therefore, 6 µl of sample mixture recovered from the Bioanalyzer chip were digested with 0.2 µl of Benzonase of *Sigma Aldrich, Steinheim Germany*, at 30 °C for 2 hours mixing on the Thermomixer at 8×10^2 rpm and afterwards analysed on the Bioanalyzer system.

2.7. Study of the interaction between liposome, receptor and viral capsid

Additionally, the interaction of the Ni^{2+} - carrying lipid with the receptor and consequently with the viral capsid was studied on the GEMMA instrument. Therefore liposome preparations #26 and #27 (see Appenix B) were diluted 1:10 (v/v) in solution B containing 1 μM of MBP-V33333 receptor. The samples were incubated for 5 min at 30 °C. Afterwards the liposome-receptor complex was desalted with solution G as described in 2.3.2. For the study of the interaction of the liposome with the receptor material a 1:25 (v/v) dilution in solution G was required.

In case of introducing the virus to the liposome, a dilution of the liposome-receptor complex of 1:12.5 (v/v) was achieved. Subsequently, an equal volume of already desalted HRV-A2 in solution G was added to the liposome-receptor mixture yielding in a 1:25 (v/v) dilution of the liposome. The samples were analyzed on the GEMMA instrument as described in 2.3.2.

3. Results and Discussion

This section is separated into three subsections – the viral RNA release into solution, the liposome preparation and their quality control and the viral RNA release into liposomes.

3.1. RNA release into solution

First experiments I carried out during my master thesis dealt with release of viral RNA into solution in order to collect experimental experience with the different analytes of interest and the used oligonucleotides. With some of these experiments I was able to contribute to the manuscript “*In vitro RNA release from a human rhinovirus monitored by means of molecular beacons and chip electrophoresis*” published in *Analytical and Bioanalytical Chemistry* in April 2016 (V.U.Weiss et al.) as Paper in Forefront (selected by the journal editor) [52].

Here a short summary of the manuscript is given:

The aim of the work was to design a fast and sensitive method to detect viral RNA on a chip capillary electrophoresis system in combination with molecular beacons. Thereby, *in vitro* RNA release from the human rhinovirus into solution was monitored using MB P14.

MB P14 was especially designed to bind near the 3' end of the viral RNA of HRV-A2 serotype. The sequence of this probe (tcgcaCAAAGCAAATCATACGGAGGGATGcga) form a helix-like stem carrying Atto 633 as fluorophore and a Iowa Black RQ-Sp quencher to keep the fluorescence signal low as long as fluorophore and quencher are in close proximity. The specificity of the MB towards a perfectly complementary sequence was tested by applying an especially synthesized single-stranded DNA target that includes eight additional nucleotides, which are identical to the viral genome of HRV-A2 on each end of the complementary sequence to the MB. The MB was incubated with different amounts of positive control at 30 °C for 30 min. Hybridization of the MB resulting in the opening of the stem structure was detected on the *Agilent* Bioanalyzer 2100 system. It was shown that increasing target concentrations led to an increase of the fluorescence signal. Incubation of the MB with any irrelevant region of the viral genome or with an RNA ladder containing six sequences of various lengths led to no measurable interaction of the MB with the target.

One step further, the MB was introduced to the HRV-A2 genome. For this purpose the RNA release was triggered by heating the sample to 56 °C for 15 min. Introducing a desalting step of the viral preparation prior to the RNA release was found beneficial for the fluorescence signal in case of MBs hybridisation to the released RNA.

We were able to show that the synthesized MB is able to bind specifically to the released RNA of HRV-A2 serotype of the common cold virus. Implementation of the desalting procedure before initiating viral RNA release through increased temperature showed clearer signals of the MB-RNA complex than without buffer exchange.

HRV-B14, belonging to the group of major type viruses, was applied to the MB as a negative control. RNA release was also triggered by heating the sample to 56 °C for 15 min. No interaction of the MB with the viral genome of HRV-B14 serotype was detected.

Moreover, it was shown that addition of Trolox (6-hydroxy-2,5,7,8-tetramethylchorman-2-carboxylic acid) to the BGE increases the fluorescence yield by up to a factor of three. On the other hand Trolox in BGE is mainly influencing the storability of the MBs. Hence, the reactivity of the probes towards the viral RNA decreases significantly over a period of storage for more than one day. Therefore, samples in Trolox buffer have to be analysed within one day.

My direct contribution to this manuscript was:

- the study the reactivity of the MBs towards the RNA ladder provided by *Agilent Technologies (Waldbronn, Germany)*
- the study regarding the influence of heating the MBs to 56 °C for 15 min
- the study of viral RNA release into solution through increased temperature of HRV-A2 preparation D (see ESM S1 of the attached manuscript [52])
- the study of viral RNA release into solution through increased temperature of HRV-B14 as negative control

Experiments which I have carried out during my thesis exceeding these results are given after the published manuscript in following sections. They concern the pre-experiments concerning the behaviour of the two MB batches towards controls, the storability of the MBs in different buffers and in buffer containing MgCl₂ as well as the reactivity of MB P12 and MB P13 towards the RNA release of HRV-A2 in solution. Furthermore, results regarding the liposomes on the GEMMA instrument and on the Bioanalyzer system are discussed. Finally the monitoring of the viral RNA transfer into the liposomes is discussed in details for different liposomes.

In vitro RNA release from a human rhinovirus monitored by means of a molecular beacon and chip electrophoresis

Victor U. Weiss¹ · Christina Bliem¹ · Irene Gösler² · Sofiya Fedosyuk² · Martin Kratzmeier³ · Dieter Blaas² · Günter Allmaier¹

Received: 28 December 2015 / Revised: 19 February 2016 / Accepted: 1 March 2016
© The Author(s) 2016. This article is published with open access at Springerlink.com

Abstract Liquid-phase electrophoresis either in the classical capillary format or miniaturized (chip CE) is a valuable tool for quality control of virus preparations and for targeting questions related to conformational changes of viruses during infection. We present an in vitro assay to follow the release of the RNA genome from a human rhinovirus (common cold virus) by using a molecular beacon (MB) and chip CE. The MB, a probe that becomes fluorescent upon hybridization to a complementary sequence, was designed to bind close to the 3' end of the viral genome. Addition of Trolox (6-hydroxy-2,5,7,8-tetramethylchroman-2-carboxylic acid), a well-known additive for reduction of bleaching and blinking of fluorophores in fluorescence microscopy, to the background electrolyte increased the sensitivity of our chip CE set-up. Hence, a fast, sensitive and straightforward method for the detection of viral RNA is introduced. Additionally, challenges of our assay will be discussed. In particular, we found that (i) desalting of virus preparations prior to analysis increased the recorded signal and (ii) the MB–RNA complex signal decreased with the time of virus storage at –70 °C. This suggests that 3'-proximal sequences of the viral

RNA, if not the whole genome, underwent degradation during storage and/or freezing and thawing. In summary, we demonstrate, for two independent virus batches, that chip electrophoresis can be used to monitor MB hybridization to RNA released upon incubation of the native virus at 56 °C.

Keywords Virus · Electrophoresis · Molecular beacon · Fluorescence · RNA uncoating

Introduction

Human rhinoviruses (HRVs) are non-enveloped, icosahedral particles of approx. 30 nm diameter [1, 2]. They are composed of four viral proteins (VP1–VP4), 60 copies each, forming the virus capsid, and a single-stranded, positive sense RNA genome of approx. 7.1 kb covalently linked to the approx. 20 amino acid residue peptide VPg at the 5' end. The 3' end carries a poly-(A) tail [3]. To date, more than 160 serotypes have been characterized with respect to their genome sequence. On top of the phylogenetic classification into species A, B and C, the first two have also been divided into a minor and a major receptor group [4]. Minor group viruses bind members of the low density lipoprotein receptor (LDLR) family and major group viruses bind intercellular adhesion molecule 1 (ICAM1) for cell entry. In the current work HRV serotype 2 (HRV-A2), a minor group prototype strain, was used.

Upon binding its receptor on the plasma membrane of the host cell, HRV-A2 is taken up into endosomes where the acidic pH induces structural changes culminating in the release of the viral RNA genome that is supposedly shuttled across the endosomal membrane into the cytosol in a process termed virus uncoating. There, it is translated into a polyprotein that undergoes proteolytic cleavages resulting in the structural and the non-structural proteins responsible for replication [4].

Electronic supplementary material The online version of this article (doi:10.1007/s00216-016-9459-2) contains supplementary material, which is available to authorized users.

✉ Günter Allmaier
guenter.allmaier@tuwien.ac.at

¹ Institute of Chemical Technologies and Analytics, Vienna University of Technology (TU Wien), Getreidemarkt 9/164, 1060 Vienna, Austria

² Department of Medical Biochemistry, Medical University of Vienna, Vienna Biocenter, Dr. Bohr-Gasse 9, 1030 Vienna, Austria

³ Agilent Technologies, Hewlett-Packard-Straße 8, 76337 Waldbronn, Germany

Subviral particles in which the RNA genome is prepared for release from the protective, proteinaceous viral shell can also be obtained *in vitro* and have been extensively characterized [5, 6]; in the process of virus uncoating native virions (composed of VP1 through VP4 and RNA/VPg and sedimenting at 150S) first release VP4 and expose amino-terminal sequences of VP1. Resulting subviral A particles composed of VP1 through VP3 and RNA/VPg sediment at 135S. In a second step, the viral RNA (with the attached VPg) is released and empty capsids (particles sedimenting at 80S) are obtained [5]. *In vitro*, the alteration of HRV-A2 can either be triggered by acidification ($\text{pH} \leq 5.8$), which mimics the *in vivo* situation in endosomes, or by heating (≥ 10 min to ≥ 56 °C) [7]. Depending on the concentration of divalent cations, subviral A particles or empty viral capsids are formed [8, 9]. Several orthogonal analytical methods like sucrose density centrifugation (e.g. ref. [5]), transmission electron microscopy [10], nano electrospray gas-phase electrophoretic mobility molecular analysis (nES GEMMA) [2, 11] and capillary electrophoresis (CE) [7, 8, 12, 13] have been employed in their characterization. Fluorescence (FL) labelling of the virus capsid with *N*-hydroxysuccinimide-activated dyes targeting primary amines i.e. mainly lysine residues on the virus surface [14] or non-covalent labelling of the RNA genome [15] or both [16] allowed detection of virus particles with high sensitivity.

Furthermore, in a series of publications we reported the electrophoretic analysis of fluorescently labelled HRV-A2 in the chip format [17, 18]. We employed a commercially available instrument (Agilent 2100 Bioanalyzer) equipped with simultaneous FL detection at two wavelengths ($\lambda_{\text{ex/em}} = 470/525$ and $635/685$ nm, respectively) and chips from soda-lime glass in the absence of any sieving material and in the presence of electroosmosis. Other than classical CE in the capillary format, chip electrophoresis allowed analysis within less than 2 min (including electrophoretic sample injection). Additionally, electrophoresis of virions in the capillary format required the presence of detergents to avoid unreproducible spikes from particle aggregation [13]. Upon application of chips for electrophoresis owing to (i) differences in the supporting material (soda-lime glass instead of fused silica) and (ii) the short separation distance, as well as (iii) the FL labelling of virus particles, electrophoresis of virions in the absence of detergents could be achieved. This was a necessary prerequisite to target processes occurring early in infection by using an *in vitro* model in which the inner endosomal membrane was mimicked by the lipid membrane of liposomes (vesicles consisting of a lipid bilayer enclosing an aqueous lumen). The possibility (i) to follow the attachment of virions to liposomes [19, 20] and (ii) to detect changes in liposome membrane permeability upon virus uncoating [21, 22] by means of chip electrophoresis have been demonstrated. On the other hand, transfer of the viral RNA genome through this vesicle membrane was assessed via encapsulation of reverse

transcriptase in the lumen of liposomes. The released viral RNA served as a template for cDNA synthesis inside vesicles followed by subsequent amplification by PCR and detection via agarose gel electrophoresis [22].

In the current manuscript, we now demonstrate that the combination of molecular beacons (MBs) with chip electrophoresis is also suitable to assess the *in vitro* release of viral RNA into an aqueous buffer (see Electronic Supplementary Material (ESM) Fig. S1 for a schematic of the study outline). MBs, short, single-stranded oligonucleotides, carry a fluorophore/quencher pair at their respective ends. Under favourable conditions (e.g. the ionic strength, *I*, of a corresponding buffer), sequences at the 3' and 5' ends of the MB form a short helix structure (stem) leading to spatial proximity between the fluorophore/quencher pair (closed hairpin) and no FL is recorded. Hybridization of nucleotides not involved in stem formation (i.e. the loop) to a complementary target sequence results in loss of the stem helix structure and hence to an increase in FL (open hairpin) [23].

To date several publications describe the application of MBs for virus genome detection e.g. as FL probes in living cells [24, 25]. Su et al. [26] recently introduced a microfluidic approach to detect fish pathogens via MBs and magnetic beads. In the current manuscript we demonstrate the specific detection of viral RNA by a fast and easy-to-handle chip electrophoresis method. With this we set the stage for a more detailed analysis of the release of the HRV-A2 RNA genome from the protective virus capsid by using MBs. We expect this analytical method to help in obtaining a more detailed view of how the viral RNA genome that is tightly packed inside the viral shell passes through a small orifice in the subviral capsid during infection. The current hypothesis suggests RNA release in the form of a completely unfolded single strand implying that nucleotide sequences along the genome must become available for hybridization in a time-dependent manner from the 3' towards the 5' end; by using a set of suitable MBs, such analyses might become possible with the methodology described in the present report.

Materials and methods

Chemicals and reagents

Boric acid and DMSO (both pro analysis) were obtained from Fluka (Steinheim, Germany) and sodium hydroxide (≥ 99 %) from Merck (Darmstadt, Germany). Atto 488, Atto 495 and Atto 633 were from Atto Tec (Siegen, Germany). The three individual fluorophore molecules were dissolved in DMSO (at 2.5, 3.3 and 2.5 mM, respectively) and further diluted as described below. Trolox (6-hydroxy-2,5,7,8-tetramethylchroman-2-carboxylic acid) and Benzonase nuclease (ultrapure grade) were purchased from Sigma Aldrich (Steinheim, Germany). Water

(18.2 M Ω cm resistivity at 25 °C) was from a Millipore (Billerica, MA, USA) apparatus.

Biological material

HRV-A2 was prepared and its infectivity was assessed as described [27]. The 50 % tissue culture infectious dose (TCID₅₀/mL) of preparations was typically between 10¹⁰ and 10¹¹ infectious units per mL (refer to ESM Fig. S2 summarizing the data of the virus preparations used). The concentration of virus particles was obtained from nES GEMMA measurements [2, 11, 28] yielding virus peak heights. Comparison of these values to the nES GEMMA peak height obtained for an HRV-A2 preparation whose concentration had previously been measured by CE [27] and taking sample dilution into account enabled us to calculate virus concentrations of all employed batches. It is of note that lipase-treated virus preparations [11] still contained low but detectable amounts of so far unidentified contaminating material. Therefore, it has to be concluded that the purity of HRV-A2 preparations is dependent (i) on the original amount of this contaminating material (prior to lipase digestion) and (ii) on the activity of lipase which differs between enzyme batches. HRV-A2 quality control either via nES GEMMA or TEM [27] thus appears to be necessary to check whether the purity of a given preparation is sufficient for a particular experiment. HRV-B14, another rhinovirus strain, was prepared as above and employed at 2 mg/ml (3.65 × 10¹¹ TCID₅₀/mL) in 50 mM Tris, pH 7.4 as a negative control for the specificity of the MB.

Oligonucleotides were obtained from Integrated DNA Technologies (Leuven, Belgium). The MB (Atto 633 - tcgcaCAAAAGCAAATCATA CGGAGGGATGcga - Iowa Black RQ-Sp quencher) targets a region close to the 3' end of the HRV-A2 genome (nucleotides 7017–7041, see ESM Fig. S3 for the position of complementarity on the viral RNA genome [29]). Uppercase letters are bases complementary to the viral RNA. MB nucleotides were modified with locked nucleotides (LNAs, in bold and italics). Care was exercised to exclude intramolecular recognition of LNAs. An oligonucleotide complementary to the MB (with eight additional nucleotides identical to the viral genome at each end) was employed as positive, single-stranded DNA (ssDNA) control for MB binding. An oligonucleotide of the same length but with a sequence of a different region of the viral RNA was employed as a negative ssDNA control. ssDNA controls did not contain LNA. The MB and controls were purified by HPLC and lyophilised. They were dissolved in 2 mM ammonium acetate, pH 7.2 to yield 0.5 mM stock solutions (based on the amounts specified by the manufacturer). Aliquots were kept at −20 °C. The MB stock solution was subsequently diluted for preparation of samples used in experiments as specified below. It is of note that the MB in the presence of Trolox suffered an alteration over time that

impacted on its FL output. The long-term storage of the MB in background electrolyte (BGE) solutions containing Trolox was therefore avoided (unpublished data). When contact of MB with Trolox was limited to a sample preparation step on the day of measurement, no such alteration was observed.

As an additional control to exclude unspecific binding, MB was incubated with RNAs of irrelevant sequence (RNA ladder from Agilent Technologies, Waldbronn, Germany, a mixture of six RNAs of lengths between 0.2 and 6 kb at a total concentration of 150 ng/μL in 0.1 mM EDTA). ESM Fig. S4 depicts the corresponding electropherogram for such a ladder sample obtained from a standard chip gel electrophoresis set-up.

Instrumentation

Chip electrophoresis was carried out on an Agilent 2100 Bioanalyzer instrument in the presence of electroosmosis employing commercially available, single-use chips [17, 18]. Modifications of the script (software of the instrument) allowed electrophoresis of samples at ambient temperature (typically $T = 22.5 \pm 0.3$ °C). Sodium borate, pH 8.5, with and without Trolox as indicated (total ionic strength, I , was kept constant at approx. 40 mM) was employed as BGE and sample buffer (SB). Sodium borate was filtered (0.2 μm pore size, surfactant-free cellulose acetate membranes from Sartorius, Göttingen, Germany). Analyte detection was simultaneously at two wavelengths ($\lambda_{\text{ex/em}} = 470/525$ and 635/685 nm). The instrument optics was adjusted to the position of a respective single-use chip inside the instrument after electrophoretic flushing of the separation channel with 100 nM Atto 633 in BGE. Subsequently, the fluorophore was removed from the separation channel via electrophoresis.

Sample preparation

Samples contained MB at 40 nM as well as Atto 488 (2.5 μM) and Atto 495 (3.3 μM) as internal standards. Positive control ssDNA target concentrations of up to 400 nM and negative control ssDNA target concentrations of 200 nM were employed as indicated in the respective figures. When RNA ladder was used as negative control, 6 ng/μL was employed (yielding a comparable molar concentration of the RNA and DNA controls). Samples were incubated at 30 °C for 30 min at 800 rpm employing an Eppendorf Thermomixer instrument to check for MB reactivity employing control oligonucleotides. Subsequently, samples were cooled and stored on ice until analysis on the same day. For detection of the RNA released from HRV-A2, the control nucleotides were substituted by HRV-A2. The virus was either directly diluted in BGE or employed after additional removal of low molecular weight components followed by such a dilution step. In both cases, the dilution factor of virus stock was 1:15 (v/v). Removal of low molecular weight

sample components was carried out as described elsewhere [30] employing polyethersulfone membrane filters with a 10-kDa molecular weight cutoff (VWR, Vienna, Austria). The final virus concentration was around 80 nM with an infectivity of 2.8×10^{10} TCID₅₀/mL (overall dilution of HRV-A2 preparation A of 1:16.7 (v/v); for a list of all employed HRV-A2 preparations refer to ESM Fig. S2). Samples were heated for 15 min to 56 °C (800 rpm, Eppendorf Thermomixer) to trigger RNA release. Subsequently, samples were cooled on ice to allow for MB binding and subjected to chip electrophoresis. Negative controls (i) omitted the heating step or (ii) replaced HRV-A2 by HRV-B14, whose RNA sequence has no regions complementary to the MB. (iii) The impact of 15 min heating to 56 °C on MBs was assessed, too.

Data evaluation

Raw data were exported from the Agilent 2100 Bioanalyzer software. For inter- and intrachip comparability, electropherograms were adjusted with respect to analyte migration according to Reijenga et al. [31] and to the signal heights of the internal standards as detected with the blue LED of the instrument (see “Results and discussion”). The area of the recorded FL signals was obtained by fitting Gaussian-shaped peaks to the data (OriginPro 9.1.0; see ESM Fig. S5 for an exemplary electropherogram).

Results and discussion

To generate a specific fluorescence signal the closed hairpin of the MB must open, which needs to be triggered via binding of its loop sequence to the complementary sequence of a target. Unfolding without hybridization, which might occur at low *I* or elevated temperature, results in a false positive signal. Therefore, orienting experiments were conducted with various MBs (same stem, different loop) to investigate the dependence of unfolding on *I* of the BGE (not shown). As expected, increase of *I* led to a reduction of the observed electroosmotic flow as well as to a higher proportion of the MB in its closed hairpin conformation, i.e. less FL was recorded. The maximal possible FL gain under the finally chosen *I* conditions was determined via nuclease digestion of the MB, which leads to its complete dequenching. Addition of divalent cations (e.g. Mg²⁺) known to stabilize the MB stem was omitted as these had been found to stabilize viral uncoating intermediates [9].

Chip electrophoresis of MBs

We carried out chip CE measurements in sodium borate, *I*=40 mM (pH 8.5). For intra- and interchip comparison of the

electropherograms, we included two additional fluorophores in samples similar to Bidulock and colleagues, who used caesium and lithium chloride as internal standards in sodium chloride analysis on home-made chips [32]. In our case, Atto 488 and Atto 495 gave rise to FL signals detectable with the blue LED of the applied instrument and did not interfere with analyte signals detected at $\lambda_{\text{ex/em}} = 635/685$ nm (see ESM Fig. S6A). In the specified BGE, Atto 495 is zwitterionic and migrates with the electroosmotic flow (EOF), whereas Atto 488 is negatively charged (the structure of dyes is available from the homepage of the manufacturing company). Migration of both peaks of the internal standards is such that electropherogram normalization, as described by Reijenga and colleagues [31], is feasible and slight changes in the EOF can be corrected. As all samples included the same amount of both dyes, we were also able to correct for slight changes in FL intensities. An intensity correction factor for each of the two internal FL standards was calculated separately and the average of these two numbers was employed to finally correct the FL intensity of a corresponding electropherogram. ESM Figs. S6B and C demonstrate the utility of this approach for correction of the blue traces of several electropherograms obtained from different chips. Upon normalization of both axes the signals were comparable.

Although we expected a completely closed state of the MBs under the given electrophoresis conditions and in the absence of a target molecule, our analyses showed that the MB exhibited residual FL in the absence of cognate oligonucleotides or viral RNA targets (ESM Fig. S7). However, compared to the high signal obtained after digestion with Benzonase this background was found to be negligible (an approx. 25-fold increase of FL was recorded upon Benzonase treatment). Therefore, we were indeed able to set the stage for our intended in vitro viral RNA release detection method by slight advancements of chip CE in comparison to our originally published set-up [17, 18] i.e. by inclusion of two internal standards as well as by choosing conditions where the majority of the MB is in its closed hairpin state (i.e. by adjustment of *I* of the BGE). Additionally, we modified the software of the instrument (script) to allow electrophoretic separations at ambient temperature ($T = 22.5 \pm 0.3$ °C).

Impact of BGE additives on FL response of MB

Subsequent experiments targeted the MB's reactivity in the presence of the respective positive control ssDNA oligonucleotide. With increasing concentration of this oligonucleotide an increase of FL was recorded (Fig. 1). No such increase was detected with the negative control oligonucleotide or with the RNA ladder (ESM Fig. S8A, B).

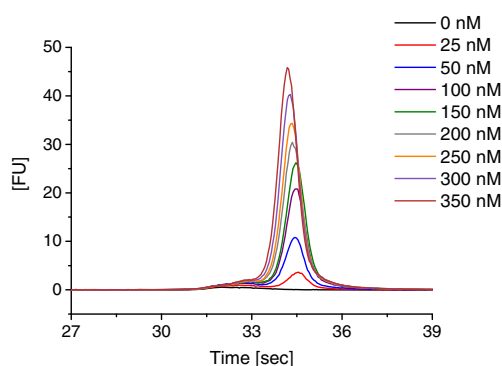


Fig. 1 Chip CE results for MB binding to positive control ssDNA oligonucleotides employed at indicated concentrations. With increasing concentrations of the control oligonucleotide an increase of the FL signal is observed in the electropherograms. Sodium borate, pH 8.5 ($I = 40$ mM) without any additives was employed as SB and BGE. Data was aligned as described in the text

Several compounds reduce blinking and photobleaching of fluorophores [33] in FL microscopy. In our case Trolox (6-hydroxy-2,5,7,8-tetramethylchroman-2-carboxylic acid) at 10 mM concentration in the BGE and SB increased the FL signal by approximately two- to threefold (Fig. 2). Fitting Gaussians to the electropherogram peaks yielded a linear correlation between the concentration of the positive control oligonucleotide and the area of the FL peak. In the presence of 10 mM Trolox, the FL signal equalled 0.282 times the concentration of the positive control oligonucleotide (in nanomoles per litre). In the absence of Trolox the slope of the linear correlation dropped to 0.108. Higher concentrations were not tested because of the limited solubility of Trolox (around 3 mg/mL which corresponds to approx. 12 mM in phosphate buffered saline, pH 7.2; www.scbt.com/datasheet-200810-trolox.html). Additive concentrations close to its solubility limit might lead to clogging of the chip channels.

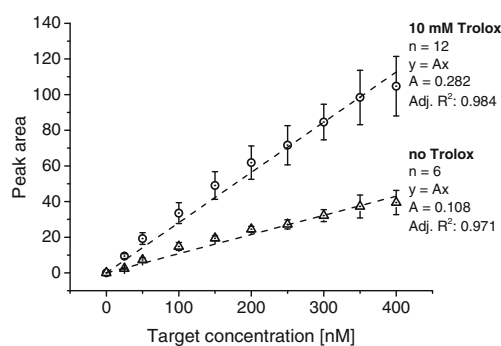


Fig. 2 Addition of 10 mM Trolox to the BGE (I constant at 40 mM) resulted in a two- to threefold increase of FL signals obtained for the MB/positive control ssDNA oligonucleotide complex as a result of reduced photobleaching and blinking. Values of symmetric Gaussian peaks fitted to electropherograms were taken for calculation. The number of repeats per data point is indicated in the figure, standard deviation values are shown. Data points are approximated via linear fits

Use of ascorbic acid as an alternative additive (up to 6 mM) failed to increase the FL yield (data not shown).

Detecting RNA release via MBs and chip electrophoresis

Following our experiments with control oligonucleotides we mixed MB with HRV-A2, triggered virus uncoating via heating for 15 min to 56 °C, and carried out chip CE as above. Desalting of HRV-A2 preparations was beneficial for the FL signal obtained from MB binding the viral RNA possibly because uncoating might have been reduced owing to the stabilizing effect of Mg^{2+} and other divalent cations present in the HRV-A2 stock solution [9]. After this buffer exchange we observed clear and specific signals for the MB–RNA complex (compare Fig. 3a without HRV-A2 desalting prior virus uncoating to Fig. 3b where HRV-A2 desalting had been carried out before initiating viral RNA release at 56 °C). The test with MB alone (in the absence of virus) showed only a low response to sample heating to 56 °C indicating that it folded

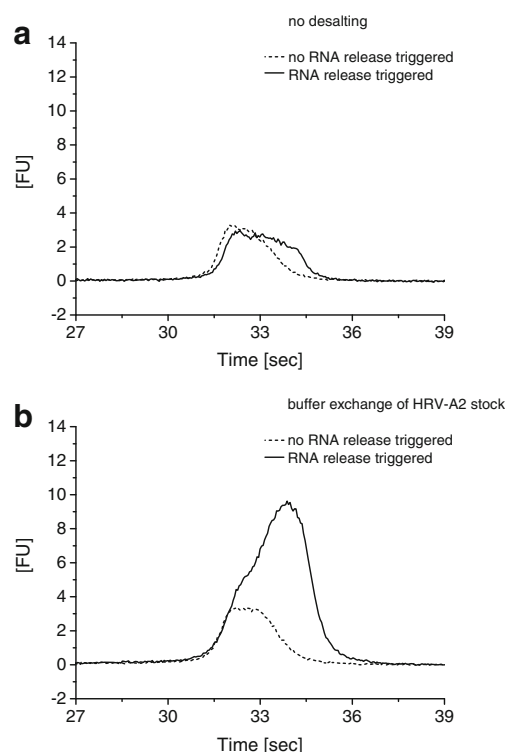


Fig. 3 Detection of free viral RNA by using our chip CE set-up. RNA release was triggered through heating of the virus preparation (15 min to 56 °C). As a negative control, the sample was kept in ice and the viral RNA remains inside the protein shell and inaccessible to the MB. Buffer exchange of the HRV-A2 batch was found to strongly increase the signal of the viral RNA (compare a, which is the result without buffer exchange, and b, which is the result including a sample buffer exchange step). Sodium borate, pH 8.5 including 10 mM Trolox ($I = 40$ mM) was employed as SB and BGE. Data was aligned as described in the text

back on cooling (ESM Fig. S8C). Likewise, no reactivity of the MB with RNA from HRV-B14 was recorded indicating that the obtained MB/RNA signal was specific (ESM Fig. S8D). RNase activity after release of the viral genome slightly impacted the obtained MB–RNA complex signal. Given samples were stored on ice as well as under light protection and measurements were carried out within a few hours after sample preparation areas recorded for the complex were found to be within approx. 10 % of an average (ESM Fig. S9).

Challenges of the experimental set-up

Having demonstrated the applicability of our set-up to qualitatively follow the release of HRV-A2 RNA employing an MB and chip CE, we were interested in the quantification of the obtained FL signals. However, measurements of identically prepared samples showed a significant decline of the MB–

RNA signal over time of storage at -70°C and the numbers of freezing and thawing cycles of the virus stock solution (Fig. 4a; note that samples were prepared freshly for each experiment). It is important to mention that a decline of infectivity by as much as one log $\text{TCID}_{50}/\text{mL}$ even during storage at -80°C for several weeks was frequently observed. However, fluorescence of the MB measured on incubation with native HRV-A2 whose RNA is inaccessible (Fig. 4b) did not alter in FL over time. This makes it unlikely (i) that the MB interacts with virus and/or virus aggregates, which might reduce the concentration of free MB in solution and (ii) that the MB is degraded. Instead we assume that repeated freezing/thawing of the virus stock solution impacted on the signal as a result of the viral RNA being degraded.

Breathing, i.e. transient exposure of capsid-internal N-terminal sequences, of VP1 and VP4 was reported for picornaviruses [15] and similar dynamics of virus capsid components have been observed for hepatitis B virus capsids [34]. These transient rearrangements of the capsid proteins might account for the RNA becoming accessible for RNases, especially during freezing and thawing. In this context it is of note that Gauntt had observed fragmentation of the RNA in virions of another serotype [35].

Material apparently released from HRV-A2 later in the experimental series (i.e. after virus storage at -70°C and repeated freezing/thawing leading to viral RNA degradation) resulted in quenching of overall FL. Hence, special care has to be exercised with virus storage and freezing/thawing. Also, inclusion of RNase inhibitors in samples and stocks might be beneficial to avoid eventual degradation of the viral RNA via RNases that might gain access during temporary opening of pores given that an impact of these additional components on chip CE can be excluded.

On the basis of the linear correlation between the concentration of the control oligonucleotide and FL, we calculated the amount of viral RNA that was released on heating. This yielded 43 nM for the most prominent MB–RNA complex signal (at day 177 after HRV-A2 preparation; Fig. 4a). When the virus was then frozen and thawed the RNA concentration was found to be decreased, which is in line with the well-known natural decay of viruses.

Analysis of HRV-A2 preparations other than A led to similar results (see ESM Fig. S2 for an overview of virus preparations) when the $\text{TCID}_{50}/\text{mL}$ values and purities were comparable, as in preparation D. In the case of low virus concentrations (e.g. batch B, see ESM S1) or highly impure virus preparations (e.g. batch C, see ESM S1), no MB–RNA complex could be detected (Fig. 5a–d for indicated HRV-A2 preparations). Batch C showed considerable amounts of the previously described contaminant as well as a protein impurity,

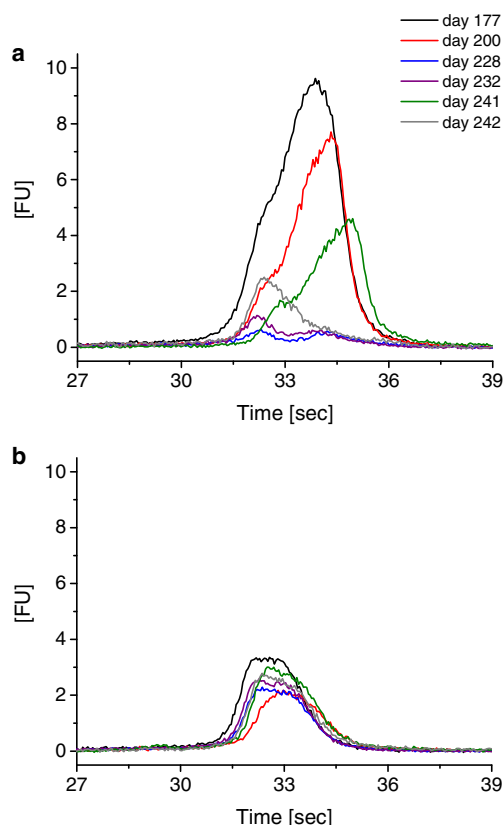
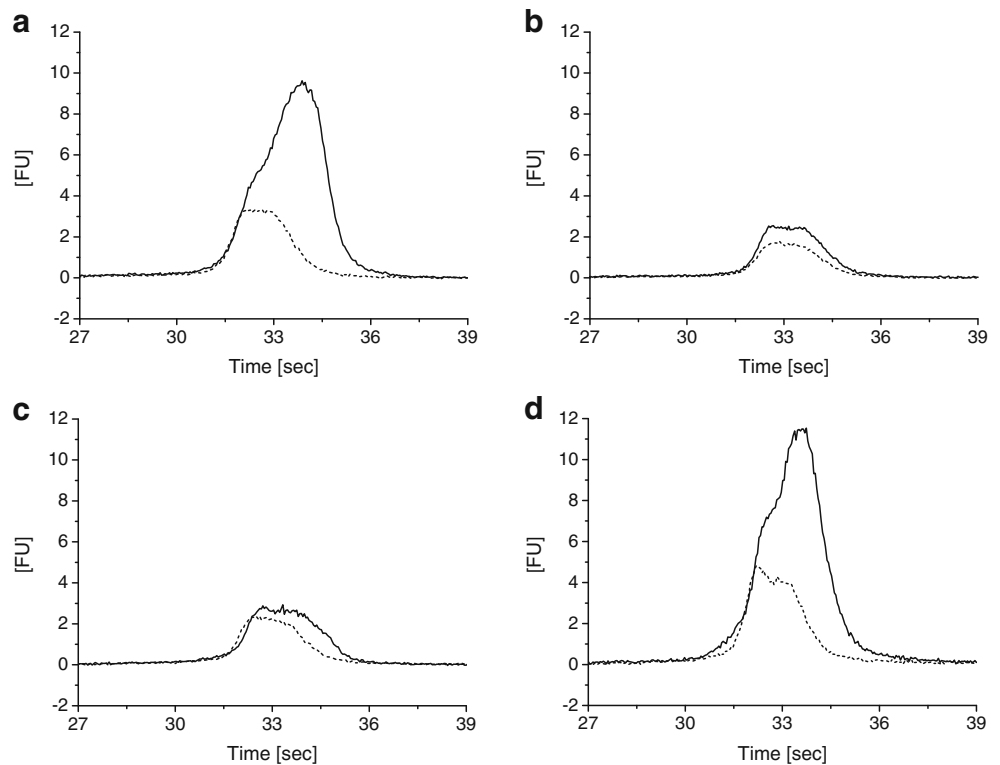


Fig. 4 Decline of the MB/RNA signal in the course of chip CE experiments over time. Viral RNA release experiments as presented in Fig. 3 were repeated at the indicated times (days) after preparation of the original HRV-A2 batch. Samples were prepared freshly from an HRV-A2 stock for each time point. A decline in the FL signal for the MB/RNA signal (a) was observed over time which was ascribed to degradation of the viral RNA genome. No significant decline is observed for the negative control electropherograms for the MB in the presence of HRV-A2 but without triggering of viral RNA release (b)

Fig. 5 Chip CE results for different HRV-A2 batches **a–d**. (see ESM Fig. S2). Virus stock solutions were subjected to buffer exchange. Depending on the quality of the preparation (purity and infectivity), a signal for the MB–RNA complex is obtained. Conditions as noted for Fig. 3. No RNA release triggered via sample heating, *dashed line*; RNA release triggered by sample heating for 15 min to 56 °C, *solid line*



possibly ferritin, as inferred from gas-phase electrophoresis (nES GEMMA).

Conclusions

The major aim of this study was the development of a fast, sensitive and easy-to-handle analytical method to detect viral RNA by using an MB and chip CE to set the stage for further investigation of the mode of release of the RNA genome of a human rhinovirus. Intra- and interchip comparison of results by using internal standards was good (analytes were detected with the second wavelength of the instrument without interference from internal standard signals). Addition of Trolox to the BGE increased the FL signals substantially. Our results demonstrate that the release of the viral RNA genome from the viral capsid can indeed be monitored via the combination of an MB and chip CE. However, during our investigations we noted a significant decrease of the signal measured with the MB over time of storage at -70°C and repeated freezing/thawing, which we attributed to degradation of the viral RNA genome. Nevertheless, given that an HRV-A2 preparation was of sufficiently high purity and the virus concentration was in the range of at least 10^{10} TCID₅₀ in the final sample, results between preparation batches were very similar. Future

work might substantially lower this detection threshold and will also allow the extension of our presented in vitro set-up to the analysis of other viruses.

Acknowledgments Open access funding provided by TU Wien (TUW). Funding was provided by the FWF Austrian Science Fund (grant P25749-B20 to VUW and P23308-B13 to DB). The device was partly funded by a non-specified grant — University Relations Program (Agilent Technologies) – to TU Wien (GA).

Contributions Experimental design by VUW; experimental work by VUW and CL; HRV preparation and TCID₅₀/mL determination by IG; HRV-B14 purification by SF; guidance by GA, VUW, DB; instrumentation by GA; funding by VUW, GA, DB; all authors contributed to the manuscript.

Compliance with ethical standards The authors declare that they have no conflict of interest and that MK is a full-time employee of Agilent Technologies.

Open Access This article is distributed under the terms of the Creative Commons Attribution 4.0 International License (<http://creativecommons.org/licenses/by/4.0/>), which permits unrestricted use, distribution, and reproduction in any medium, provided you give appropriate credit to the original author(s) and the source, provide a link to the Creative Commons license, and indicate if changes were made.

References

- Hewat EA, Blaas D. Structure of a neutralizing antibody bound bivalently to human rhinovirus 2. *EMBO J*. 1996;15(7):1515–23.
- Bacher G, Szymanski WW, Kaufman SL, Zollner P, Blaas D, Allmaier G. Charge-reduced nano electrospray ionization combined with differential mobility analysis of peptides, proteins, glycoproteins, noncovalent protein complexes and viruses. *J Mass Spectrom*. 2001;36(9):1038–52.
- Fuchs R, Blaas D. Uncoating of human rhinoviruses. *Rev Med Virol*. 2010;20(5):281–97.
- Fuchs R, Blaas D. Human rhinovirus cell entry and uncoating. In: Cheng RH, Miyamura T, editors. *Structure-based study of viral replication*. Singapore: World Scientific Publishing; 2008. p. 1–42.
- Lonberg-Holm K, Yin FH. Antigenic determinants of infective and inactivated human rhinovirus type 2. *J Virol*. 1973;12(1):114–23.
- Korant BD, Lonberg-Holm K, Noble J, Stasny JT. Naturally occurring and artificially produced components of three rhinoviruses. *Virology*. 1972;48(1):71–86.
- Okun VM, Blaas D, Kenndler E. Separation and biospecific identification of subviral particles of human rhinovirus serotype 2 by capillary zone electrophoresis. *Anal Chem*. 1999;71(20):4480–5.
- Weiss VU, Subirats X, Pickl-Herk A, Bilek G, Winkler W, Kumar M, et al. Characterization of rhinovirus subviral A particles via capillary electrophoresis, electron microscopy and gas-phase electrophoretic mobility molecular analysis: part I. *Electrophoresis*. 2012;33(12):1833–41.
- Subirats X, Weiss VU, Gosler I, Puls C, Limbeck A, Allmaier G, et al. Characterization of rhinovirus subviral A particles via capillary electrophoresis, electron microscopy and gas phase electrophoretic mobility molecular analysis: part II. *Electrophoresis*. 2013;34(11):1600–9.
- Harutyunyan S, Kumar M, Sedivy A, Subirats X, Kowalski H, Kohler G, et al. Viral uncoating is directional: exit of the genomic RNA in a common cold virus starts with the poly-(A) tail at the 3'-end. *PLoS Pathog*. 2013. doi:10.1371/journal.ppat.1003270.
- Weiss VU, Bereszcak JZ, Kallinger P, Goesler I, Havlik M, Kumar M, et al. Analysis of a common cold virus and its subviral particles by gas-phase electrophoretic mobility molecular analysis and native mass spectrometry. *Anal Chem*. 2015;87(17):8709–17.
- Okun VM, Ronacher B, Blaas D, Kenndler E. Analysis of common cold virus (human rhinovirus serotype 2) by capillary zone electrophoresis: the problem of peak identification. *Anal Chem*. 1999;71(10):2028–32.
- Kremser L, Petsch M, Blaas D, Kenndler E. Influence of detergent additives on mobility of native and subviral rhinovirus particles in capillary electrophoresis. *Electrophoresis*. 2006;27(5-6):1112–21.
- Kremser L, Konecni T, Blaas D, Kenndler E. Fluorescence labeling of human rhinovirus capsid and analysis by capillary electrophoresis. *Anal Chem*. 2004;76(14):4175–81.
- Kremser L, Okun VM, Nicodemou A, Blaas D, Kenndler E. Binding of fluorescent dye to genomic RNA inside intact human rhinovirus after viral capsid penetration investigated by capillary electrophoresis. *Anal Chem*. 2004;76(4):882–7.
- Kremser L, Petsch M, Blaas D, Kenndler E. Labeling of capsid proteins and genomic RNA of human rhinovirus with two different fluorescent dyes for selective detection by capillary electrophoresis. *Anal Chem*. 2004;76(24):7360–5.
- Kolivoska V, Weiss VU, Kremser L, Gas B, Blaas D, Kenndler E. Electrophoresis on a microfluidic chip for analysis of fluorescence-labeled human rhinovirus. *Electrophoresis*. 2007;28(24):4734–40.
- Weiss VU, Kolivoska V, Kremser L, Gas B, Blaas D, Kenndler E. Virus analysis by electrophoresis on a microfluidic chip. *J Chromatogr B*. 2007;860(2):173–9.
- Weiss VU, Bilek G, Pickl-Herk A, Blaas D, Kenndler E. Mimicking virus attachment to host cells employing liposomes: analysis by chip electrophoresis. *Electrophoresis*. 2009;30(12):2123–8.
- Bilek G, Weiss VU, Pickl-Herk A, Blaas D, Kenndler E. Chip electrophoretic characterization of liposomes with biological lipid composition: coming closer to a model for viral infection. *Electrophoresis*. 2009;30(24):4292–9.
- Weiss VU, Bilek G, Pickl-Herk A, Subirats X, Niespodziana K, Valenta R, et al. Liposomal leakage induced by virus-derived peptides, viral proteins, and entire virions: rapid analysis by chip electrophoresis. *Anal Chem*. 2010;82(19):8146–52.
- Bilek G, Matscheko NM, Pickl-Herk A, Weiss VU, Subirats X, Kenndler E, et al. Liposomal nanocontainers as models for viral infection: monitoring viral genomic RNA transfer through lipid membranes. *J Virol*. 2011;85(16):8368–75.
- Tyagi S, Kramer FR. Molecular beacons: probes that fluoresce upon hybridization. *Nat Biotechnol*. 1996;14(3):303–8.
- Cui ZQ, Zhang ZP, Zhang XE, Wen JK, Zhou YF, Xie WH. Visualizing the dynamic behavior of poliovirus plus-strand RNA in living host cells. *Nucleic Acids Res*. 2005;33(10):3245–52.
- Dunams D, Sarkar P, Chen W, Yates MV. Simultaneous detection of infectious human echoviruses and adenoviruses by an in situ nuclease-resistant molecular beacon-based assay. *Appl Environ Microbiol*. 2012;78(5):1584–8.
- Su YC, Wang CH, Chang WH, Chen TY, Lee GB. Rapid and amplification-free detection of fish pathogens by utilizing a molecular beacon-based microfluidic system. *Biosens Bioelectron*. 2015;63:196–203.
- Weiss VU, Subirats X, Kumar M, Harutyunyan S, Gosler I, Kowalski H, et al. Capillary electrophoresis, gas-phase electrophoretic mobility molecular analysis, and electron microscopy: effective tools for quality assessment and basic rhinovirus research. *Methods Mol Biol*. 2015;1221:101–28.
- Kaufman SL, Skogen JW, Dorman FD, Zarrin F, Lewis KC. Macromolecule analysis based on electrophoretic mobility in air: globular proteins. *Anal Chem*. 1996;68(11):1895–904.
- Skern T, Sommergruber W, Blaas D, Gruendler P, Fraundorfer F, Pieler C, et al. Human rhinovirus 2: complete nucleotide sequence and proteolytic processing signals in the capsid protein region. *Nucleic Acids Res*. 1985;13(6):2111–26.
- Weiss VU, Lehner A, Kerul L, Grombe R, Kratzmeier M, Marchetti-Deschmann M, et al. Characterization of cross-linked gelatin nanoparticles by electrophoretic techniques in the liquid and the gas phase. *Electrophoresis*. 2013;34(24):3267–76.
- Reijenga JC, Martens JH, Giuliani A, Chiari M. Pherogram normalization in capillary electrophoresis and micellar electrokinetic chromatography analyses in cases of sample matrix-induced migration time shifts. *J Chromatogr B*. 2002;770(1-2):45–51.
- Bidulock AC, van den Berg A, Eijkel JC. Improving chip-to-chip precision in disposable microchip capillary electrophoresis devices with internal standards. *Electrophoresis*. 2015;36(6):875–83.
- Vogelsang J, Kasper R, Steinhauer C, Person B, Heilemann M, Sauer M, et al. A reducing and oxidizing system minimizes photobleaching and blinking of fluorescent dyes. *Angew Chem Int Ed*. 2008;47(29):5465–9.
- Utrecht C, Watts NR, Stahl SJ, Wingfield PT, Steven AC, Heck AJ. Subunit exchange rates in hepatitis B virus capsids are geometry- and temperature-dependent. *Phys Chem Chem Phys*. 2010;12(41):13368–71.
- Gauntt CJ. Fragmentation of RNA in virus-particles of rhinovirus type-14. *J Virol*. 1974;13(3):762–4.

Analytical and Bioanalytical Chemistry

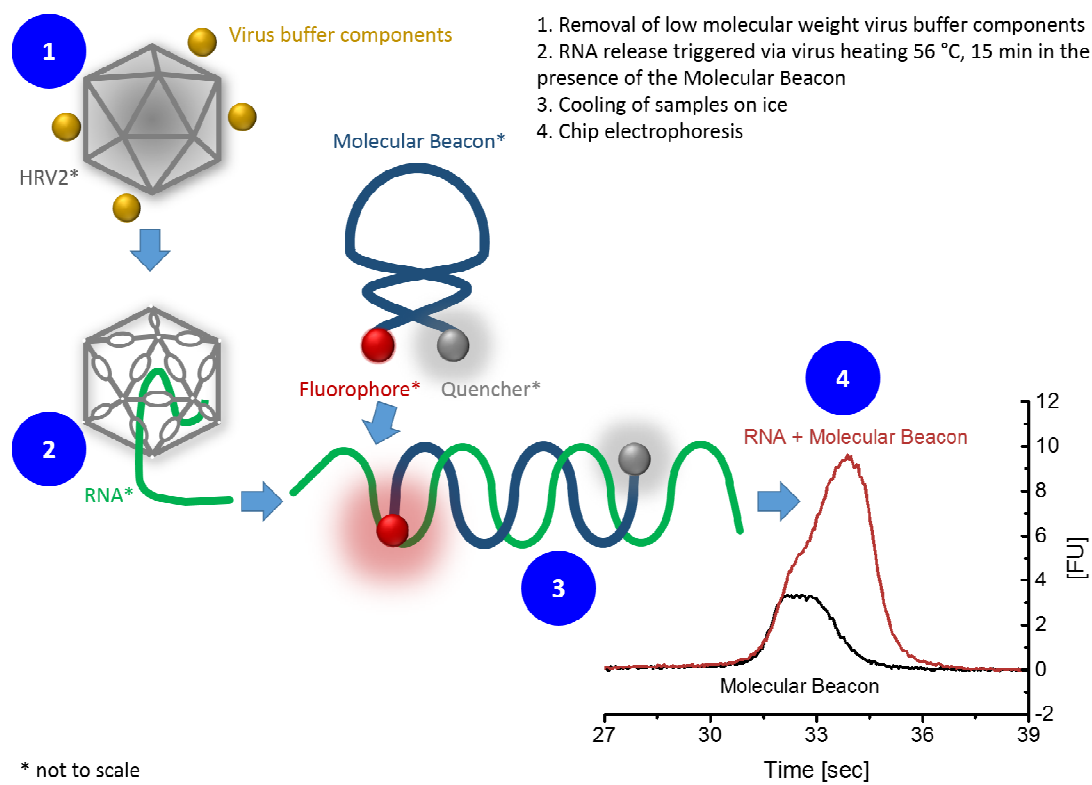
Electronic Supplementary Material

In vitro RNA release from a human rhinovirus monitored by means of a molecular beacon and chip electrophoresis

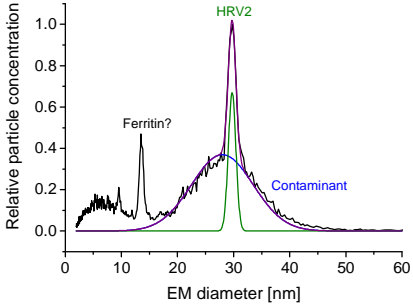
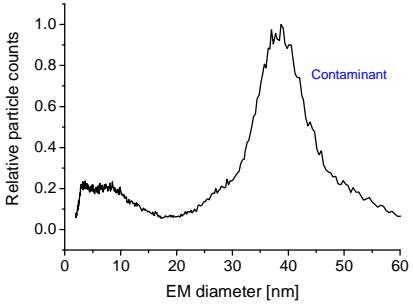
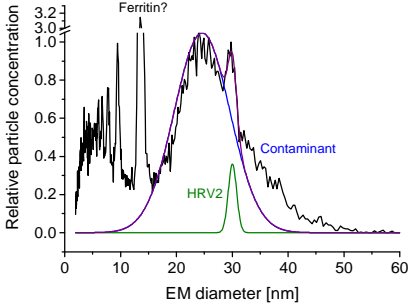
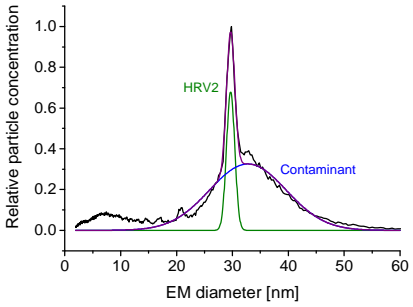
Victor U. Weiss, Christina Bliem, Irene Gösler, Sofiya Fedosyuk, Martin Kratzmeier,
Dieter Blaas, Günter Allmaier

The supplementary part of the manuscript gives additional information on:

- (i) the study principle (S1),
- (ii) HRV-A2 preparation batches (S2),
- (iii) position of complementary to the MB on the HRV-A2 RNA genome (S3),
- (iv) the RNA ladder including six RNA transcripts of various length used as negative control (S4); a chip gel electropherogram (Agilent 2100 Bioanalyzer RNA Nano kit) is presented,
- (v) data evaluation of FL signals obtained upon MB binding to positive control ssDNA oligonucleotides (S5),
- (vi) the concept of electropherogram alignment (S6),
- (vii) the FL increase obtained upon MB digestion via the nuclease benzonase (S7),
- (viii) signals obtained for negative controls (S8) including ssDNA (A), RNA ladder (B), MB heated for 15 min to 56°C (C) and HRV-B14 (D),
- (ix) the impact of RNase digestion over time on MB / RNA complexes after triggering of viral RNA release from protective capsids (S9); samples were stored on ice and under light protection after RNA genome release; between first (left) and last (right) measurement lay approx. 4 hours.



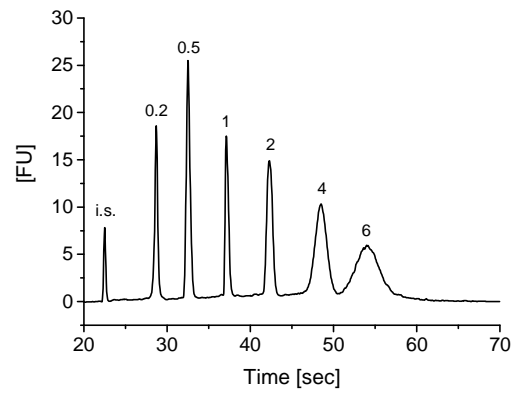
Supplementary Figure S1: Schematic of the study principle

HRV-A2: Preparation date Preparation mode	Preparation ID	TCID ₅₀ /mL	Virus particles [mg/mL]	nES GEMMA spectra
03.02.2014 2 nd fraction Standard preparation with additional lipase digestion [Weiss, V. U. et al, 2015 Analytical Chemistry]	#A	$4.64 \cdot 10^{11}$	11.9	
03.02.2014 1 st fraction Standard preparation with additional lipase digestion [Weiss, V. U. et al, 2015 Analytical Chemistry]	#B	$2.02 \cdot 10^{10}$	n.d.	
04.07.2014 2 nd fraction Standard preparation with additional lipase digestion [Weiss, V. U. et al, 2015 Analytical Chemistry]	#C	$5.62 \cdot 10^{10}$	0.3	
30.01.2015 1 st fraction Standard preparation with additional PEG precipitation step prior sucrose density centrifugation	#D	$4.64 \cdot 10^{11}$	4.7	

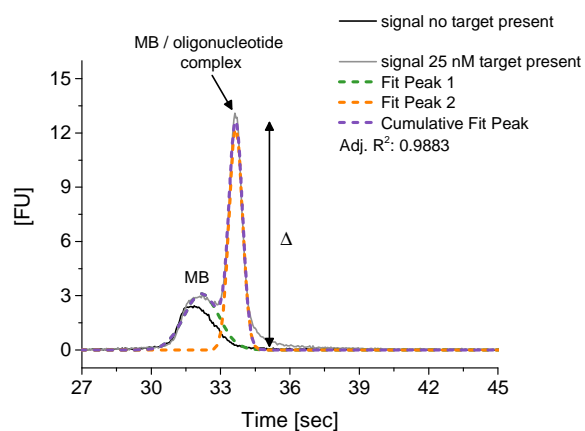
Supplementary Figure S2: Overview on HRV-A2 preparation batches; n.d. value not determinable

(5')VP_ttaaaactggatccagggtgttccacctggattcccacaggagtggtactctgtattacggttaactttgtacgccagttttatctccctccccatgttaacttagaagttttcacaagac
caatagccggtaatacagcagattactgaagtcacagcttctgtttcccggtcaatgttgatcttcccaacaggggcaaaaacactgcgatgttaacgcgctacgcgctcaagccttagta
gcatctttgaaactgtttggctgcatccgcatcttccctggtagacctggcagatgaggtagaaataccccactggcgacagtggtttagcctgctggtgctgctgacacccataggtgtgaag
cacaacaaatggacaagggtgtgaagagcccgtgtgctgcgtcttgatctcctggccctgaatgtgggttaaccttaacccctgcagctagagcagcgaacaaatgtgtatctagctgaatgagcaatg
cgggatgggaccaactactttgggtgtccgtgttcacttttctttatattgtcttagtgacaataatacaatataatattggcaccatgggtgacaggtttcaagacaaaatgttggaactcact
cacgcacaaactctgtatcaaatgggtctagtttaaatattttaacatcaaatattttaaaagatgtcttcaaatgggtcatcaaaactggaaattcacacaagatcctagtaaatttactgaccagtt
aaggatgtttggaaaagggaataccaacactacagctccccacagtgaggctgttggtactctgtagaggattatagattaccagaggagattcaaccataacctcacaagatgttgctaagtc
tatcgttgcgtatgtgttggccacattatctatctccaaggatgcctctgcaattgataaacctctcaaccagatatacttctaatagattttatactctaaggagtgtagctggagcagttcctca
aagggtgttggtggaaactacatgctacacaggaacaggtggttattgttgaaacatgtttatcattacctgggtaggagtggtacacaatacatgtgcagtgtaagtctagtaaatccacc
agggtacactaaatgtgtcctgatacctgagcagattgcaagtccttacatggcgaatgtgaatgttggttaactacacacaccagggtgaacaggcagggaagttaaagctgagacgaga
ttgaatcctgatctacaacctactgaagagtattggtaaaactgttgggacactccttggaataattaccatttccctcatcaatttatcaactgaggagtaataattctgccacaataattgccct
tatgtcaatgcagttctatgattcaatgcggagccacaataattggagtttggttaataatacaaatatgtcccttgagacatcaagtgaattaacacaatacctattacaatctataagccccat
gtgtgcagagttttccggcgctgccaagcgtcaaggattaccagtttcatcacaccaggttcaggacagttttgacaacagatgatttccaatccccatgtgcacttccctggtatcacccaactaa
ggaaatttctatccaggtagggttaaaatgttggtgaattgtcaagtagacagcctagtaacaaataaactgcacactacatcaatagtgaaatagttatctgttgattgtcaatcatca
ataatgcaccagataagattctctctatctcaacagatgtgttctccaacctgtgctcactcttgattgttgtagatctagctatttcaaccactggacaggaggtcattggtcagctctgtttgt
tggtactgccaacactactgttaagctttgttggtacacacaccctggtatcgagaaccacccaagaaggatgcaatgtcaggcactcatgttatatgggtgtgggtgtgagctcacaata
tcaatggtatgtccatgattagcgtagctattatagaacacatcacacaggtagatctacatctgggtacataacatcgtggtatcagactagattagctattcaccctcagacccccaacagcta
gattgttatgtttgtatctgggtgcaaaagactttgtctgcatggcagagatacctacacactgcaaaagggtgcaatagcacagaacccctgttgagaattatagatgaagttcttaatgaa
ttttgtgttcccaaatattatagtagtagtaacccaacacatacctcaaatctgccccagctacagtagctgagaaacagggcacactagtagtttcaaccagaggatgcttgaatgtgagctatgtc
agacatcacaacaagagatgaatagtttagagagttttctggcagatcaggatgcatacgaatcaaatagagggtacacttgcaaatatacaaggagaattttacagtggtggctatta
atctacaagaaatggctcaaatagaaagaaattgaattgttcaactatactaggtttgattctgaaataacccctagttccatgatttccgctctagtcaggacattggacacatcaaatcaatc
atgtatgttccacagggtgcacgggtcccaatagtagggacgattatgcatggcagctggcactaatgcctctgttttggcaacatggacagggttcaagattttcttacccttctcaatgtgtg
gcatctgtctattacatgtttatgtatgggtatgatacaagatcaaaactatgttcagcaaacacaaataacatgggtcactatgctcaggatagtaacagacacatctataagttacat
ataatgacaagaatctatcaaggctaaacatgtcaaggatgtgttccacgccccacagcgcttgagtatactctgctcactcaattttaaaataggagtaggagtagttacagacagca
attgtgaccagacaattatcactacagctggccccagtgacatgtatgttcatgtaggttaacattttatagaatcttcatctttcaactctgagatgcatgaatctatttggatcttattcatcaga
tttaactatttaccgaacaaactgtaggtagattacattccctctgtgattgtaccaaagctactattattgcaaacataaaatagatacttccaatcacagttacaagcctagctggtatga
aatacagggaagttagtactatcccaaacacatacagctacaattgttattgttgtaggggccccgttggaacagggtgactgttggtggaagtgtctatgcaaacatgggtgctatagttatgaacgc
tggtgtgataatcatgtggcttttattgaccttagacacttccattgtgtcgaagaacaagggtgtacagattatatacatatgctagggagaagcatttggaatggatttggtagtgttaaaagaa
catatacatgccataaacccagtaggaataatcagcaagaaattatgaatggatgttgagaataatcagcaatggtcataataatagaactcttctgacccccaaactatattagcaacactc
acactgattgggtgttctggtacacccctggagatttttaaggaaaaatctgttaaatggacacagcttaattatatacacaagaatcagattcatggtttaagaaatattactgaagcagcgaatgca
gctagagggttgatgtagtagggaataagatatctaaatttattgaatggatgaagtcgagctccccgaagctcaattgaagggttaagtactaaacagagcttaaaaaactcaacctatcagaaaa
aatgaattgagagcttgcgggtgctgacatgaataacacagaaaaaatgaatggaaactcagacttcatgatttgcagtaaatctcacttctgtaggaggtgagcaaaaggagataaa
accctatacattaaatgtgataatcatcaagcagaagaaagatgtgaaccagtagctatgtttatctggaccctgggtgctgcaaatctatacaacaaatcttctggccaaaatgataact
aatgatagtgacatactctcactcctgacaaaatattttagtggttatgacacagagtgtagtaataatggatgacattatgcagaatccagcggggatgacatgacatttctgcca
tggtttctagtggtacattataaccacaaatggctgactaccagataaaggcaaggcttttattctaggtttgtattatgcagcaaaatcattcccttcaacccccgacaataacttactacactgc
aatgaattgagagcttgcgggtgctgacatgaataacacagaaaaaatgaatggaaactcagacttcatgatttgcagtaaatctcacttctgtaggaggtgagcaaaaggagataaa
accctatacattaaatgtgataatcatcaagcagaagaaagatgtgaaccagtagctatgtttatctggaccctgggtgctgcaaatctatacaacaaatcttctggccaaaatgataact
aatgatagtgacatactctcactcctgacaaaatattttagtggttatgacacagagtgtagtaataatggatgacattatgcagaatccagcggggatgacatgacatttctgcca
tggtttctagtggtacattataaccacaaatggctgactaccagataaaggcaaggcttttattctaggtttgtattatgcagcaaaatcattcccttcaacccccgacaataacttactacactgc
aggagaacccaaagccaaagatacatctcccaaaaggcgtgtgtagtaacacaggagcagaggaatttgggtgtctttaaataacataactcatgtgttataacagaaagacaggttaagtgacg
cacaggcttggagtatacagacagatttgggtgtaccaacacatgcagatcctggaaaggaaatcagggttgatgtgataactcaaaaagtcattgactcatatgacctatacaacaagaatgggat
aaagctagaataacagctacttaaatagatagaatgaaaaatttagagatagcaggagatataacacaaatgaagatgattaccacaaatgcaacttagcactgtagcaaacacgcctgaa
ccaactataatcaatgttgagatgtgtatcctatggcaatactatgctcagtggaacaaacaggctagaatgcttaataacagttaccaactaaatctggttactgtggaggtgtcttatacaaaa
tgggcaagtccttggaatacatgttgggggcaatgttagggatgggttttctcagctatgttactcagactgttgcagggccaaataacgttatcaagaagacaggttaagtgtaactgtaac
accagatatacacaacccatgcaaaacaaatgcagcctaggttttctatgatttccctggttcaaaagaacacagctgtgtgtctgaaagagatcccgggttaacagttgatttcaatgaagca
ctattttctaatacaaaagggaatagagttgctcctaataatgacacataagaattgcatcatcacattatgcagcaacactattaccttagatattgacccaaaacattacacttgaggacagtg
tctttggcactgatggattagaggtcttctgattgaacactagcgcaggatttccatattgcaatggggatgaaagagagatttaataaacaacagacaaagataaagcaaaactaaagaa
gcaattgacaataacggagtgacttaccatggtcaccttcttgaagatgaactcagaagcatgaaaaggtaattaaaggtaaaactagagttattgaagctagtagtgtaagtagatccctatta
tttagaacaacttttggcaaccttttcaagttccactgaatcctggaattgttactggtcagcagcagtggtgtgatccagagggttttgggtcaaaaataccagcaaatgttgatgataaatgtatt
atggcttttgattatacaaatatgagttgtagtataccctatttggttgaagctcttaaacaggtagctgtagatctatcttaatacattatagatagactatgcaagctcaaacacatcttc
aaaaatacactatgaagtgaggagggtgtagcttgggttccaggtactagatttttaacataatgatacaataatattatcataaggaccttagtttagatgcatacaagaatagatctag
ataagcttaagataattgcctatggtgatgtcatattctatatacatgaactggacatggagggtatagcaatagagggtgtaaatatgtttgactataactcctgctgataaatctaacac
atttgaataatgagctatagcaatgttactttttaaagagggtttaagcaagatgataaacttcttaatacatcacttccctgaagatgaaatatttgaatcactcagatggacaaaag
aaacatcacaatgcatgaacatgtgtgtctgtgctacttaattggcacaatggacgtgacgcatacaaaaaatttggagaagatagcagtgtaagcgctggtgctgactgtatcatccct
ccgtatgatttgccttttcagtagtggtatgaaaaattttaaagatatgaaaaatagtaactgattttattgtttataaaaaaataaaaaaataaaaaaataaaaaaataaaaaa
aaaaaaaaaaaaaaaaaaaaaaaaaaaaa (3')

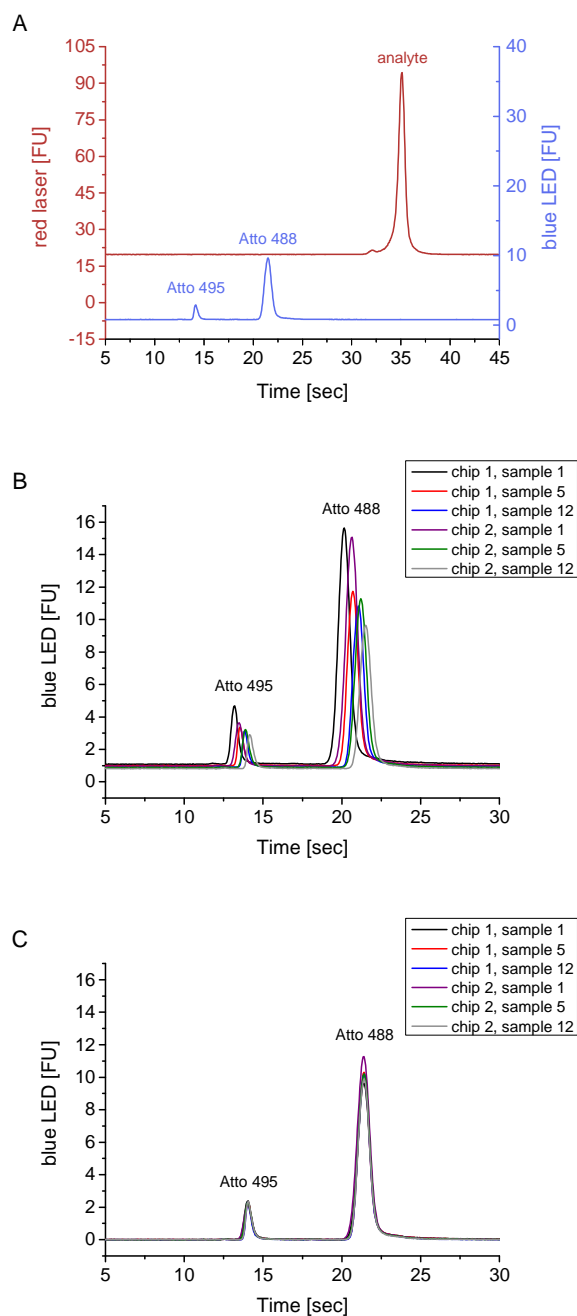
Supplementary Figure S3: The position of complementary to the MB on HRV-A2 RNA [29] is marked. Additionally, the position of the poly-A tail at the 3' end is indicated; note that this poly(A) tail is between 70 and 150 bases long.



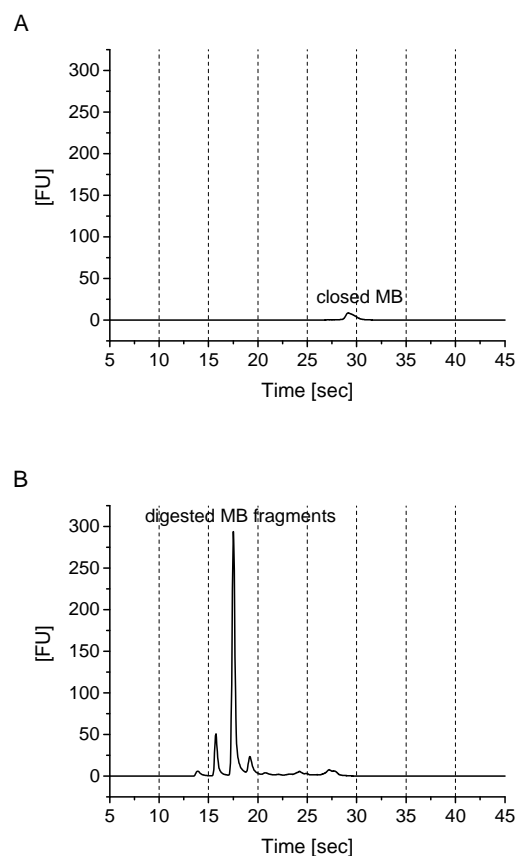
Supplementary Figure S4: Chip gel electropherogram (Agilent 2100 Bioanalyzer RNA Nano Kit) of a RNA ladder with six transcripts of the indicated lengths (in kbases). Note that gel-filled channels were used in this analysis. i.s. internal standard



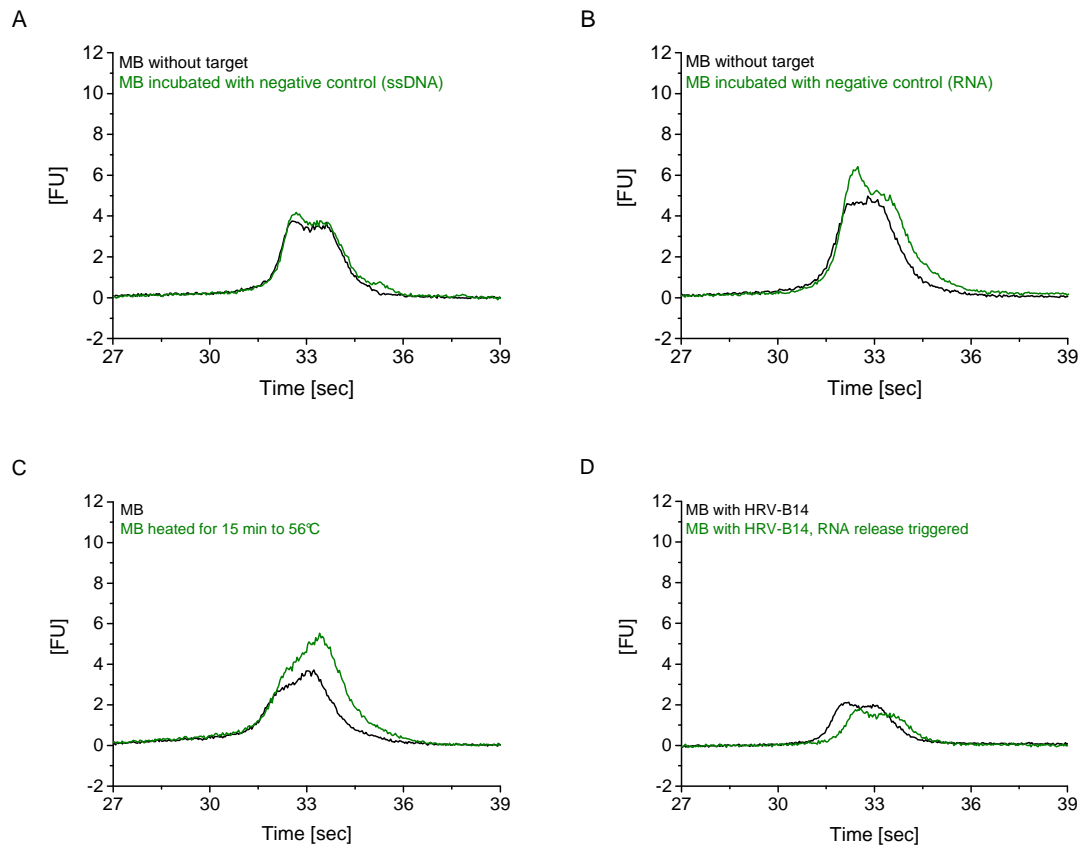
Supplementary Figure S5: Exemplary electropherograms to demonstrate data evaluation of FL signals obtained for the MB complexed to positive control ssDNA oligonucleotides (25 nM target concentration). Gaussian shaped peaks were fitted to data (OriginPro 9.1.0). An increase in FL upon complex formation with the complementary target is indicated by ' Δ '. Area values of fitted peaks are taken for calculation.



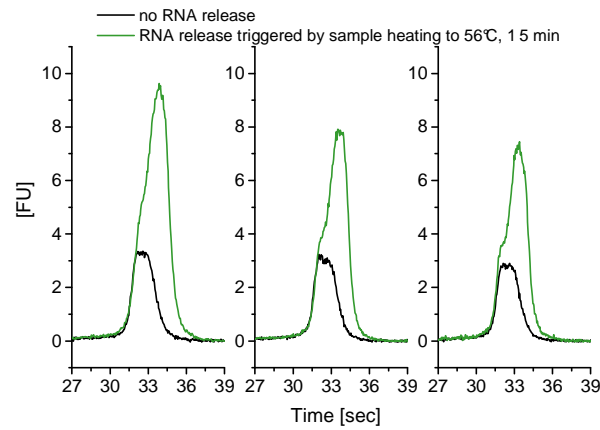
Supplementary Figure S6: Chip CE on the Agilent 2100 Bioanalyzer offers the possibility of simultaneous analyte detection at two wavelengths, $\lambda_{\text{ex/em}} = 470 / 525 \text{ nm}$ (blue LED) and $635 / 685 \text{ nm}$ (red laser), respectively (A). The blue trace of the instrument is employed for the analysis of internal standards (Atto 495 and Atto 488) spiked to samples. Inter- and intrachip variations in analyte migration and sensitivity (B) are compensated according to Reijenga et al. (x-axis) [31] and according to the height of FL signals (y-axis), (C).



Supplementary Figure S7: Chip CE data of the MB under conditions (sodium borate, pH 8.5, ionic strength of 40 mM) preferably yielding closed probes (A) and after digestion of molecules with benzonase (B) indicating the maximum possible increase in FL. It is of note that the MB concentration (other than for subsequent measurements) was at 100 nM. Digestion was for 2 hours at 30°C and 800 rpm on an Eppendorf Thermomixer employing 0.6 units enzyme in the sample.



Supplementary Figure S8: Negative controls demonstrating no MB interaction with the negative ssDNA control (A) or the RNA ladder (B) as well as no significant signal increase for the MB alone upon sample heating for 15 min to 56°C followed by cooling (C) or incubation with another HRV strain (HRV-B14) and heating for 15 min to 56°C followed by cooling (D).



Supplementary Figure S9: In case RNA release and sample measurement were within several hours and sample storage was on ice and under light protection the obtained signals for the MB / RNA complex were in the range of approx. 10 % from an average - between first (left) and last (right) measurement lay approx. 4 hours.

3.1.1. Comparison of two MB preparation batches

A comparison of two MBs preparation batches was carried out by chip CE using the RNA 6000 Nano Kit of *Agilent Technologies*. The result of the comparison of the two MB preparation batches can be displayed as a gel image. Figure 18 gives an overview of the MBs preparations from 2014 (sample 1-3) and from 2015 (sample 7-9) as well as of the three targets that were synthesized in 2014. A provided RNA ladder containing up to six RNA sequences of different length was applied as an internal marker on the Bioanalyzer RNA 6000 Nano chip. The actual composition of the RNA segments was not published by the company. The electropherogram of the ladder is plotted in Figure 19. An overlay of the corresponding electropherograms of each of the three MB is provided in Figure 20.

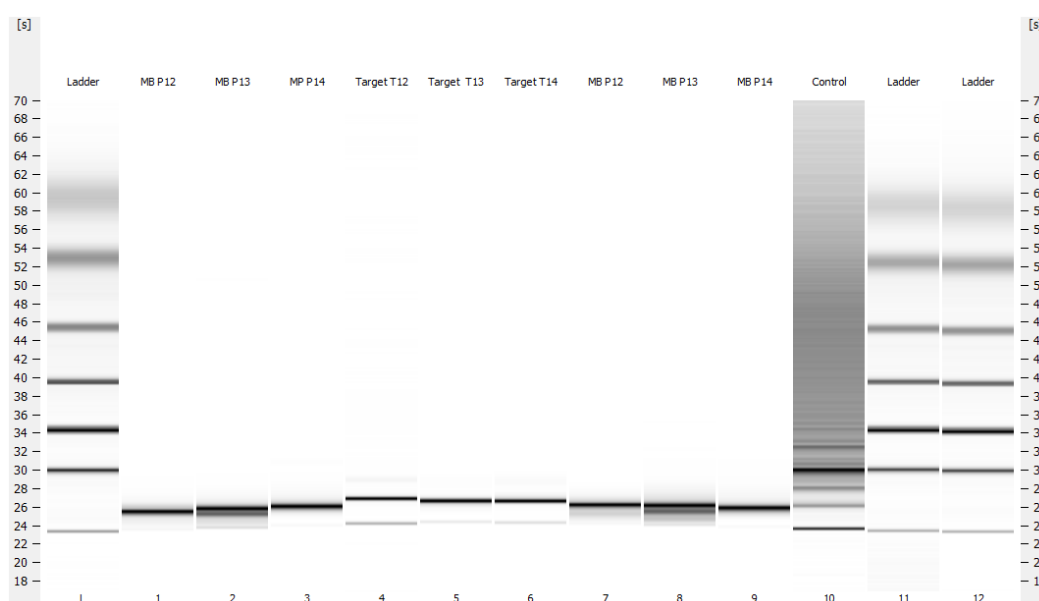


Figure 18: Gel-like image obtained on the Bioanalyzer RNA chip for the comparison of two different MB preparations: sample 1-3: older MB batch (P12, P13, P14), sample 4-6: DNA targets (T12, T13, T14), sample 7-9 newer MB batch (P12, P13, P14)

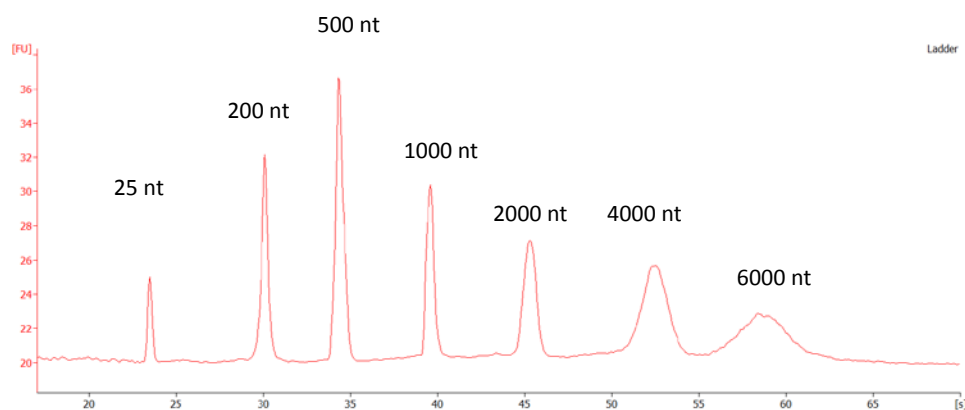


Figure 19: Electropherogram of the RNA ladder provided by Agilent; BGE is part of the provided RNA 6000 Nano Kit (Gel-Dye- mix)

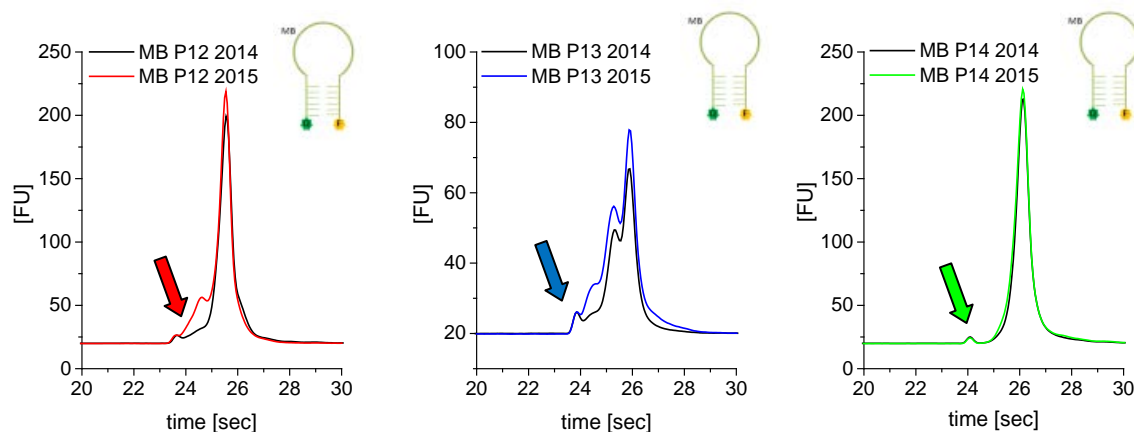


Figure 20: Overlay of the corresponding electropherograms of the previous and the new preparation batch of MB P12 (left), MB P13 (middle) and MB P14 (right); BGE is part of the provided RNA 6000 Nano Kit (Gel-Dye- mix); concentration of MB: 1 μ M in UHQ; electropherograms are manually aligned to the peak of the internal standard (arrow)

The electropherograms of the MBs are comparable to each other. A degradation of the MB synthesized in 2014 was not detectable in comparison to the newer batch. As a consequence of these experiments the older and newer MB preparation batch were mixed for further experiments. It is still unknown why MB P13 (blue) gives several peaks. This could probably appear from partly misfolding or problems in synthesis, i.e. impurities.

3.1.2. Specificity of the MB towards positive and negative controls

In the paper mentioned above [52] only MB P14, which binds specifically to the complementary sequence close to the 3' end of the viral genome, was considered. However, the equivalent experiments were also performed with two other MBs (MB P13, MB P12). MB P13 hybridizes to the complementary sequence in the central area, while MB P12 binds specifically near the 5' end of the viral RNA of HRV-A2 serotype.

A representative selection of the results obtained on the *Agilent* Bioanalyzer 2100 system is shown here. Further results are shown in the Appendix A.

Future experiments schedule the RNA release out of the viral capsid either by heating the samples or via acidification to mimic the endosomal environment. Hence, in order to ensure good comparability control experiments were also carried out to investigate the behaviour of the MBs alone at different incubation conditions:

- incubation at ambient temperature
- incubation at increased temperature at 56 °C for 15 min
- incubation at lower pH (< 5.6) at 30 °C for 30 min

The impact of increased temperature is shown in Figure 21, the impact of treatment with acid on the MB in Figure 22.

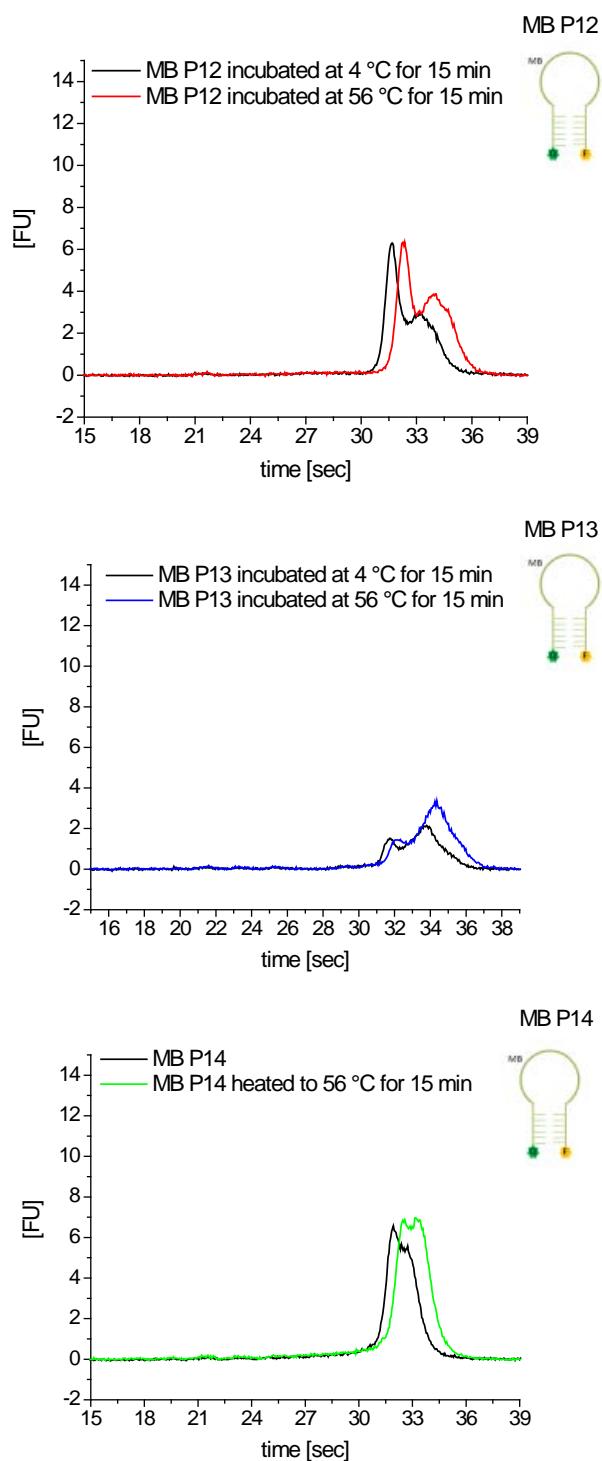


Figure 21: Impact of temperature on the fluorescence signal of the MBs: MB P12 shown in red, MB P13 in blue and MB P14 in green; BGE and sample buffer: solution C containing 10 mM Trolox; concentration of MBs: 40 nM; Electropherograms are aligned to the peaks of the internal standards.

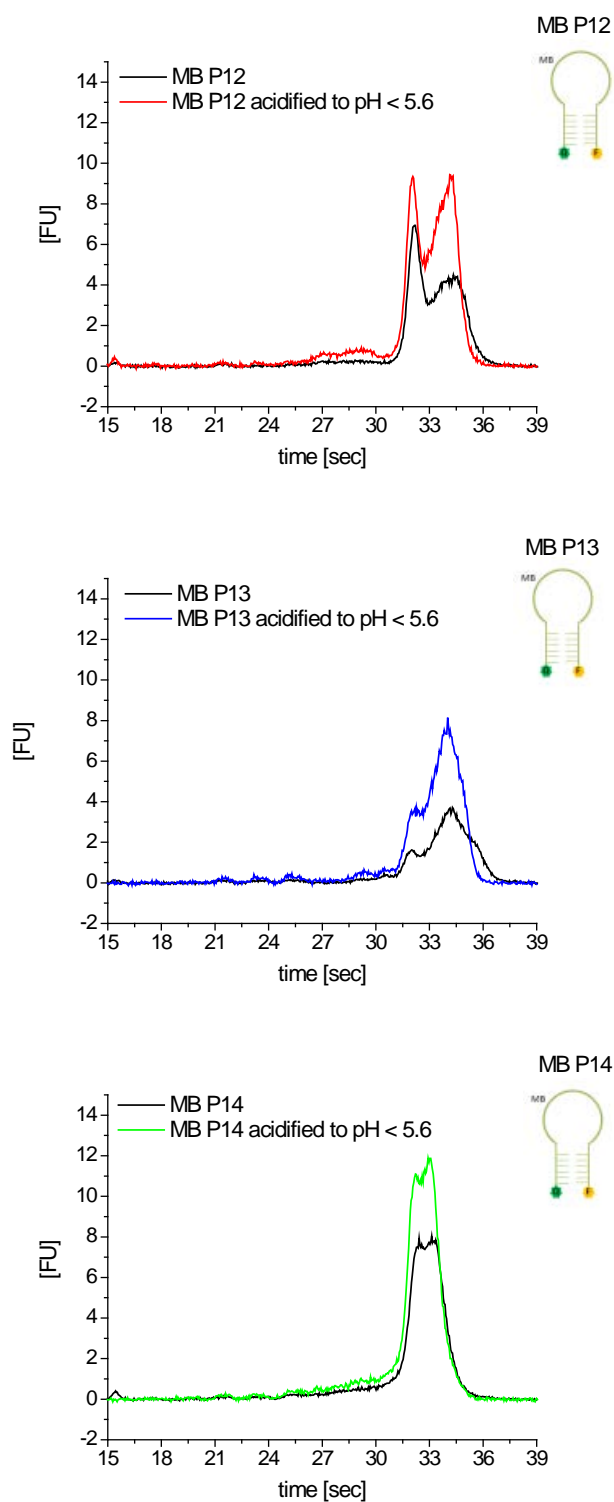


Figure 22: Impact of acidification to pH < 5.6 on the fluorescence signal of the MBs: MB P12 shown in red, MB P13 in blue and third MB P14 in green; BGE and sample buffer: solution C containing 10 mM Trolox; concentration of MBs: 40 nM; Electropherograms are aligned to the peaks of the internal standards.

Treatment of the MB with acid or by heat leads to slightly increased fluorescence signals especially for the former case. However, as shown in Figure 21 and 22 the signal differs from the increase in fluorescence resulting from hybridization of the MB to the corresponding target (see below in

3.1.2.1). Nevertheless, these slight changes of the signals have to be considered in case of detection of the hybridization of the MB to the released RNA of HRV-A2 or the positive controls.

3.1.2.1. Reactivity of the MBs towards positive control

In addition to each MB preparation, a specific single-stranded DNA target was synthesized based on the viral RNA sequence. The MBs were incubated with different concentrations of these DNA targets. *Weiss et al.* described a linear connection between an increasing concentration of the target and the increase of the fluorescence signal of MB P14 [52]. This behaviour can also be obtained for MB P12 and P13 by VUW in detail and additionally in my experiments as given in Figure 23 and Figure 24.

At this point it should be noted, that the signal of MB P13 is significantly lower than the fluorescence signal obtained from the two other MBs. This behaviour is also shown in Figure 20 concerning the comparison of the MBs batches. A direct comparison of the absolute fluorescence increase in case of hybridization to the target of the three applied MBs is not possible.

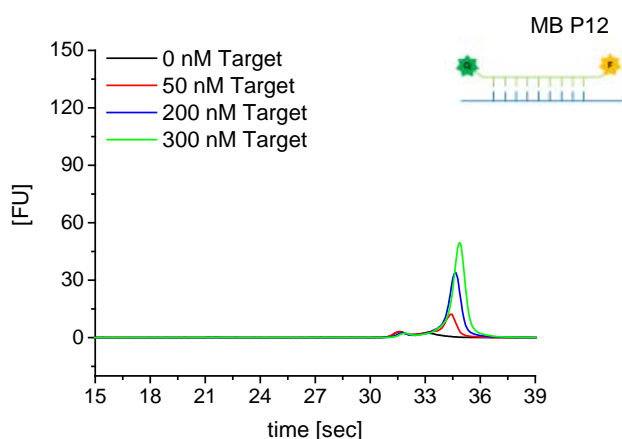


Figure 23: MB P12 incubated with different concentrations of specific DNA target to check the reactivity of the MB towards a perfectly complementary sequence; BGE and sample buffer: solution C containing 10 mM Trolox; concentration of MBs: 40 nM; concentration of the target as indicated; Electropherograms are aligned to the peaks of the internal standards.

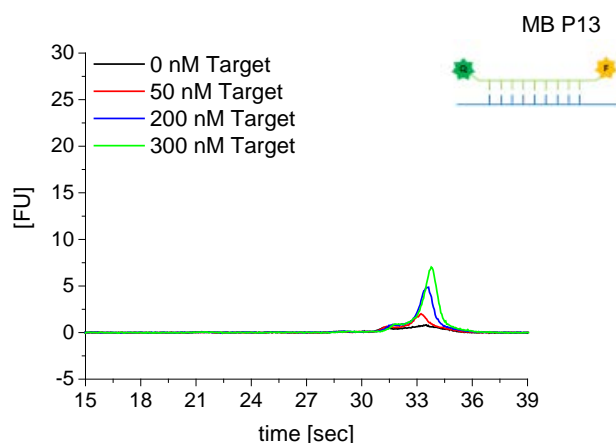


Figure 24: MB P13 incubated with different concentrations of specific DNA target to check the reactivity of the MB towards a perfectly complementary sequence; BGE and sample buffer: solution C containing 10 mM Trolox; concentration of MBs: 40 nM; concentration of the target as indicated. Electropherograms are aligned to the peaks of the internal standards.

3.1.2.2. *Reactivity of the MBs towards negative control*

The same experiments as with the complementary DNA targets were also performed with irrelevant single-stranded DNA target sequences. Again different concentrations of target were considered in these experiments. The corresponding electropherograms for each MB obtained at the Bioanalyzer are shown in Figure 25 for 200 nM DNA target concentration.

MB P12 and MB P13 did not show any interaction with an unspecific DNA target, as already observed for MB P14 [52].

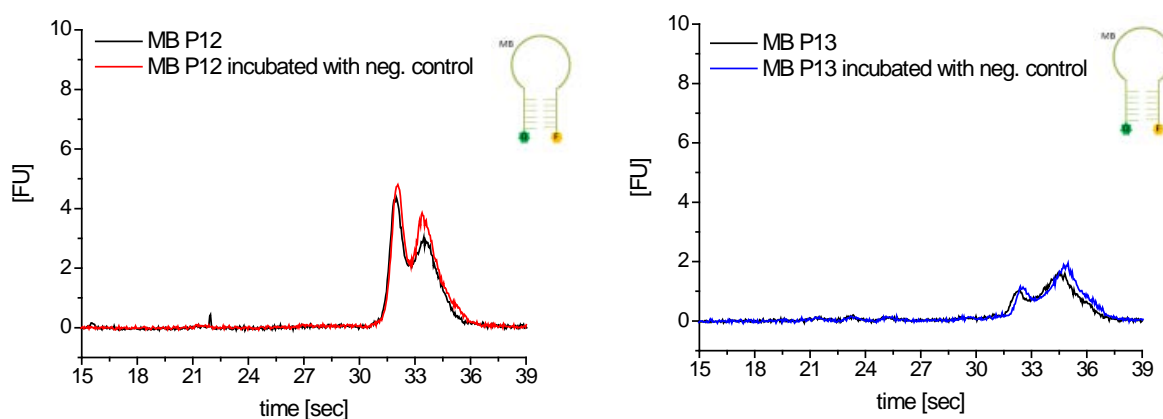


Figure 25: Control experiments introducing irrelevant DNA sequences as negative control to MB P12 and P13; BGE and sample buffer: solution C containing 10 mM Trolox; concentration of MBs: 40 nM; concentration of single-stranded DNA target: 200 nM; Electropherograms are aligned to the peaks of the internal standards.

3.1.2.3. *RNA ladder as negative control*

Additionally to the single-stranded DNA targets, a RNA target was applied to the MBs as negative control. A RNA ladder from the Agilent RNA Nano Chip kit was used for this experiment. This ladder contains six RNA transcripts of various lengths between 0.2 and 6 kb (see also the electropherogram in Figure 19). The actual concentration of the RNA transcripts is not given by the company. Hence, different volumes of ladder were added to the MBs.

This ladder material contains large amounts of additional components such as divalent cations or EDTA that could influence the behaviour of the MBs. Thus we attempted to desalt this RNA ladder with 200 mM Na-Borate, pH 8.4, by filtration through a 10 kDa spin filter membrane. Figure 26 shows that desalting of the RNA ladder led to degradation of the RNA fragments. Hence, this additional sample preparation step was not considered further.

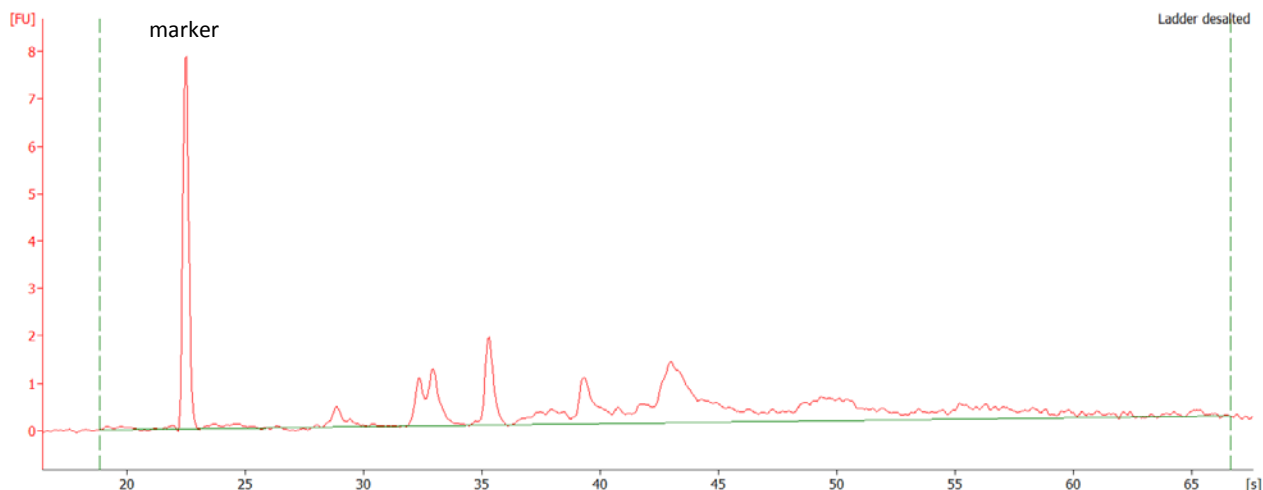


Figure 26: Electropherogram of the RNA ladder after desalting with solution B; BGE is part of the provided RNA 6000 Nano Kit (Gel-Dye- mix)

The incubation of the RNA ladder (without desalting step during sample preparation) in different quantities with the MB (P12, P13, P14) led to no detectable interaction. The results for MB P12 and P13 obtained on the Bioanalyzer are provided here as an addition to the already published data.

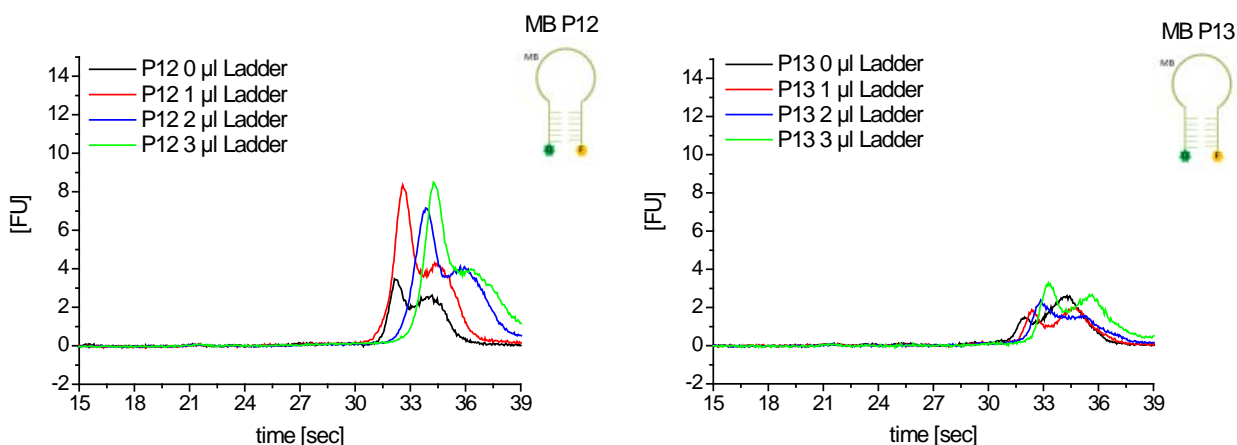


Figure 27: Electropherograms of MB P12 (left) and MB P13 (right) incubated with different amounts of RNA ladder as negative control; BGE and sample buffer: solution C containing 10 mM Trolox; concentration of MBs: 40 nM; Electropherograms are aligned to the peaks of the internal standards.

The fluorescence signal of MB P12 shows a small increase when incubating the MB with the RNA ladder. However, a positive reaction with the target sequence would give an increased fluorescence peak at a latter migration position, i.e. on the back of the MBs signal (see also electropherograms of the positive controls in 3.1.2.1). Hence, increase of fluorescence signals is possible related to additional buffer components of the RNA ladder, especially influencing electrophoretic sample injection to the separation channel of the Bioanalyzer chip. Likewise, slight changes in analyte migration despite sample alignment can probably be related to additional buffer components of the RNA ladder as well.

3.1.3. Stability of the MB in different buffers

Previous experiments showed that the additive Trolox increases the fluorescence signal though reduction of bleaching und blinking of the fluorophore [57]. However, long-term storage of the MB in the buffer containing 10 mM Trolox significantly influences the reactivity of these probes towards the target, while the signal of the closed hairpin-shaped MB increases even in absence of a corresponding target. Studies over a longer period confirm these observations. Electropherograms obtained on the Bioanalyzer system for MBs stored over a certain time period in Trolox buffer are depicted in Figure 28.

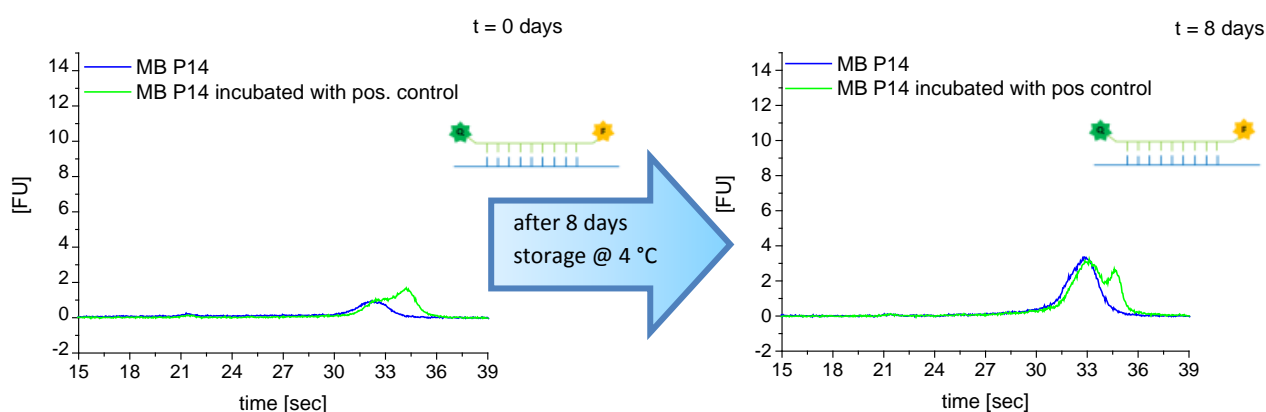


Figure 28: Comparison of the reactivity of MB towards a positive control obtained on analysis day 0 (left) and after storage of the MB in buffer containing 155 mM Na-Borate, 10 mM Trolox after 8 days (right); BGE and sample buffer: solution C containing 10 mM Trolox; concentration of MBs: 10 nM; concentration of DNA target: 40 nM; Electropherograms are aligned to the peaks of the internal standards.

Considering the fluorescence increase forced by the opening of the hairpin structure as result of the binding of the MB to the target sequence, one should note that there is only a weak signal resulting after a storage time of 8 days (Figure 28, right).

After storage in Trolox buffer over more than two weeks, the reactivity of the MB towards a single-stranded DNA target is not given any more, while the signal of the MB itself increases significantly. In addition, the degradation/aggregation/folding of the MB was detected in the leading part of the electropherogram in the range of 16 to 28 s (Figure 29)

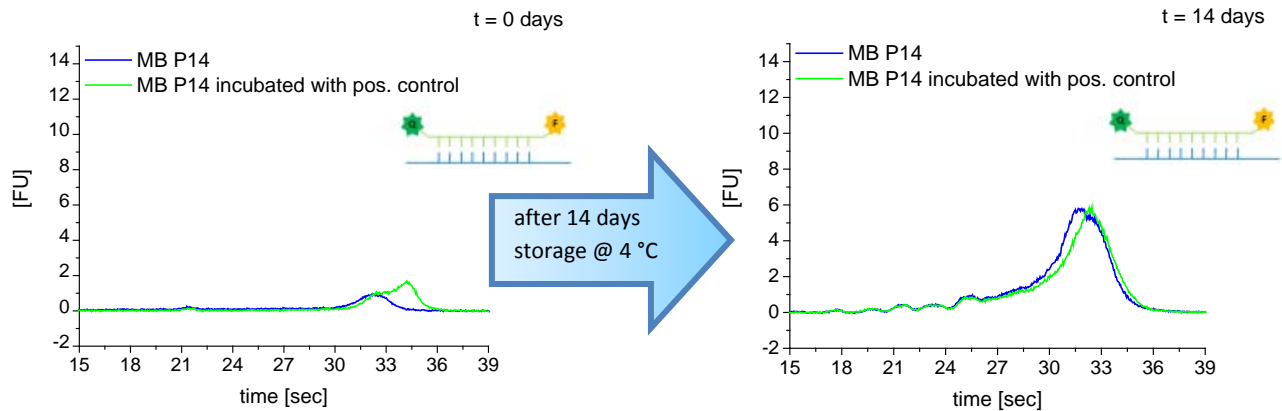


Figure 29: Long time storage of MB P14 in a buffer containing Trolox led to inactivity towards a positive control; BGE and sample buffer: solution C containing 10 mM Trolox; concentration of MBs: 10 nM; concentration of DNA target: 40 nM; Electropherograms are aligned to the peaks of the internal standards.

Therefore, adaptations in the storage buffer system were necessary. In order to encapsulate MBs in liposomes for detection of RNA transfer into the chosen cell model, a buffer system for the MBs with sufficient storability was required. To find out a suitable buffer system, different compositions were considered. The stability of the MBs and their reactivity towards respective positive controls were tested after defined storage times and compared to freshly prepared MB solutions.

In the following sections, the results obtained from these experiments are explained in detail for each buffer system separately. UHQ, ammonium acetate and sodium borate were considered. These experiments were performed with MB P14.

A) Buffer system: UHQ

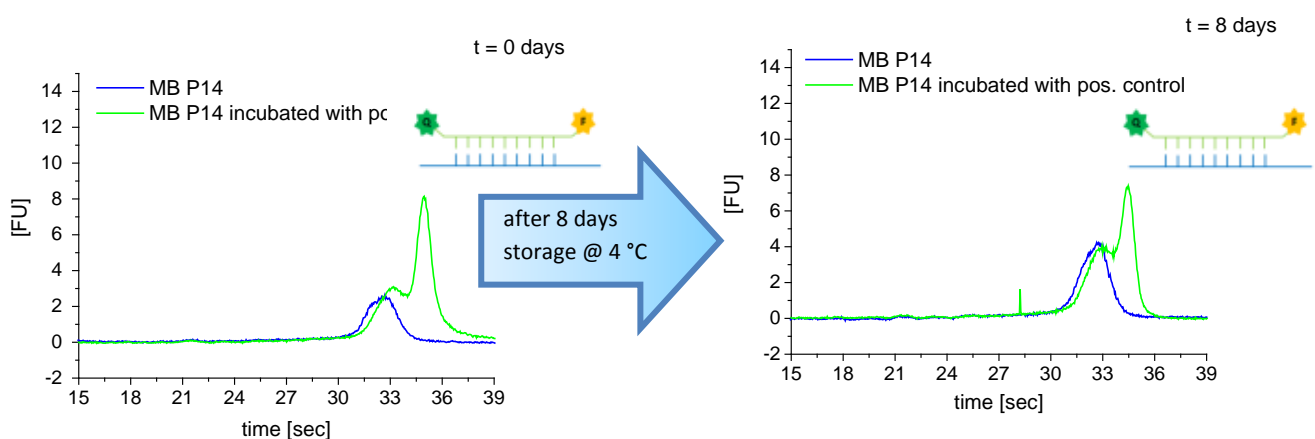


Figure 30: Comparison of the reactivity of MB P14 towards a perfectly complementary DNA target T14 stored in UHQ for 8 days (right) to fresh diluted solutions (left); BGE: solution C containing 10 mM Trolox; concentration of MBs: 10 nM; concentration of DNA target: 40 nM; Electropherograms are aligned to the peaks of the internal standards.

Storage in UHQ without any buffering system led to a decrease in reactivity of the MB and to changes in the structure of the probes. The changes of the MB structure result in an increase of the fluorescence signal of the MB itself (given in blue in Figure 30).

UHQ from the Millipore system is desalted via ion exchange and treated with UV light as well as particle filtration. Hence, UHQ water should contain very low residual amounts of salts that buffer the system. Therefore, the pH of UHQ might vary significantly because of its missing buffering capacity, which can influence the structure of MBs.

Additionally, the experiment was carried out with two different batches of UHQ. The results are equivalent; no difference between the two water batches was detected.

B) Buffer system: 10 mM NH₄Ac, pH 7.15

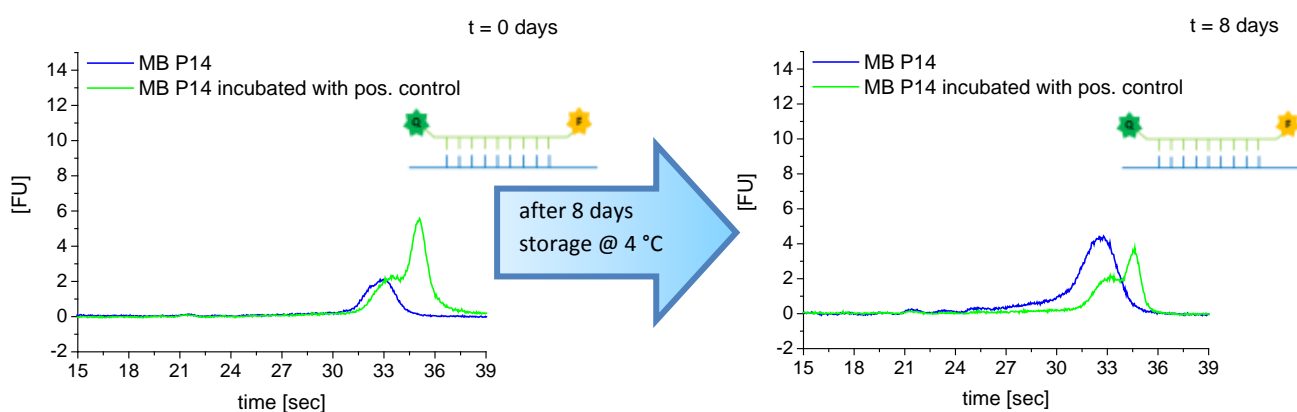


Figure 31: Comparison of the reactivity of MB P14 towards its complementary single-stranded DNA target T14 stored in 10 mM NH₄OAc for 8 days (right) to fresh diluted solutions (left); BGE: solution C containing 10 mM Trolox; concentration of MBs: 10 nM; concentration of DNA target: 40 nM; Electropherograms are aligned to the peaks of the internal standards.

In contrast to previous experiments the MBs stock solutions (0.5 mM) were already prepared in NH₄OAc, because of a sufficient stability of the MBs and the target sequences in case of long-time storage in this buffer. Ten mM NH₄OAc at pH 7.15 giving an ionic strength of approx. 10 mM in contrast to 42 mM of the BGE was used. As shown in the electropherograms in Figure 31 the reactivity of MB P14 towards the positive DNA target T14 decreases during storage of the probes in this buffer. A significant increase of the fluorescence signal of the beacon itself is also detectable after 8 days of storage time at 4 °C.

C) Buffer system: 200 mM Na-Borate, pH 8.4

In order to keep the differences between the background electrolyte (BGE) on the chip (containing 10 mM Trolox to enhance the fluorescence signal) and the buffer system during sample preparation as small as possible, in a third set of samples 200 mM Na-Borate, pH 8.4, without any additives was chosen. (The ionic strength I of 42 mM in the sample buffer is equal to I in the BGE.)

As shown in the following electropherograms the influence to the stability of the MBs during storage in this buffer is negligible.

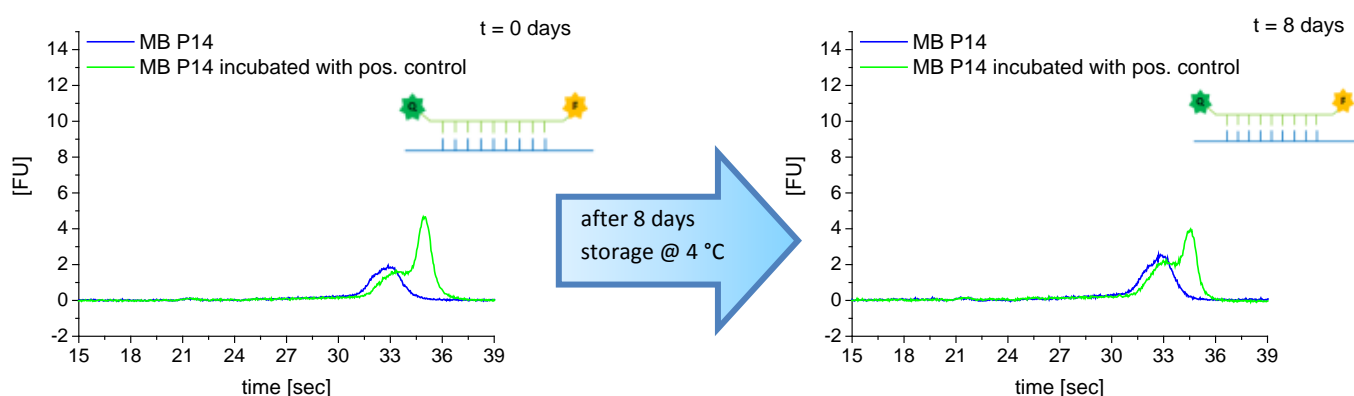


Figure 32: Comparison of the reactivity of MB P14 towards a perfectly complementary DNA target T14 stored in 200 mM Na-Borate, pH 8.4 without Trolox for 8 days (right) to fresh prepared solutions (left); BGE: solution C containing 10 mM Trolox; concentration of MBs: 10 nM; concentration of DNA target: 40 nM; Electropherograms are aligned to the peaks of the internal standards.

The total increase of the fluorescence signal resulting through hybridization of the MB to the target sequence is lower in comparison to MB stored in UHQ (Figure 30), but the reactivity after 8 days storage is significantly better (Figure 32). Even after a storage period of more than two weeks in this buffer, the MBs still show an acceptable reactivity. For this reason 200 mM Na-Borate, pH 8.4, was chosen for preparation of MB and target stock solutions for further experiments and for liposome preparation.

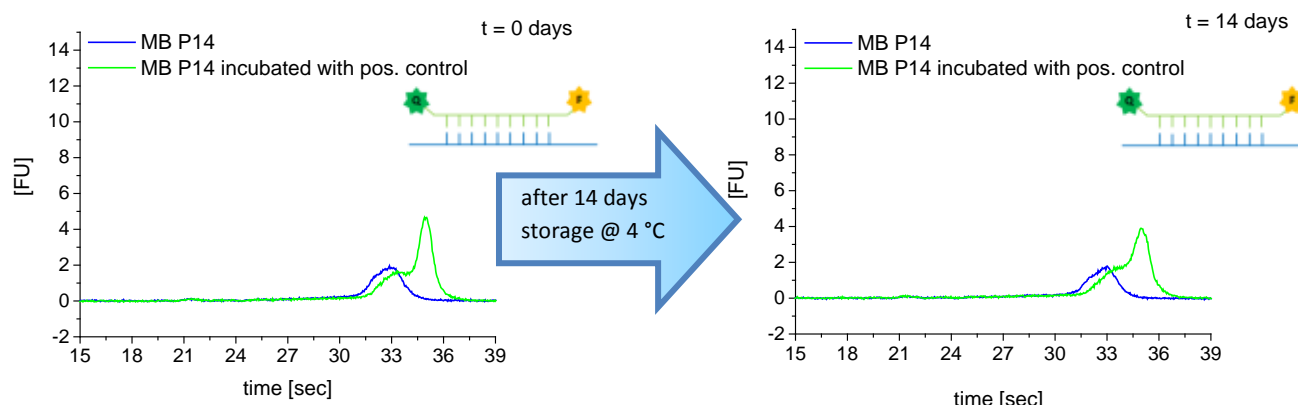


Figure 33: Comparison of the reactivity of MB P14 towards a perfectly complementary DNA target T14 stored in 200 mM Na-Borate, pH 8.4 without Trolox for 14 days (right) to fresh prepared solutions (left); BGE: solution C containing 10 mM Trolox; concentration of MBs: 10 nM; concentration of DNA target: 40 nM; Electropherograms are aligned to the peaks of the internal standards.

3.1.4. Influence of MgCl_2 on the MB

As in future work a cations gradient across a lipid membrane should be formed in order to facilitate the release of viral RNA into the liposomes, the impact of MgCl_2 on the MBs behaviour was assessed. The concentration of the total available MgCl_2 inside the cell [58] differs significantly from the concentration outside the cell [59]. MgCl_2 is also known for stabilizing the helix-like stem structure of the MB. In order to determine the ideal MgCl_2 concentration, MBs were stored in buffers containing different amounts of MgCl_2 . The stability of the MBs in the different buffers were tested in the same way described for the various buffer systems above - either in freshly prepared dilutions or after storage of MBs for at least 25 hours in buffers containing 0, 1, or 2 mM MgCl_2 . The aim of the experiments was to determine the maximum concentration of MgCl_2 that does not have any significant effect on the reactivity of the MB towards a positive control.

Figure 34 gives an overview of the influence of very low concentrations of MgCl_2 . The influence of 1 and 2 mM MgCl_2 on the reactivity of the MBs is shown in detail in Figure 35.

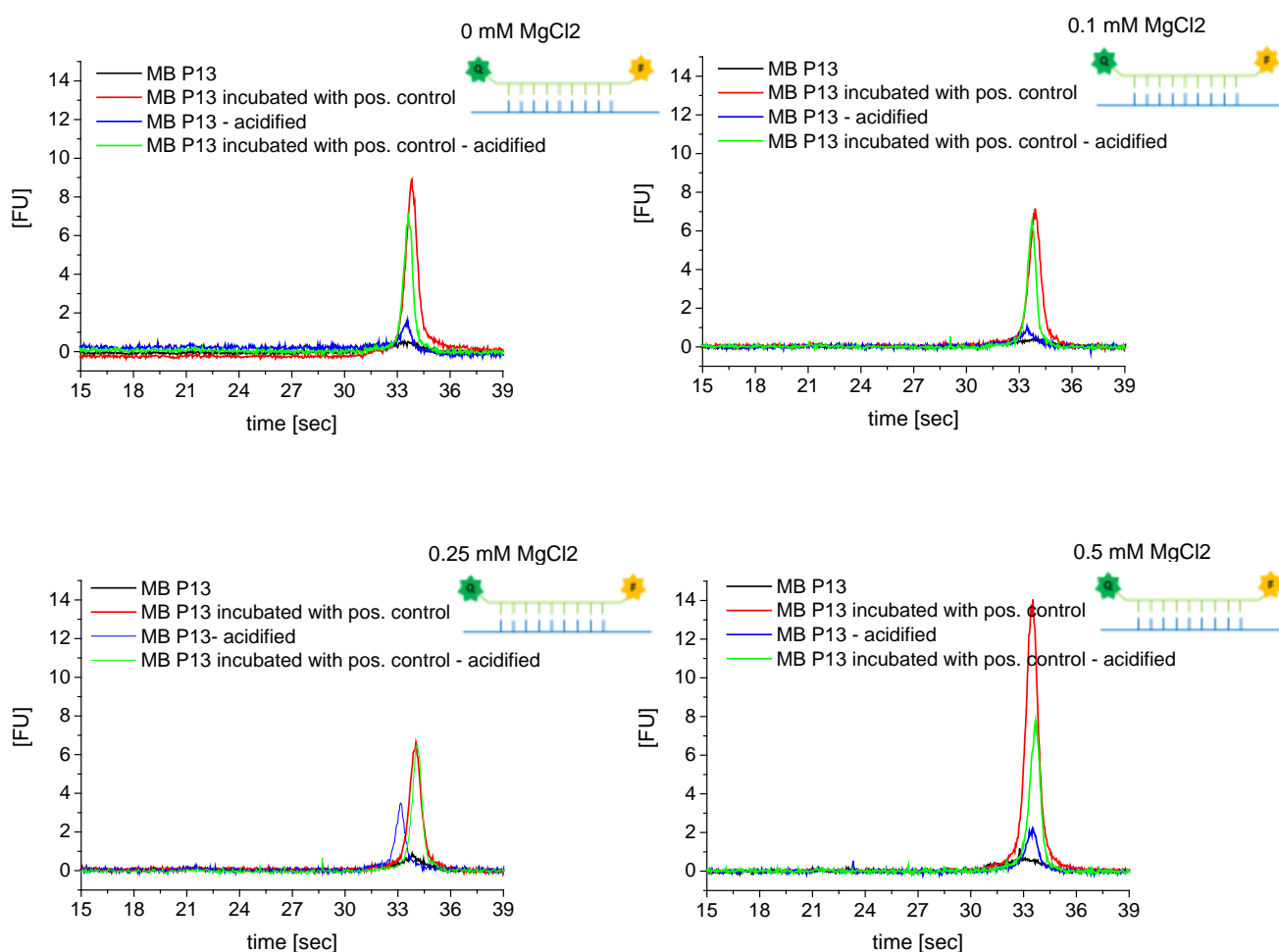


Figure 34: Influence of different amounts of the divalent cation MgCl_2 on the reactivity of the MBs towards the positive control; BGE: solution C containing 10 mM Trolox; concentration of MBs: 10 nM; concentration of DNA target: 40 nM; Electropherograms are aligned to the peaks of the internal standards.

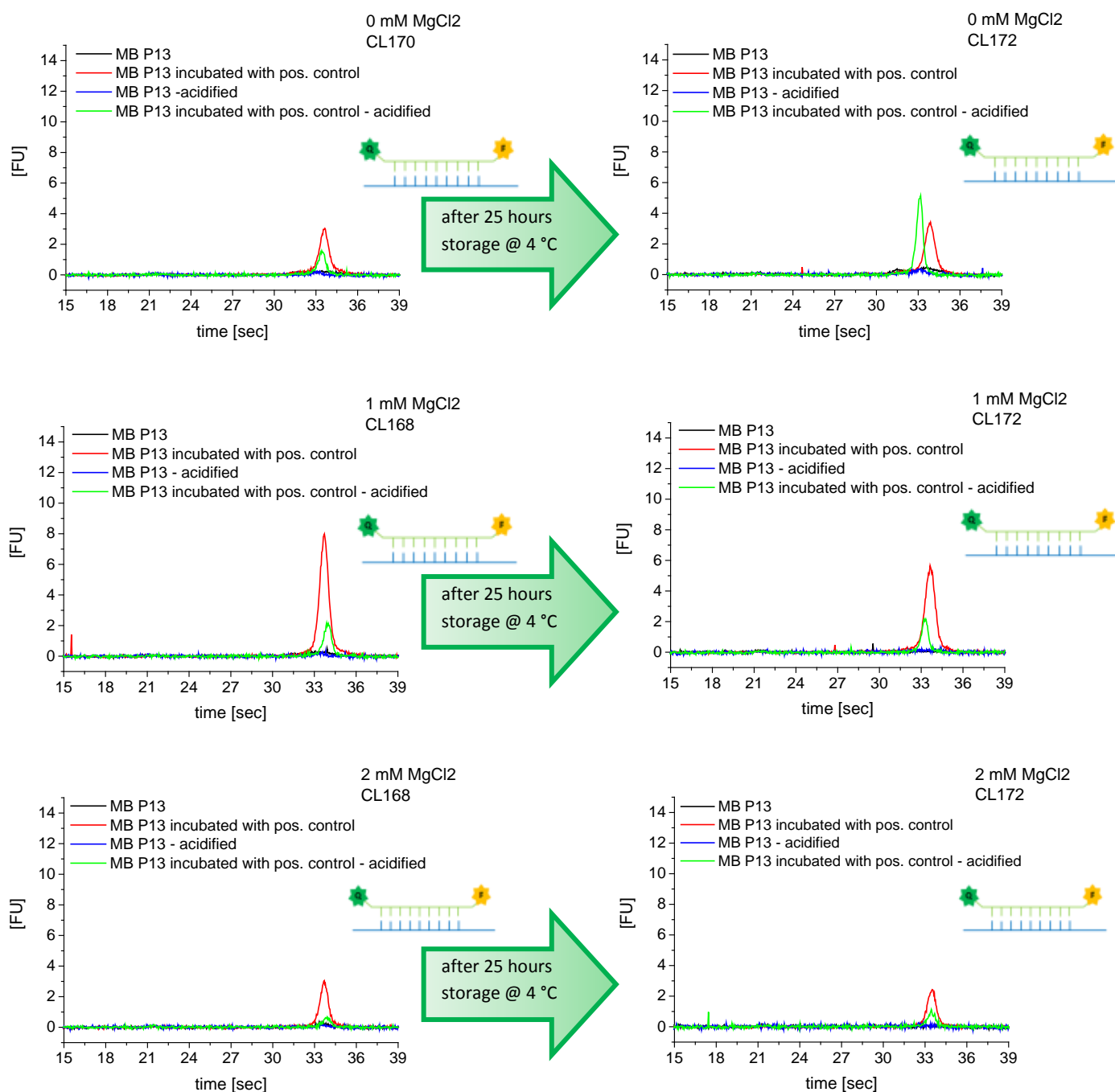


Figure 35: Comparison of the reactivity of MB P13 towards a complementary single-stranded DNA target when storing in buffers containing 0 mM MgCl_2 (first row), 1 mM MgCl_2 (second row) and 2 mM MgCl_2 (third row) for 1 hour (left) and at least 25 hours (right); BGE: solution C containing 10 mM Trolox; concentration of MBs: 10 nM; concentration of DNA target: 40 nM; Electropherograms are aligned to the peaks of the internal standards.

The influence of 1 mM MgCl_2 to the reactivity of the MB P14 towards the positive control is small in comparison to the influence of 2 mM MgCl_2 . As shown in Figure 33, the storage of MBs in higher MgCl_2 concentration led to significantly lower reactivity of the probes. This can be explained by the stabilizing effect of divalent cations like Mg^{2+} on the stem formation of the MB mentioned previously. As already described in chapter 1.4 the length of the complementary sequences of the probe arms forming the stem as well as the presence of certain positively charged ions influences the formation of the stem as well as the hybridization step of the MB to the specific target sequence. From my results it appears that the influence of a concentration of 1 mM MgCl_2 is low enough to give the MB the possibility to open and bind the target sequence without any additional help of e.g. temperature that would additionally force an opening of the stem helix. Furthermore, a concentration of 1 mM MgCl_2 allows to generate a distinct cation gradient across the liposomal lipid bilayer, the cell models membrane, by diluting the liposomes in the future experimental approaches (see also section 3.3.1.3). To confirm the sufficiently low influence of magnesium on the MB, the reactivity of the MB was tested again after 22 days of storage in this buffer system. As shown Figure 34 the MBs are still able to interact with the complementary target sequence. The decrease of the fluorescence signal in case of opening the stem structure of the MB upon binding to its target can be explained by the stabilizing effect of Mg^{2+} on the stem. This led to the assumption that the reactivity of the MB during a long-time storage in Mg^{2+} buffer system is not completely guaranteed and storage periods in excess of more than 2 weeks should be avoided.

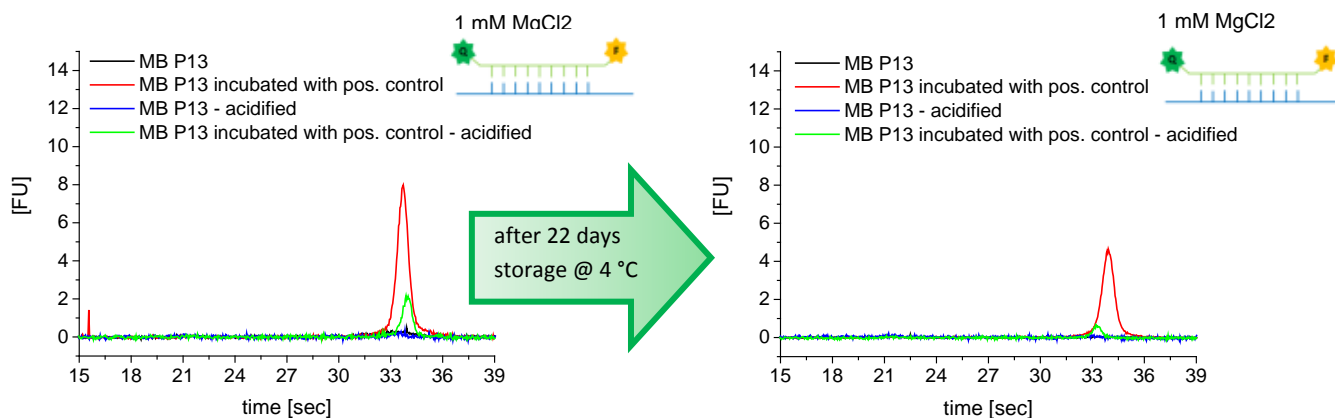


Figure 36: Reactivity of MB P13 towards positive control in buffer containing 1 mM MgCl_2 after 22 days of storage in comparison to 1 hour storage in buffer; BGE: solution C containing 10 mM Trolox; concentration of MBs: 10 nM; concentration of DNA target: 40 nM; Electropherograms are aligned to the peaks of the internal standards.

3.1.5. Influence of incubation temperature

Additional experiments concerning the influence of the incubation temperature (ambient temperature at around 22 °C, 30 °C or 37 °C) on MBs reactivity were also performed. As depicted in Figure 37 the existing protocol, which suggests an incubation step at 30 °C during the acidification of the samples to force the RNA release out of the viral capsid, does not need to be adapted.

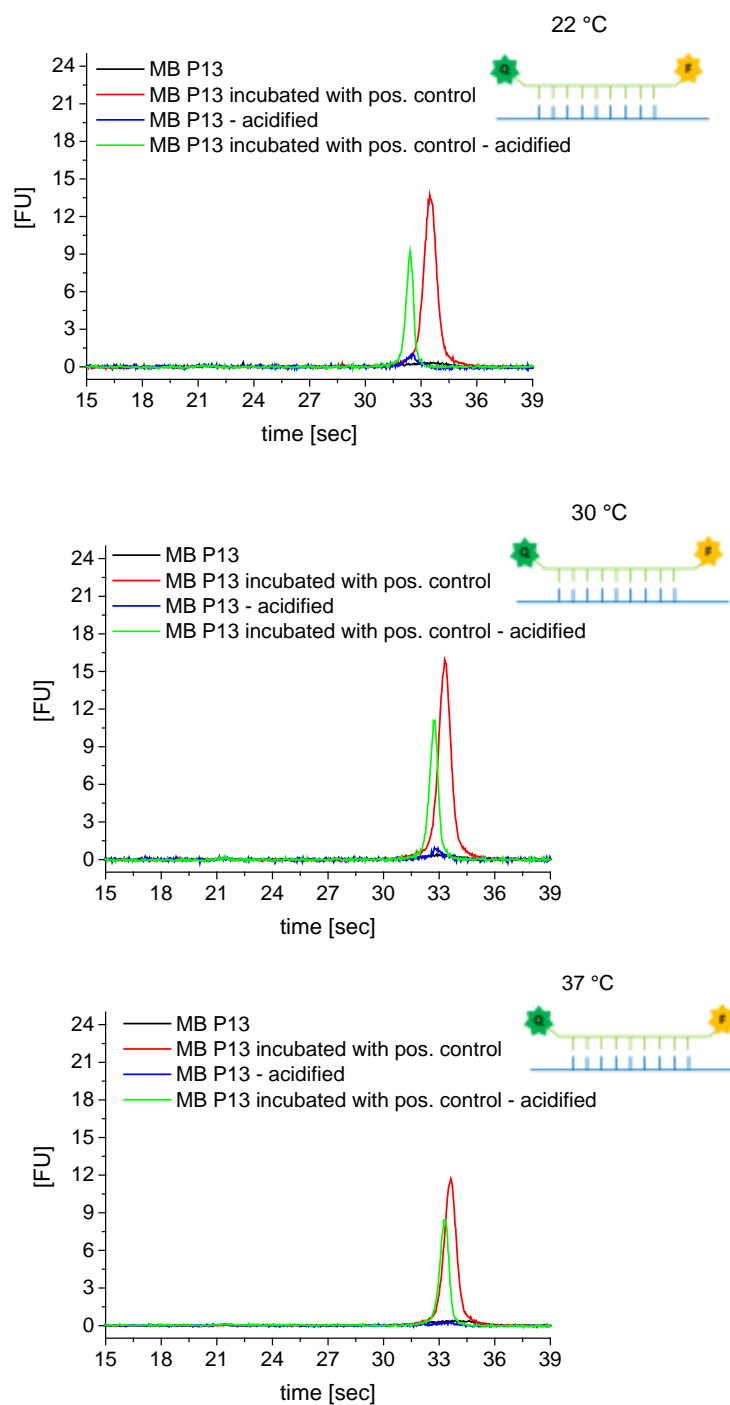


Figure 37: Influence of the incubation temperature to the reactivity of the MBs towards complementary single-stranded DNA target; BGE: solution C containing 10 mM Trolox; concentration of MBs: 10 nM; concentration of DNA target: 40 nM; Electropherograms are aligned to the peaks of the internal standards.

3.1.6. MBs reactivity towards released viral RNA

Before encapsulating MBs into liposomes to follow the viral material transfer through membranes, the specificity of the MB towards the released viral genome of human rhinovirus serotype A2 was tested. RNA release was either triggered through heating of the samples to 56 °C for 15 min or by acidification of the samples to a pH lower than 5.6 to mimic the endosomal environment.

In present work six different preparations of HRV-A2 and one preparation of HRV-B14 were available in different purity and concentration. Concentration was determined on GEMMA by fitting a Gaussian curve to the peak area. Table 23 provides a list of HRV preparations.

Table 23: Overview of the used HRV-A2 preparations: preparation A and B are not pure, preparations C-F are highly pure; HRV-B14 was used as negative control

Preparation #	Preparation date	Purification	Storage buffer	concentration [mg/ml]
HRV-A2				
A	04.10.2013, 1 st fraction	pyranosid treatment	50 mM Tris	5.7
B	30.01.2015, 1 st fraction	PEG precipitation	50 mM Tris	4.7
C	05.11.2015	CIM purified	50 mM Tris	5.3
D	25.11.2015	CIM purified	50 mM HEPES	1.7
E	22.01.2016, 1 st aliquot	CIM purified	50 mM Tris *	2.4
F	22.01.2016, 2 nd aliquot	CIM purified	50 mM Tris	2.4
HRV-B14				
I	n.a.	n.a	50 mM Tris	2.0

HRV-A2 preparation A and B have to be regarded separately from the remaining HRV-A2 preparations (C-F), because these two preparations are not CIM purified and contain an unknown contaminant that could influence the viral uncoating.

3.1.6.1. RNA release triggered by temperature

The interaction of the three MBs with the viral RNA after heating the samples to 56 °C is shown as an example for virus preparation #B (30.01.2015). These experiments are only valid for those virus preparations that are not CIM purified (#A and #B). Peaks for the respective MB/RNA complexes appear at positions as detected for MBs complexed to positive controls.

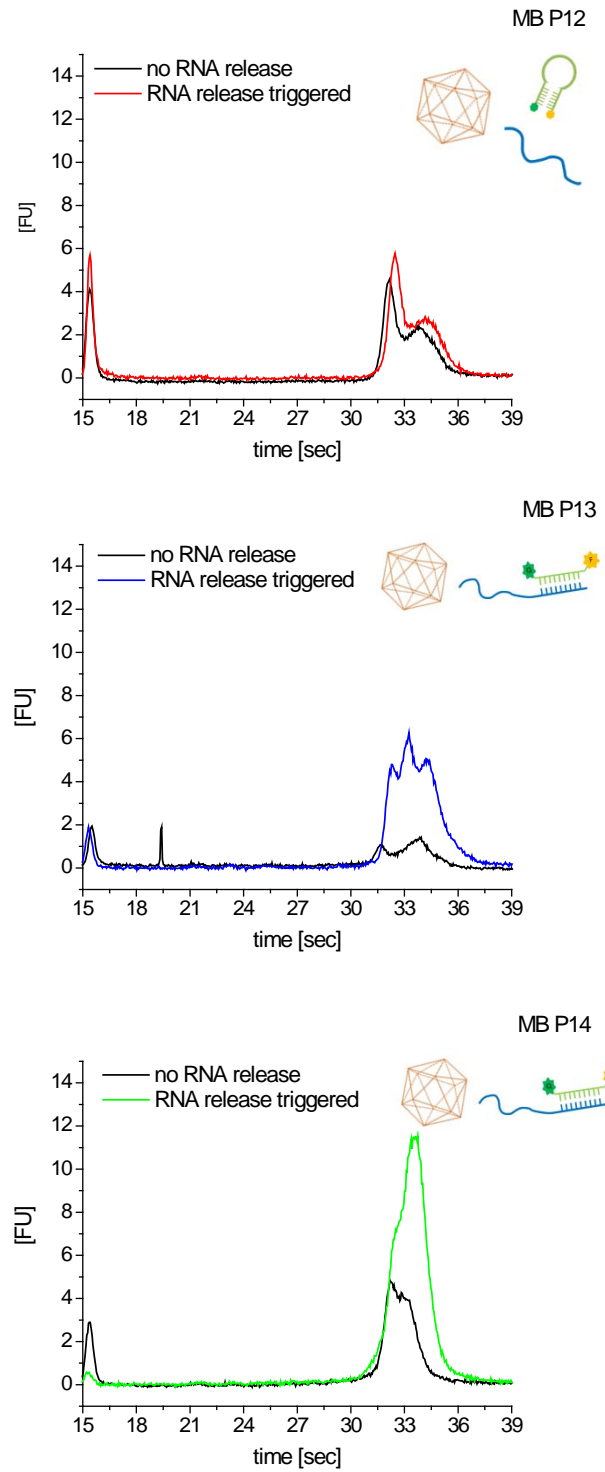


Figure 38: Reactivity of MB P12 (first), MB P13 (second) and MB P14 (third) towards released viral RNA of HRV-A2, preparation B – RNA release was triggered by heating the sample to 56 °C for 15 min; BGE and sample buffer: solution C containing 10 mM Trolox; concentration of MBs: 40 nM; Electropherograms are aligned to the peaks of the internal standards.

MB P13 as well as MB P14 were able to bind specifically to the complementary sequence of the released viral RNA. As plotted in the first electropherogram in Figure 38, MB P12 does not interact with the released RNA. However, this could be explained by point mutations of the cultivated HRV-A2 or problems in MB synthesis.

In case of MB P13 and MB P14, which bind regions near the 3' end of the viral RNA, a significant increase of the fluorescence signal was detectable.

In contrast, incubation of the CIM purified HRV-A2 preparations (#C - #F) with these three MBs did not result in a signal. Neither hybridization of the MB to the released RNA nor a detectable signal of the MB after heating the sample was recorded. The corresponding electropherograms are shown in Figure 39, exemplary for MB P14.

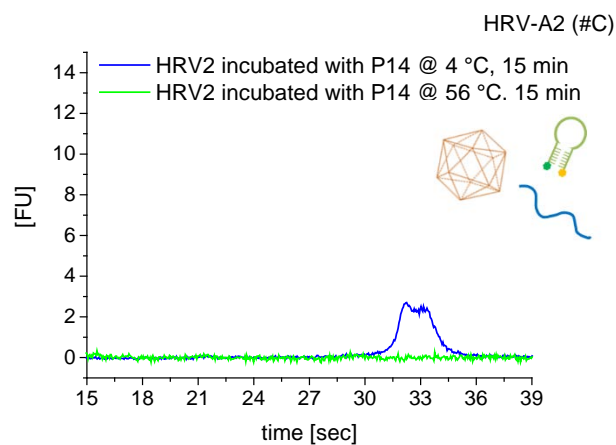


Figure 39: Incubation of HRV-A2 with MB P14 at 56 °C for 15 min to trigger RNA release out CIM purified virus preparations led to no detectable fluorescence signal; BGE: solution C containing 10 mM Trolox; sample buffer: solution B; concentration of MBs: 40 nM; Electropherograms are aligned to the peaks of the internal standards.

During CIM purification of virus preparations, high amounts of salts are necessary. However, these high amounts of mono- and divalent cations could influence the changes of the viral capsid and hence the RNA release out of the capsid is hindered. Additionally, divalent ions are known to stabilize the RNA structure also influencing the viral RNA release. Due to this reason an incubation step at 37 °C for 10 min was integrated in the desalting procedure to allow a buffer exchange even through the viral membrane. Upon virus incubation at 37 °C the interior of the viral capsid is accessible due to temporal formation of pores in the course of the so called “viral breathing”. Applying this step during desalting led to detectable signals of released RNA as shown in Figure 40 exemplary for MB P14 and RNA release through a temperature increase.

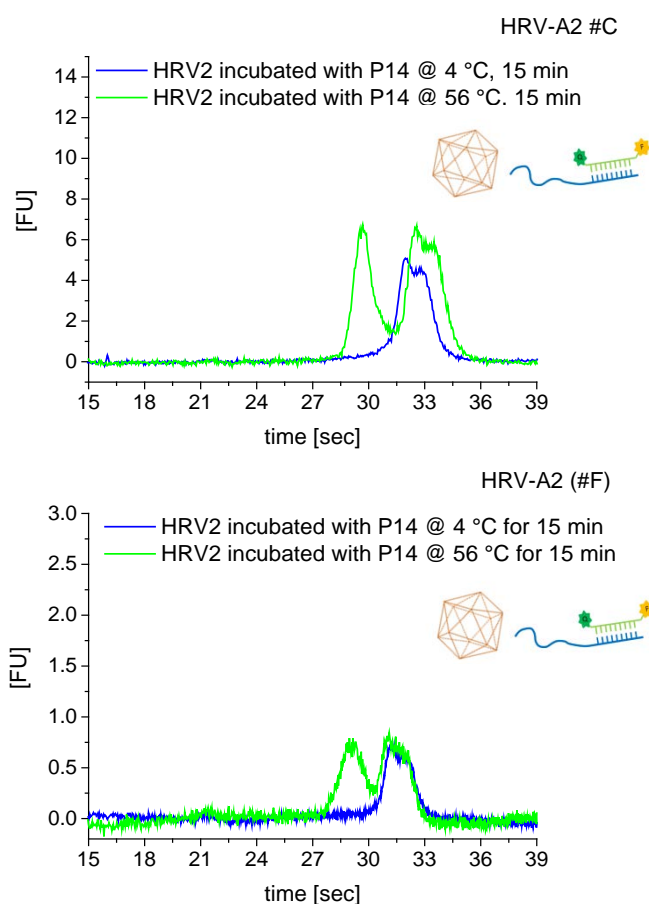


Figure 40: Detection of viral RNA release forced through increased temperature out of a CIM purified HRV-A2 preparation #C and #F with MB P14 after introducing an incubation step at 37 °C for 10 min during desalting; BGE: solution C containing 10 mM Trolox; sample buffer: solution B; concentration of MBs: 40 nM; Electropherograms are aligned to the peaks of the internal standards.

In contrast to the electropherograms for standards and previous HRV-A2 preparation a signal at around 29 s was recorded. This signal corresponds probably to the MB/RNA complex. However, a shift in migration time detected in comparison to experiments employing positive control DNA targets might be explained by additional proteins bound to the released RNA or by its complex folding.

Adding a contaminant with an until now unknown composition to the virus preparation before desalting and incubation at 37 °C led to slightly lower fluorescence signals for MB P14 hybridization to the RNA. This let us assume that the contaminant influences the viral uncoating and needs to be removed from the virus preparation (by e.g. CIM purification) before simulation the *in vivo* cell infection employing liposomes.

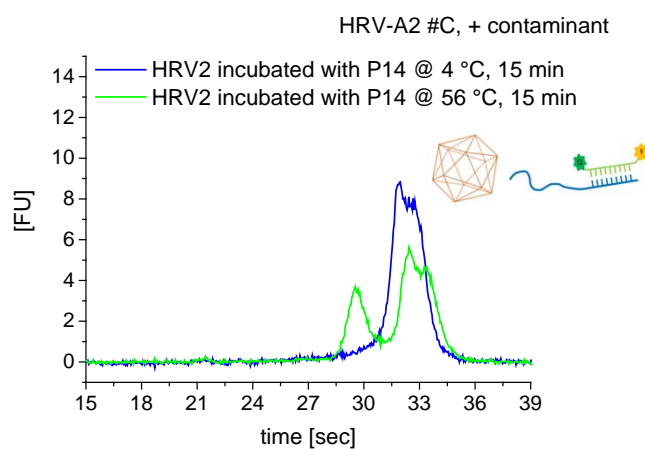


Figure 41: Adding the contaminant to CIM purified HRV-A2 influences the viral RNA– fluorescence signals are less intense than in absence of the contaminant; BGE: solution C containing 10 mM Trolox; sample buffer: solution B; concentration of MBs: 40 nM; Electropherograms are aligned to the peaks of the internal standards.

3.1.6.2. RNA release triggered by acidification

Future experiments plan to monitor the RNA transfer from the viral capsid into the liposome as cell model. Therefore, RNA release was also triggered by acidification to pH 5.3. The results obtained in these experiments are depicted in Figure 42.

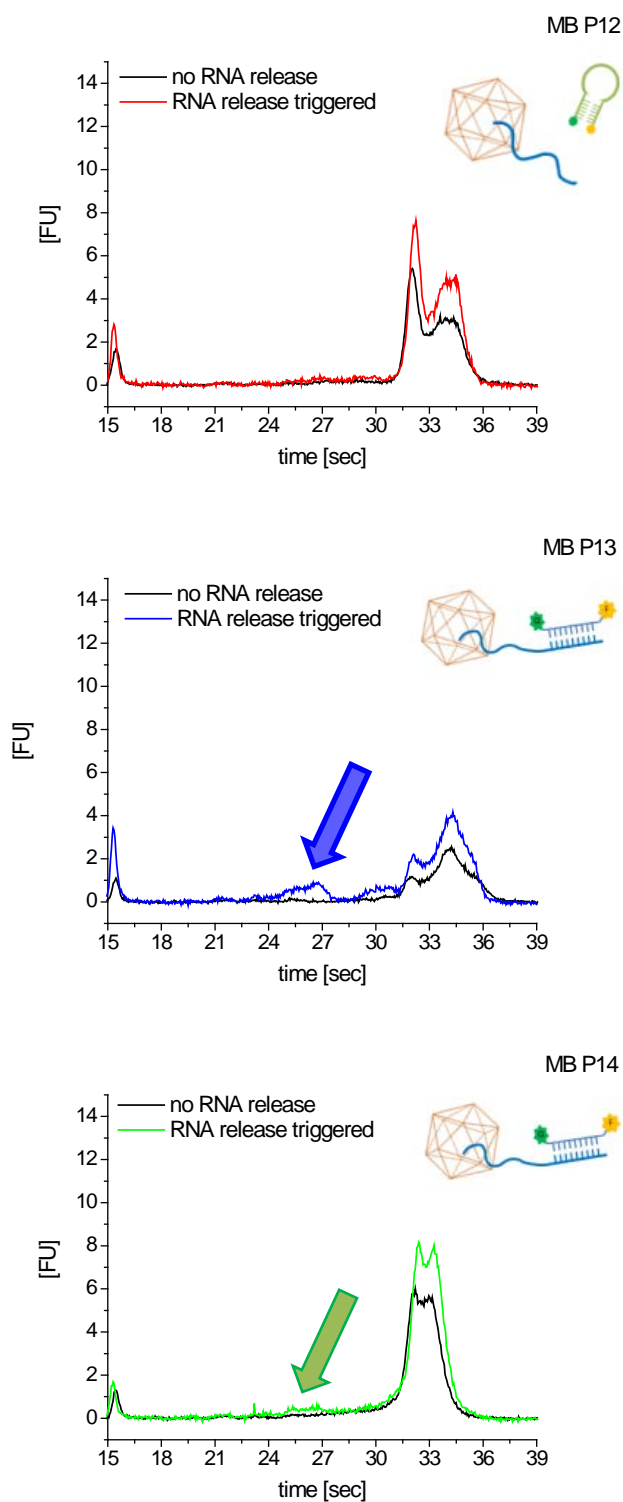


Figure 42: Reactivity of MB P12 (first), MB P13 (second) and MB P14 (third) towards released viral RNA of HRV-A2, preparation B – RNA release triggered by acidification to a pH of ~ 5.3; BGE: solution C containing 10 mM Trolox; sample buffer: solution B; concentration of MBs: 40 nM; Electropherograms are aligned to the peaks of the internal standards.

As for previous experiments, in which RNA release was triggered through sample heating, also the RNA release triggered by acidification resulted in a no detectable hybridization of MB P12 to the released RNA. In case of MB P13 in the second and in case of MB P14 in the third row a fluorescence signal at around 26 s migration time was detected: In contrast to heating the samples only partial RNA release and subviral particles attached to RNA that influences the migration of the complex on the chip were detected. It is of note that MB P13 yielded higher fluorescent signals for the MB/RNA complex than MB P14 upon triggering of viral RNA release via acidification. Therefore, MB P13 was employed for experiments including liposomes (see also 3.3.1).

3.1.6.3. HRV-B14 as negative control -RNA release triggered by temperature

As additional negative control a human rhinovirus serotype that is not specific for the here applied MBs, HRV-B14, was used. RNA release was triggered by heating the samples to 56 °C for 15 as in the previous experiments with HRV-A2. The results obtained at the Bioanalyzer are plotted in Figure 43.

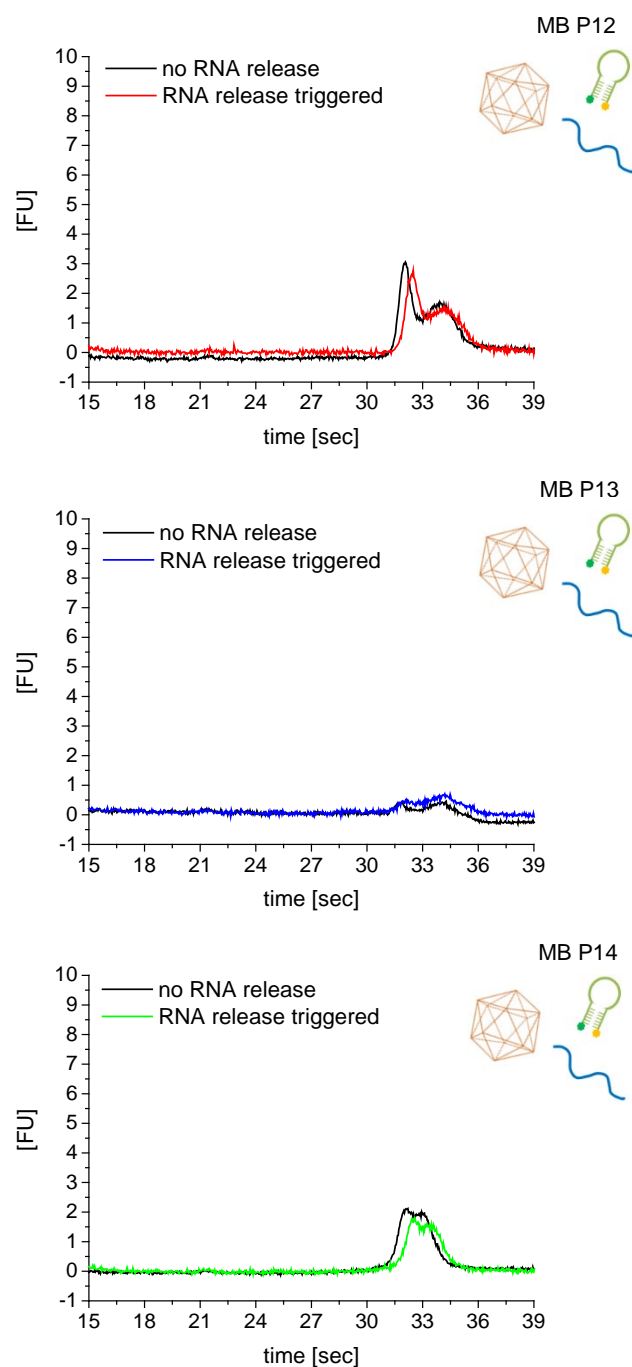


Figure 43: HRV-B14 as negative control for the MB P12 (red), MB P13 (blue) and MB P14 (green) – RNA release triggered by heating the samples to 56 °C for 15 min led to no interaction between the MBs and the released RNA; BGE: solution C containing 10 mM Trolox; sample buffer: solution B; concentration of MBs: 40 nM; Electropherograms are aligned to the peaks of the internal standards.

None of the three MBs was able to interact with the released RNA of HRV-B14. Hence, the applied MBs are specific for HRV-A2, but are not able to bind the tested different serotypes.

3.2. Liposome preparation

3.2.1. Quality control of liposomes at the GEMMA instrument

Each liposome preparation was measured at the gas-phase electrophoretic mobility molecular analyzer (GEMMA) instrument to control the quality of the vesicles preparation and to determine the dry particle size of the liposomes.

The produced liposomes can be divided into groups of non-physiological liposomes, liposomes of physiological lipid composition without Ni-NTA and those of physiological lipid composition carrying Ni²⁺ on the vesicle surface. The amount of lipids in the different preparations is already given in chapter 2.3.1. Depending on the lipid composition, different dry vesicle sizes were obtained. An overview on prepared liposome batches is given in the Appendix B.

Non-physiological liposomes

Non-physiological liposomes that consist only of HSPC, DSPE, Cholesterol and the fluorescence label NBD-PC are significantly larger in diameter as physiological ones (compare Figure 44 and Figure 46). The dry particle size of the liposomes that are passed through a 100 nm filter membrane during extrusion to form unilamellar particles is around 90 nm. Thus, the particle counts are relatively low when compared to physiological liposome due to the larger particle diameter.

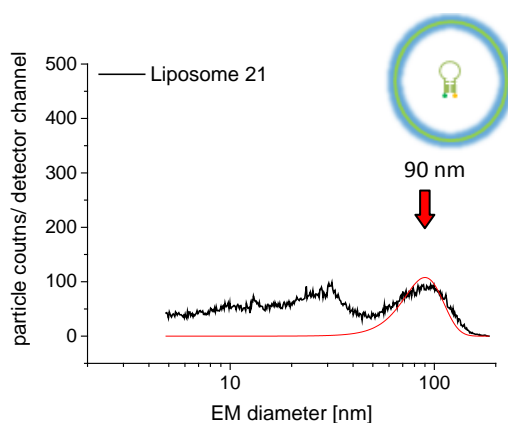


Figure 44: GEMMA spectra of non-physiological liposomes, extrusion at 100 nm results to dry particle sizes of liposomes around 90 nm; sample buffer: solution G

Physiological liposomes

Liposomes resembling more closely the composition of a cell wall consist of SOPC, SoyPE, Chicken Egg SM, Cholesterol and NBD-PC (fluorescence label). They are significantly smaller in their dry particle size than non-physiological liposomes. Particles that are passed through 200 nm filter membranes during extrusion are about 45 nm in diameter (Figure 45).

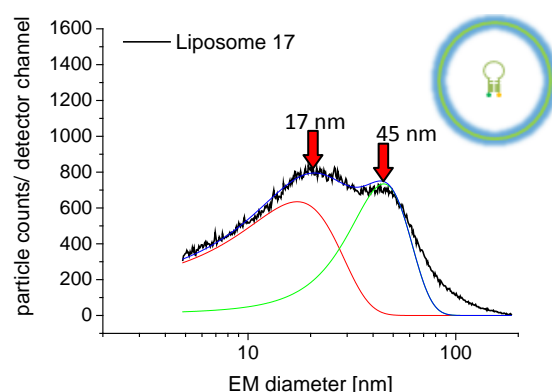


Figure 45: GEMMA spectra of a physiological liposome after extrusion through a 200 nm filter membran- the dry particle size is approximately 45 nm

The dry particle size is mainly influenced by the extrusion step in the liposomal production and the lipid composition. Normally, liposomes were extruded to 100 nm. Depending on the extrusion procedure the liposomes show different behaviors at the GEMMA instrument.

Figure 46 gives a comparison of two liposomal preparations of the same lipid composition and concentration and containing 250 nM MB P13 solution B, each. The GEMMA spectra differ significantly in their shape. Liposome 25 was extruded first 21times through a 200 nm filter membrane to achieve larger liposomes. An Aliquot was taken, then another 21 extrusion cycles through a 100 nm filter membrane for smaller particles were carried out. The result is a dry particle size of around 43 nm for the latter preparation. In contrast, liposomes 26 were only passed through a 100 nm filter membrane 21 times, which led to a larger dry particle size of around 65 nm. It can be assumed that the dry particle size depends strongly on number of extrusion cycles and on drawing of sample aliquots in between cycles.

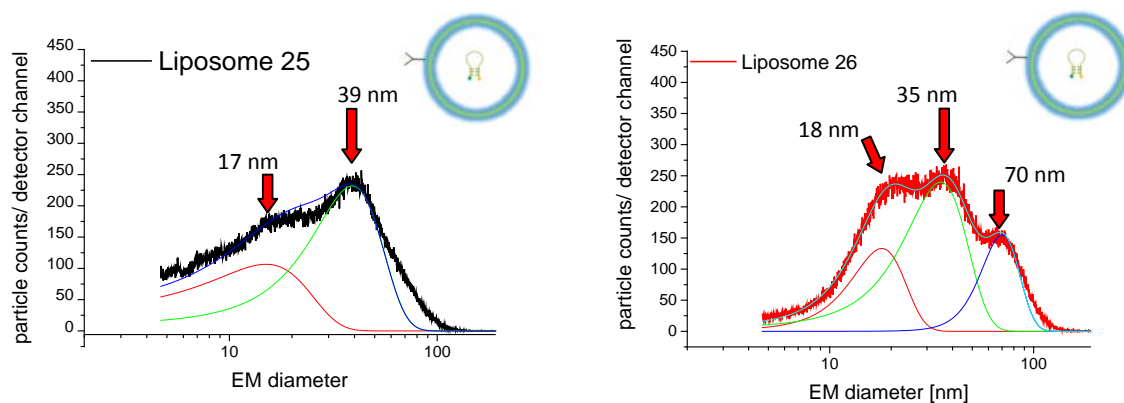


Figure 46: Comparison of two liposome preparations that show different behavior at GEMMA. Liposomes 25 were extruded sequential to 100 nm, while liposomes 26 were extruded in one step 10 100 nm. Sample buffer: solution G

Most of the liposome preparations showed a smaller dry particle size (around 43 nm; see also the list of liposomes in Appendix B) than non-physiological liposomes. The determined diameters were used for calculation of the necessary viral material for monitoring of the viral RNA transfer into the liposomes. For comparison reasons the ratio between liposomes and virus was kept constant at 1:2.

It is of note that the buffer for rehydration and consequently the buffer inside the liposomes showed only a slight impact on the dry particle size. Liposomes that were rehydrated with buffer containing Trolox were in average slightly smaller than liposomes without Trolox.

Due to loss of reactivity of the MB in Trolox buffer liposomes (preparation ID greater # 11) were produced without the buffer containing Trolox. In Figure 47, liposomes in Trolox buffer are compared to liposomes in 200 mM Na-Borate only.

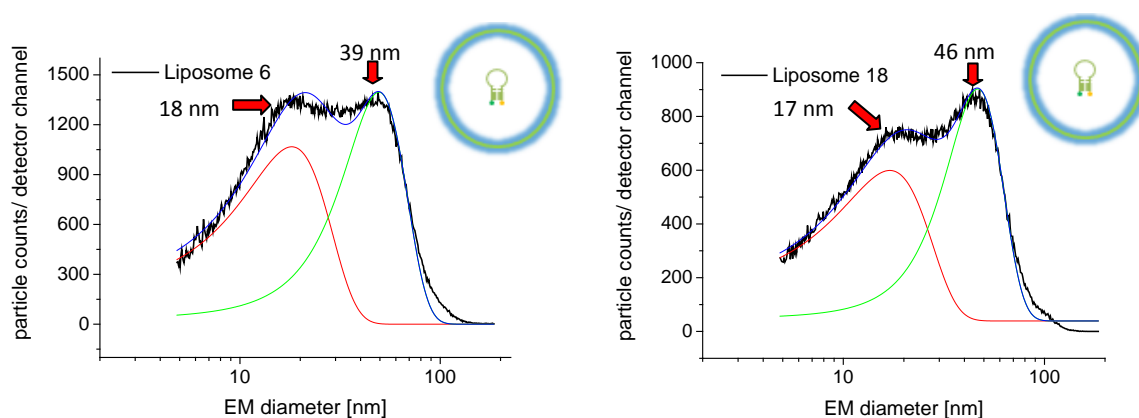


Figure 47: Comparison of liposome 6 containing 250 nM MB P14 in 155 mM Na-Borate, 10 mM Trolox, pH 8.4, and liposome 18 containing 250 nM MB P13 in 200 mM Na-Borate, pH 8.4, to show the impact of the buffer on the liposome dry particle size given in nm obtained at GEMMA; sample buffer: solution G

An impact of acidification or higher temperature to the liposomes was not detectable by the GEMMA instrument as shown in Figure 48. Sonicating of the liposomes for at least 20 min led to size reduction and well-expected destruction of the liposomes (Figure 49).

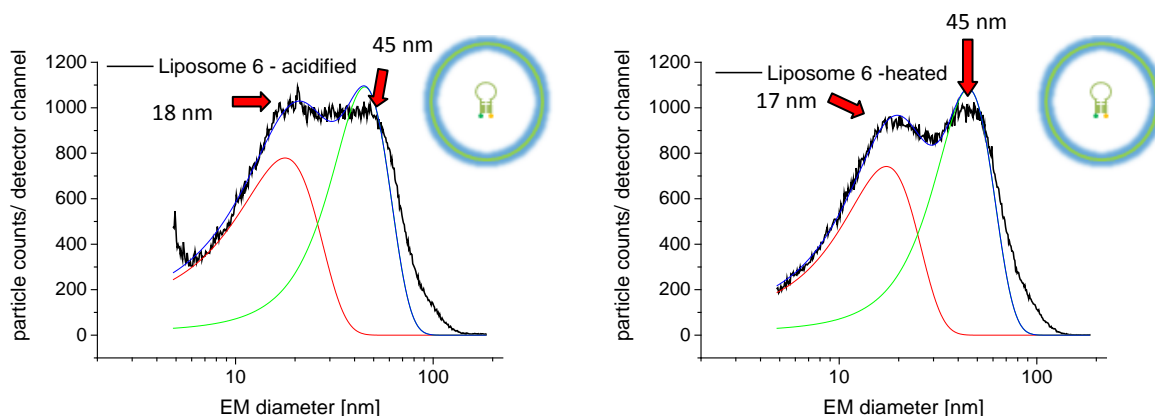


Figure 48: influence of acidification and increased temperature on the liposomes, determined at the GEMMA instrument; sample buffer: solution G

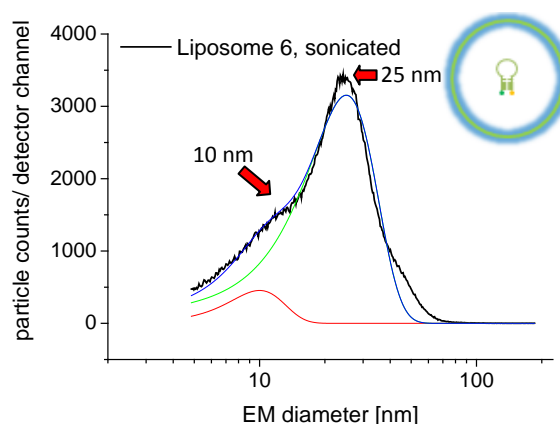


Figure 49: Sonification of the liposomes led to a reduction of the vesicle size and an increase of the detected counts in lower diameter range; sample buffer: solution G

Adding 5 mol% Ni-NTA (NGS-NTA), a Ni^{2+} complexing lipid, to the physiological lipid composition had no significant impact on the liposomal size. The average particle size of these liposomes is around 45 nm after a sequential extrusion (400/200/100 nm filter pore size, 21 passes each). An interaction between the recombinant MBP-V33333 receptor and liposomes was not detectable by the GEMMA instrument so far. As plotted in Figure 50, although liposome preparation #26 was incubated with MBP-V33333 receptor material no significant shift of the liposome peak to higher EM diameter values was detected (i.e. no attachment of the receptor molecules in sufficient amount or no attachment at all. It might be possible that the receptor molecules are inside the liposomes and therefore no size increase is detectable).

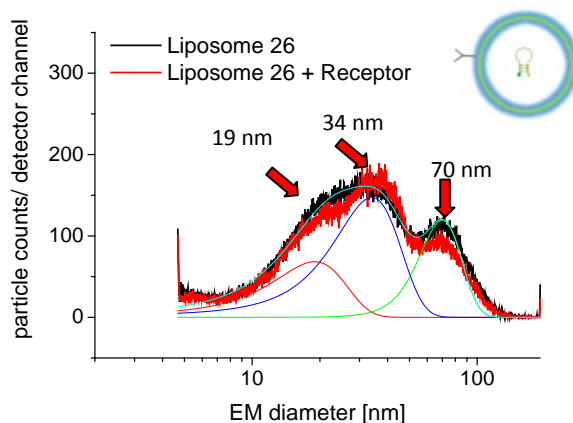


Figure 50: Comparison of liposome 26 without receptor (black) and incubated with receptor (red); sample buffer: solution G

3.2.2. Liposomes at the Bioanalyzer 2100 system

Additionally, the liposomes were tested in different dilutions on the Agilent Bioanalyzer 2100 system. Liposomes were loaded on the chip in dilutions of 1:2, 1:5, 1:10, 1:20, 1:25, 1:30 and 1:40 (v/v) in solution B to determine the lowest possible liposome concentration that can be detected. Depending on the liposome preparation, dilutions of 1:10 (v/v) up to 1:25 (v/v) of the liposomes (carrying a fluorescence labeled lipid) were detectable with the blue LED of the instrument. An example is plotted in Figure 51.

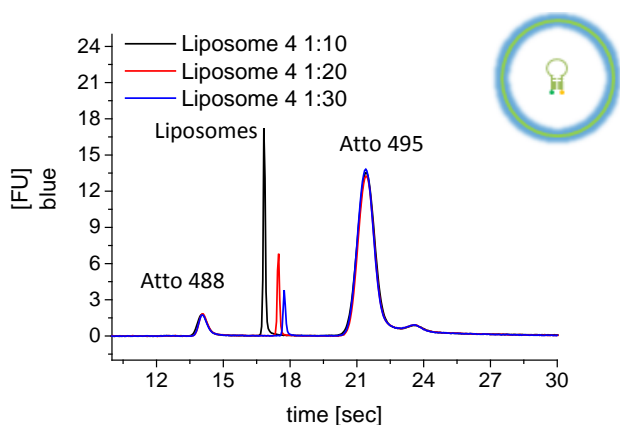


Figure 51: Detection of various liposome dilutions in the blue LED channel of the Bioanalyzer to determine the lowest detectable liposome concentration; sample buffer: solution G; Electropherograms are aligned to the peaks of the internal standards.

Furthermore the reactivity of the MBs outside of the liposome was tested after the whole preparation procedure against positive as well as against negative single-stranded DNA controls. Therefore the liposomes were diluted 1:10 (v/v) and incubated with a corresponding DNA target. For comparison reasons with future experiments samples were also acidified to a pH lower 5.6 as in the viral RNA release experiments. In the following, the results of these experiments for physiological liposomes without receptor (Figure 52), physiological liposomes containing additional MgCl_2 (Figure 53) and physiological liposomes with receptor (Figure 54) are given. No signal upon incubation of MBs with negative control single-stranded DNA is obtained.

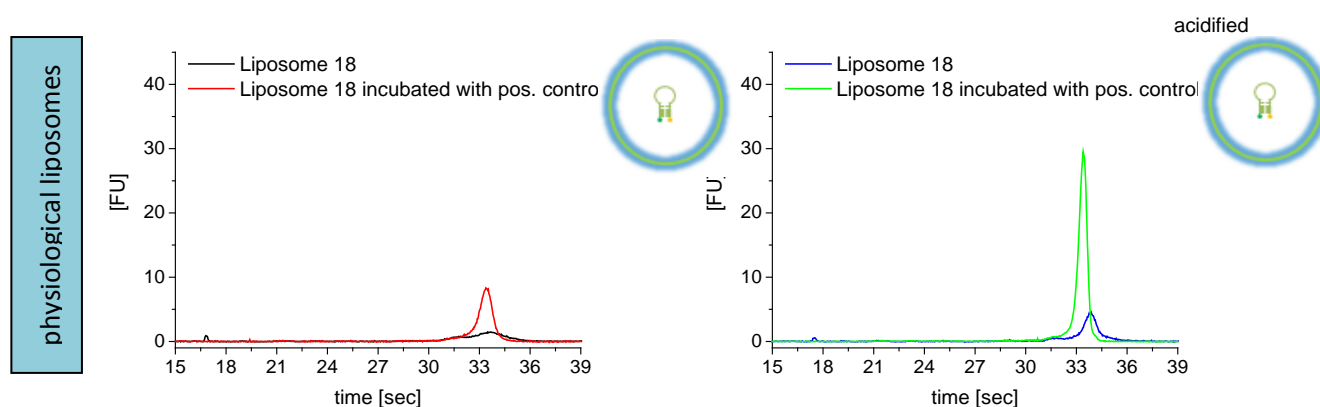


Figure 52: Reactivity of MB P13 outside the liposome towards a positive control- either in non-acidified (left) or in acidified (right) state; sample buffer: solution G; Electropherograms are aligned to the peaks of the internal standards.

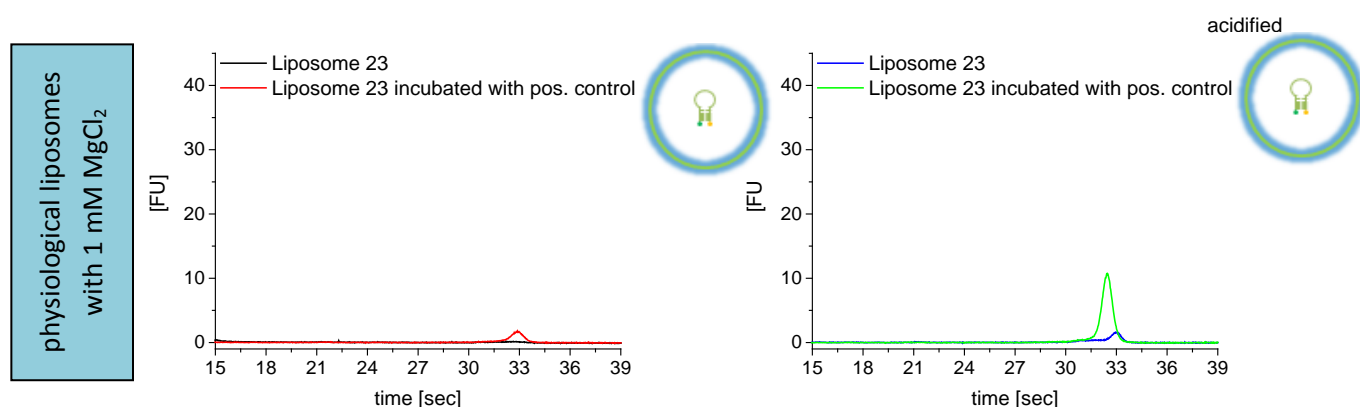


Figure 53: Reactivity of MB P13 outside the liposome containing 1 mM MgCl_2 inside towards a positive control- either in non-acidified (left) or in acidified (right) state; sample buffer: solution G; Electropherograms are aligned to the peaks of the internal standards.

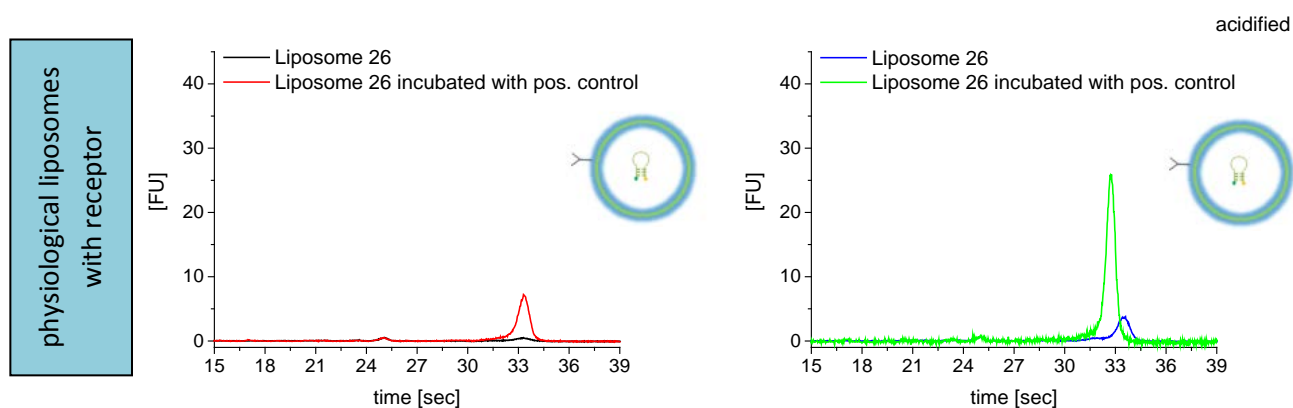


Figure 54: Reactivity of MB P13 outside the liposome with receptor towards a positive control- either in non-acidified (left) or in acidified (right) state; sample buffer: solution G; Electropherograms are aligned to the peaks of the internal standards.

The requirement of active MBs outside of the liposomes after the preparation and extrusion step was fulfilled for each liposomal preparation that was considered in further experiments with HRV-A2.

As shown in Figure 53 the reactivity of the MB in presence of divalent cations is reduced after longer storage. This phenomenon was also observed in the previous experiments, in which the influence of $MgCl_2$ was tested (3.1.4).

The presence of a receptor in the sample mixture did not influence the reactivity of the MB outside the liposomal vesicles as depicted in Figure 54 compared to Figure 52. No receptor was added to the latter liposome/MB sample. Acidification led to an increased fluorescence signal in all observed situations, even after correction of the electropherograms according to *Reijenga et al.* [51] and based on the intensity of the internal standards.

3.3. Viral RNA release into liposomes

3.3.1. Results on the Bioanalyzer 2100 system

The signals obtained on the Bioanalyzer 2100 system can be connected to certain analyte species in the experiments: Based on the migration time in the chip CE the electrophoretic mobility can be calculated and compared to the mobility values in literature [59]. The electrophoretic mobility of analytes that are not listed in literature, like liposomes, MBP-V33333 receptor or liposomes with bound receptor were determined on a CE (sample preparation: CL; measurement: VUW).

The calculation of μ ($\text{m}^2 \text{V}^{-1} \text{s}^{-1}$) is based on the total length of the capillary and the effective length of the separation part as well as on the applied voltage and the migration time. μ was calculated according to Equation 9.

$$\mu_{app} = \mu_{EOF} - \mu_{eff}$$

Equation 9

$$\mu_{eff} = \frac{l_{total} * l_{effective}}{voltage * t}$$

Equation 10

Table 24: Total length of the capillary and effective length of to calculate μ

l_{total}	0.598	m
$l_{effective}$	0.515	m
Voltage	20000	V

$$\mu_{EOF} = \mu_{eff} + \mu_{app}$$

Equation 11

μ_{EOF} ... electroosmotic flow

l_{total} ... total length of the capillary [m]

μ_{eff} ... electrophoretic mobility of particle i

$l_{effective}$... effective length of separation [m]

μ_{app} ... apparent electrophoretic mobility

μ_{EOF} was calculated based on the migration time of Atto 495. Atto 495 is a neutral marker that migrates with the electroosmotic flow. Hence, μ_{eff} is zero and μ_{app} is calculated according to Equation 10 ($\mu_{EOF} = \mu_{app}$).

A list of the electrophoretic mobilities, μ , and the migration time of the main components in the here present experiments is given in Table 25. A corresponding scheme based on migration time and the mobility is given in Figure 55 and can be used as template to assign the signal in the electropherograms more easily.

Table 25: Electrophoretic mobilities μ of native viral and subviral particles, liposomes, MBs and receptor MBP-V33333; purple marked values are literature given values [60], blue marked values were determined at CE and green marked values were determined on the Bioanalyzer 2100 system

Particle	μ^a	SD ^a	T	n	Migration time [s]
Atto 488*	-12.9	0.0	22.5	4	21.4
Atto 495*	0.0	0.0	22.5	4	14.05
Native 150S ^c	-5.7	0.3	20	36	16.6
135S ^c	-16.6	0.4	20	5	25.2
Intermediate All ^c	-13.0	1.4	20	11	21.5
Subviral 80S ^c (heat)	-9.5	0.2	25	21	18.6
	-8.2	0.3	20	21	18.0
Subviral 80S ^c (pH)	-9.6	0.1	25	21	18.9
	-8.5	0.3	20	21	18.2
Receptor MBP- V33333	18.7	0.1	22.5	4	28.1
Liposome	23.2	0.6	22.5	13	35.3
Liposome + Receptor MBP-V33333 + HRV2	14.1 HRV2 from 05.11.15	-	22.5	2	22.5
	15.1 HRV2 from 25.11.15	-		2	23.5
Molecular Beacon	21.6	0.1	22.5	5	33.0

T ... measuring temperature (°C)

SD ... standard deviation

^a [10⁻⁹ m²/Vs]

^c 100 mM sodium borate (pH 8.3), 10 mM Thesit

* Internal standards for electropherogram alignment

μ ... averaged from n measurements;

n ... number of measurmentes

^b 100 mM sodium borate (pH 8.3), 10 mM SDS

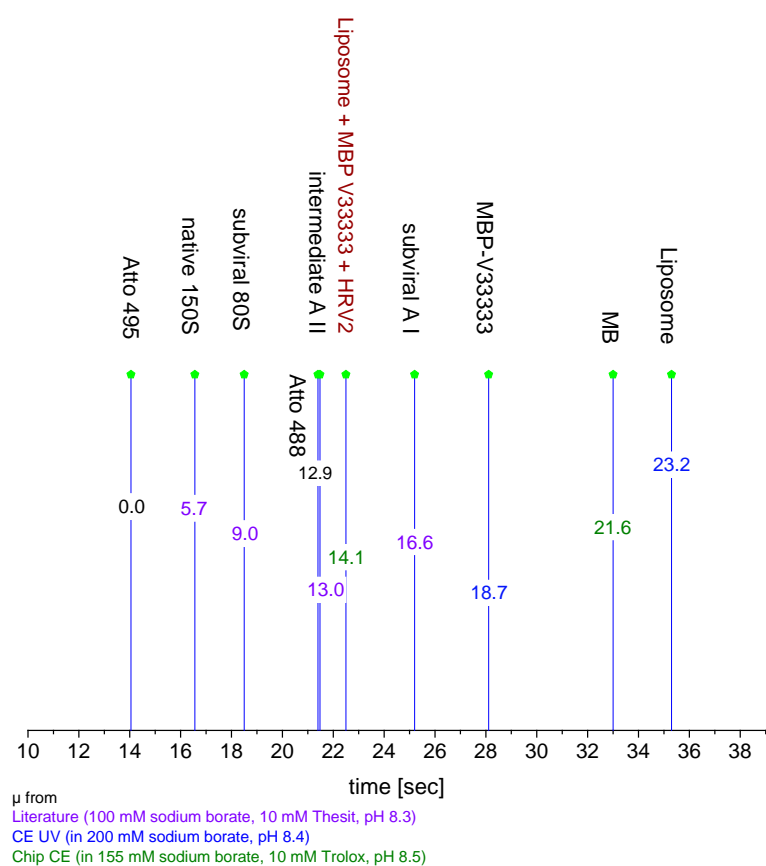


Figure 55: Electrophoretic mobility μ of native viral and subviral particles, liposomes, MBs, and receptor MBP-V33333 correlated to the migration time on the RNA Nano chip

3.3.1.1. Liposomes with physiological lipid composition without NGS-NTA

Liposomes in 155 mM Na-Borate, 10 mM Trolox, pH 8.4

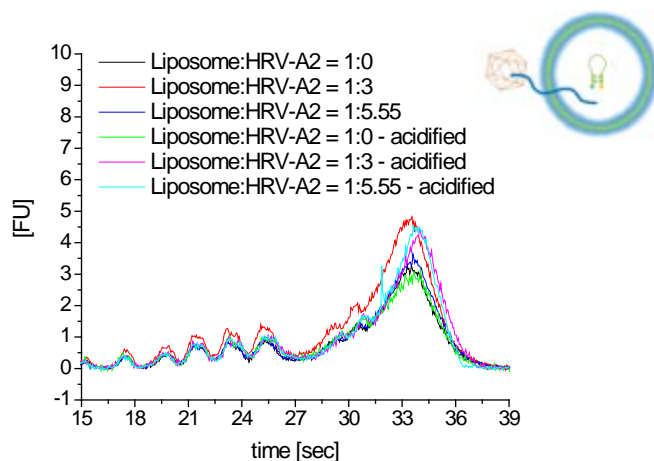


Figure 56: Liposome 10 incubated with different amounts of HRV-A2 preparation #C: no RNA release, but degradation of the MBs outside the liposomes in 155 mM Na-Borate, 10 mM Trolox, pH 8.4, is seen; Electropherograms are aligned to the peaks of the internal standards.

The electropherogram in Figure 56 shows a degradation of the MB outside of the liposome (signals between 15 and 30 s migration time) and hence no reactivity towards an eventually released RNA. Different ratios of liposome/virus were chosen to determine the detectable virus concentration in case of RNA release. No RNA release was detected even at the highest applied virus concentration that is about 5.55 times greater than the liposomal concentration (i.e. virus to vesicle ratio of 5.55 :1)

This liposome preparation (#10) contains Trolox buffer that is mainly influencing the MBs stability as already shown in 3.1.3. Due to this reason following liposome preparations were prepared with 200 mM Na-Borate buffer, pH 8.4, for rehydration of the lipid film.

Liposomes in 200 mM Na-Borate, pH 8.4

For subsequent experiments liposomes containing 250 nM MB P13 in 200 mM Na-Borate, pH 8.4, were incubated with three different HRV-A2 preparations. The first row in Figure 57 shows the results for virus preparation #C, the second one shows the result for virus preparation #D, while the third row gives the electropherograms of virus preparation #E. Furthermore the influence of the size of liposomal vesicle in physiological composition without receptor was tested. Liposomes #17 were extruded through a 200 nm filter membrane, while liposomes #18 were additionally extruded through 100 nm membrane. The particle size determined at the GEMMA instrument were used for calculation of the necessary viral concentration to keep a constant ratio of liposome:virus of 1:2. Due to very low concentrations of virus preparation #D the experiment was only done for liposomes #18, the smaller vesicles.

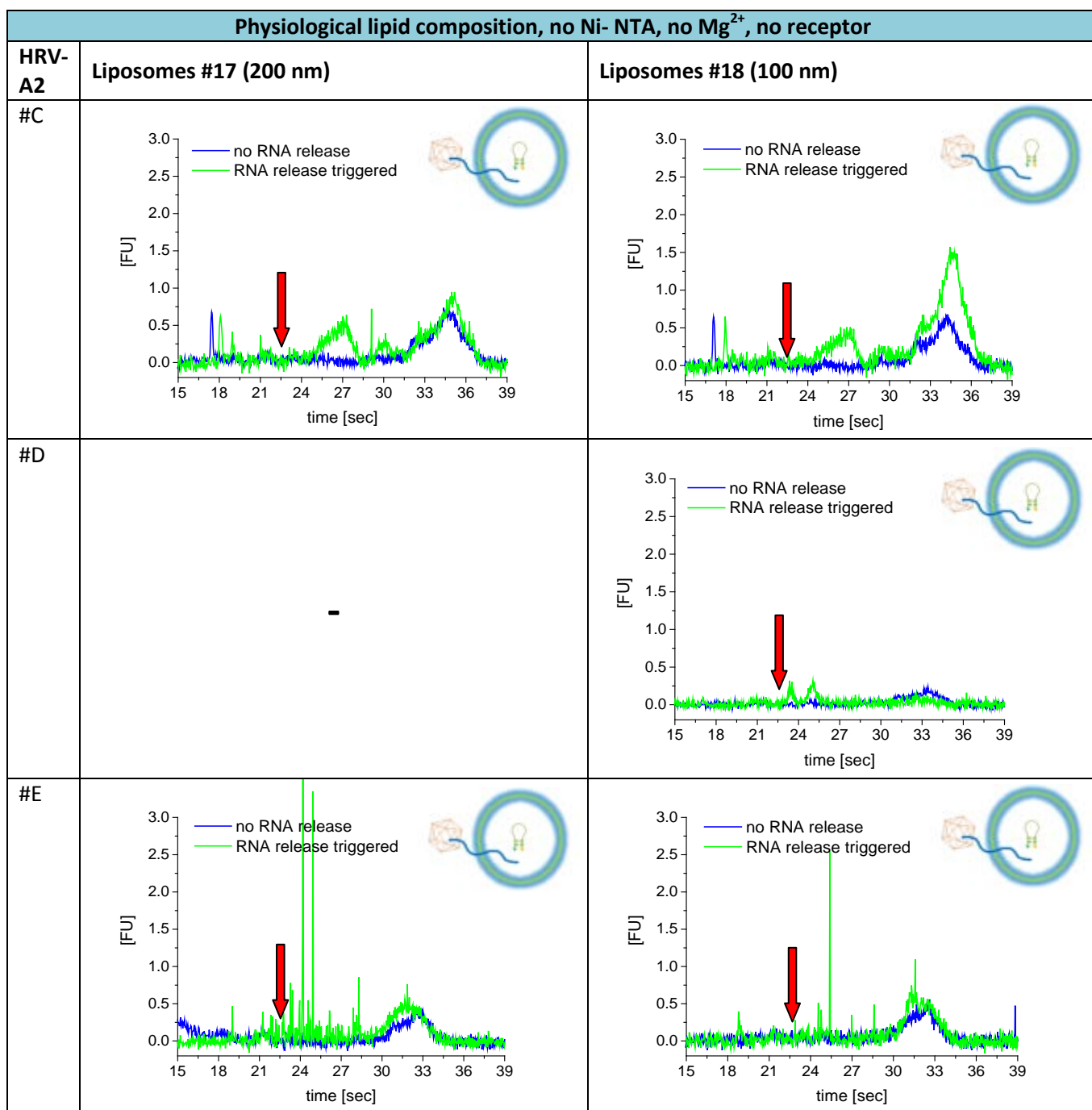


Figure 57: Incubation of HRV-A2 #C, #D and #E with physiological liposomes extruded to the indicated diameter of 200 nm or 100 nm out of PC, PE, SM, Cholesterol and NBD-PC as fluorescence labelled lipid, RNA release triggered through acidification to pH < 5.6; The expected viral RNA transfer into the liposome is marked by the red arrow. BGE: solution C containing 10 mM Trolox; sample buffer: solution B; concentration MBs inside liposome: 250 nM; concentration liposome outside: 25 nM; Electropherograms are aligned to the peaks of the internal standards.

In Figure 57 a signal at around 26 seconds appears in the green graph in the corresponding electropherograms of HRV-A2 preparation #C in the first line. This signal increase can be dedicated to a partial RNA release out of the capsid, but most probably not into liposomes. It is not clear if such an

increased signal at this position was also detected in case of incubation of HRV-A2 #E with liposome 17, because of spikes between 21 and 28 seconds migration time. The complex whereby RNA released partial is also known as subviral A I particle.

HRV-A2 preparation #D was dissolved in 50 mM HEPES buffer after purification. *Buchmueller and Weeks* published in 2004 a study regarding the influence of HEPES and Tris buffer to the viral RNA structure and the virus uncoating process [60]. Based on this study it was supposed that the viral uncoating and hence the RNA release is might be hindered in HEPES buffer, which would explain the missing signal of the presumed partial RNA release in case of this experiment.

Transfer of RNA into the liposome should be detectable at around 23.5 seconds based on the previous mentioned calculations for the Bioanalyzer 2100 system. It is non surprisingly that such a RNA release into the liposome is not detectable in this simplified experiments without any support of a gradient of ions across the cell membrane or even a receptor to bind the viral capsid directly to the cell model.

3.3.1.2. *Liposomes with non-physiological lipid composition*

The composition of liposome preparation #19, #20 and #21 do not correspond to the physiological composition of a natural cell wall. Lipids employed for vesicle formation were HSPC, DSPE, Cholesterol and the fluorescence labelled lipid NBD-PC. This composition was chosen as a simplified cell model with known behaviour in capillary electrophoresis and GEMMA. The liposomes were prepared with 250 nM MB P13 in 200 mM Na-Borate, pH 8.4, inside and sequentially extruded, whereby after each extrusion step (400 nm, 200 nm, 100 nm) an aliquot was taken for analysis and the remaining dispersion was passed through the filter membrane with smaller pore size.

Again, in these experiments no Ni-NTA lipid and hence no receptor binding possibility was included in the liposomal bilayer. Due to this fact, no receptor material was introduced to the liposome-virus mixture. The results obtained from incubation of the liposomes in non-physiological composition and HRV-A2 preparation #C and #E at acidified conditions are given in Figure 58 for larger (left) and smaller (right) vesicles. HRV-A2 #E was only analysed with the liposome preparation #21, the smaller vesicles.

Although these liposomes are significantly larger in diameter and hence provide a greater surface for docking of the viral capsid, only partial RNA release was detected in case of HRV-A2 preparation #C with both sizes of liposome as well as for the HRV-A2 #E preparation with liposomes #21. Due to the already mentioned low amount of HRV-A2, experiments with larger liposomal particles were neglected for preparation #D - #F. RNA transfer into these liposomes was also not detectable on the chip CE system. Thus, these liposomes were not considered for further experiments.

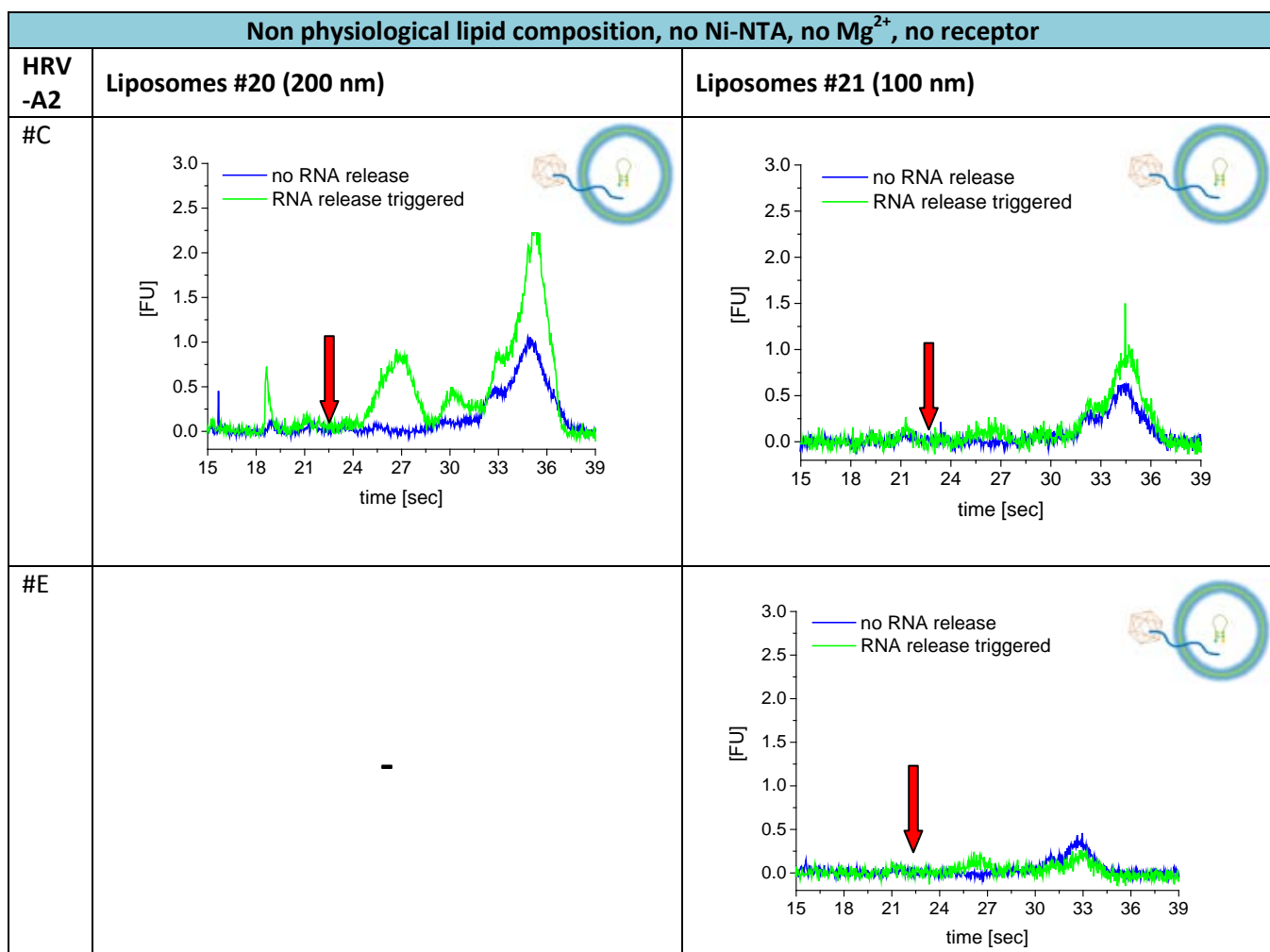


Figure 58: Electropherogram of the incubation of HRV-A2 #C with non-physiological liposomes in two sizes (#20: 200 nm; #21: 100 nm) containing only PC, PE, Cholesterol and the fluorescence labelled lipid (NBD-PC) under acidified conditions for RNA release (green)). The expected viral RNA transfer into the liposome is marked by the red arrow. BGE: solution C containing 10 mM Trolox; sample buffer: solution B; MB concentration inside liposome: 250 nM; MB concentration outside liposome: 25 nM; Electropherograms are aligned to the peaks of internal standards.

3.3.1.3. Liposomes with physiological lipid composition without NGS-NTA including 1 mM MgCl₂

Further liposome preparations with physiological composition were prepared. A cations gradient across the lipid membrane was suggested to facilitate the transfer of viral RNA from inside the virion into the lipid vesicle. Either RNA transfer driven as antiporter system based on a concentration difference between inside and outside liposomes or via RNA complexation to Mg²⁺ inside vesicles, as soon as RNA at least partial passes through the membrane, was supposed.

In order to generate this gradient across the membrane, 1 mM MgCl₂ was encapsulated besides 250 nM MB P13 inside the liposomes. After dilution of the liposomes in the sample an MgCl₂ concentration of 1 mM occurs inside the cell model, while the concentration outside was decrease to 0.1 mM. Experiments were carried out only with liposomes that were passed through 100 nm filter membranes to form unilamellar vesicles. These liposomes were incubated with HRV-A2 #C, #D as well as #E. The results obtained thereby are given below.

Independently from the HRV-A2 preparation a signal corresponding to subviral A I particles at around 26 s was detectable in case of acidification of samples containing liposome 23 and HRV-A2. The assumption that the presence of HEPES buffer in HRV-A2 preparation #D could influence the viral uncoating [60] was not supported by these experiments. As plotted in the second graph in Figure 59 even applying this virus preparation (#D) to the liposomes led to a partial RNA release in the course of virus acidification.

As can be derived from these experiments a gradient of cations across the membrane is still not sufficient to force the released RNA to enter the lipid bilayer.

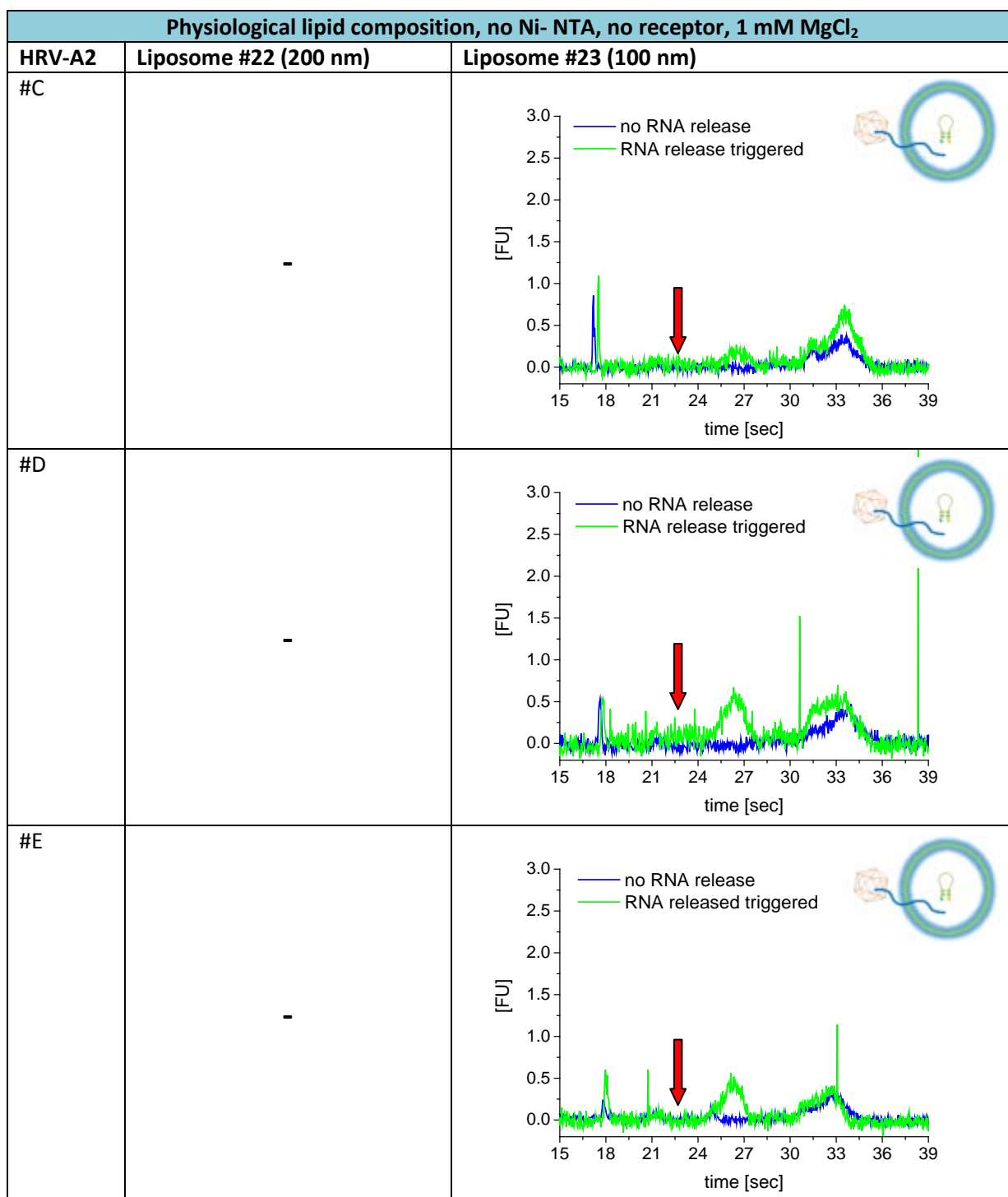


Figure 59: Electropherograms obtained on the chip CE after incubation of liposome #23 containing 1 mM MgCl₂ inside with HRV-A2 #C, #D and #E after RNA release triggered through acidification (green). The expected viral RNA transfer into the liposome is marked by the red arrow. BGE: solution C containing 10 mM Trolox; sample buffer: solution O containing 1 mM MgCl₂; MB concentration inside liposome: 250 nM; MB concentration outside liposome: 25 nM; Electropherograms are aligned to the peaks of the internal standards.

3.3.1.4. Liposomes with physiological lipid composition including NGS-NTA, but without receptor

In order to introduce a specific receptor for HRV-A2 to the liposome-virus system, a Ni^{2+} -complexing lipid (NGS-NTA) was added to the mixture of lipids for liposomes of physiological lipid composition. This lipid carrying Ni^{2+} allows a specific binding of a His6-tagged recombinant receptor (MBP-V33333, see following section) to the liposome to form a direct connection between the viral capsid and the cell model membrane.

However, before introduction the receptor material, the influence of Ni^{2+} to the viral uncoating and an eventual docking of the virus capsid to the liposome, was tested. It was assumed that because of the positively charged liposomes the viral capsid could already bind to the liposome which would make a RNA transfer into vesicles more likely. Therefore, three liposome preparations containing this Ni^{2+} -complexing lipid in their bilayer and 250 nM MB P13 inside were prepared and used for the monitoring of viral RNA into the liposomes. A selection of the results for HRV-A2 #C and #E is given here.

As depicted in Figure 60 below again no RNA transfer into the liposome was recognizable although liposome carrying positively charged ions were applied to bring the viral capsid in closer proximity to vesicles. Only a partial RNA release out of the capsid at around 26 seconds was detectable like in previous experiments without NGS-NTA or during experiments including a cations gradient.

Those results let us assume that the virus does not bind to the cell model membrane without application of a specific receptor molecule or a number of these molecules.

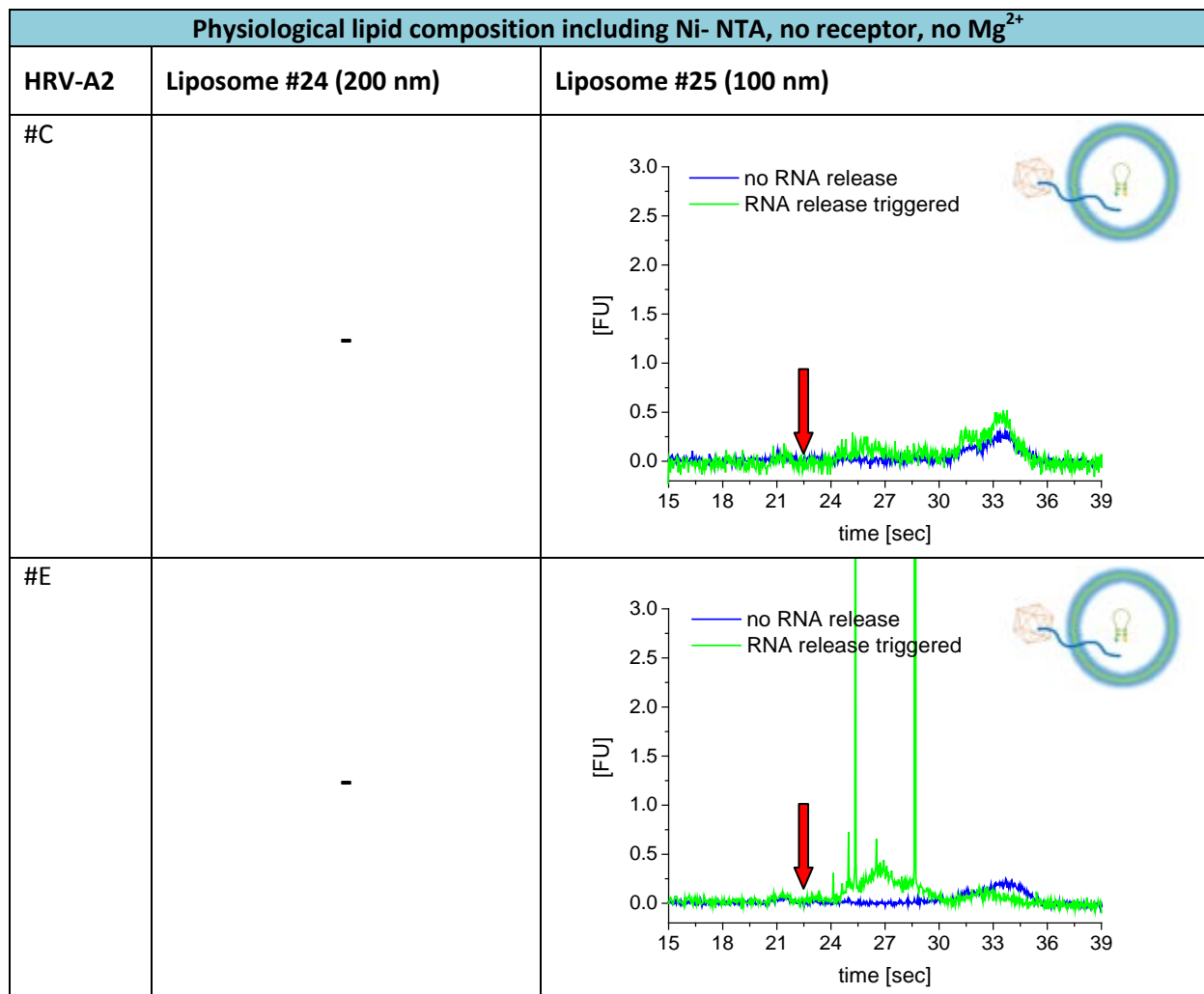
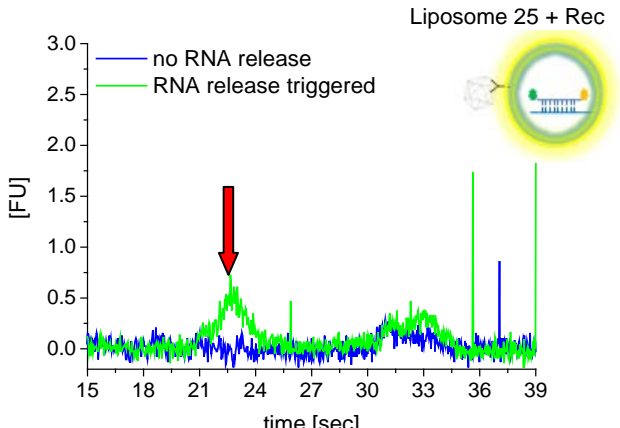
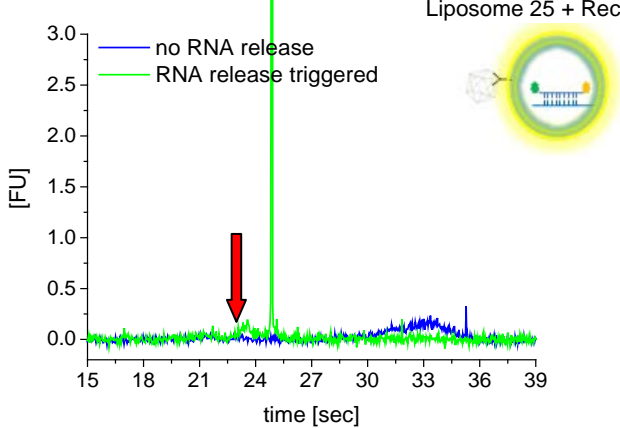


Figure 60: Result of the incubation of HRV-A2 preparation #C and #E with liposomes carrying a Ni-complexing lipid in the lipid bilayer at acidified conditions to force RNA release out of the viral capsid given in green and the corresponding control experiment given in blue. The expected viral RNA transfer into the liposome is marked by the red arrow. BGE: solution C containing 10 mM Trolox; sample buffer: solution B; MB concentration inside liposome: 250 nM; MB concentration outside liposome: 25 nM; Electropherograms are aligned to the peaks of the internal standards.

3.3.1.5. Liposomes with physiological lipid composition including NGS-NTA with receptor

Members of the very low density lipoprotein receptor (VLDLR) group bind minor group viruses. One VLDLR domain, domain 3, was combined fivefold in a recombinant receptor fragment to enable a higher binding affinity of the viral capsid to the receptor. This receptor was additionally modified with a His6-tag that allows a binding of the receptor to the liposomes carrying the prior mentioned Ni^{2+} -complexing lipid (NGS-NTA). Introducing the recombinant MBP-V33333 receptor to the liposomes and the virus allows the formation of a direct link between the cell model membrane and the viral capsid.

In the experiments five different liposomes containing Ni-NTA were prepared. Liposome #25, #26 and #29 were prepared with 250 nM MB P13 inside, while in liposome #27 and #28 250 nM MB P14 was encapsulated. The results obtained on the Bioanalyzer system after inducing RNA release by acidification are depicted below for all CIM purified HRV-A2 preparations (#C, #D, #E, #F).

Physiological lipid composition including Ni- NTA and a receptor, no Mg^{2+}		
HRV-A2	Liposomes #24 (200 nm)	Liposomes #25 or #26 (100 nm)
#C	-	
#D	-	

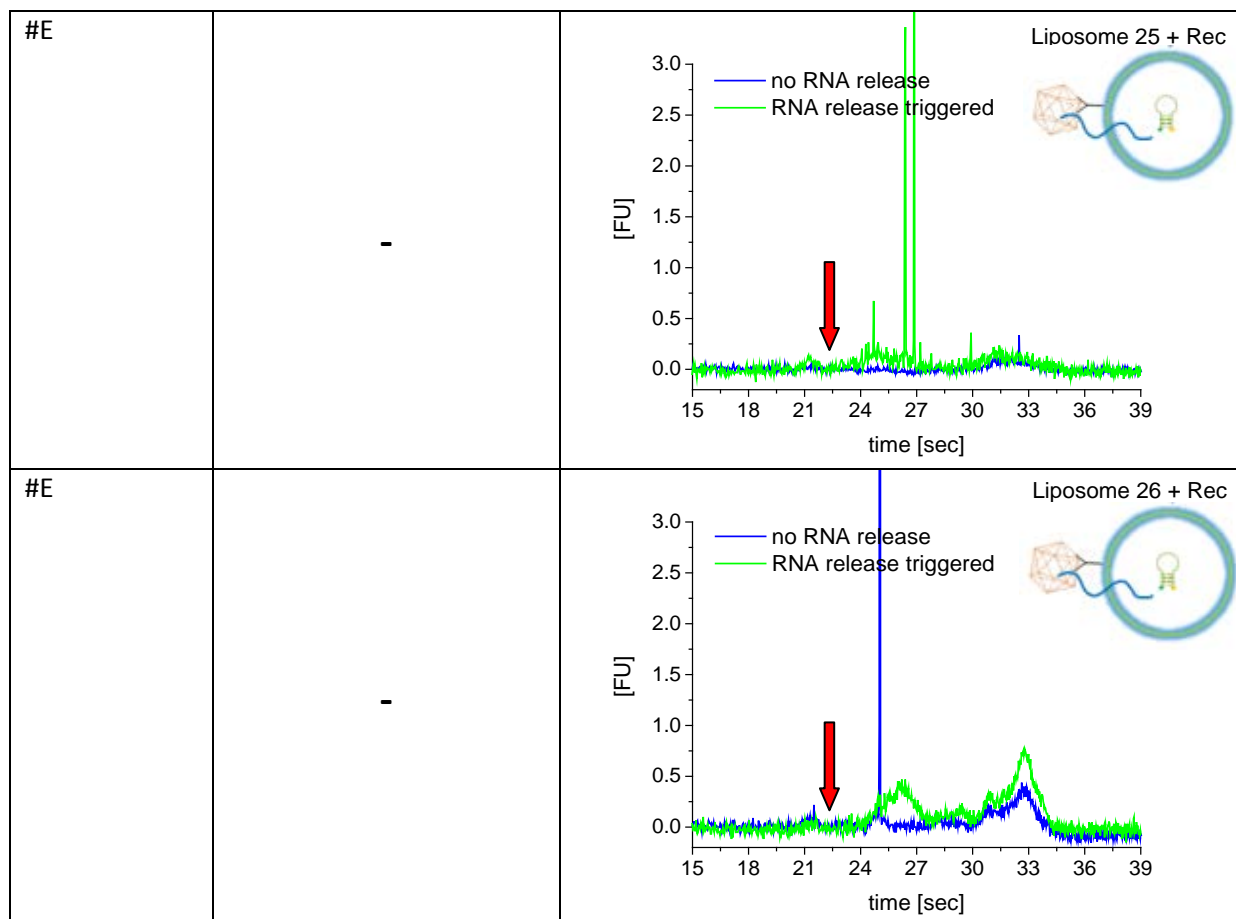


Figure 61: Presumed RNA transfer out of the viral capsid into liposomes: HRV-A2 preparation #C and #D, liposomes #25 with docked MBP-V33333 receptor and partial RNA release out of HRV-A2 preparation #E, liposomes #25 and #26; The expected viral RNA transfer into the liposome is marked by the red arrow. BGE: solution C containing 10 mM Trolox; sample buffer: solution O containing 1 mM $MgCl_2$; MB concentration inside liposome: 250 nM; MB concentration outside liposome: 25 nM; Electropherograms are aligned to the peaks of the internal standards.

Figure 61 gives an overview of the results obtained upon addition of the MBP-V33333 to liposome preparation #25 and HRV-A2 preparation #C and #D. Presumably a RNA release into the liposome was detectable on the Bioanalyzer. The signal at around 22.5 seconds in the respective green graph of the overlaid electropherograms supposedly originate from the transfer of the viral RNA into vesicles, because of the migration time of the peak. While the signals in the first experiments with HRV-A2 #C are quiet distinctive, the signals in case of HRV-A2 #D are considerable less intensive, but still recognizable.

HRV-A2 preparations #E and #F behaved differently than HRV-A2 #C and #D. In case of HRV-A2 #E a partial RNA release out of capsid at around 26 seconds migration time was detected instead. Differences between these experiments could possibly be explained by degradation or aggregation of the receptor material. Hence, the receptor is not active anymore and no direct link between the liposome and the viral capsid can be formed.

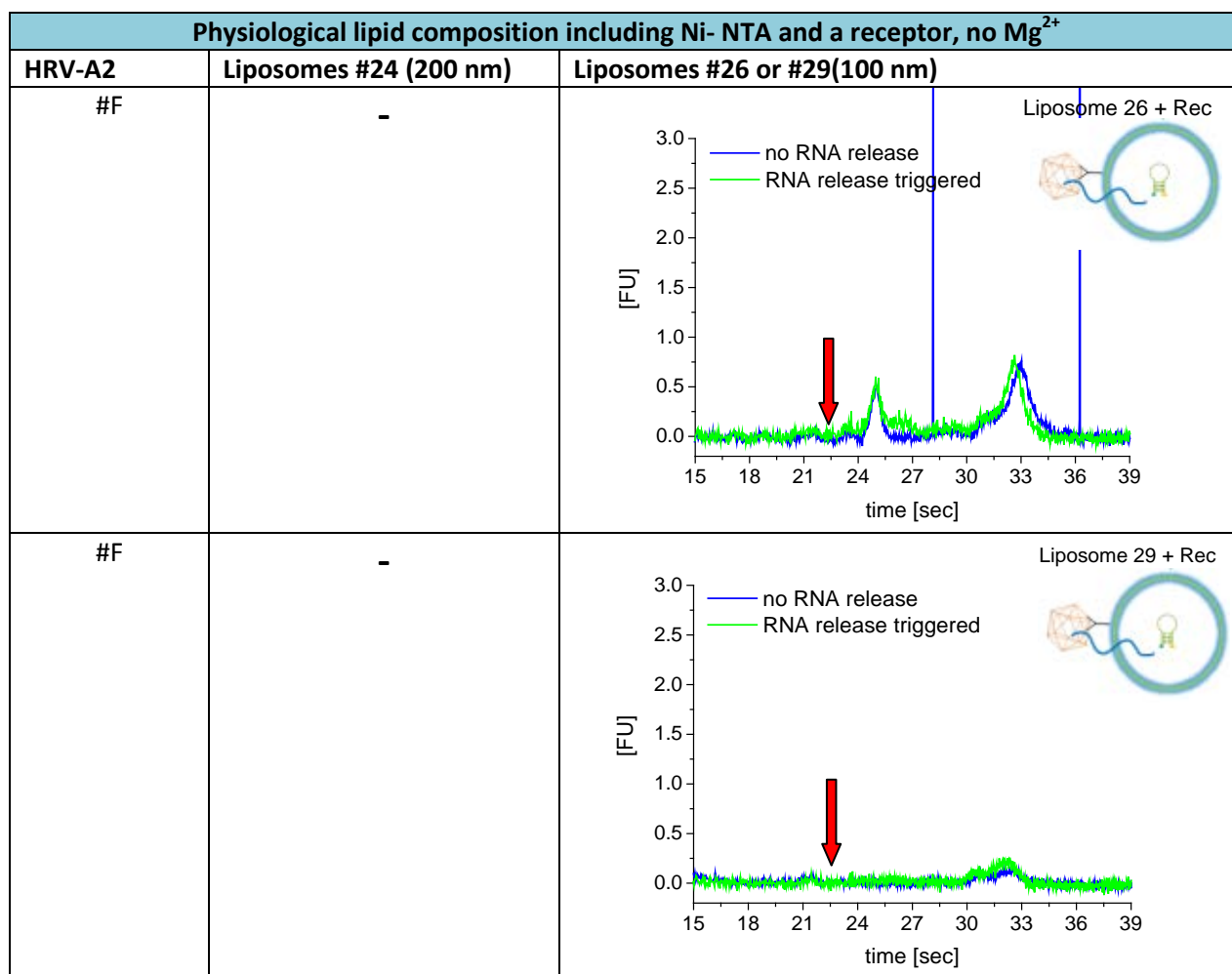


Figure 62: Neither RNA release into the liposome nor partial RNA release in case of applying HRV-A2 #F to liposomes #26 or liposomes #29 with receptor mediation was detected, although RNA release should be triggered by acidification; The expected viral RNA transfer into the liposome is marked by the red arrow. BGE: solution C containing 10 mM Trolox; sample buffer: solution O containing 1 mM $MgCl_2$; MB concentration inside liposome: 250 nM; MB concentration outside liposome: 25 nM; Electropherograms are aligned to the peaks of the internal standards.

For HRV-A2 #F not even a partial RNA release was detectable (Figure 62). This let us assume that the viral material was degraded because of storage and multiply freezing/thawing cycles. Due to this reason RNA release was initiated by heating of the samples in addition to the acidification step. As shown in Figure 63 heating the samples to 56 °C for 15 min led to RNA release out of the capsid that was detected via the MBs outside the liposomes. As expected, samples heating did not led to RNA transfer into liposomes.

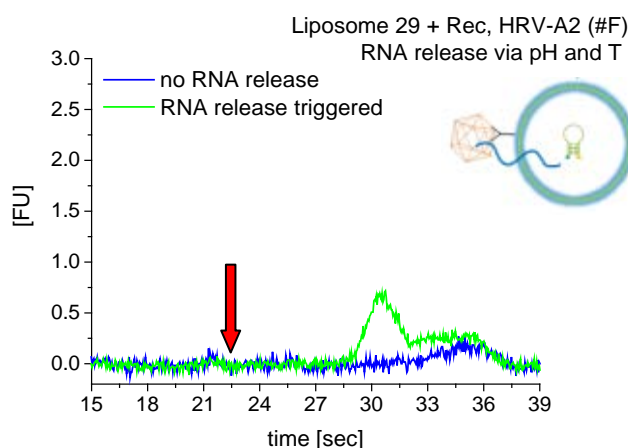


Figure 63: Additional heating step after acidification of HRV-A2 #F with liposome #29 and receptor to force RNA release out of the viral capsid to check the viral material; heating the sample to 56 °C for 15 min led to released RNA detected by the MBs outside the liposome; The expected viral RNA transfer into the liposome is marked by the red arrow. BGE: solution C containing 10 mM Trolox; sample buffer: solution O containing 1 mM MgCl_2 ; MB concentration inside liposome: 250 nM; MB concentration outside liposome: 25 nM; Electropherograms are aligned to the peaks of the internal standards.

MB P14 encapsulated inside liposomes

Furthermore, liposomes with MB P14 inside (#27 and #28) were used for additional experiments, because MB P14 binds specific to the 3' end of the HRV-A2 RNA. This sequence segment of the viral genome will be released first out of the capsid. Hence, a detection of released RNA should also be possible in case of only partial release. Therefore liposome #27 was incubated with HRV-A2 #F under conditions including sample acidification. As shown in Figure 64, neither partial RNA transfer out of the capsid nor a transfer of the genetic material into the liposome was detectable. Hence, a so far unidentified parameter either hinders RNA release out of this HRV-A2 preparation by acidification of samples or is needed for genome release

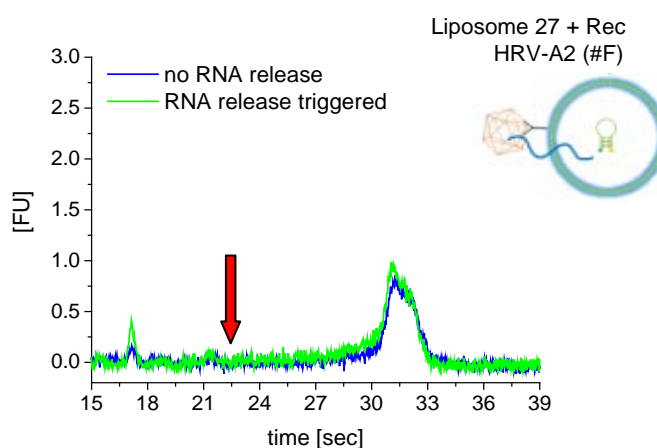


Figure 64: Incubation of HRV-A2 #F with liposome #27 (including 250 nM MB P14) and receptor under conditions including sample acidification to initiate RNA release; RNA release out of viral capsid was not detectable; The expected viral RNA transfer into the liposome is marked by the red arrow. BGE: solution C containing 10 mM Trolox; sample buffer: solution O containing 1 mM MgCl_2 ; MB concentration inside liposome: 250 nM; MB concentration outside liposome: 25 nM; Electropherograms are aligned to the peaks of the internal standards.

3.3.1.6. *Benzonase digest of free RNA and MBs*

The idea was to digest released RNA and the remaining MBs outside the liposomes to verify the RNA transfer into the liposomes. Oligonucleotides inside vesicles should be protected from the enzyme. As plotted in following graphs digested MB fragments in the lower size range were detected with high intensity. The signal of the MBs outside the liposomes is not present any more in the corresponding electropherograms. Hence, the digestion of the genetic material works well. Zooming into the electropherograms a signal of the purposed RNA/MB complex inside liposomes is still detectable. However, due to the high intensity of small fragments after digestion signals of the RNA transfer into the liposome are only visible upon magnification of the corresponding electropherogram regions. However, as for these virus preparations initially no transfer of the viral genome to vesicles was detected (see Figure 61), those results have to be interpreted with caution.

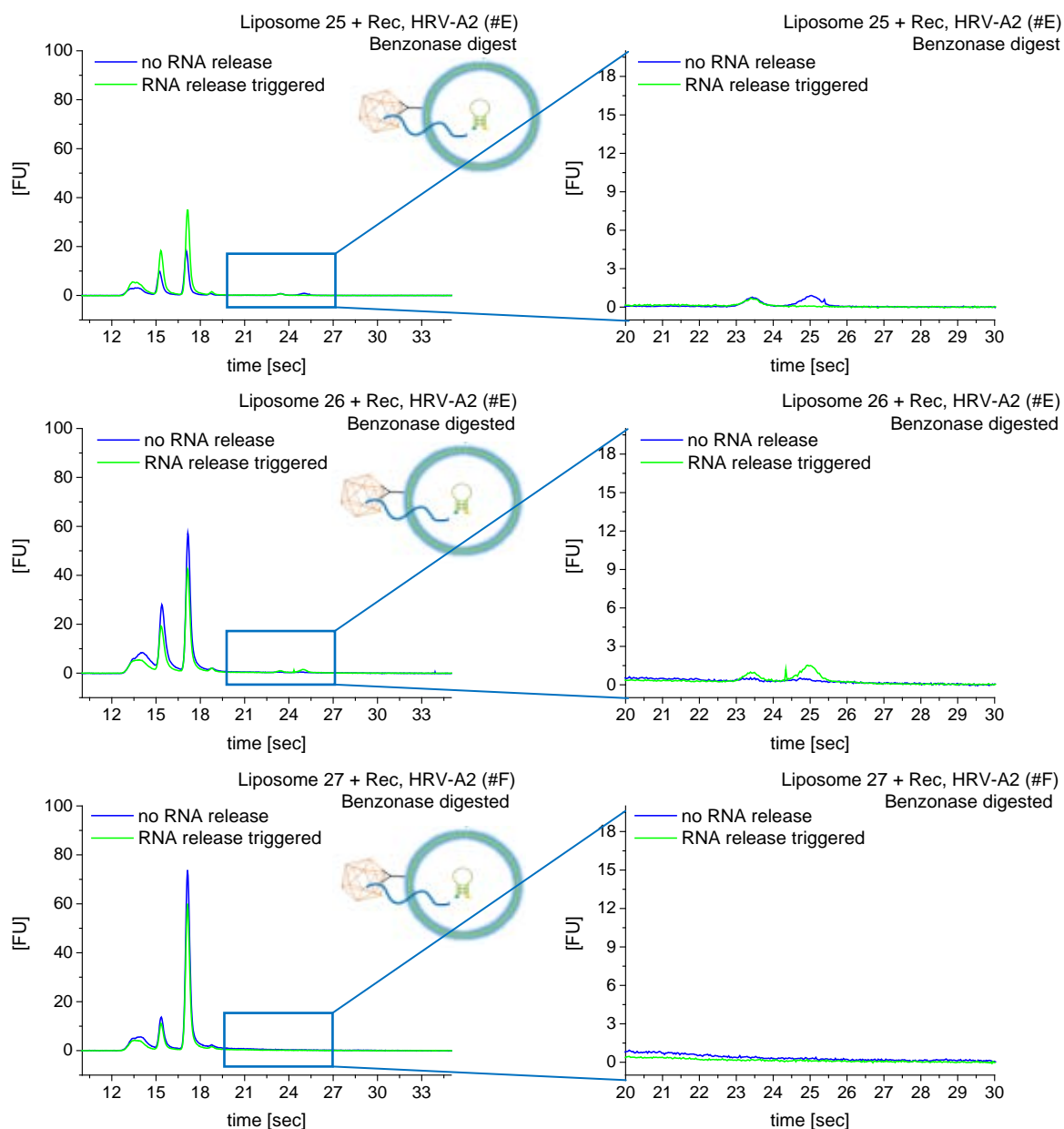


Figure 65: Benzonase treatment of the liposomes incubated with receptor and HRV-A2 to digest the MBs and free RNA outside the liposomes; BGE: solution C containing 10 mM Trolox; sample buffer: solution O containing 1 mM MgCl_2 ; MB concentration inside liposome: 250 nM; MB concentration outside liposome: 25 nM; Electropherograms are aligned to the peaks of the internal standards.

3.3.2. GEMMA results

Additionally to the chip CE experiments the interaction of virus and liposome was studied by means of the GEMMA device. Therefore, desalted HRV-A2 preparations in solution G were used. The viral material was incubated with liposomes #26 and #27 and the MBP-V33333 receptor. The binding of the receptor to the liposomes in absence of virions was also checked via gas-phase electrophoresis.

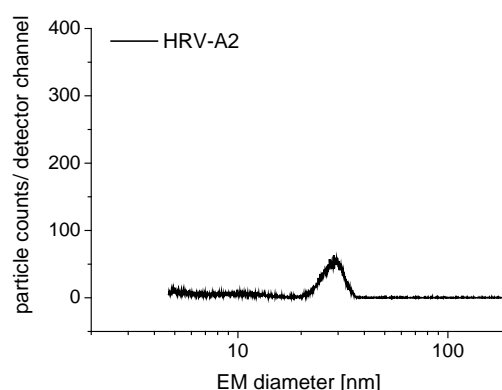


Figure 66: GEMMA spectra of HRV-A2 preparation in 40 mM NH_4OAc , using a 25 μm capillary for sample delivery to the nES process

In Figure 66 the GEMMA spectrum of the HRV-A2 solution G is plotted. This measurement was performed using a 25 μm capillary for sample delivery to the nES process and a sheath flow of 2.5 lpm during separation in the DMA. Due to the latter parameter and in contrast to measurements found in literature employing significant higher sheath flow values, a broader virus peak was obtained.

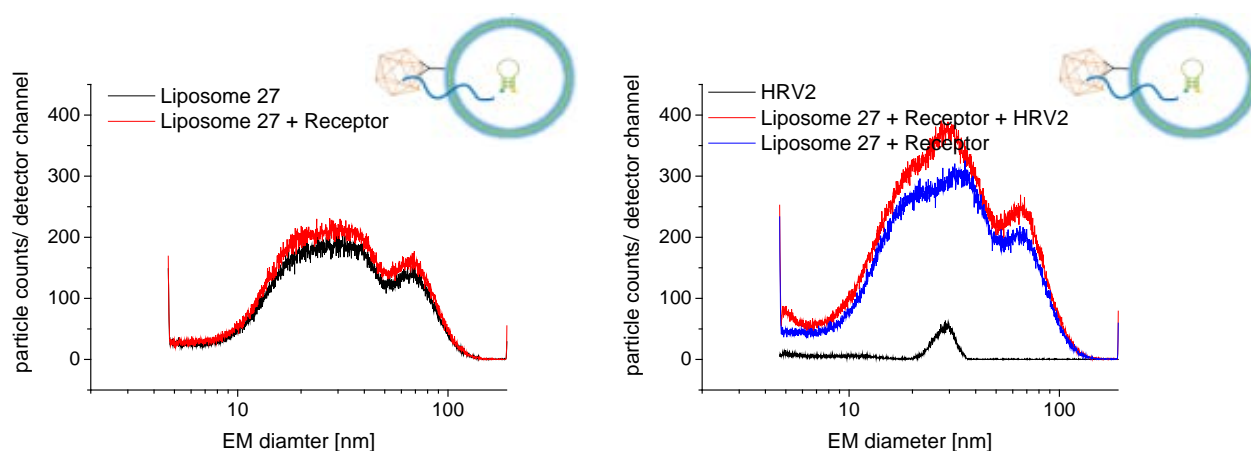


Figure 67: GEMMA spectra of liposomes #27 with and without receptor, respectively, (left) in comparison to the spectra in which liposomes were incubated with HRV-A2 and receptor (right)

Figure 67 shows a comparison of the liposomes and liposomes with receptor (left) and the samples with additional HRV-A2 on the right. Neither incubation of the liposome with the receptor nor the addition of virus resulted in a significant change of the particle size, which would be the consequence in case of virus binding predicted by the cell model. No interaction between liposome and receptor or liposome, receptor and virus could be detected via GEMMA measurements for the selected molecule/particle ratios and time frame as well concentrations.

These experiments let us assume that the receptor material is probably not able to bind to the liposomes anymore, because of degradation. This suspicion appeared already during the Bioanalyzer experiments with liposome preparation # ≥ 26 and HRV-A2 preparation #E and #F whereby RNA transfer into the liposomes was no longer detectable.

3.3.3. TEM results

Samples were additionally visualized via TEM (transmission electron microscopy) at *MFPL* to study the interaction of the liposome with the viral particles under the microscope with kind assistance of *Sofiya Fedosyuk* (group of *Dieter Blass*). Therefore samples were analysed first at the Bioanalyzer 2100 system, afterwards transferred to the sample carrier for TEM and negatively stained with 2 % phosphotungstate.

Some of the results obtained from samples with liposome #18 (no Ni-NTA) and liposome #25 (with Ni-NTA and receptor) with HRV-A2 preparation #D are shown here.

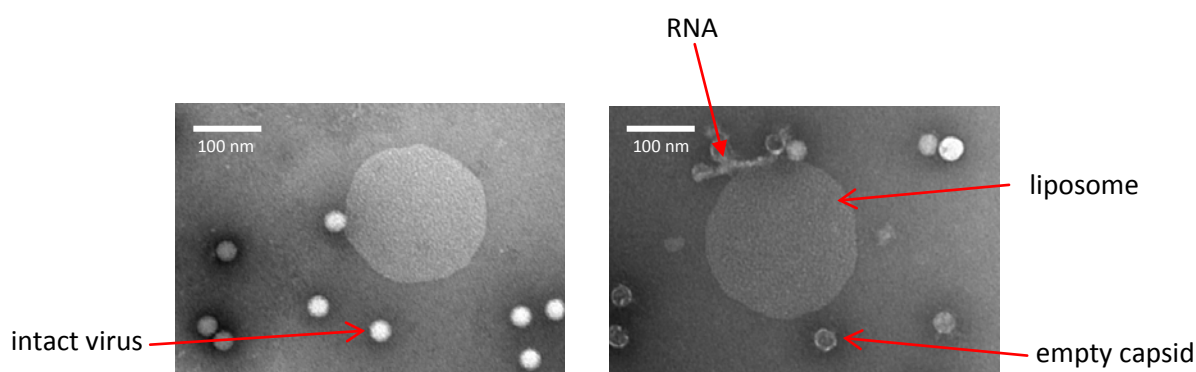


Figure 68: TEM image of liposome #18 with HRV-A2 #D (left) and after RNA release through acidification (right); © by SF

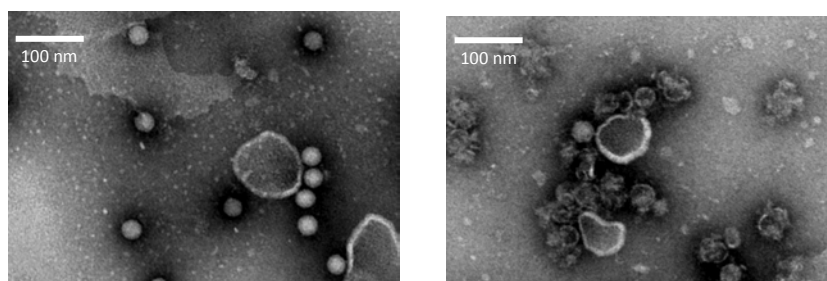


Figure 69: TEM image of liposome #25 with receptor and HRV-A2 #D (left) and after acidification of the sample to trigger RNA release (right); © by SF

As shown in the TEM images in Figure 68 and Figure 69 the viral particles are more concentrated around the liposomes in case of receptor introduction (Figure 69).

Acidification of the samples led to viral RNA release possibly into the solutions shown as bundle of threads around the viral capsids. RNA release into the liposome itself was not visible on these TEM images due to method inherent problems in preparation of TEM specimens. It was noticed, that liposomes are mostly broken upon contact with the TEM sample carrier (C-grid), so the found images are derived in large part from artefacts of the TEM preparation (which has to be verified in the future in detail).

4. Summary

In the here presented master thesis the RNA transfer of the human rhinovirus serotype HRV-A2 into liposomes as cell model was monitored via molecular beacons and chip capillary electrophoresis to simulate an *in vivo* cell infection.

For detection of the viral RNA, three different MB batches that bind to distinct sequence regions of the HRV-A2 genome were considered. In order to understand the behaviour of these probes a number of pre-experiments were performed. It was shown that the presence of Trolox (6-hydroxy-2,5,7,8-tetramethylchroman-2-carboxylic acid) in the sample buffer increases the detectable fluorescence signal up to the 3fold and by reduction of blinking and bleaching of the MBs fluorophore [52]. On the other hand, storage of the MBs in Trolox buffer led to increased degradation and makes a long-time storage impossible. Due to this reason the buffer system needed to be adapt to guarantee a sufficient reactivity of the probes towards the complementary target sequence even after more than 2 days stored in buffer, e.g. upon encapsulation in the liposomes.

The specificity towards complementary DNA sequences as well as towards any irrelevant target oligonucleotide sequences was tested prior to experiments including viral material. As already published in *Analytical and Bioanalytical Chemistry* RNA release into solution was detectable with MB P14, a probe that binds specific near the 3' end of the viral genome [52]. RNA release was triggered by heating the sample to 56 °C for 15 min or by acidification to a pH lower 5.6 to simulate the *in vivo* situation in endosomes. During this thesis it was also shown that released RNA can be detected by another molecular beacon, MB P13, while the third applied MB, MB P12, was not able to bind to the released viral RNA in solution.

Based on this information, MBs were encapsulated in liposomes in various lipid composition. Liposomes were prepared with different amounts of MBs inside and in different buffer systems. For quality control the liposomes were analysed on the GEMMA instrument to get an idea about the vesicle size and the number of particles.

Four HRV-A2 preparations provided by *MFPL* were introduced to various liposomes. RNA release into the liposomes was triggered by acidification with acetic acid to a pH \approx 5.3 and detected on the *Agilent* Bioanalyzer 2100 system, a chip capillary electrophoresis device. Signals were assigned based on the migration time on the CE chip and the electrophoretic mobility μ , given in literature or determined on a CE.

Transfer of released RNA into liposomes in physiological constitution (corresponding to the constitution of natural cells) was not detectable with this setup. Independently form the particle size only a partial RNA release out of the viral capsid was detected. Furthermore, MgCl₂ was implemented into the liposomes in order to generate a cations gradient across the liposomal membrane to support the transfer of viral RNA into the cell model. Also for the cations gradient across the membrane it was shown that this was not sufficient to pull the released RNA into the liposomes. Hence, a specific receptor to form a direct link between cell model and viral capsid was required. A recombinant MBP-V33333 receptor carrying a His6-tag was used. The receptor was introduced to liposomes containing a Ni²⁺-complexing lipid in which the receptor can bind. Most probably, RNA transfer into the liposome was detected on the Bioanalyzer 2100 system with the help of the recombinant MBP-V33333 receptor for two HRV-A2 preparations. However, further experiments using fresh biological material are necessary to confirm this result.

5. Outlook

Prior to further improvements of the bioanalytical strategy, the process of virus cultivation and purification needed to be adapted. CIM purification as additional purification step after viral cultivation is absolutely necessary to remove the so-called contaminant. The exact composition of this contaminant is still not known, but it influences the viral RNA release out of the capsid. Its actual structural composition has to be determined to get an idea how the contaminant might influencing the viral uncoating. On the other hand further purification steps also lead to a loss of active biological material. Very low concentrations and only low amounts of biological material were mainly influencing and to certain extent limiting the progress of this work. Due to this reason, the applied virus purification need to be improved towards higher yields and larger homogeneous batches.

Furthermore, it was already shown and is known to a certain extent for HRV that freezing and thawing cycles influences the final viral activity. Hence, fresh viral preparations should be used as soon as possible after improved purification. Long storage periods (although the virus was stored at – 70 °C) and repeating freezing-thawing cycles need to be avoided.

In order to confirm the RNA transfer into the liposomes (carrying a specific receptor), further analytical techniques should be considered and experiments including the enzyme Benzonase should be repeated.

Besides the chip capillary electrophoresis system, a classic CE system should be considered to study the viral RNA transfer. The Bioanalyzer 2100 system was preferred in this project because of the significantly shorter analysis time and the huge number of samples than can be handled in one step. Furthermore the short inner wall-interaction time in the chip CE system is beneficial. Due to this reason the here presented setup show a huge potential for clinical applications that requires easy to handle and fast methods. In order to confirm the probable viral RNA transfer into the liposome by means of the chip CE device, repeated experiments with fresh biological material as well as control experiments employing any unspecific serotype of the human rhinovirus, e.g. HRV-B14, to the liposomes are required.

Additionally, first experiments regarding the study of the complex interaction between intact virus, receptor(s) and liposome derived from the cell model were already done on the GEMMA instrument. Thereby the binding of the receptor to the liposome and consequently the attachment of the viral capsid to the construct should be studied in detail. Due to presumed degradation of the biological material it is not possible to draw a clear conclusion concerning an actual binding of the receptor to liposomes and consequently to the viral capsid surface. Hence, it is of great interest to repeat these experiments with fresh biological material of higher purity.

References

- [1] Tyrrell, D. A. J., & Parsons, R. (1960). Some virus isolations from common colds: III. Cytopathic effects in tissue cultures. *The Lancet*, 275(7118), 239-242.
- [2] Snyers, L., Zwickl, H., & Blaas, D. (2003). Human rhinovirus type 2 is internalized by clathrin-mediated endocytosis. *Journal of virology*, 77(9), 5360-5369.
- [3] Bilek, G., Matscheko, N. M., Pickl-Herk, A., Weiss, V. U., Subirats, X., Kenndler, E., & Blaas, D. (2011). Liposomal nanocontainers as models for viral infection: monitoring viral genomic RNA transfer through lipid membranes. *Journal of virology*, 85(16), 8368-8375.
- [4] <http://www.picornaviridae.com>; downloaded on 15/04/2016
- [5] Verdaguer, N., Blaas, D., & Fita, I. (2000). Structure of human rhinovirus serotype 2 (HRV2). *Journal of molecular biology*, 300(5), 1179-1194.
- [6] Davis, M. P., Bottley, G., Beales, L. P., Killington, R. A., Rowlands, D. J., & Tuthill, T. J. (2008). Recombinant VP4 of human rhinovirus induces permeability in model membranes. *Journal of virology*, 82(8), 4169-4174.
- [7] Greve, J. M., Davis, G., Meyer, A. M., Forte, C. P., Yost, S. C., Marlor, C. W., Kamarck, M.E, McClelland, A. (1989). The major human rhinovirus receptor is ICAM-1. *Cell*, 56(5), 839-847.
- [8] Gruenberger, M., Wandl, R., Nimpf, J., Hiesberger, T., Schneider, W. J., Kuechler, E., & Blaas, D. (1995). Avian homologs of the mammalian low-density lipoprotein receptor family bind minor receptor group human rhinovirus. *Journal of virology*, 69(11), 7244-7247.
- [9] Hofer, F., Gruenberger, M., Kowalski, H., Machat, H., Huettinger, M., Kuechler, E., & Blass, D. (1994). Members of the low density lipoprotein receptor family mediate cell entry of a minor-group common cold virus. *Proceedings of the National Academy of Sciences*, 91(5), 1839-1842.
- [10] Lau, S. K., Yip, C. C., Tsoi, H. W., Lee, R. A., So, L. Y., Lau, Y. L., Chan, K. H., Woo, P. C. Y., Yuen, K. Y. (2007). Clinical features and complete genome characterization of a distinct human rhinovirus (HRV) genetic cluster, probably representing a previously undetected HRV species, HRV-C, associated with acute respiratory illness in children. *Journal of clinical microbiology*, 45(11), 3655-3664.
- [11] Fuchs, R., & Blaas, D. (2008). Human rhinovirus cell entry and uncoating. Structure-Based Study of Viral Replication, World Scientific publishing, Singapur, 1. Ausgabe, p. 1-41.
- [12] Mercer, J., Schelhaas, M., & Helenius, A. (2010). Virus entry by endocytosis. *Annual review of biochemistry*, 79(79), 803-833.
- [13] Brabec, M., Baravalle, G., Blaas, D., & Fuchs, R. (2003). Conformational changes, plasma membrane penetration, and infection by human rhinovirus type 2: role of receptors and low pH. *Journal of virology*, 77(9), 5370-5377.

- [14] Okun, V. M., Blaas, D., & Kenndler, E. (1999). Separation and biospecific identification of subviral particles of human rhinovirus serotype 2 by capillary zone electrophoresis. *Analytical chemistry*, 71(20), 4480-4485.
- [15] Andersen, O. M., Christensen, L. L., Christensen, P. A., Sørensen, E. S., Jacobsen, C., Moestrup, S. K., Etzerodt, M., Thøgersen, H. C. (2000). Identification of the Minimal Functional Unit in the Low Density Lipoprotein Receptor-related Protein for Binding the Receptor-associated Protein (RAP) A conserved acidic residue in the complement-type repeats is important for recognition of RAP. *Journal of biological chemistry*, 275(28), 21017-21024.
- [16] Nizet, S., Wruss, J., Landstetter, N., Snyers, L., & Blaas, D. (2005). A mutation in the first ligand-binding repeat of the human very-low-density lipoprotein receptor results in high-affinity binding of the single V1 module to human rhinovirus 2. *Journal of virology*, 79(23), 14730-14736.
- [17] Pattni, B. S., Chupin, V. V., & Torchilin, V. P. (2015). New developments in liposomal drug delivery. *Chemical reviews*, 115(19), 10938-10966.
- [18] Kirby, C., Clarke, J., & Gregoriadis, G. (1980). Effect of the cholesterol content of small unilamellar liposomes on their stability in vivo and in vitro. *Biochemical journal*, 186(2), 591-598.
- [19] Lopez-Pinto, J. M., Gonzalez-Rodriguez, M. L., & Rabasco, A. M. (2005). Effect of cholesterol and ethanol on dermal delivery from DPPC liposomes. *International journal of pharmaceutics*, 298(1), 1-12.
- [20] <http://news.upenn.edu/sites/default/files/news/images/hires/Liposome%20and%20Dendrimers%20ome.jpg>, downloaded on 15/04/2016
- [21] Hope, M. J., Bally, M. B., Webb, G., & Cullis, P. R. (1985). Production of large unilamellar vesicles by a rapid extrusion procedure. Characterization of size distribution, trapped volume and ability to maintain a membrane potential. *Biochimica et biophysica acta-Biomembranes*, 812(1), 55-65.
- [22] Popa, R., Vranceanu, M., Nikolaus, S., Nirschl, H., & Lenewit, G. (2008). Entrance effects at nanopores of nanocapsules functionalized with poly (ethylene glycol) and their flow through nanochannels. *Langmuir*, 24(22), 13030-13036.
- [23] Stano, P., Bufali, S., Pisano, C., Bucci, F., Barbarino, M., Santaniello, M., Carminati, P., Luisi, P. L. (2004). Novel camptothecin analogue (Gimatecan)-containing Liposomes Prepared by the Ethanol Injection Method. *Journal of liposome research*, 14(1-2), 87-109.
- [24] <http://eu.idtdna.com/pages/products/gene-expression/molecular-beacons>; downloaded on 15/05/2016
- [25] Tyagi, S., & Kramer, F. R. (1996). Molecular beacons: probes that fluoresce upon hybridization. *Nature biotechnology*, 14(3), 303-308.

- [26] Vogelstein, B., & Kinzler, K. W. (1999). Digital Pcr. *Proceedings of the National Academy of Sciences*, 96(16), 9236-9241.
- [27] Chen, W., Martinez, G., & Mulchandani, A. (2000). Molecular beacons: a real-time polymerase chain reaction assay for detecting *Salmonella*. *Analytical biochemistry*, 280(1), 166-172.
- [28] Fang, X., Li, J. J., & Tan, W. (2000). Using molecular beacons to probe molecular interactions between lactate dehydrogenase and single-stranded DNA. *Analytical chemistry*, 72(14), 3280-3285.
- [29] Sokol, D. L., Zhang, X., Lu, P., & Gewirtz, A. M. (1998). Real time detection of DNA-RNA hybridization in living cells. *Proceedings of the National Academy of Sciences*, 95(20), 11538-11543.
- [30] http://www.premierbiosoft.com/tech_notes/molecular_beacons.html; downloaded on 13/05/2016
- [31]: Wang, L., Yang, C. J., Medley, C. D., Benner, S. A., & Tan, W. (2005). Locked nucleic acid molecular beacons. *Journal of the american chemical society*, 127(45), 15664-15665.
- [32] Tiselius, A. (1937). Electrophoresis of serum globulin. *Biochemistry journal*, 31: 313–317
- [33] Lottspeich, F., Engels, J.W., Bioanalytik, Springer Spektrum Verlag, Berlin Heidelberg, Germany, 3. Ausgabe, p. 267- 274
- [34] Lottspeich, F., Engels, J.W., Bioanalytik, Springer Spektrum Verlag, Berlin Heidelberg, Germany, 3. Ausgabe, p. 280-281
- [35] <http://www.wiley-vch.de/books/info/3-527-30300-6/itp.html>; downloaded on 06/05/2015
- [36] Lottspeich, F., Engels, J.W., Bioanalytik, Springer Spektrum Verlag, Berlin Heidelberg, Germany, 3. Ausgabe, p. 286-290
- [37] Gey, M.; Instrumentelle Analytik und Bioanalytik, Springer Spektrum Verlag, Berlin Heidelberg, Germany, 2.Ausgabe, p. 183-184
- [38] Jorgenson, J. W., & Lukacs, K. D. (1981). Free-zone electrophoresis in glass capillaries. *Clinical chemistry*, 27(9), 1551-1553.
- [39] Lottspeich, F., Engels, J.W., Bioanalytik, Springer Spektrum Verlag, Berlin Heidelberg, Germany, 3. Ausgabe, p. 302-327
- [40] Landers, J. P. (Ed.). (1996). *Handbook of capillary electrophoresis*. CRC Press, Boca Raton, Florida, USA.
- [41] <http://www.genomics.agilent.com/en/Bioanalyzer-System/2100-Bioanalyzer-Instruments/?cid=AG-PT-106&tabId=AG-PR-1001>, downloaded on 05/05/2016

- [42] Kolivoška, V., Weiss, V. U., Kremser, L., Gaš, B., Blaas, D., & Kenndler, E. (2007). Electrophoresis on a microfluidic chip for analysis of fluorescence-labeled human rhinovirus. *Electrophoresis*, 28(24), 4734-4740.
- [43] http://www.cmmmt.ubc.ca/sites/default/files/pdf_Bioanalyzer_brochure.pdf, downloaded on 05/05/2015
- [44] <http://www.spektrum.de/lexikon/optik/photolithographie/2522>, downloaded on 09/05/2016
- [45] Bunch, R. (2011). Rapid, high-resolution microfluidic separations for nucleic acid analysis, Perkin Elmar, <http://www.genengnews.com/media/pdf/516650-slide-deck-complete.pdf>, downloaded on 20/05/2106
- [46] Allmaier, G., Laschober, C., & Szymanski, W. W. (2008). Nano ES GEMMA and PDMA, new tools for the analysis of nanobioparticles—Protein complexes, lipoparticles, and viruses. *Journal of the american society for mass spectrometry*, 19(8), 1062-1068.
- [47] Bacher, G., Szymanski, W. W., Kaufman, S. L., Zöllner, P., Blaas, D., & Allmaier, G. (2001). Charge-reduced nano electrospray ionization combined with differential mobility analysis of peptides, proteins, glycoproteins, noncovalent protein complexes and viruses. *Journal of mass spectrometry*, 36(9), 1038-1052.
- [48] Thomas, J. J., Bothner, B., Traina, J., Benner, W. H., & Siuzdak, G. (2004). Electrospray ion mobility spectrometry of intact viruses. *Journal of spectroscopy*, 18(1), 31-36.
- [49] Skern, T., Sommergruber, W., Blaas, D., Gruendler, P., Fraundorfer, F., Pieler, C., Fogy, I., Kuechler, E. (1985). Human rhinovirus 2: complete nucleotide sequence and proteolytic processing signals in the capsid protein region. *Nucleic acids research*, 13(6), 2111-2126.
- [50] https://www.agilent.com/cs/library/usermanuals/Public/G2938-90034_RNA6000Nano_KG.pdf, downloaded on 05/05/2016
- [51] Reijenga, J. C., Martens, J. H., Giuliani, A., & Chiari, M. (2002). Pherogram normalization in capillary electrophoresis and micellar electrokinetic chromatography analyses in cases of sample matrix-induced migration time shifts. *Journal of chromatography B*, 770(1), 45-51.
- [52] Weiss, V. U., Bliem, C., Gösler, I., Fedosyuk, S., Kratzmeier, M., Blaas, D., & Allmaier, G. (2016). In vitro RNA release from a human rhinovirus monitored by means of a molecular beacon and chip electrophoresis. *Analytical and bioanalytical chemistry*, 408 (16), 1-9.
- [53] Subirats, X., Weiss, V. U., Gösler, I., Puls, C., Limbeck, A., Allmaier, G., & Kenndler, E. (2013). Characterization of rhinovirus subviral A particles via capillary electrophoresis, electron microscopy and gas phase electrophoretic mobility molecular analysis: part II. *Electrophoresis*, 34(11), 1600-1609.

[54] Ušelová-Včeláková, K., Zuskova, I., & Gaš, B. (2007). Stability constants of amino acids, peptides, proteins, and other biomolecules determined by CE and related methods: recapitulation of published data. *Electrophoresis*, 28(13), 2145-2152.

[55] <http://avantilipids.com/divisions/equipment/>; downloaded on 15/03/2016

[56] Pickl-Herk, A. M. (2011). *Structural changes of minor group human rhinoviruses during uncoating* (Ph. D. thesis, University of Vienna, Vienna, Austria).

[57] Vogelsang, J., Kasper, R., Steinhauer, C., Person, B., Heilemann, M., Sauer, M., & Tinnefeld, P. (2008). A reducing and oxidizing system minimizes photobleaching and blinking of fluorescent dyes. *Angewandte chemie international edition*, 47(29), 5465-5469.

[58] <http://www.med-college.hu/hu/wiki/artikel.php?id=1233&lan=1>, downloaded on 16/11/2015

[59] Weiss, V. U., Subirats, X., Pickl-Herk, A., Bilek, G., Winkler, W., Kumar, M., Allmaier, G., Blaas, D., Kenndler, E. (2012). Characterization of rhinovirus subviral A particles via capillary electrophoresis, electron microscopy and gas-phase electrophoretic mobility molecular analysis: Part I. *Electrophoresis*, 33(12), 1833-1841.

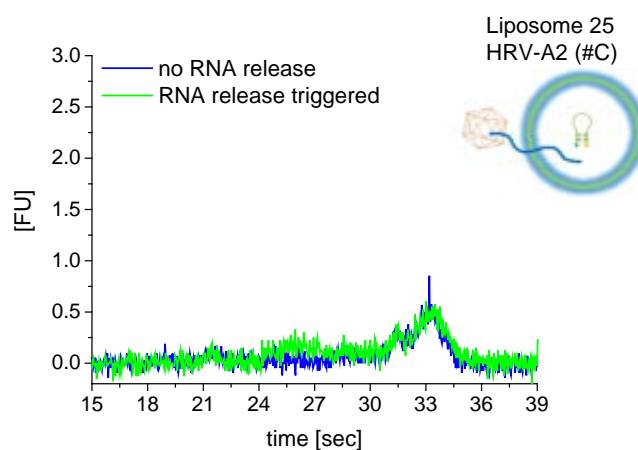
[60] Buchmueller, K. L., & Weeks, K. M. (2004). Tris-borate is a poor counterion for RNA: a cautionary tale for RNA folding studies. *Nucleic acids research*, 32(22), e184-e184.

Appendix A

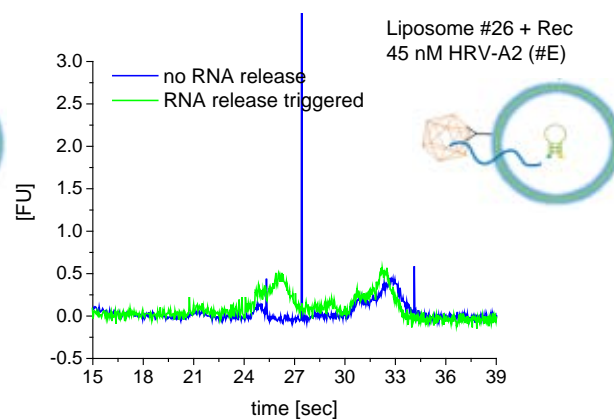
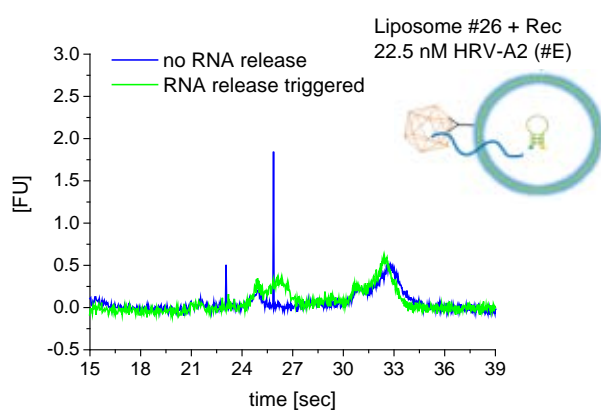
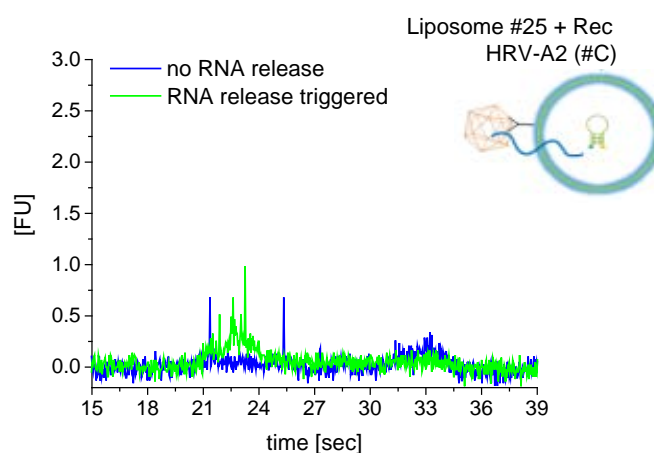
Further results obtained at the Bioanalyzer 2100 system

1. Further results regarding RNA release into liposomes

1.1. Liposomes in physiological lipid composition with NGS-NTA, but without receptor

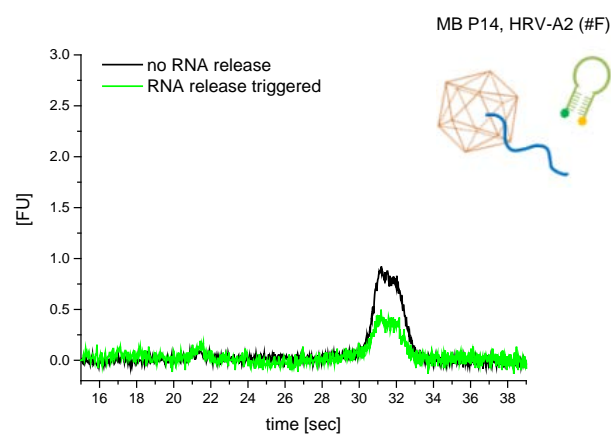
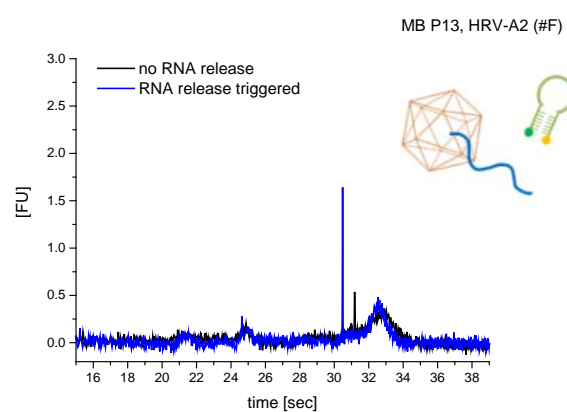
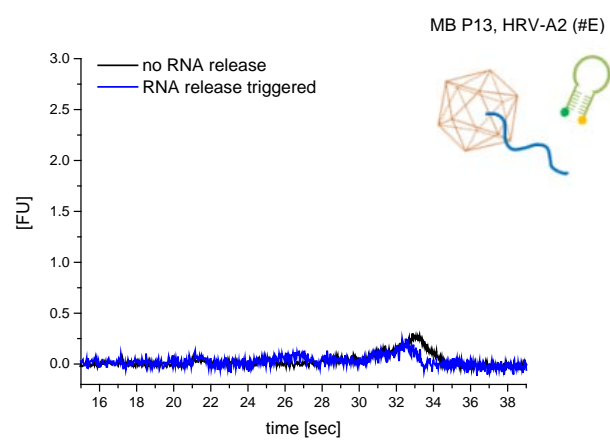


1.2. Liposomes in physiological lipid composition with NGS-NTA and receptor



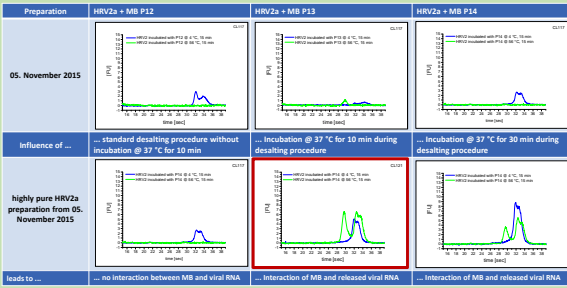
2. Further results regarding RNA release into solution (HRV-A2 #E and #F)

2.1. RNA release triggered by acidification

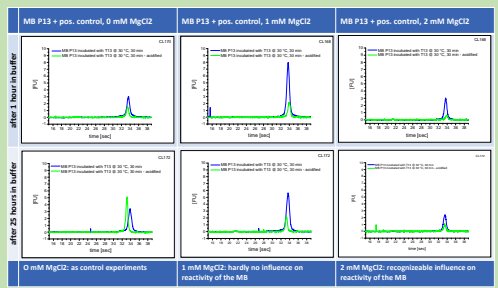


Further experiments for a Human Rhinovirus Serotype 2 (HRV-A2) RNA transfer setup to

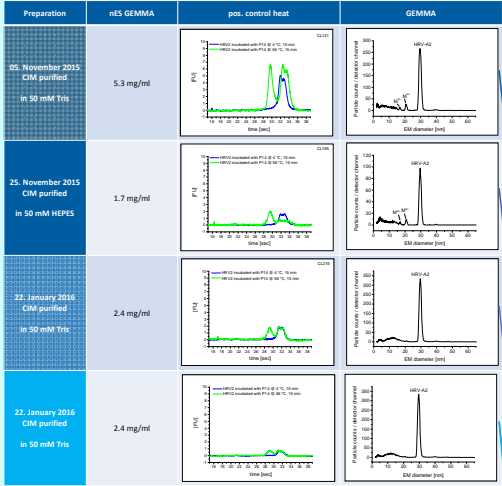
Adaptions in sample preparation



Differences in storage buffer



HRV2 preparations reactivity towards MB P14



Viral & subviral particle mobilities

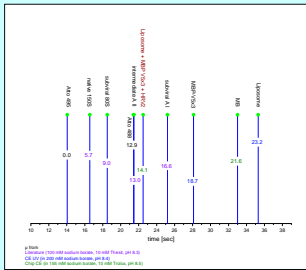
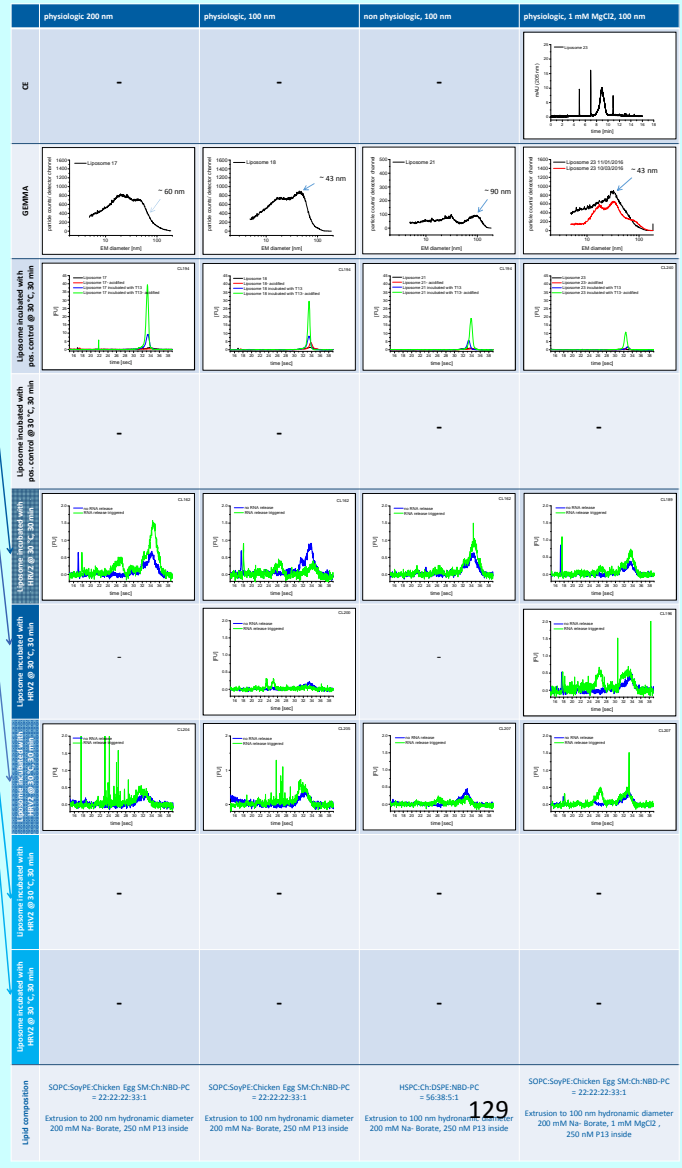


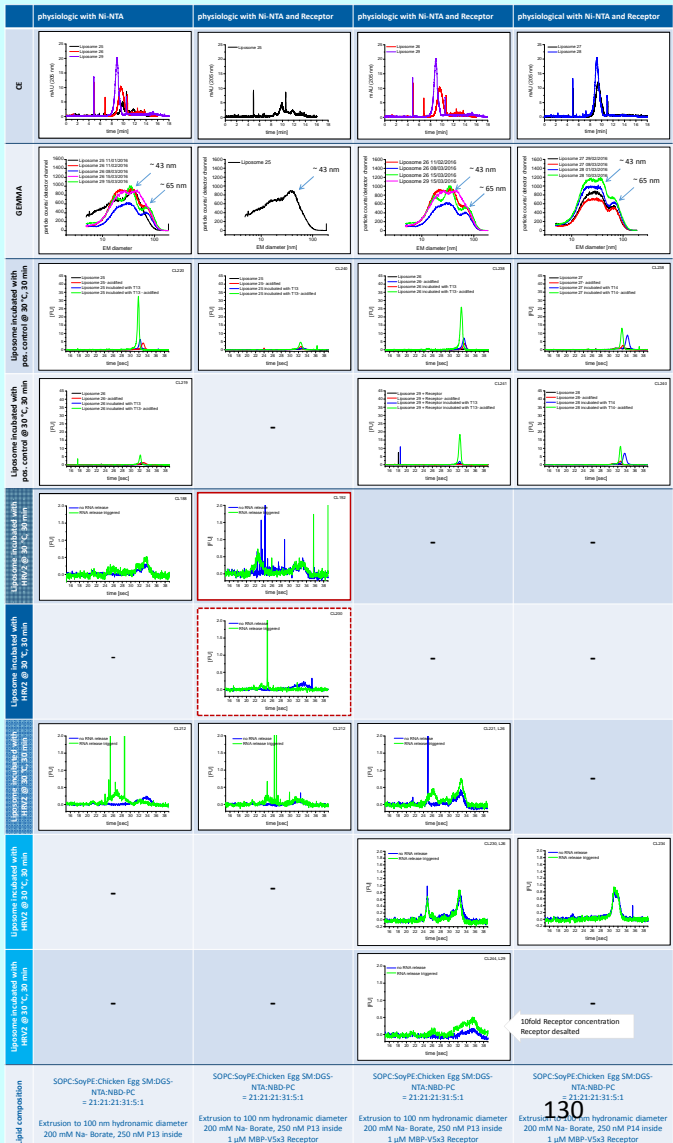
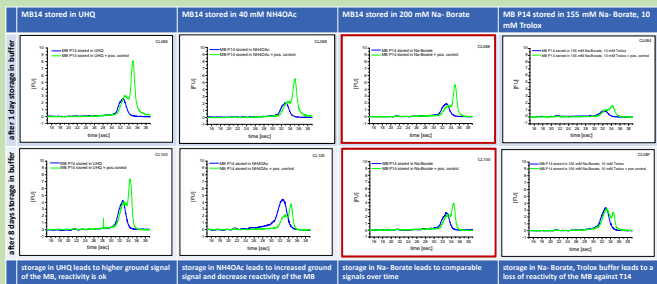
Figure 1 – Electrophoretic mobilities, pI, of viral and subviral particles, liposomes, MB and receptor MBP-V5x3 according to Table 1

Particle	pI*	SD*	t	n
native 135S ¹	-5.7	0.3	20	36
135S ¹ + V*	-16.6	0.4	20	5
intermediate AII ¹	-13.0	1.4	20	11
subviral B05 ¹ (heat)	-9.5	0.2	25	21
subviral B05 ¹ (pH)	-8.2	0.3	20	21
compare to 8.5 from [16]				
subviral B05 ¹ (pH)	-9.6	0.1	25	21
Receptor MBP V5x3	18.7	0.1	22.5	4
Liposome	23.2	0.6	22.5	13
Liposome + Receptor MBP V5x3 + HRV2	18.1 HRV2 from 05.10.15 15.1 HRV2 from 25.10.15	-	22.5	2
Molecular Beacon	21.6	0.1	22.5	5

Table 1 – Electrophoretic net mobilities, pI, of native virus and subviral particles (from doi: 10.1002/ds.201106647), liposomes, MB and receptor MBP-V5x3
* measuring temperature (°C): Heat: sample incubated at 56°C for 10 min.
pH: sample incubated at pH 5.0 for 15 min; pI averaged from 4 measurements;
SD, standard deviation.
* [10]¹ mV/Vs
* 100 mM sodium borate (pH 8.3), 10 mM Tris.
* 100 mM sodium borate (pH 8.3), 10 mM Tris.
* Preparation according to [2]



liposomes employing Molecular Beacons and Chip Electrophoresis



List of Bioanalyzer 2100 chips used				
Chip No.	Date	Script	samples	comments
CL001	18.08.2015	Eukaryotes Total RNA Nano Series	MB, Targets	
CL002	18.08.2015	Liposomes II, 1000 V, RT, DNA Series	MB ohne & pos control	failed
CL003	18.08.2015	Liposomes II, 1000 V, RT, DNA Series	MB ohne & neg control	
CL004	18.08.2015	Liposomes II, 1000 V, RT, DNA Series	MB ohne & pos control	
CL005	21.08.2015	Liposomes II, 1000 V, RT, DNA Series	Liposomen check: 1:20, 1:30, 1:40 (v/v)	
CL006	21.08.2015	Liposomes II, 1000 V, RT, DNA Series	Liposomen check: 1:20, 1:30, 1:40 (v/v)	
CL007	24.08.2015	Liposomes II, 1000 V, RT, DNA Series	Liposomen check: 1:2, 1:5, 1:10 (v/v)	
CL008	24.08.2015	Liposomes II, 1000 V, RT, DNA Series	MB + RNA Ladder as neg control	
CL009	25.08.2015	Liposomes II, 1000 V, RT, DNA Series	Liposomen check: 1:2 – 1:40 (v/v) new	extrusion failed
CL010	26.08.2015	Liposomes II, 1000 V, RT, DNA Series	Liposomen check: 1:2 – 1:40 (v/v) new	
CL011	26.08.2015	Liposomes II, 1000 V, RT, DNA Series	WH Liposomen 250 nM MB (Dupl.)	failed
CL012	27.08.2015	Liposomes II, 1000 V, RT, DNA Series	WH Liposomen 250 nM MB (Dupl.)	1_40 – 1:2 (v/v)
CL013	27.08.2015	Liposomes II, 1000 V, RT, DNA Series	MB + HRV2, +/- T	
CL014	27.08.2015	Liposomes II, 1000 V, RT, DNA Series	MB + HRV2, +/- T	Basislinie shifted
CL015	27.08.2015	Liposomes II, 1000 V, RT, DNA Series	MB + HRV2, ohne & mit erhitzen	Basislinie shifted
CL016	27.08.2015	Liposomes II, 1000 V, RT, DNA Series	MB +/- T (control)	
CL017	27.08.2015	Liposomes II, 1000 V, RT, DNA Series	MB +/- T (control)	
CL018	27.08.2015	Liposomes II, 1000 V, RT, DNA Series	WH Liposomen 250 nM, 1_40 -1:2 (v/v)	
CL019	28.08.2015	Liposomes II, 1000 V, RT, DNA Series	MB + HRV2, acidified	
CL020	28.08.2015	Liposomes II, 1000 V, RT, DNA Series	MB + HRV2, acidified	
CL021	28.08.2015	Liposomes II, 1000 V, RT, DNA Series	MB + HRV2, acidified	
CL022	28.08.2015	Liposomes II, 1000 V, RT, DNA Series	MB, acidified (control)	
CL023	28.08.2015	Liposomes II, 1000 V, RT, DNA Series	MB, acidified (control)	
CL024	31.08.2015	Liposomes II, 1000 V, RT, DNA Series	Liposomen 7 check: 1:40 – 1:2 (v/v)	BGE = 0 mM Trolox, 200 mM Na-Borate
CL025	02.09.2015	Liposomes II, 1000 V, RT, DNA Series	WH MB P12, 13, 14 +/- T	
CL026	02.09.2015	Liposomes II, 1000 V, RT, DNA Series	WH MB P12, 13, 14 +/- T	

CL027	02.09.2015	Liposomes II, 1000 V, RT, DNA Series	Liposome 4 acidified: 1:40 -1:2 (v/v)	
CL028	02.09.2015	Liposomes II, 1000 V, RT, DNA Series	Liposome 4 acidified: 1:40 -1:2 (v/v)	
CL029	03.09.2015	Liposomes II, 1000 V, RT, DNA Series	MB P14 + HRV2, +/- T	Virus inactive?
CL030	03.09.2015	Liposomes II, 1000 V, RT, DNA Series	HRV2 + Liposomes (6), +/- T	Virus inactive?
CL031	03.09.2015	Liposomes II, 1000 V, RT, DNA Series	HRV2 + Liposomes (6), +/- T	Virus inactive?
CL032	03.09.2015	Liposomes II, 1000 V, RT, DNA Series	HRV2 + Liposomes (6), +/- T	Virus inactive?
CL033	03.09.2015	Liposomes II, 1000 V, RT, DNA Series	HRV2 + MB P14, +/- T	Virus inactive?
CL034	04.09.2015	Liposomes II, 1000 V, RT, DNA Series	HRV2 (04/10/13) + MB, +/- T	Signal @ MB P13?
CL035	04.09.2015	Liposomes II, 1000 V, RT, DNA Series	HRV2 (04/10/13) + MB, +/- T	Signal @ MB P13?
CL036	04.09.2015	Liposomes II, 1000 V, RT, DNA Series	HRV2 (04/10/13) + MB, +/- T	Signal @ MB P13?
CL037	08.09.2015	Liposomes II, 1000 V, RT, DNA Series	Liposomes 9 & 10 check: 1:40 -1:2 (v/v)	
CL038	08.09.2015	Liposomes II, 1000 V, RT, DNA Series	Liposomes 9 & 10 check: 1:40 -1:2 (v/v)	
CL039	08.09.2015	Liposomes II, 1000 V, RT, DNA Series	Liposomes 8 & 4 check: 1:40 -1:2 (v/v)	
CL040	08.09.2015	Liposomes II, 1000 V, RT, DNA Series	Liposomes 8 & 4 check: 1:40 -1:2 (v/v)	
CL041	09.09.2015	Liposomes II, 1000 V, RT, DNA Series	Liposome 6 + pos contr. (T14) + pH	5,10,15,20,25 nM T
CL042	09.09.2015	Liposomes II, 1000 V, RT, DNA Series	Liposome 6 + pos contr. (T14) + pH	5,10,15,20,25 nM T
CL043	09.09.2015	Liposomes II, 1000 V, RT, DNA Series	Liposome 6 + neg contr. (T12) +pH	5,10,15,20,25 nM T
CL044	09.09.2015	Liposomes II, 1000 V, RT, DNA Series	Liposome 6 + neg contr. (T12) +pH	5,10,15,20,25 nM T
CL045	09.09.2015	Liposomes II, 1000 V, RT, DNA Series	Liposome 6 pos +neg control +pH	20, 40 nM T
CL046	10.09.2015	Liposomes II, 1000 V, RT, DNA Series	Liposome 6 pos +neg control + pH	100,150,200 nM T
CL047	10.09.2015	Liposomes II, 1000 V, RT, DNA Series	Liposome 6 pos +neg control + pH	100,150,200 nM T
CL048	10.09.2015	Liposomes II, 1000 V, RT, DNA Series	HRV2 (04/10/13) + Lipo 10 +pH	
CL049	10.09.2015	Liposomes II, 1000 V, RT, DNA Series	HRV2 (04/10/13) + Lipo 10 +pH	
CL050	10.09.2015	Liposomes II, 1000 V, RT, DNA Series	HRV2 (04/10/13) + Lipo 10 +pH	Signal increased?
CL051	10.09.2015	Liposomes II, 1000 V, RT, DNA Series	HRV2 (04/10/13) + Lipo 10 +pH	
CL052	14.09.2015	Liposomes II, 1000 V, RT, DNA Series	MB 12, 13, 14 + Target + pH	
CL053	14.09.2015	Liposomes II, 1000 V, RT, DNA Series	MB 12, 13, 14 + Target - pH	
CL054	14.09.2015	Liposomes II, 1000 V, RT, DNA Series	MB 12, 13, 14 + Target + pH	

CL055	14.09.2015	Liposomes II, 1000 V, RT, DNA Series	MB 12, 13, 14 + Target - pH	
CL056	16.09.2015	Liposomes II, 1000 V, RT, DNA Series	new MB 12, 13, 14 + Target + pH	
CL057	16.09.2015	Liposomes II, 1000 V, RT, DNA Series	new MB 12, 13, 14 + Target + pH	
CL058	16.09.2015	Liposomes II, 1000 V, RT, DNA Series	new MB 12, 13, 14 + Target - pH	
CL059	16.09.2015	Liposomes II, 1000 V, RT, DNA Series	new MB 12, 13, 14 + Target - pH	
CL060	21.09.2015	Liposomes II, 1000 V, RT, DNA Series	Comparison old & new P14, diff. T	4, 30, 50, 60,70 °C
CL061	21.09.2015	Liposomes II, 1000 V, RT, DNA Series	Comparison old & new P14, diff. T	4, 30, 50, 60,70 °C
CL062	22.09.2015	Liposomes II, 1000 V, RT, DNA Series	Comparison old & new P12, diff. T	4, 30, 50, 60,70 °C
CL063	22.09.2015	Liposomes II, 1000 V, RT, DNA Series	Comparison old & new P12, diff. T	4, 30, 50, 60,70 °C
CL064	22.09.2015	Eukaryotes Total RNA Nano Series	RNA chip, MB and Ladder (desalt.)	Desalted Ladder not stable
CL065	22.09.2015	Liposomes II, 1000 V, RT, DNA Series	Comp. old & new P12 + P14, diff. T	80 °C, 90 °C, + Target
CL066	22.09.2015	Liposomes II, 1000 V, RT, DNA Series	Comp. old & new P12 + P14, diff. T	80 °C, 90°C, + Target
CL067	23.09.2015	Liposomes II, 1000 V, RT, DNA Series	MB P12, P13, P14 new +/- T	
CL068	23.09.2015	Liposomes II, 1000 V, RT, DNA Series	MB P12, P13, P14 new +/- T	
CL069	24.09.2015	Liposomes II, 1000 V, RT, DNA Series	MB old & new, diff. T, +/- pH	
CL070	24.09.2015	Liposomes II, 1000 V, RT, DNA Series	MB old & new, diff. T, +/- pH	
CL071	24.09.2015	Liposomes II, 1000 V, RT, DNA Series	MB old & new, diff. T, +/- pH + Tar.	
CL072	24.09.2015	Liposomes II, 1000 V, RT, DNA Series	MB old & new, diff. T, +/- pH + Tar.	
CL073	25.09.2015	Liposomes II, 1000 V, RT, DNA Series	Liposome 4, diff. T, +/- pH	
CL074	25.09.2015	Liposomes II, 1000 V, RT, DNA Series	Liposome 4, diff. T, +/- pH	
CL075	28.09.2015	Liposomes II, 1000 V, RT, DNA Series	MB new + Lipo 4 + T + Target	
CL076	28.09.2015	Liposomes II, 1000 V, RT, DNA Series	MB new + Lipo 4 + T + Target	
CL077	29.09.2015	Liposomes II, 1000 V, RT, DNA Series	MB old + Lipo 6 + T + Target	
CL078	29.09.2015	Liposomes II, 1000 V, RT, DNA Series	MB old + Lipo 6 + T + Target	
CL079	01.10.2015	Liposomes II, 1000 V, RT, DNA Series	MB P14 V1-V4, + Target V2 & V4	
CL080	01.10.2015	Liposomes II, 1000 V, RT, DNA Series	MB P14 V1-V4, + Target V2 & V4	
CL081	06.10.2015	Liposomes II, 1000 V, RT, DNA Series	MB P14 V1-V4, + Target V2 & V4	After 4 days
CL082	06.10.2015	Liposomes II, 1000 V, RT, DNA Series	MB P14 V1-V4, + Target V2 & V4	After 4 days

CL083	07.10.2015	Liposomes II, 1000 V, RT, DNA Series	MB P14 V1-V4, + Target V2 & V4	After 5 days
CL084	08.10.2015	Liposomes II, 1000 V, RT, DNA Series	MB P14 V I-V IV, + Target V I & V III	New 50 μ M Intermediates
CL085	08.10.2015	Liposomes II, 1000 V, RT, DNA Series	MB P14 V I-V IV, + Target V I & V III	New 50 μ M Intermediates
CL086	09.10.2015	Liposomes II, 1000 V, RT, DNA Series	diff. old P14 + Target V2 & V III	
CL087	09.10.2015	Liposomes II, 1000 V, RT, DNA Series	diff. old P14 + Target V2 & V III	
CL088	12.10.2015	Liposomes II, 1000 V, RT, DNA Series	MB P14 V I-V IV, + Target V I & V III	new 1 μ M in BGE
CL089	12.10.2015	Liposomes II, 1000 V, RT, DNA Series	MB P14 V I-V IV, + Target V I & V III	based on 1 μ M Intermediates from 08/10
CL090	12.10.2015	Liposomes II, 1000 V, RT, DNA Series	MB P14 V I-V IV, + Target V I & V III	new 1 μ M in BGE
CL091	12.10.2015	Liposomes II, 1000 V, RT, DNA Series	MB P14 V I-V IV, + Target V I & V III	based on 1 μ M Intermediates from 08/10
CL092	12.10.2015	Liposomes II, 1000 V, RT, DNA Series	MB P14 V I-V IV, + Target V I & V III	new 1 μ M in diff. buffers
CL093	15.10.2015	Liposomes II, 1000 V, RT, DNA Series	MB P14 V I – V IV +T14 V I & V III	new 1 μ M Interm. in diff. buffers
CL094	15.10.2015	Liposomes II, 1000 V, RT, DNA Series	MB P14 V I – V IV +T14 V I & V III	1 μ M Interm. from 12/10/15
CL095	15.10.2015	Liposomes II, 1000 V, RT, DNA Series	MB P14 V I – V IV +T14 V I & V III	1 μ M Interm. from 12/10/15
CL096	15.10.2015	Liposomes II, 1000 V, RT, DNA Series	MB P14 V I – V IV +T14 V I & V III	new 1 μ M Interm. in diff. buffers
CL097	19.10.2015	Liposomes II, 1000 V, RT, DNA Series	HRV2 (04/10/13) + MB V III, +/- T	P12, P13, P14; HRV2 is broken
CL098	19.10.2015	Liposomes II, 1000 V, RT, DNA Series	HRV14 + MB V III, +/- T	Neg. control
CL099	19.10.2015	Liposomes II, 1000 V, RT, DNA Series	HRV14 + MB V III, +/- T	
CL100	20.10.2015	Liposomes II, 1000 V, RT, DNA Series	MB V I – V IV (1 μ M Interm. 12/10)	
CL101	23.10.2015	Liposomes II, 1000 V, RT, DNA Series	Lipo 11-12-13 check (1:5- 1:40 (v/v))	
CL102	23.10.2015	Liposomes II, 1000 V, RT, DNA Series	Lipo 11-12-13 + pos control, \pm pH	
CL103	23.10.2015	Liposomes II, 1000 V, RT, DNA Series	Lipo 11-12-13 + neg control, \pm pH	
CL104	23.10.2015	Liposomes II, 1000 V, RT, DNA Series	Lipo 11-12-13 + pos control, \pm pH	
CL105	23.10.2015	Liposomes II, 1000 V, RT, DNA Series	Lipo 11-12-13 + neg control, \pm pH	
CL106	27.10.2015	Liposomes II, 1000 V, RT, DNA Series	Lipo 11-12-13 + pos control, \pm T	
CL107	27.10.2015	Liposomes II, 1000 V, RT, DNA Series	Lipo 11-12-13 + neg control, \pm T	
CL108	28.10.2015	Liposomes II, 1000 V, RT, DNA Series	Lipo 11-12-13 + pos control, \pm pH	Higher conc.
CL119	02.11.2015	Liposomes II, 1000 V, RT, DNA Series	Lipo 12-13 + pos control, \pm pH	Diff. reneutralisation strategies

CL110	02.11.2015	Liposomes II, 1000 V, RT, DNA Series	Lipo 12-13 + pos control, \pm pH	Diff. reneutralisation strategies
CL111	03.11.2015	Liposomes II, 1000 V, RT, DNA Series	Lipo 11-12-13 check (1:5- 1:40 (v/v))	65 mM Na Borate, 10 mM Trolox, pH 9.4
CL112	03.11.2015	Liposomes II, 1000 V, RT, DNA Series	Lipo 11-12-13 check (1:5- 1:40 (v/v))	65 mM Na Borate, 10 mM Trolox, pH 9.4
CL113	04.11.2015	Liposomes II, 1000 V, RT, DNA Series	Lipo 11-12-13 check (1:5- 1:40 (v/v))	155 mM Na Borate, 10 mM Trolox, pH 8.4
CL114	04.11.2015	Liposomes II, 1000 V, RT, DNA Series	Lipo 11-12-13 check (1:5- 1:40 (v/v))	BGE: 65mM Na Borate, 10mM Trolox, pH 9.4
CL115	05.11.2015	Liposomes II, 1000 V, RT, DNA Series	Lipo 13, diff. tests (Δ pH, 1:x, + T14)	BGE: pH 8.4
CL116	05.11.2015	Liposomes II, 1000 V, RT, DNA Series	Lipo 11-12-13 (1:10, 1:25 (v/v)) + Target	BGE: pH 8.4
CL117	06.11.2015	Liposomes II, 1000 V, RT, DNA Series	HRV2 (11/15) check with MB, \pm T	
CL118	06.11.2015	Liposomes II, 1000 V, RT, DNA Series	HRV2 (11/15) check with MB, \pm T	
CL119	06.11.2015	Liposomes II, 1000 V, RT, DNA Series	MB P12, P13, P14 \pm T	
CL120	09.11.2015	Liposomes II, 1000 V, RT, DNA Series	Lipo 11-12-13 check (1:5- 1:40 (v/v))	Prepared in Agilent Eppendorf vials only
CL121	09.11.2015	Liposomes II, 1000 V, RT, DNA Series	HRV2 (11/15) + P14, \pm T	Incubation @ 37 °C for desalting
CL122	09.11.2015	Liposomes II, 1000 V, RT, DNA Series	HRV2 (11/15) + P14, \pm T	Incubation @ 37 °C for desalting
CL123	10.11.2015	Liposomes II, 1000 V, RT, DNA Series	Lipo 11-12-13 check (1:5-1:40 (v/v))	BGE: 200 mM Na-Borate, pH 8.4
CL124	12.11.2015	Liposomes II, 1000 V, RT, DNA Series	HRV2 (11/15) + P14 + contam., \pm T	
CL125	12.11.2015	Liposomes II, 1000 V, RT, DNA Series	HRV2 (11/15) + P14 + contam., \pm T	
CL126	17.11.2015	Liposomes II, 1000 V, RT, DNA Series	Liposome 11-14-15 check	
CL127	17.11.2015	Liposomes II, 1000 V, RT, DNA Series	Liposome 11-14-15 check	
CL128	17.11.2015	Liposomes II, 1000 V, RT, DNA Series	Liposome & MB + Target, \pm pH	
CL129	17.11.2015	Liposomes II, 1000 V, RT, DNA Series	Liposome & MB + Target, \pm pH	
CL130	19.11.2015	Liposomes II, 1000 V, RT, DNA Series	Liposome 11-14-15, + Target, \pm pH	BGE = 55 mM Na-Borate, 10 mM Trolox, pH 9.6
CL131	19.11.2015	Liposomes II, 1000 V, RT, DNA Series	Liposome 11-14-15, + Target, \pm pH	BGE = 155 mM Na-Borate, 10 mM Trolox, pH 8.4
CL132	19.11.2015	Liposomes II, 1000 V, RT, DNA Series	Liposome 11-14-15, + Target, \pm pH	BGE = 57 mM Na-Borate, 9,71 mM Trolox, pH 9.4
CL133	19.11.2015	Liposomes II, 1000 V, RT, DNA Series	Liposome 11-14-15, + Target, \pm pH	BGE = 77 mM Na-Borate, 7,7 mM Trolox, pH 9.0
CL134	20.11.2015	Liposomes II, 1000 V, RT, DNA Series	Liposome 11-14-15, + Target, \pm pH	BGE = 155 mM Na-Borate, 10 mM Trolox, pH 8.4

CL135	20.11.2015	Liposomes II, 1000 V, RT, DNA Series	Liposome 14-15-11, + Target, \pm pH	BGE = 155 mM Na-Borate, 10 mM Trolox, pH 8.4
CL136	20.11.2015	Liposomes II, 1000 V, RT, DNA Series	Liposome 15-11-14, + Target, \pm pH	BGE = 155 mM Na-Borate, 10 mM Trolox, pH 8.4
CL137	20.11.2015	Liposomes II, 1000 V, RT, DNA Series	Liposome 11-14-15, + Target, \pm pH	BGE = 77 mM Na-Borate, 10 mM Trolox, pH 9.0
CL138	20.11.2015	Liposomes II, 1000 V, RT, DNA Series	Liposome 14-15-11, + Target, \pm pH	BGE = 77 mM Na-Borate, 10 mM Trolox, pH 9.0
CL139	20.11.2015	Liposomes II, 1000 V, RT, DNA Series	Liposome 15-11-14, + Target, \pm pH	BGE = 77 mM Na-Borate, 10 mM Trolox, pH 9.0
CL140	20.11.2015	Liposomes II, 1000 V, RT, DNA Series	Liposome 15-11-14, + Target, \pm pH	BGE = 155 mM Na-Borate, 10 mM Trolox, pH 8.4
CL141	24.11.2015	Liposomes II, 1000 V, RT, DNA Series	Liposome 11-14-15, + Target, \pm pH	above: - pH, bottom: + pH
CL142	24.11.2015	Liposomes II, 1000 V, RT, DNA Series	Liposome 11-14-15, + Target, \pm pH	above: + pH, bottom: - pH
CL143	24.11.2015	Liposomes II, 1000 V, RT, DNA Series	HRV2 (11/15) + Lipo 11-14-15, \pm pH	BGE = 155 mM Na-Borate, 10 mM Trolox, pH 8.4
CL144	24.11.2015	Liposomes II, 1000 V, RT, DNA Series	HRV2 (11/15) + Lipo 11-14-15, \pm pH	BGE = 155 mM Na-Borate, 10 mM Trolox, pH 8.4
CL145	24.11.2015	Liposomes II, 1000 V, RT, DNA Series	HRV2 (11/15) + Lipo 11-14-15, \pm pH	BGE = 77 mM Na-Borate, 10 mM Trolox, pH 9.0
CL146	24.11.2015	Liposomes II, 1000 V, RT, DNA Series	HRV2 (11/15) + Lipo 11-14-15, \pm pH	BGE = 155 mM Na-Borate, 10 mM Trolox, pH 8.4
CL147	26.11.2015	Liposomes II, 1000 V, RT, DNA Series	HRV2 (11/15) + Lipo 14 & P13, \pm pH	BGE = 155 mM Na-Borate, 10 mM Trolox, pH 8.4
CL148	26.11.2015	Liposomes II, 1000 V, RT, DNA Series	HRV2 (11/15) + Lipo 15 & P15, \pm pH	BGE = 155 mM Na-Borate, 10 mM Trolox, pH 8.4
CL149	26.11.2015	Liposomes II, 1000 V, RT, DNA Series	HRV2 (11/15) + Lipo 14 & P13, \pm pH	BGE = 155 mM Na-Borate, 10 mM Trolox, pH 8.4
CL150	26.11.2015	Liposomes II, 1000 V, RT, DNA Series	HRV2 (11/15) + Lipo 15 & P15, \pm pH	BGE = 155 mM Na-Borate, 10 mM Trolox, pH 8.4
CL151	26.11.2015	Liposomes II, 1000 V, RT, DNA Series	HRV2 (11/15) + Lipo 14 & P13, \pm pH	BGE = 77 mM Na-Borate, 10 mM Trolox, pH 9.0
CL152	26.11.2015	Liposomes II, 1000 V, RT, DNA Series	HRV2 (11/15) + Lipo 14 & P13, \pm pH	BGE = 77 mM Na-Borate, 10 mM Trolox, pH 9.0
CL153	26.11.2015	Liposomes II, 1000 V, RT, DNA Series	HRV2 (11/15) + Lipo 15 & P15, \pm pH	BGE = 77 mM Na-Borate, 10 mM Trolox, pH 9.0

CL154	30.11.2015	Liposomes II, 1000 V, RT, DNA Series	Lipo 11-14-15 & MB + Target, \pm pH	BGE = 155 mM Na-Borate, 10 mM Trolox, pH 8.4
CL155	04.12.2015	Liposomes II, 1000 V, RT, DNA Series	Lipo 17-18-20-21 check(1:40-1:10 (v/v))	
CL156	04.12.2015	Liposomes II, 1000 V, RT, DNA Series	Lipo 17-18-20-21 check(1:40-1:10 (v/v))	
CL157	07.12.2015	Liposomes II, 1000 V, RT, DNA Series	Lipo 17-18-20-21, \pm pH, \pm Target	
CL158	09.12.2015	Liposomes II, 1000 V, RT, DNA Series	Lipo 17-18-20-21 check(1:5-1:1.5(v/v))	
CL159	09.12.2015	Liposomes II, 1000 V, RT, DNA Series	Lipo 17-18 (1:5 (v/v)), \pm pH, \pm Target	
CL160	09.12.2015	Liposomes II, 1000 V, RT, DNA Series	Lipo 20-21 (1:5 (v/v)), \pm pH, \pm Target	
CL161	09.12.2015	Liposomes II, 1000 V, RT, DNA Series	Lipo 20-21 (1:5 (v/v)), \pm pH, \pm Target	
CL162	10.12.2015	Liposomes II, 1000 V, RT, DNA Series	HRV2 + Lipo 17-18-20-21, \pm pH	
CL163	10.12.2015	Liposomes II, 1000 V, RT, DNA Series	HRV2 + Lipo 17-18-20-21, \pm pH	
CL164	11.12.2015	Liposomes II, 1000 V, RT, DNA Series	Lipo 17-18-20-21, \pm pH	
CL165	11.12.2015	Liposomes II, 1000 V, RT, DNA Series	Lipo 17-18-20-21, \pm pH	
CL166	15.12.2015	Liposomes II, 1000 V, RT, DNA Series	MB P13, \pm T13, 0; 0.1;0,25 mM Mg	\pm pH
CL167	15.12.2015	Liposomes II, 1000 V, RT, DNA Series	MB P13, \pm T13, 0.5;1;2 mM Mg	FAILED
CL168	15.12.2015	Liposomes II, 1000 V, RT, DNA Series	MB P13, \pm T13, 0.5;1;2 mM Mg	\pm pH
CL169	15.12.2015	Liposomes II, 1000 V, RT, DNA Series	MB P13, \pm T13, 0.5;1;2 mM Mg	\pm pH
CL170	15.12.2015	Liposomes II, 1000 V, RT, DNA Series	MB P13, \pm T13, 0; 0.1;0,25 mM Mg	\pm pH
CL171	16.12.2015	Liposomes II, 1000 V, RT, DNA Series	MB P13, \pm T13, 0;1;2 mM Mg \pm pH	
CL172	16.12.2015	Liposomes II, 1000 V, RT, DNA Series	MB P13, \pm T13, 0;1;2 mM Mg \pm pH	
CL173	16.12.2015	Liposomes II, 1000 V, RT, DNA Series	MB P13, \pm T13, 1 mM Mg \pm pH	Incubation @ RT, 30°C, 37°C, stored @ RT
CL174	16.12.2015	Liposomes II, 1000 V, RT, DNA Series	MB P13, \pm T13, 1 mM Mg \pm pH	Incubation @ RT, 30°C, 37°C, stored @ ice
CL175	16.12.2015	Liposomes II, 1000 V, RT, DNA Series	MB P13, \pm T13, 1 mM Mg \pm pH (WH)	Incubation @ RT, 30°C, 37°C, stored @ RT
CL176	17.12.2015	Liposomes II, 1000 V, RT, DNA Series	MB P13, \pm T13, 1 mM Mg \pm pH	Incubation @ RT, 30°C, 37°C, stored @ RT
CL177	17.12.2015	Liposomes II, 1000 V, RT, DNA Series	MB P13, \pm T13, 1 mM Mg \pm pH	Incubation @ RT, 30°C, 37°C, stored @ ice
CL178	17.12.2015	Liposomes II, 1000 V, RT, DNA Series	MB P13, \pm T13, 1 mM Mg \pm pH (WH)	Incubation @ RT, 30°C, 37°C, stored @ RT
CL179	21.12.2015	Liposomes II, 1000 V, RT, DNA Series	MB P13, \pm T13, 1 mM Mg \pm pH	Incubation @ RT, 30°C, 37°C, stored @ RT
CL180	21.12.2015	Liposomes II, 1000 V, RT, DNA Series	MB P13, \pm T13, 1 mM Mg \pm pH	Incubation @ RT, 30°C, 37°C, stored @ ice

CL181	07.01.2016	Liposomes II, 1000 V, RT, DNA Series	MB P13, \pm T13, 1 mM Mg \pm pH	Incubation @ RT, 30°C, 37°C, stored @ ice
CL182	07.01.2016	Liposomes II, 1000 V, RT, DNA Series	Lipo 18, \pm T13, 1 mM Mg \pm pH	Incubation @ RT, 30°C, 37°C, stored @ ice
CL183	07.01.2016	Liposomes II, 1000 V, RT, DNA Series	MB P13, \pm T13, 1 mM Mg \pm pH	Incubation @ RT, 30°C, 37°C, stored @ RT
CL184	07.01.2016	Liposomes II, 1000 V, RT, DNA Series	Lipo 18, \pm T13, 1 mM Mg \pm pH	Incubation @ RT, 30°C, 37°C, stored @ RT
CL185	11.01.2016	Liposomes II, 1000 V, RT, DNA Series	Lipo 22-23-24-25, \pm T13, \pm pH	
CL186	11.01.2016	Liposomes II, 1000 V, RT, DNA Series	Lipo 22-23-24-25, \pm Target, \pm pH	
CL187	12.01.2016	Liposomes II, 1000 V, RT, DNA Series	Lipo 22-23-24-25 check (1:10-1:2 (v/v))	
CL188	13.01.2016	Liposomes II, 1000 V, RT, DNA Series	HRV2 (11/15) + Lipo 23-25, \pm pH	
CL189	13.01.2016	Liposomes II, 1000 V, RT, DNA Series	HRV2 (11/15) + Lipo 23-25, \pm pH	
CL190	13.01.2016	Liposomes II, 1000 V, RT, DNA Series	HRV2 (11/15) + Lipo 23-25, \pm pH	recovered from CL188
CL191	14.01.2016	Liposomes II, 1000 V, RT, DNA Series	HRV2 (11/15) + Lipo 25 + Rec \pm pH	
CL192	14.01.2016	Liposomes II, 1000 V, RT, DNA Series	HRV2 (11/15) + Lipo 25 + Rec \pm pH	
CL193	19.01.2016	Liposomes II, 1000 V, RT, DNA Series	Lipo 17-18-21 (1:5 (v/v)), Lipo 25+R +T13	\pm pH
CL194	19.01.2016	Liposomes II, 1000 V, RT, DNA Series	Lipo 17-18-21 (1:5 (v/v)), Lipo 25+R +T13	\pm pH
CL195	22.01.2016	Liposomes II, 1000 V, RT, DNA Series	HRV2(12/15)+P14 Δ T, Lipo 23 \pm pH	
CL196	22.01.2016	Liposomes II, 1000 V, RT, DNA Series	HRV2(12/15)+P14 Δ T, Lipo 23 \pm pH	
CL197	22.01.2016	Liposomes II, 1000 V, RT, DNA Series	HRV2(12/15)+P14 Δ T, Lipo 23 \pm pH	recovered
CL198	25.01.2016	Liposomes II, 1000 V, RT, DNA Series	Benzonase check on MB P13, \pm pH	
CL199	26.01.2016	Liposomes II, 1000 V, RT, DNA Series	Benzonase check on MB P13, \pm pH	overnight @ RT
CL200	26.01.2016	Liposomes II, 1000 V, RT, DNA Series	HRV2(12/15) + Lipo 18_25+R, \pm pH	
CL201	26.01.2016	Liposomes II, 1000 V, RT, DNA Series	HRV2(12/15) + Lipo 18_25+R, \pm pH	TEM
CL202	26.01.2016	Liposomes II, 1000 V, RT, DNA Series	HRV2(12/15) + Lipo 18_25+R, \pm pH	recovered from CL200
CL203	27.01.2016	Liposomes II, 1000 V, RT, DNA Series	new Benzonase check on P13, \pm pH	
CL204	01.02.2016	Liposomes II, 1000 V, RT, DNA Series	HRV2(01/16) + Lipo 17_18, \pm pH	
CL205	01.02.2016	Liposomes II, 1000 V, RT, DNA Series	HRV2(01/16) + Lipo 17_18, \pm pH	
CL206	01.02.2016	Liposomes II, 1000 V, RT, DNA Series	HRV2(01/16) + Lipo 17_18, \pm pH	Recovered from CL204
CL207	02.02.2016	Liposomes II, 1000 V, RT, DNA Series	HRV2(01/16) + Lipo 21_23, \pm pH	
CL208	02.02.2016	Liposomes II, 1000 V, RT, DNA Series	HRV2(01/16) + Lipo 21_23, \pm pH	

CL209	02.02.2016	Liposomes II, 1000 V, RT, DNA Series	HRV2(01/16) + Lipo 21_23, \pm pH	Recovered from CL208
CL210	02.02.2016	Liposomes II, 1000 V, RT, DNA Series	HRV2(01/16) + Lipo 21_23, \pm pH	benzonase digested
CL211	04.02.2016	Liposomes II, 1000 V, RT, DNA Series	HRV2(01/16) + Lipo 25 \pm Rec, \pm pH	
CL212	04.02.2016	Liposomes II, 1000 V, RT, DNA Series	HRV2(01/16) + Lipo 25 \pm Rec, \pm pH	
CL213	04.02.2016	Liposomes II, 1000 V, RT, DNA Series	HRV2(01/16) + Lipo 25 \pm Rec, \pm pH	recovered from CL212
CL214	04.02.2016	Liposomes II, 1000 V, RT, DNA Series	HRV2(01/16) + Lipo 25 \pm Rec, \pm pH	benzonase digested
CL215	08.02.2016	Liposomes II, 1000 V, RT, DNA Series	HRV2(01/16) + MB P14 new, Δ T	
CL216	08.02.2016	Liposomes II, 1000 V, RT, DNA Series	HRV2(01/16) + Lipo 25 \pm Rec, \pm pH	$\frac{1}{2}$ conc. Of HRV2 (22,5 nM)
CL217	08.02.2016	Liposomes II, 1000 V, RT, DNA Series	HRV2(01/16) + Lipo 25 \pm Rec, \pm pH	$\frac{1}{2}$ conc. Of HRV2 (22,5 nM)
CL218	08.02.2016	Liposomes II, 1000 V, RT, DNA Series	HRV2(01/16) + Lipo 25 \pm Rec, \pm pH	$\frac{1}{2}$ conc. Of HRV2 (22,5 nM), recovered
CL219	12.02.2016	Liposomes II, 1000 V, RT, DNA Series	Lipo 25, 26 \pm Rec, \pm Target, \pm pH	
CL220	12.02.2016	Liposomes II, 1000 V, RT, DNA Series	Lipo 25, 26 \pm Rec, \pm Target, \pm pH	
CL221	16.02.2016	Liposomes II, 1000 V, RT, DNA Series	HRV2(01/16) + Lipo 26 \pm Rec, \pm pH	22,5 nM & 45 nM HRV2
CL222	16.02.2016	Liposomes II, 1000 V, RT, DNA Series	HRV2(01/16) + Lipo 26 \pm Rec, \pm pH	22,5 nM & 45 nM HRV2
CL223	16.02.2016	Liposomes II, 1000 V, RT, DNA Series	HRV2(01/16) + Lipo 26 \pm Rec, \pm pH	22,5 nM & 45 nM HRV2
CL224	16.02.2016	Liposomes II, 1000 V, RT, DNA Series	HRV2(01/16) + Lipo 26 \pm Rec, \pm pH	22,5 nM & 45 nM HRV2, Benzonase digested
CL225	18.02.2016	Liposomes II, 1000 V, RT, DNA Series	HRV2 (01/16) + MB P13, \pm pH	+ P13 + Rec \pm pH
CL226	18.02.2016	Liposomes II, 1000 V, RT, DNA Series	HRV2 (01/16) + MB P13, \pm pH	+ P13 + Rec \pm pH, recovered
CL227	18.02.2016	Liposomes II, 1000 V, RT, DNA Series	HRV2 (01/16) + MB P13, \pm pH	+ P13 + Rec \pm pH, Benzonase digested
CL228	01.03.2016	Liposomes II, 1000 V, RT, DNA Series	HRV2(01/16_2) + MB P14 Δ T	
CL229	02.03.2016	Liposomes II, 1000 V, RT, DNA Series	HRV2(01/16_2) + Lipo26/ P13, \pm pH	
CL230	02.03.2016	Liposomes II, 1000 V, RT, DNA Series	HRV2(01/16_2) + Lipo26/ P13, \pm pH	
CL231	02.03.2016	Liposomes II, 1000 V, RT, DNA Series	HRV2(01/16_2) + Lipo26/ P13, \pm pH	recovered from CL230
CL232	02.03.2016	Liposomes II, 1000 V, RT, DNA Series	HRV2(01/16_2) + Lipo26/ P13, \pm pH	recover from CL228, Benzonase digested
CL233	03.03.2016	Liposomes II, 1000 V, RT, DNA Series	HRV2(01/16_2) + Lipo27/ P14, \pm pH	
CL234	03.03.2016	Liposomes II, 1000 V, RT, DNA Series	HRV2(01/16_2) + Lipo27/ P14, \pm pH	
CL235	03.03.2016	Liposomes II, 1000 V, RT, DNA Series	HRV2(01/16_2) + Lipo27/ P14, \pm pH	recovered from CL234
CL236	03.03.2016	Liposomes II, 1000 V, RT, DNA Series	HRV2(01/16_2) + Lipo27/ P14, \pm pH	recovered from CL233, Benzonase digest

CL237	04.03.2016	Liposomes II, 1000 V, RT, DNA Series	Lipo 26, 27, 27 + Rec + pos. control	± pH
CL238	04.03.2016	Liposomes II, 1000 V, RT, DNA Series	Lipo 26, 27, 27 + Rec + pos. control	± pH
CL239	10.03.2016	Liposomes II, 1000 V, RT, DNA Series	Lipo 23,25 +Rec,28 +Rec +pos.control	± pH
CL240	10.03.2016	Liposomes II, 1000 V, RT, DNA Series	Lipo 23,25 +Rec,28 +Rec +pos.control	± pH
CL241	15.03.2016	Liposomes II, 1000 V, RT, DNA Series	Lipo 29 + Rec + pos control, ± pH	
CL242	15.03.2016	Liposomes II, 1000 V, RT, DNA Series	Lipo 29 + Rec + pos control, ± pH	
CL243	16.03.2016	Liposomes II, 1000 V, RT, DNA Series	Lipo 29 + HRV2(01/16_2) + Rec ± pH	
CL244	16.03.2016	Liposomes II, 1000 V, RT, DNA Series	Lipo 29 + HRV2(01/16_2) + Rec ± pH	
CL245	16.03.2016	Liposomes II, 1000 V, RT, DNA Series	Lipo 29 + HRV2(01/16_2) + Rec ± pH	recovered from CL243, ΔT for RNA release
CL246	16.03.2016	Liposomes II, 1000 V, RT, DNA Series	Lipo 29 + HRV2(01/16_2) + Rec ± pH	recovered from CL244
CL247	16.03.2016	Liposomes II, 1000 V, RT, DNA Series	Lipo 29 + HRV2(01/16_2) + Rec ± pH	recovered from CL245, ΔT for RNA release
CL248	17.03.2016	Liposomes II, 1000 V, RT, DNA Series	HRV2(01/16_2) + MB P13 ΔT	

Bioanalyzer scripts

1. Eukaryotes Total RNA Nano Series

#	Duration	[D1]	D1	[C1]	C1	[B1]	B1	[A1]	A1	[D2]	D2	[C2]	C2	[B2]	B2	[A2]	A2
0	0.1	0	350	0	350	0	350	0	350	0	350	0	350	0	1100	0	350
1	3.5	1	-0.3	1	-0.3	1	-0.3	1	-0.3	1	-0.3	1	-0.3	0	1100	1	-0.3
2	60	1	0	1	0	1	0	1	0	0	100	1	0	0	1500	1	0
3	90	1	0	1	0	1	0	1	0	1	0	0	1500	1	0	0	100
4	60	1	0	1	0	1	0	1	0	1	-3.8	1	0.1	0	1500	1	-0.38
5	60	1	0	1	0	1	0	1	0	1	-3.8	1	0.1	0	1500	1	-0.38
6	60	1	0	1	0	1	0	1	0	0	100	1	0.1	0	1500	1	0.1
7	15	1	0	1	0	1	0	1	0	1	-1.5	0	1400	1	-1.5	1	-2
8	2	1	0	1	0	1	0	1	0	1	-4	1	1	0	1500	1	1
9	0	0	0	0	0	0	0	0	0	0	0	4	0	0	0	3	0
10	85	1	0	1	0	1	0	1	0	0	100	1	3.3	0	1200	1	0.1
11	7	1	0	1	0	1	0	1	0	1	-1.5	1	0	1	-1.5	0	1400
12	2	1	0	1	0	1	0	1	0	1	-4	1	0	0	1500	1	1
13	0	0	0	0	0	0	0	0	0	0	0	4	0	0	0	3	0
14	85	1	0.05	1	0.05	1	0	1	0	0	100	1	3.3	0	1200	1	0.1
15	7	1	0	1	0	1	0	1	0	1	-1.5	1	0	1	-1.5	0	1400
16	2	1	0	1	0	1	0	1	0	1	-4	1	0	0	1500	1	1
17	0	2	240	0	0	0	0	0	0	0	0	4	0	0	0	3	0
18	85	1	-3.45	1	0.05	1	0	1	0	0	100	1	3.3	0	1200	1	0.1
19	7	1	-2	1	0	1	0	1	0	1	-1.5	1	0	1	-1.5	0	1400
20	2	1	1	1	0	1	0	1	0	1	-4	1	0	0	1500	1	1
21	0	0	0	0	0	0	0	0	0	0	0	4	0	0	0	3	0
22	85	1	0.05	1	0.05	1	0	1	0	0	100	1	3.3	0	1200	1	0.1
23	7	1	0	1	0	1	0	1	0	1	-1.5	1	0	1	-1.5	0	1400
24	2	1	0	1	0	1	0	1	0	1	-4	1	0	0	1500	1	1
25	0	0	0	0	0	0	0	0	0	0	0	4	0	0	0	3	0
26	85	1	0.05	1	0.05	1	0	1	0	0	100	1	3.3	0	1200	1	0.1
27	7	1	0	1	0	1	0	1	0	1	-1.5	1	0	1	-1.5	0	1400
28	2	1	0	1	0	1	0	1	0	1	-4	1	0	0	1500	1	1
29	0	0	0	2	240	0	0	0	0	0	0	4	0	0	0	3	0
30	85	1	0.05	1	-3.45	1	0	1	0	0	100	1	3.3	0	1200	1	0.1
31	7	1	0	1	-2	1	0	1	0	1	-1.5	1	0	1	-1.5	0	1400
32	2	1	0	1	1	1	0	1	0	1	-4	1	0	0	1500	1	1
33	0	0	0	0	0	0	0	0	0	0	0	3	0	0	0	4	0
34	85	1	0	1	0	1	0.05	1	0.05	0	100	1	0.1	0	1200	1	3.3
35	7	1	0	1	0	1	0	1	0	1	-1.5	0	1400	1	-1.5	1	0
36	2	1	0	1	0	1	0	1	0	1	-4	1	1	0	1500	1	0
37	0	0	0	0	0	0	0	0	0	0	0	3	0	0	0	4	0
38	85	1	0	1	0	1	0.05	1	0.05	0	100	1	0.1	0	1200	1	3.3
39	7	1	0	1	0	1	0	1	0	1	-1.5	0	1400	1	-1.5	1	0
40	2	1	0	1	0	1	0	1	0	1	-4	1	1	0	1500	1	0
41	0	0	0	0	0	2	240	0	0	0	0	3	0	0	0	4	0
42	85	1	0	1	0	1	-3.45	1	0.05	0	100	1	0.1	0	1200	1	3.3
43	7	1	0	1	0	1	-2	1	0	1	-1.5	0	1400	1	-1.5	1	0
44	2	1	0	1	0	1	1	1	0	1	-4	1	1	0	1500	1	0
45	0	0	0	0	0	0	0	0	0	0	0	3	0	0	0	4	0
46	85	1	0	1	0	1	0.05	1	0.05	0	100	1	0.1	0	1200	1	3.3
47	7	1	0	1	0	1	0	1	0	1	-1.5	0	1400	1	-1.5	1	0
48	2	1	0	1	0	1	0	1	0	1	-4	1	1	0	1500	1	0
49	0	0	0	0	0	0	0	0	0	0	0	3	0	0	0	4	0
50	85	1	0	1	0	1	0.05	1	0.05	0	100	1	0.1	0	1200	1	3.3
51	7	1	0	1	0	1	0	1	0	1	-1.5	0	1400	1	-1.5	1	0
52	2	1	0	1	0	1	0	1	0	1	-4	1	1	0	1500	1	0
53	0	0	0	0	0	0	0	2	240	0	0	3	0	0	0	4	0
54	85	1	0	1	0	1	0.05	1	-3.45	0	100	1	0.1	0	1200	1	3.3
55	7	1	0	1	0	1	0	1	-2	1	-1.5	0	1400	1	-1.5	1	0
56	2	1	0	1	0	1	0	1	1	1	-4	1	1	0	1500	1	0
57	85	1	0	1	0	1	0	1	0	0	100	1	0.1	0	1200	1	0.1
58	1	0	0	0	0	0	0	0	0	0	0	0	0	0	0	0	0

#	Duration	[D3]	D3	[C3]	C3	[B3]	B3	[A3]	A3	[D4]	D4	[C4]	C4	[B4]	B4	[A4]	A4
0	0.1	0	350	0	350	0	350	0	350	0	350	0	350	0	350	0	350
1	3.5	1	-0.3	1	-0.3	1	-0.3	1	-0.3	1	-0.3	1	-0.3	1	-0.3	1	-0.3
2	60	1	0	1	0	1	0	1	0	1	0	1	0	1	0	1	0
3	90	1	0	1	0	1	0	1	0	1	0	1	0	1	0	1	0
4	60	1	0	1	0	1	0	1	0	1	0	1	0	1	0	1	0
5	60	1	0	1	0	1	0	1	0	1	0	1	0	1	0	1	0
6	60	1	0	1	0	1	0	1	0	1	0	1	0	1	0	1	0
7	15	1	0	1	0	1	0	1	0	1	0	1	0	1	0	1	0
8	2	1	0	1	0	1	0	1	0	1	0	1	0	1	0	1	0
9	0	2	240	0	0	0	0	0	0	0	0	0	0	0	0	0	0
10	85	1	-3.2	1	0	1	0	1	0	1	0	1	0	1	0	1	0
11	7	1	-2	1	0	1	0	1	0	1	0	1	0	1	0	1	0
12	2	1	1	1	0	1	0	1	0	1	0	1	0	1	0	1	0
13	0	0	0	0	0	0	0	0	0	2	240	0	0	0	0	0	0
14	85	1	0.05	1	0.05	1	0	1	0	1	-3.45	1	0.05	1	0	1	0
15	7	1	0	1	0	1	0	1	0	1	-2	1	0	1	0	1	0
16	2	1	0	1	0	1	0	1	0	1	1	1	0	1	0	1	0
17	0	0	0	0	0	0	0	0	0	0	0	0	0	0	0	0	0
18	85	1	0.05	1	0.05	1	0	1	0	1	0.05	1	0.05	1	0	1	0
19	7	1	0	1	0	1	0	1	0	1	0	1	0	1	0	1	0
20	2	1	0	1	0	1	0	1	0	1	0	1	0	1	0	1	0
21	0	0	0	2	240	0	0	0	0	0	0	0	0	0	0	0	0
22	85	1	0.05	1	-3.45	1	0	1	0	1	0.05	1	0.05	1	0	1	0
23	7	1	0	1	-2	1	0	1	0	1	0	1	0	1	0	1	0
24	2	1	0	1	1	1	0	1	0	1	0	1	0	1	0	1	0
25	0	0	0	0	0	0	0	0	0	0	0	2	240	0	0	0	0
26	85	1	0.05	1	0.05	1	0	1	0	1	0.05	1	-3.45	1	0	1	0
27	7	1	0	1	0	1	0	1	0	1	0	1	-2	1	0	1	0
28	2	1	0	1	0	1	0	1	0	1	0	1	1	1	0	1	0
29	0	0	0	0	0	0	0	0	0	0	0	0	0	0	0	0	0
30	85	1	0.05	1	0.05	1	0	1	0	1	0.05	1	0.05	1	0	1	0
31	7	1	0	1	0	1	0	1	0	1	0	1	0	1	0	1	0
32	2	1	0	1	0	1	0	1	0	1	0	1	0	1	0	1	0
33	0	0	0	0	0	2	240	0	0	0	0	0	0	0	0	0	0
34	85	1	0	1	0	1	-3.45	1	0.05	1	0	1	0	1	0.05	1	0.05
35	7	1	0	1	0	1	-2	1	0	1	0	1	0	1	0	1	0
36	2	1	0	1	0	1	1	1	0	1	0	1	0	1	0	1	0
37	0	0	0	0	0	0	0	0	0	0	0	0	0	2	240	0	0
38	85	1	0	1	0	1	0.05	1	0.05	1	0	1	0	1	-3.45	1	0.05
39	7	1	0	1	0	1	0	1	0	1	0	1	0	1	-2	1	0
40	2	1	0	1	0	1	0	1	0	1	0	1	0	1	1	1	0
41	0	0	0	0	0	0	0	0	0	0	0	0	0	0	0	0	0
42	85	1	0	1	0	1	0.05	1	0.05	1	0	1	0	1	0.05	1	0.05
43	7	1	0	1	0	1	0	1	0	1	0	1	0	1	0	1	0
44	2	1	0	1	0	1	0	1	0	1	0	1	0	1	0	1	0
45	0	0	0	0	0	0	0	2	240	0	0	0	0	0	0	0	0
46	85	1	0	1	0	1	0.05	1	-3.45	1	0	1	0	1	0.05	1	0.05
47	7	1	0	1	0	1	0	1	-2	1	0	1	0	1	0	1	0
48	2	1	0	1	0	1	0	1	1	1	0	1	0	1	0	1	0
49	0	0	0	0	0	0	0	0	0	0	0	0	0	0	0	2	240
50	85	1	0	1	0	1	0.05	1	0.05	1	0	1	0	1	0.05	1	-3.45
51	7	1	0	1	0	1	0	1	0	1	0	1	0	1	0	1	-2
52	2	1	0	1	0	1	0	1	0	1	0	1	0	1	0	1	1
53	0	0	0	0	0	0	0	0	0	0	0	0	0	0	0	0	0
54	85	1	0	1	0	1	0.05	1	0.05	1	0	1	0	1	0.05	1	0.05
55	7	1	0	1	0	1	0	1	0	1	0	1	0	1	0	1	0
56	2	1	0	1	0	1	0	1	0	1	0	1	0	1	0	1	0
57	85	1	0	1	0	1	0	1	0	1	0	1	0	1	0	1	0
58	1	0	0	0	0	0	0	0	0	0	0	0	0	0	0	0	0

#	Duration	Control	Temperature	LoopTo	LoopCount	Step	
0	0.1	101	30	0	0	97	-1
1	3.5	101	30	0	0	97	-1
2	60	117	30	0	0	90	-1
3	90	101	30	0	0	80	-1
4	60	101	30	0	0	80	-1
5	60	109	30	0	0	98	-1
6	60	101	30	0	0	97	-1
7	15	101	30	0	0	80	-1
8	2	101	30	0	0	80	-1
9	0	97	30	0	0	91	-1
10	85	101	30	0	0	12	12
11	7	101	30	0	0	80	-1
12	2	101	30	0	0	80	-1
13	0	97	30	0	0	91	-1
14	85	101	30	0	0	3	0
15	7	101	30	0	0	80	-1
16	2	101	30	0	0	80	-1
17	0	97	30	0	0	91	-1
18	85	101	30	0	0	7	1
19	7	101	30	0	0	80	-1
20	2	101	30	0	0	80	-1
21	0	97	30	0	0	91	-1
22	85	101	30	0	0	11	2
23	7	101	30	0	0	80	-1
24	2	101	30	0	0	80	-1
25	0	97	30	0	0	91	-1
26	85	101	30	0	0	2	3
27	7	101	30	0	0	80	-1
28	2	101	30	0	0	80	-1
29	0	97	30	0	0	91	-1
30	85	101	30	0	0	6	4
31	7	101	30	0	0	80	-1
32	2	101	30	0	0	80	-1
33	0	97	30	0	0	91	-1
34	85	101	30	0	0	10	5
35	7	101	30	0	0	80	-1
36	2	101	30	0	0	80	-1
37	0	97	30	0	0	91	-1
38	85	101	30	0	0	1	6
39	7	101	30	0	0	80	-1
40	2	101	30	0	0	80	-1
41	0	97	30	0	0	91	-1
42	85	101	30	0	0	5	7
43	7	101	30	0	0	80	-1
44	2	101	30	0	0	80	-1
45	0	97	30	0	0	91	-1
46	85	101	30	0	0	9	8
47	7	101	30	0	0	80	-1
48	2	101	30	0	0	80	-1
49	0	97	30	0	0	91	-1
50	85	101	30	0	0	0	9
51	7	101	30	0	0	80	-1
52	2	101	30	0	0	80	-1
53	0	97	30	0	0	91	-1
54	85	101	30	0	0	4	10
55	7	101	30	0	0	80	-1
56	2	101	30	0	0	80	-1
57	85	101	30	0	0	8	11
58	1	97	30	0	0	91	-1

2. DNA 7500 Series, Liposomes II, 1000 V, RT

#	Duration	[D1]	D1	[C1]	C1	[B1]	B1	[A1]	A1	[D2]	D2	[C2]	C2	[B2]	B2	[A2]	A2
0	0.1	0	350	0	350	0	350	0	350	0	350	0	350	0	1100	0	350
1	120	1	0	1	0	1	0	1	0	1	0	1	0	0	350	0	1500
2	60	1	0	1	0	1	0	1	0	1	0	1	0	0	350	0	1500
3	60	1	0	1	0	1	0	1	0	0	1500	1	0	0	350	0	350
4	1	1	0	1	0	1	0	1	0	1	0	1	0	1	0	1	0
5	100	1	0	1	0	1	0	1	0	0	1500	1	0	0	700	1	0
6	35	1	0	1	0	1	0	1	0	1	0	0	200	1	0	1	0
7	10	1	0	1	0	1	0	1	0	1	0	1	0	1	0	0	200
8	80	1	0	1	0	1	0	1	0	0	1500	1	0	0	500	1	0
9	35	1	0	1	0	1	0	1	0	1	0	0	200	1	0	1	0
10	10	1	0	1	0	1	0	1	0	1	0	1	0	1	0	0	200
11	80	1	0	1	0	1	0	1	0	0	1500	1	0	0	500	1	0
12	35	0	1500	1	0	1	0	1	0	1	0	0	200	1	0	1	0
13	10	0	1500	1	0	1	0	1	0	1	0	1	0	1	0	0	200
14	80	1	0	1	0	1	0	1	0	0	1500	1	0	0	500	1	0
15	35	1	0	1	0	1	0	1	0	1	0	0	200	1	0	1	0
16	10	1	0	1	0	1	0	1	0	1	0	1	0	1	0	0	200
17	80	1	0	1	0	1	0	1	0	0	1500	1	0	0	500	1	0
18	35	1	0	1	0	1	0	1	0	1	0	0	200	1	0	1	0
19	10	1	0	1	0	1	0	1	0	1	0	1	0	1	0	0	200
20	80	1	0	1	0	1	0	1	0	0	1500	1	0	0	500	1	0
21	35	1	0	0	1500	1	0	1	0	1	0	0	200	1	0	1	0
22	10	1	0	0	1500	1	0	1	0	1	0	1	0	1	0	0	200
23	80	1	0	1	0	1	0	1	0	0	1500	1	0	0	500	1	0
24	35	1	0	1	0	1	0	1	0	1	0	1	0	1	0	0	200
25	10	1	0	1	0	1	0	1	0	1	0	0	200	1	0	1	0
26	80	1	0	1	0	1	0	1	0	0	1500	1	0	0	500	1	0
27	35	1	0	1	0	1	0	1	0	1	0	1	0	1	0	0	200
28	10	1	0	1	0	1	0	1	0	1	0	0	200	1	0	1	0
29	80	1	0	1	0	1	0	1	0	0	1500	1	0	0	500	1	0
30	35	1	0	1	0	0	1500	1	0	1	0	1	0	1	0	0	200
31	10	1	0	1	0	0	1500	1	0	1	0	0	200	1	0	1	0
32	80	1	0	1	0	1	0	1	0	0	1500	1	0	0	500	1	0
33	35	1	0	1	0	1	0	1	0	1	0	1	0	1	0	0	200
34	10	1	0	1	0	1	0	1	0	1	0	0	200	1	0	1	0
35	80	1	0	1	0	1	0	1	0	0	1500	1	0	0	500	1	0
36	35	1	0	1	0	1	0	1	0	1	0	1	0	1	0	0	200
37	10	1	0	1	0	1	0	1	0	1	0	0	200	1	0	1	0
38	80	1	0	1	0	1	0	1	0	0	1500	1	0	0	500	1	0
39	35	1	0	1	0	1	0	0	1500	1	0	1	0	1	0	0	200
40	10	1	0	1	0	1	0	0	1500	1	0	0	200	1	0	1	0
41	80	1	0	1	0	1	0	1	0	0	1500	1	0	0	500	1	0
42	1	1	0	1	0	1	0	1	0	1	0	1	0	1	0	1	0

#	Duration	[D3]	D3	[C3]	C3	[B3]	B3	[A3]	A3	[D4]	D4	[C4]	C4	[B4]	B4	[A4]	A4
0	0.1	0	350	0	350	0	350	0	350	0	350	0	350	0	350	0	350
1	120	1	0	1	0	1	0	1	0	1	0	1	0	1	0	1	0
2	60	1	0	1	0	1	0	1	0	1	0	1	0	1	0	1	0
3	60	1	0	1	0	1	0	1	0	1	0	1	0	1	0	1	0
4	1	1	0	1	0	1	0	1	0	1	0	1	0	1	0	1	0
5	100	1	0	1	0	1	0	1	0	1	0	1	0	1	0	1	0
6	35	0	1500	1	0	1	0	1	0	1	0	1	0	1	0	1	0
7	10	0	1500	1	0	1	0	1	0	1	0	1	0	1	0	1	0
8	80	1	0	1	0	1	0	1	0	1	0	1	0	1	0	1	0
9	35	1	0	1	0	1	0	1	0	0	1500	1	0	1	0	1	0
10	10	1	0	1	0	1	0	1	0	0	1500	1	0	1	0	1	0
11	80	1	0	1	0	1	0	1	0	1	0	1	0	1	0	1	0
12	35	1	0	1	0	1	0	1	0	1	0	1	0	1	0	1	0
13	10	1	0	1	0	1	0	1	0	1	0	1	0	1	0	1	0
14	80	1	0	1	0	1	0	1	0	1	0	1	0	1	0	1	0
15	35	1	0	0	1500	1	0	1	0	1	0	1	0	1	0	1	0
16	10	1	0	0	1500	1	0	1	0	1	0	1	0	1	0	1	0
17	80	1	0	1	0	1	0	1	0	1	0	1	0	1	0	1	0
18	35	1	0	1	0	1	0	1	0	1	0	0	1500	1	0	1	0
19	10	1	0	1	0	1	0	1	0	1	0	0	1500	1	0	1	0
20	80	1	0	1	0	1	0	1	0	1	0	1	0	1	0	1	0
21	35	1	0	1	0	1	0	1	0	1	0	1	0	1	0	1	0
22	10	1	0	1	0	1	0	1	0	1	0	1	0	1	0	1	0
23	80	1	0	1	0	1	0	1	0	1	0	1	0	1	0	1	0
24	35	1	0	1	0	0	1500	1	0	1	0	1	0	1	0	1	0
25	10	1	0	1	0	0	1500	1	0	1	0	1	0	1	0	1	0
26	80	1	0	1	0	1	0	1	0	1	0	1	0	1	0	1	0
27	35	1	0	1	0	1	0	1	0	1	0	1	0	0	1500	1	0
28	10	1	0	1	0	1	0	1	0	1	0	1	0	0	1500	1	0
29	80	1	0	1	0	1	0	1	0	1	0	1	0	1	0	1	0
30	35	1	0	1	0	1	0	1	0	1	0	1	0	1	0	1	0
31	10	1	0	1	0	1	0	1	0	1	0	1	0	1	0	1	0
32	80	1	0	1	0	1	0	1	0	1	0	1	0	1	0	1	0
33	35	1	0	1	0	1	0	0	1500	1	0	1	0	1	0	1	0
34	10	1	0	1	0	1	0	0	1500	1	0	1	0	1	0	1	0
35	80	1	0	1	0	1	0	1	0	1	0	1	0	1	0	1	0
36	35	1	0	1	0	1	0	1	0	1	0	1	0	1	0	0	1500
37	10	1	0	1	0	1	0	1	0	1	0	1	0	1	0	0	1500
38	80	1	0	1	0	1	0	1	0	1	0	1	0	1	0	1	0
39	35	1	0	1	0	1	0	1	0	1	0	1	0	1	0	1	0
40	10	1	0	1	0	1	0	1	0	1	0	1	0	1	0	1	0
41	80	1	0	1	0	1	0	1	0	1	0	1	0	1	0	1	0
42	1	1	0	1	0	1	0	1	0	1	0	1	0	1	0	1	0

#	Duration	Control	Temperature	LoopTo	LoopCount	Step	
0	0.1	71	off	0	0	97	-1
1	120	71	off	0	0	97	-1
2	60	71	off	0	0	-1	-1
3	60	71	off	0	0	97	-1
4	1	71	off	0	0	91	-1
5	100	71	off	0	0	12	12
6	35	71	off	0	0	80	-1
7	10	71	off	0	0	80	-1
8	80	71	off	0	0	3	0
9	35	71	off	0	0	80	-1
10	10	71	off	0	0	80	-1
11	80	71	off	0	0	7	1
12	35	71	off	0	0	80	-1
13	10	71	off	0	0	80	-1
14	80	71	off	0	0	11	2
15	35	71	off	0	0	80	-1
16	10	71	off	0	0	80	-1
17	80	71	off	0	0	2	3
18	35	71	off	0	0	80	-1
19	10	71	off	0	0	80	-1
20	80	71	off	0	0	6	4
21	35	71	off	0	0	80	-1
22	10	71	off	0	0	80	-1
23	80	71	off	0	0	10	5
24	35	71	off	0	0	80	-1
25	10	71	off	0	0	80	-1
26	80	71	off	0	0	1	6
27	35	71	off	0	0	80	-1
28	10	71	off	0	0	80	-1
29	80	71	off	0	0	5	7
30	35	71	off	0	0	80	-1
31	10	71	off	0	0	80	-1
32	80	71	off	0	0	9	8
33	35	71	off	0	0	80	-1
34	10	71	off	0	0	80	-1
35	80	71	off	0	0	0	9
36	35	71	off	0	0	80	-1
37	10	71	off	0	0	80	-1
38	80	71	off	0	0	4	10
39	35	71	off	0	0	80	-1
40	10	71	off	0	0	80	-1
41	80	71	off	0	0	8	11
42	1	71	off	0	0	97	-1

Appendix B

Further data regarding liposome preparation and quality control

Liposomes No.	Date	Conc. MB (nM)	MB	comment
1	20.08.2015	0	-	
2	20.08.2015	50	P14	extrusion failed
3	20.08.2015	150	P14	2 nd extrusion
4	20.08.2015	250	P14	
5	25.08.2015	50	P14	
6	25.08.2015	250	P14	
7	31.08.2015	0	-	No Trolox, no MB, BGE = 200 mM Na-Borate
8	07.09.2015	250	P14	200 nm extrusion
9	07.09.2015	250	P12	
10	07.09.2015	250	P13	
11	21.10.2015	250	P12	BGE = 200 mM Na- Borate, pH 8.4
12	21.10.2015	250	P13	BGE = 200 mM Na- Borate, pH 8.4
13	21.10.2015	250	P14	BGE = 200 mM Na- Borate, pH 8.4
14	16.11.2015	250	P13	
15	16.11.2015	250	P14	
16	01.12.2015	250	P13	physiological composition, 400 nm
17	01.12.2015	250	P13	physiological composition, 200 nm
18	01.12.2015	250	P13	physiological composition, 100 nm
19	01.12.2015	250	P13	non physiological composition, 400 nm
20	01.12.2015	250	P13	non physiological composition, 200 nm
21	01.12.2015	250	P13	non physiological composition, 100 nm
22	08.01.2016	250	P13	Physiologic, 1 mM MgCl ₂ inside, 200 nm
23	08.01.2016	250	P13	Physiologic, 1 mM MgCl ₂ inside, 100 nm
24	08.01.2016	250	P13	Physiologic, + Ni-NTA, 200 nm
25	08.01.2016	250	P13	Physiologic, + Ni-NTA, 100 nm
26	11.02.2016	250	P13	Physiologic, + Ni-NTA, 100 nm
27	29.02.2016	250	P14	Physiologic, + Ni-NTA, 100 nm
28	01.03.2016	250	P14	Physiologic, + Ni-NTA, 100 nm
29	14.03.2016	250	P13	Physiologic, + Ni-NTA, 100 nm
30				

